NOTE TO USERS

Université d'Ottawa · University of Ottawa

Université d'Ottawa · University of Ottawa

FACULTÉ DES ÉTUDES SUPÉRIEURES ET POSTDOCTORALES

FACULTY OF GRADUATE AND POSTDOCTORAL STUDIES

Josée CLOUTIER

AUTEUR DE LA THÈSE - AUTHOR OF THESIS

M. Sc. (Chemistry)

GRADE - DEGREE

Department of Chemistry

FACULTÉ, ÉCOLE, DÉPARTEMENT - FACULTY, SCHOOL, DEPARTMENT

TITRE DE LA THÈSE - TITLE OF THE THESIS

High Throughput Methods in the Development of a New Asymmetric Reactions : Fluorescence Resonance Energy Transfer Technology for Screening Potential Catalysts

W. Ogilvie

DIRECTEUR DE LA THÈSE - THESIS SUPERVISOR

CO-DIRECTEUR DE LA THÈSE - THESIS CO-SUPERVISOR

EXAMINATEURS DE LA THÈSE - THESIS EXAMINERS

R. Ben

K. Fagnou

J.-M. De Koninck, Ph.D.

LE DOYEN DE LA FACULTÉ DES ÉTUDES SUPÉRIEURES ET POSTDOCTORALES

DEAN OF THE FACULTY OF GRADUATE AND POSTDOCTORAL STUDIES

HIGH THROUGHPUT METHODS IN THE DEVELOPMENT OF NEW ASYMMETRIC REACTIONS: FLUORESCENCE RESONANCE ENERGY TRANSFER TECHNOLOGY FOR SCREENING POTENTIAL CATALYSTS.

By

JOSÉE CLOUTIER

B.Sc. Université du Québec à Montréal, 2002

A thesis submitted to the School of Graduate Studies and Research
In partial fulfillment of the requirements for the degree of
Master of Science

Ottawa-Carleton Chemistry Institute
Department of Chemistry
University of Ottawa
Ottawa, Ontario
Canada

University of Ottawa

November 2004

Your file Votre référence
ISBN: 0-494-02594-8
Our file Notre référence
ISBN: 0-494-02594-8

TABLE OF CONTENTS

LIST OF SCHEMES

LIST OF FIGURES

LIST OF TABLES

LIST OF ABBREVIATIONS

Ac	acetyl
AUC	area under the curve
[¿]D	optical rotation, sodium lamp
HOAc	acetic acid
Bn	benzyl
br	broad
cm	centimeter
d	doublet
DCM	dichloromethane
dd	doublet of doublet
DMF	*N,N*-dimethylformamide
DIPEA	*N,N*-diisopropylethylamine
DNB	dinitrobenzene
EDC	1-(3-dimethylaminopropyl)-3-ethylcarbodiimide hydrochloride
EEDQ	2-ethoxy-1-ethoxycarbonyl-1,2-dihydroquinoline
ee	Enantiomeric excess
EI	electron impact
eq	equivalent
ESI	electrospray ionization
Et	ethyl
EtOAc	ethyl acetate
Et_2O	diethylether
FU	Fluorescence unit
HOBT	1-hydroxybenzotriazole
HPLC	High performance liquid chromatography
Hz	hertz
'	wavelength
iPr	isopropyl
IR	infrared spectrometry

m	multiplet
M	molar
Me	methyl
MeOH	methanol
MHz	megaherzt
mmol	millimoles
MS	mass spectrometry
nm	nanometer
NMR	nuclear magnetic resonance
Ph	phenyl
pmol	picomoles
ppm	parts per million
q	quartet
Rf	retention factor
rt	room temperature
s	singlet
sln	solution
t	triplet
TBAF	tetrabutylammonium fluoride
TBS	*t*-butyldimethylsilyl
TEA	triethylamine
TFA	trifluoroacetic acid
THF	tetrahydrofuran
TLC	thin layer chromatography

ABSTRACT

High throughput methods are valuable for decreasing the time needed for the development of new asymmetric reactions. Catalyst discovery may be accelerated by the rapid screening of reactions for enantioselectivity. Chiral substrates are used in a novel fluorescence resonance energy transfer (FRET) assay. A fluorophore (donor), a fluorescence quencher (acceptor) and a recognition element are part of the assay substrates. The latter are prepared using different fluorescent donor/acceptor pairs for each enantiomer of the recognition element. Screening is performed using equimolar mixture of the two substrates. Weak fluorescence indicates no reaction. Strong fluorescence at both wavelengths indicates a non-selective reaction while an enantioselective coupling would display strong fluorescence at only one wavelength.

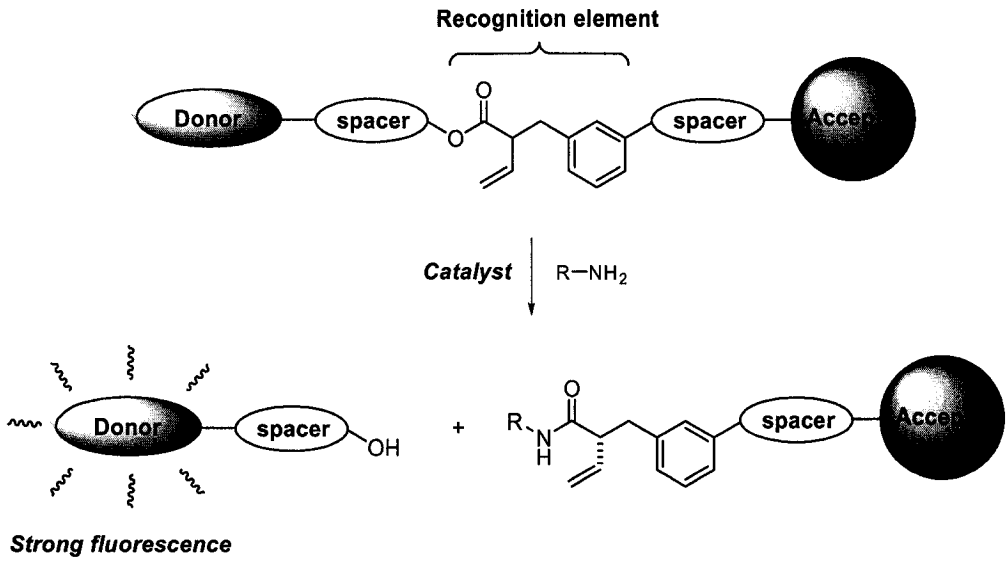

Strong fluorescence

REMERCIEMENTS

D'abord et bien entendu, j'aimerais remercier mon superviseur Dr. William W. Ogilvie de m'avoir accueillie dans son équipe. Ses ressources et ses connaissances m'ont grandement soutenues tout au cours de mon travail. J'ai bien appris à être efficace et surtout à être rigoureuse dans tout ce que j'entreprendrai.

Je tiens également à remercier mes collègues de travail et amis. Tout d'abord, Joe « esti j'ai perdu mon stir bar » Jebreen qui m'a reçue de façon tout à fait hors de l'ordinaire... La musique au boutte chantant à tue-tête, quoi demander de mieux pour agrémenter une atmosphère de travail. Aussi, je tiens sincèrement à remercier Patrick « Ti-Pet » Beaulieu pour ses connaissances illimitées et surtout pour m'avoir fait rire à l'écoeurer (sans méchancetés voyons...) sur à peu près n'importe quoi... Je ne peux oublier l'incontournable Mathieu « Pimp Shit » Lemay, mon franco-ontarien préféré. Sans lui, Mario aurait perdu son porte-feuille. Aussi, Alison « Freesbee » Lemay, je te remercie pour tes précieux conseils et surtout de ta grande détermination. Quand tu seras une vedette de l'Ultimate, j'aimerais avoir un autographe en primeur.... Merci également à ma petite Livia pour ta patience et tes encouragements, tu es formidable. Merci spécial à Ami Jun-Yee Chin pour ton incroyable aide dans mon projet, sans toi j'en aurais bavé un bon coup. Il ne faut pas que j'oublie tous les étudiants sous-gradués qui ont passé quelques temps dans notre laboratoire : Marc Lafrance, Val « aqua girl » Charbonneau, Elizabeth van Moos ainsi que Joe #2 Moran. Je n'aurais pu passer au travers tout ça sans la santé et la forme, donc je tiens à remercier Julie Farand pour m'avoir accompagnée dans les classes de steps, tae-cardio etc... Merci à tous les superviseurs et membres des autres groupes de recherches pour votre aide.

Finalement, il y a ceux qui ont été loin de moi tout ce temps, à qui je pensais très fort chaque jour, me donnant la motivation et la détermination pour accomplir tout ça : ma famille, mes amis, mon chat.....Merci d'avoir été là....

« *À mes parents, René et Francine, ainsi qu'à ma sœur, Karine, et mon neveu Maxime.* »

« *À Hélène et Pat...* »

CHAPTER 1

High Throughput Methods

1.1 Combinatorial Chemistry

1.1.1 History

The first published work on solid phase synthesis was made by R. B. Merrifield in 1963. Merrifield[1] described a new technique for the synthesis of polypeptides that resolved the solubility and purification difficulties encountered in classical approaches. His goal was to create reaction conditions that would be consistent and reliable for peptide couplings. The use of a polymeric solid phase bonded covalently to the first amino acid of the chain proved to be a suitable solution. The formation of amino acid chains followed a cyclic reaction sequence: by alternatively deprotecting, washing and coupling with the appropriate N-protected-amino acid, the desired peptide chain could be prepared. This material was then released from the polymer by hydrolysis giving the desired peptide after suitable purification. His lifetime work was rewarded nearly 20 years later when he received the Nobel Prize in 1984.

In the mid 1980's, many research teams such as those of Houghten[2] and Geysen[3], elaborated the concept of Merrifield demonstrating that the same principle could be used to make many peptides simultaneously in the same reaction vessel. The scope of this combinatorial chemistry was expanded by Furka[4] in 1988, with the development of the split-pool method. Increasing importance in drug discovery made combinatorial chemistry an essential process over the years. Since the early 1990's, companies have been attracted to this new wave as a means of reducing the time and high costs associated with the drug discovery process. "Combichem" became a new school of thought that

---

[1] Merrifield R.B., *J. Am. Chem. Soc.* **1963**, *85*, 2149.
[2] Houghten R.A., *Proc. Natl Sci. USA* **1985**, *82*, 5131.
[3] Geysen H.M.; Meloen R.H., Barteling S.J., *Proc. Natl Sci. USA* **1984**, *81*, 3998.
[4] Furka A.; Sebestyen F.; Asgedom M.; Dibo G., *Abstr. 14th Int. Congr. Biochem.*, Prague **1988**, *5*, 47.

challenged the orthodox chemistry that believed all synthetic chemical compounds should be made individually, in a fully purified and characterized state.

1.1.2 Combinatorial chemistry in the drug discovery process

Traditionally, drugs have been discovered using three major strategies. The first possibility is a systematic approach to synthesize compounds with optimal interactions with the target receptor. The second possibility comes from active ingredients in natural extracts (plants, soil, etc.) which, once isolated and purified, can be tested on different targets. Finally, the third one relies on accidental discoveries such as a drug molecule being found to be active for a different target than expected[5].

Drug discovery is both a lengthy and expensive business: it can take more than five years from launching the project to sending a potential drug into development and clinical trials. One of the main reasons for this labour is the slow synthesis of compounds. Today, however, pharmaceutical research is looking at new and improved ways to develop drugs. Combinatorial synthesis as a high throughput method enables the rapid production of hundreds to thousands of times more compounds than conventional serial organic synthesis. After collecting the compounds and grouping them in libraries, medicinal chemists can discover lead candidates and improve their activity by exploring structure-activity relationships (SAR).

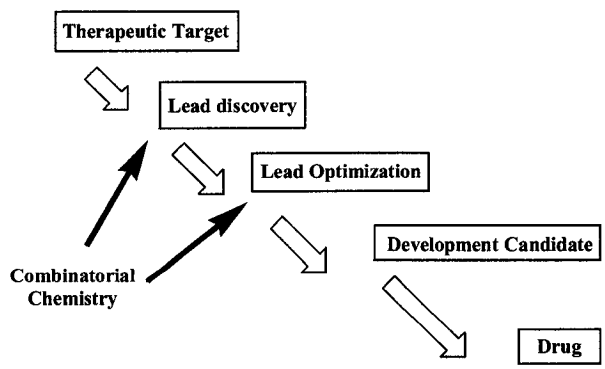

Figure 1: Key steps of drug discovery process influenced by combinatorial chemistry.

[5] Wells D.A., In *High Throughput Bioanalytical Sample Preparation* **2003**, Elsevier, Chapter 1.

Combinatorial synthesis requires high throughput screening techniques (HTS) that evaluate the potency and pharmacological activity of these compounds. Those techniques will be further discussed in this chapter. The most active compounds, or hits, are qualitatively identified from simulated biological receptors or target functions during high throughput screening. The hits then undergo an exhaustive review addressing all the key issues concerning further development: ADME (Absorption, Distribution, Metabolism and Elimination), clinical trials, etc. Combinatorial chemistry has changed the traditional way to approach synthetic chemistry. In industry, especially where the pressure to discover new agents as quickly as possible is present, these techniques make a considerable impact.

1.1.3 Principles of combinatorial chemistry

The basic idea of combinatorial chemistry is to generate a large number of compounds very quickly. In the past, chemists have made one compound at the time, in one reaction at the time. For example, compound A could react with compound B to give the product AB which then would be isolated after work-up and purification (crystallization, distillation or chromatography). In contrast, combinatorial chemistry offers the possibility of creating all the combinations of compounds A_1 to A_n with B_1 to B_n (**Figure 2**).

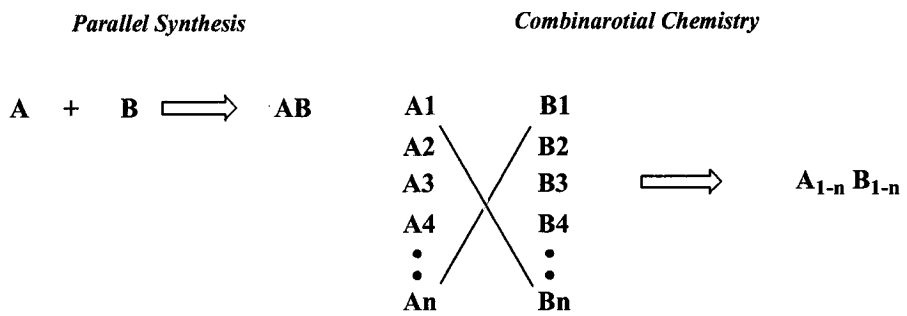

Figure 2: Contrast between orthodox chemistry (parallel synthesis) and combinatorial chemistry.

The resulting collection of compounds is referred to as a combinatorial library because of the structural relationship between the compounds or "members" (scaffold or common backbone)[6]. The range of combinatorial techniques is highly diverse and provides the potential to amplify utility over orthodox methods.

1.1.3.1 Split-Pool Synthesis

Furka[7] and co-workers pioneered the split-pool synthesis method for polypeptide libraries as previously mentioned. The approach can be summarized in three words: divide, couple and recombine. This combinatorial technique allows libraries to be created in just a few reactions.

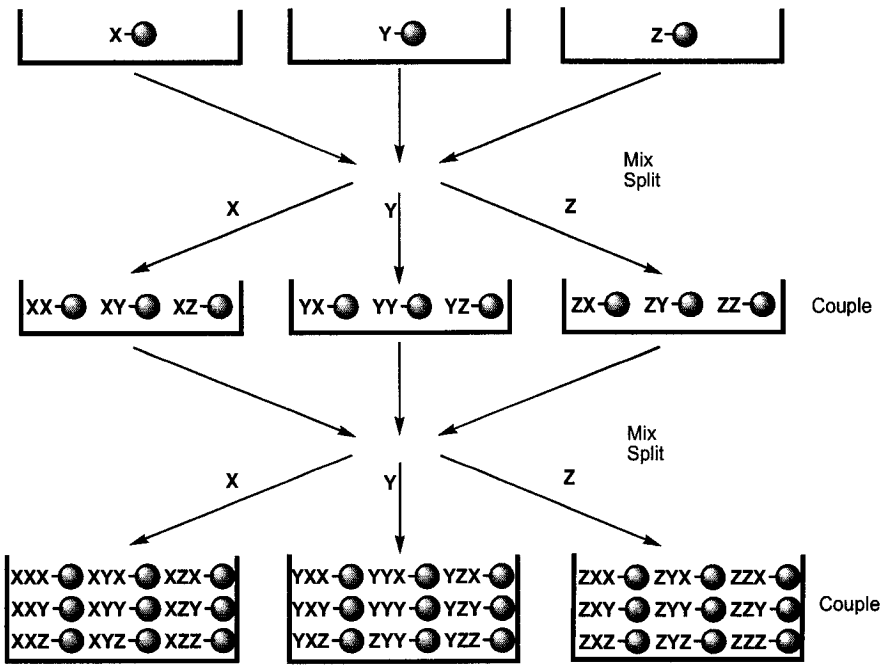

Figure 3: Split-pool synthetic scheme for the synthesis a 27 member trimer library.

A quantity of polymer beads is divided into a number of equal portions and each of these portions are individually reacted with a different monomeric starting material (**Figure 3**).

[6] Jung G., In *Combinatorial Chemistry* **1999**, Wiley-VCH, Chapter 1.
[7] Furka A.; Sebestyen F.; Asgedom M.; Dibo G., *Abstr. 14th Int. Congr. Biochem.*, Prague, **1988**, *5*, 47.

After washing away excess starting material from each container, the beads in all the reaction vessels are recombined and then split again into equal portions. A second building block is added to each vessel to produce dimeric units as mixtures. The whole process may be then repeated as necessary for a total of n times. The number of compounds resulting from the sequence equals x (monomers) to the power of n (total number of coupling steps).

For the screening of those compounds, the individual beads carrying the oligomers are tested. This technique has been criticized for its efficiency in terms of reaction time and for the difficult identification of active compounds. In general, the system has proved successfully the ability to generate a large number of compounds quickly and is currently the most popular method used in academic settings.[8] Depending on the loading capacity of the resin bead, quantities of only 200 pmol can be obtained per resin bead. Various types of split-pool protocols using solid-phase synthesis have been explored by Houghten[9], Geysen[10], and more recently by DeWitt[11] and Nicolaou[12].

1.1.4 Parallel Synthesis towards Combinatorial Libraries

Even if combinatorial synthesis generates a greater number of compounds, parallel synthesis can offer the advantage that each compound is relatively pure and easily identified. Compounds are synthesized in an automated fashion using ordered arrays of separated reaction vessels. In contrast to the split-pool method which requires a solid support, parallel synthesis can be done either on solid-phase or in solution[13]. The difficulty of purifying large numbers of compounds without automated equipment restricts the use of solution chemistry to short synthetic pathways using reliable chemistry. Also, the possibility of creating significant amounts of impurities could pose a problem. Many of these difficulties can be avoided by using solid supports. Parallel synthesis can reliably be used to mark hundreds of analogues of active substrate.

---

[8] Terrett N.K., In *Combinatorial Chemistry* **1998**, Oxford University Press, pp.15-18.
[9] Houghten R.A., *Proc. Natl Sci. USA* **1985**, *82*, 5131.
[10] Geysen H.M.; Meloen R.H.; Barteling S.J., *Proc. Natl Sci. USA* **1984**, *81*, 3998.
[11] DeWitt S.H.; Czarnik A.W., *Acc. Chem. Res.* **1996**, *29*, 114.
[12] Nicolaou K.C.; Xiao-Yi X.; Parandoosh Z.; Senyei A.; Nova M.P. *Angew. Chem. Int. Ed. Engl.* **1995**, *34*, 2289.
[13] Pirrung M.C., *Chem. Rev.* **1997**, *97*, 473.

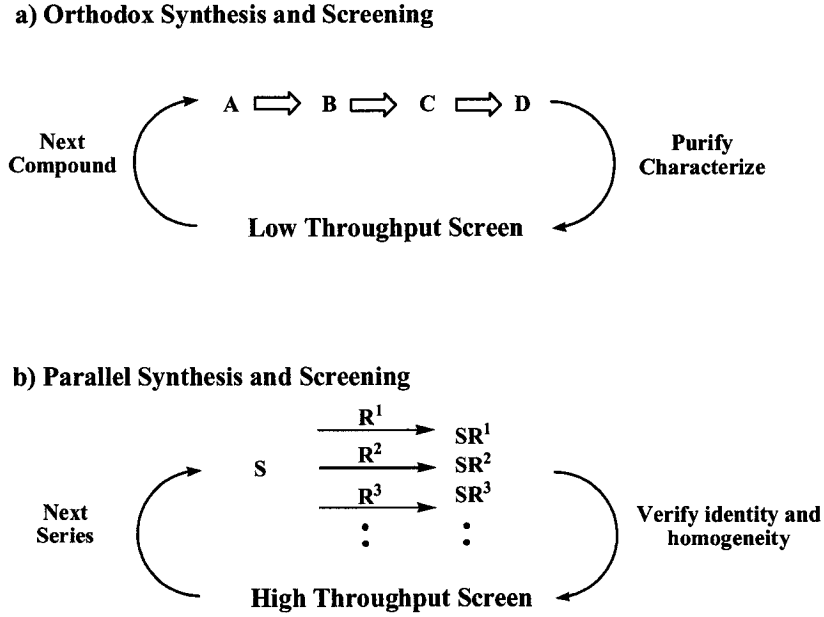

Figure 4: Comparison of orthodox and parallel synthesis.

Orthodox chemistry involves a multi-step sequence (**Figure 4a**) in which product D is purified and fully characterized before screening. The design and preparation of the next analogue depends on the biological activity of the previous compound. This process is repeated to optimize both activity and selectivity. In contrast, parallel synthesis involves the reaction of the substrate S with different reactants $\mathbf{R_n}$ to give a library of n products $\mathbf{SR_n}$ (**Figure 4b**). The created library is screened without purification using high throughput screening techniques[14].

1.2 High Throughput Screening Techniques

Besides synthesizing a large number of potentially biologically active molecules, combinatorial methods are also very good strategies for the development of new chemical transformations. For example, the preparation of libraries of potential asymmetric catalysts would accelerate the process of new catalyst discovery. The application of such

[14] Terrett N.K., In *Combinatorial Chemistry*, **1998**, Oxford University Press, Chapter 4.

strategies involves the preparation of thousands of catalysts that require high throughput screening systems capable of quickly assaying enantioselectivity. Some of the methods that have recently been developed for this purpose are discussed below.

The main goal of high throughput methods is the production of the maximum information in a minimum of time. These techniques generally use a combination of robotics, microplates (96-, 384-and more well formats), and computers for data processing. The biggest challenge for these *en masse* automated techniques relies on the choice of the best detection method. Therefore, many techniques have been developed to screen those catalysts in different systems.

1.2.1 Gas Chromatography (GC) and High Pressure Liquid Chromatography (HPLC)

Two of the most commonly used methods in organic laboratories are, perhaps, gas and high pressure liquid chromatography for purification and identification. As the development of combinatorial libraries arrived with numerous compounds or reaction vessels to analyze, many scientists opted for variations of these methods because of their reliability and accuracy. Unfortunately, the time required for each analysis, since the automated process runs one sample at the time, is fairly long for library screening.

1.2.1.1 Gas Chromatography

Studies by Gennari[15], Liskamp[16], Burgess[17], Wolf[18] and Jacobsen[19] were made for parallel analysis of reaction mixtures by GC. This type of screening cannot be qualified as a real high throughput method because one sample was analyzed in about 15 minutes:

---

[15] Gennari C.; Ceccarelli S.; Piarulli U.; Montalbetti C.A.G.N; Jackson R.F.W. *J. Org. Chem.* **1998**, *63*, 5312; Chataigner I.; Gennari C.; Piarulli U.; Ceccarelli S. *Angew. Chem. Int. Ed.* **2000**, *39*, 916; Chataigner I.; Gennari C; Ongeri S.; Piarulli U.; Ceccarelli S. *Chem. Eur. J.* **2001**, *7*, 2628; Ongeri S.; Piarulli U.; Jackson R.F.W.; Gennari C. *Eur. J. Org. Chem.* **2001**, 803.
[16] Brouwer A.J.; van der Linden J.J.; Liskamp R.M.J. *J. Org. Chem.* **2000**, *65*, 1750.
[17] Burgess K.; Porte A.M. *Tetrahedron Asymm.* **1998**, *9*, 2465.
[18] Wolf C.; Hawes P.A. *J. Org. Chem.* **2002**, *67*, 2727.
[19] Sigman M.S.; Jacobsen E.N. *J. Am. Chem. Soc.* **1998**, *120*, 4901; Francis M.B. *Angew. Chem. Int. Ed.* **1999**, *30*, 937.

less than few dozen analyses per day, when 500 to 1000 screens is normally the goal in high throughput methods. This limits throughput and defeats the original idea. However, Reetz[20] brought a significant improvement to the GC technique by using two GC instruments equipped with chiral columns were connected to a prep-and-load sample manager and a computer. This unit could analyze about 700 samples per day (yield and enantiomeric excess), meaning around 3 minutes per run.

1.2.1.2 High Pressure Liquid Chromatography

An outstanding contribution was made by Mikami in 1999[21] through the development of a super high throughput screening system (SHTS) using HPLC, a more versatile method. Normally, the separation of enantiomers by HPLC uses chiral columns in which each isomer of them is quantified. Consequently, the enantiomeric excess can be calculated. Unfortunately, the whole process takes up to 45 minutes per run which is too long for high-throughput purpose. Therefore, to remedy this problem, the Mikami group proposed to use a simple, achiral column for their separations using circular dichroism (CD) and UV-VIS detection systems. This tandem HPLC/CD/UV-VIS method was used to optimize activated diol-zinc catalysts for the asymmetric addition of diethylzinc to aldehydes. The original idea of this combination was created earlier by Mason[22] in a published work in 1980 and re-explored 10 years later by Salvadori[23] and Mannshreck[24]. From the UV (absorption ε) and CD signal ($\Delta\varepsilon$), the anisotropy factor g could be calculated ($g = \Delta\varepsilon/\varepsilon$) for a sample at a fixed wavelength in a flow system. The method was based on the assumption that the g-factor is linear with respect to the enantiomeric excess and is independent of concentration. Certain properties had to be investigated depending on the forms of the substrates (e.g. dimers or aggregates) and the reaction, where the validity of the approximation could be erroneous. The method also poses problems in terms of structural restrictions. Since UV-Vis detectors are used the molecules have to possess a chromophore and so, simple aliphatic compounds cannot be

---

[20] Reetz M.T.; Kühling K.M.; Wilensek S.; Husmann H.; Häusig U.W. *Cat. Today* **2001**, *67*, 389.
[21] Ding K.; Ishii A.; Mikami K. *Angew. Chem. Int. Ed.* **1999**, *38*, 497.
[22] Drake A.F.; Gould J.M.; Mason S.F. *J. Chromatogr. A* **1980**, *202*, 239.
[23] Salvadori P.; Bertucci C.; Rosini C. *Chirality* **1991**, *3*, 376.
[24] Mannschreck A. *Trends Anal. Chem.* **1993**, *12*, 220.

detected. However, Mikami's group polished their technique[25,26] in 2000. They successfully adapted their method to aliphatic alcohols by substituting the UV-Vis detector for a refractive index unit. The optical rotation (OR) per refractive index unit (RIU) approach could be used to analyze both aliphatic and aromatic alcohols (**Scheme 1**). Since the UV-Vis detector was no longer used, the *g* factor was replaced by the enantiomeric factor *e* which was linearly related to the % ee values. Independence over the concentration of the substrate remained.

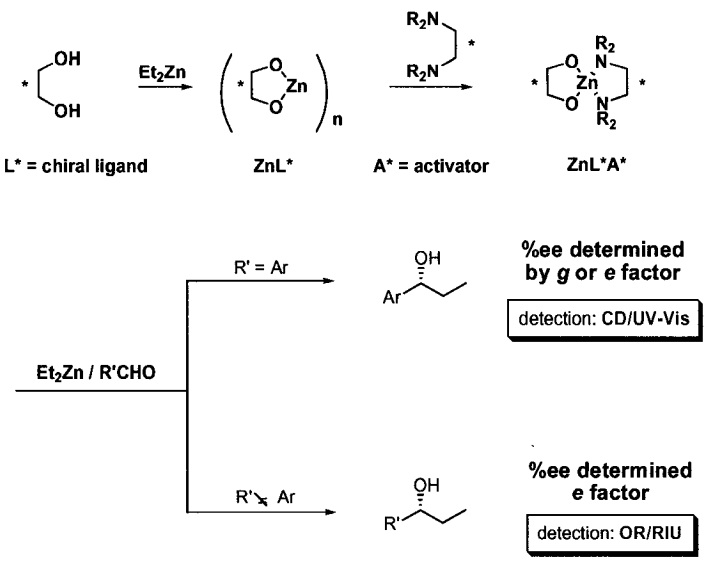

Scheme 1: Asymmetric activation of diol-zinc catalysts by nitrogen ligands used by Mikami.

Also in 2000, Reetz *et al.*[27] expanded their work on the basis of Mikami's method of HPLC/CD/UV-Vis for a different enantioselective context: measuring the % ee and yield for the asymmetric reduction of prochiral ketones with mutant reductases (**Scheme 2**).

[25] Angelaud R.; Matsumoto Y.; Korenaga T.; Kudo K.; Senda M.; Mikami K. *Chirality* **2000**, *12*, 544.
[26] Mikami K.; Angelaud R.; Ding K.; Ishii A.; Tanaka A.; Sawada N.; Kudo K.; Senda M. *Chem. Eur. J.* **2001**, *7*, 730.
[27] Reetz M.T.; Kühling K.M.; Hinrichs H.; Deege A. *Chirality* **2000**, *12*, 479.

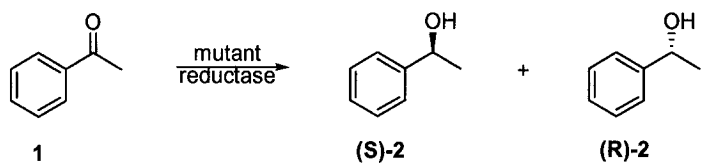

Scheme 2: Reduction of a prochiral ketone with a mutant reductase used by Reetz.

Overall, GC and HPLC methods in high throughput screening are very common and accurate. Unfortunately, these are still relatively low throughput methods because of their long time of acquisition and therefore, massive screening would be inappropriate.

1.2.2 Biological methods

Methods using biological substrates such as enzymes and antibodies for screening reactions in organic chemistry are numerous. These techniques so far have limited applications, but can be quite efficient for the high-throughput screening of particular targets.

1.2.2.1 The Quick-E test

The Quick-E Test from Kazlauskas[28] simulated competition in an enzymatic process to measure the enantioselectivity of lipases or esterases. Hydrolyses of pure enantiomers of 4-nitrophenyl 2-phenylpropanoate, **(S)-3** and **(R)-3** liberated the yellow p-nitrophenoxide which has a characteristic absorbance at 404 nm.

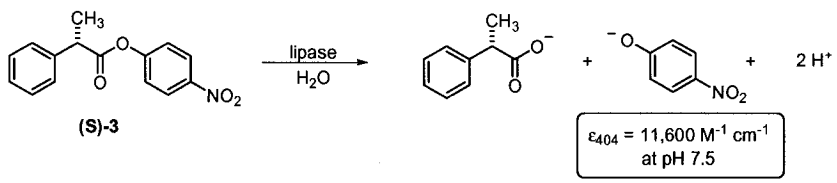

Scheme 3: Lipase-catalyzed hydrolysis of (S)-3 yielding yellow chromophore.

During the first 15 seconds of the reaction, the absorbance (404 nm) was measured on regular intervals for both pure enantiomers. The initial rates of hydrolysis of the

[28] Janes L.E.; Kazlauskas R.J. *J. Org. Chem.* (1997) *62*, 4560.

stereoisomers were calculated from these increases in absorbance, but provided no information about stereoselectivity. The enantiomeric ratio **E** could not be obtained directly from the ratio of these initial rates of reaction because it ignored the competition for binding between the two isomers. To reintroduce competition, resorufin tetradecanoate was added as a reference compound which released, after hydrolysis, a pink chromophore with a characteristic absorbance at 572 nm.

Taking into account the initial concentrations of each enantiomer with the reference compound in separate experiments (**Equation 2**), the ratio of the rates of hydrolysis of **(S)-3** and **(R)-3** was measured over the reference compound gave **E** (**Equation 3**). With this technique, the enantiomeric selectivity of an enzyme could be obtained in 60 seconds.

Enantioselectivity of an enzyme

$$\text{enantiomeric ratio} = E = \frac{(k_{cat}/K_M)_{\text{fast enantiomer}}}{(k_{cat}/K_M)_{\text{slow enantiomer}}} \qquad (1)$$

Approximation

$$\frac{(S)\text{-enantiomer}}{\text{reference}}\ \text{selectivity} = \frac{(k_{cat}/K_M)_{(S)\text{-enantiomer}}}{(k_{cat}/K_M)_{\text{reference}}} = \frac{v_{(S)\text{-enantiomer}}\ [\text{reference}]}{v_{\text{reference}}\ [(S)\text{-enantiomer}]} \qquad (2)$$

$$E = \frac{\frac{(S)\text{-enantiomer}}{\text{reference}}\ \text{selectivity}}{\frac{(R)\text{-enantiomer}}{\text{reference}}\ \text{selectivity}} \qquad (3)$$

1.2.2.2 pH Indicators

Later, Kazlauskas published a different method for hydrolase screening[29]. The reaction used to illustrate his technique was the hydrolysis of an ester at neutral pH (**Scheme 4**)

[29] Janes L.E.; Löwendahl, A.C.; Kazlauskas R.J. *Chem. Eur. J.*, **1998**, *4*, 2324.

which releases a proton detected by a pH indicator, 4-nitrophenol. The concentration of the indicator would then be measured by UV/VIS spectrometry at 404 nm.

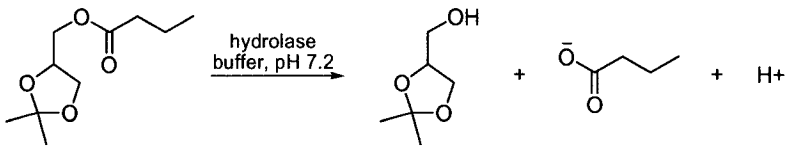

Scheme 4: Hydrolysis of solketal butyrate at neutral pH.

To make sure that the color change is proportional to the number of protons, the buffer and the indicator must have the same affinity for protons (pKa within 0.1 units). In that case, the relative amount of protonated buffer to protonated indicator stays constant as the pH shifts. Therefore, the absorbance increase was a direct measurement of the reaction rate and calibration curves were not necessary. The ratio between the rate of indicator absorbance change and the reaction rate is named the buffer factor **Q**.

Reaction rate calculation

$$Q = \frac{C_B}{C_{In}} \times \frac{1}{\Delta\varepsilon_{404\ nm}} \quad (4)$$

$$\text{rate} = \frac{dA}{dt} \times Q \times \text{reaction volume} \times 10^6 \quad (5)$$

Q = buffer factor

C = molar concentration of buffer (B) and indicator (In)

$\Delta\varepsilon_{404\ nm}$ = difference in extinctioncoefficient between the protonated and unprotonated indicator.

$\frac{dA}{dt}$ = rate of indicator absorbance change

The buffer factor **Q** can be directly calculated when the pKa of the indicator and the buffer are the same (**Equation 4**). With that value in hand, it was possible then to calculate the true reaction rate using **Equation 5**. From the ratio of initial reaction rates, the enantiomeric ratio **E** could be approximated. Unfortunately, these were not the true **E** values since the calculation did not account for competition between the two isomers for the binding site, but they could provide a reasonable approximation. For high-throughput screening methods, this was appropriate. The rate was measured for the first 60 minutes of the reaction for each pure enantiomer, however only data from the first 3-4 minutes was used in calculations so the screening time could be considerably reduced. In total, 72 hydrolases could be analyzed in 180 minutes, which corresponds to about 2 minutes per enzyme.

1.2.2.3 cat-ELISA (catalyst Enzyme-Linked Immuno-Sorbent Assay)

In 1999, Reymond[30] described an alternative technique similar to cat-ELISA (catalyst enzyme-linked immuno-sorbent assay)[31] as a new approach for continuous monitoring of catalysis by fluorescence in solution using antibody sensors. The methodology could be applied generally to reactions of non-chromogenic and nonfluorogenic substrates. This antibody sensor was made of a product-selective antibody and was based on fluorescence. In the bound state, fluorescence of the product analogue was quenched by the antibody. Fluorescence was possible only when this product analogue was released into solution. As the true reaction product was formed, it displaced this analogue from the antibody, which resulted in an increase in fluorescence (**Figure 5**).

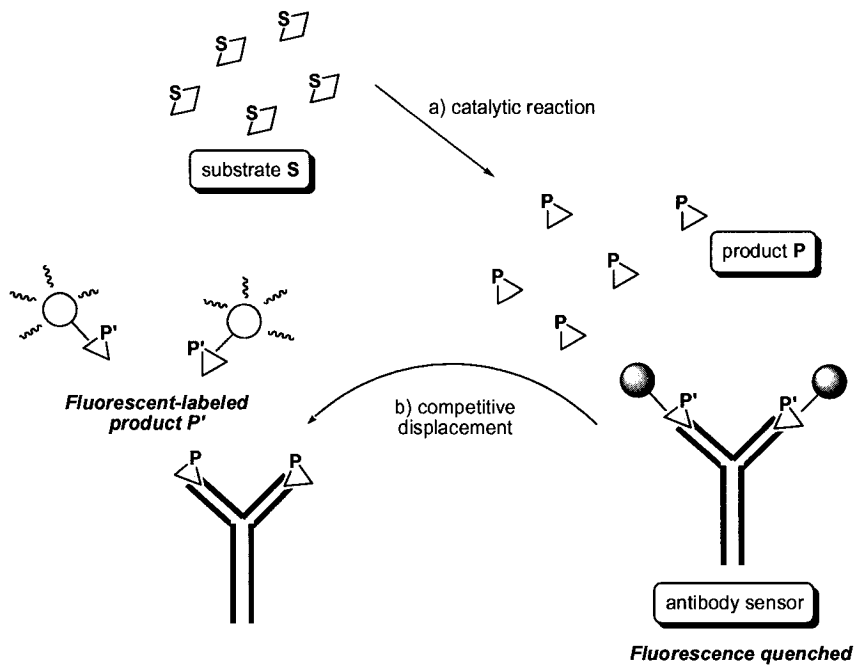

Figure 5: Real-time catalysis assay with the use of fluorescent antibody.

[30] Geymayer P.; Bahr N.; Reymond J.L. *Chem. Eur. J.*, **1999**, *5*, 1006.
[31] Tawfik D.S.; Green B. S.; Chap R.; Sela M.; Eshhar Z. *Proc. Natl Acad. Sci. USA*, **1993**, *90*, 373; MacBeath G.; Hilvert D. *J. Am. Chem. Soc.*, **1994**, *116*, 6101; Benedetti F.; Berti F.; Massimiliano F.; Resmini M.; Bastiani E. *Anal. Biochem.*, **1998**, *256*, 67.

The method was tested by monitoring the rate of hydrolysis of **4** by β-galactosidase and **5** by esterases (**Scheme 5**).

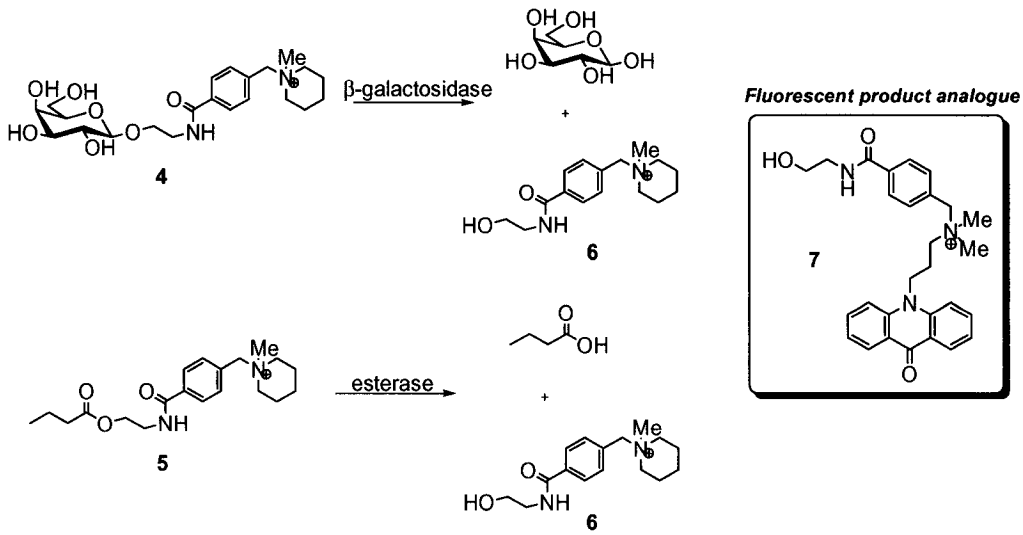

Scheme 5: Hydrolysis reaction for a fluorescence-based antibody high-throughput assay.

Both reactions released **6** as the product of hydolysis and displaced the fluorescent product analogue **7** from the antibody. The new bound-state with the antibody created a fluorescence of the acridone moiety in **7** which was quenched, but in solution (unbound-state), fluorescence at 445 nm was observed. A calibration curve could therefore be established in which the concentration of **6** could be obtained from the intensity of emission. Many variables needed to be optimized so that the reactions could be properly monitored by this method: 1) the antibody had to be able to quench the tag fluorescence, 2) the reactions had to occur in a buffered aqueous environment and 3) a proper fluorescent product analogue had to be found. Generally, this technique can be easily adapted with high-throughput screening instruments measuring in 96 or more-well plates.

1.2.2.4 cat-EIA (catalysis of competitive Enzyme Immunoassay)

A similar high-throughput screening method was developed by Wagner and Mioskowski[32] for the enantioselective reduction of α-keto acids by hydrogen transfer using chiral metal complexes. Using competitive enzyme immunoassays (EIA)[33] would allow quantification of both yields and enantiomeric excess (ee) of the reaction.

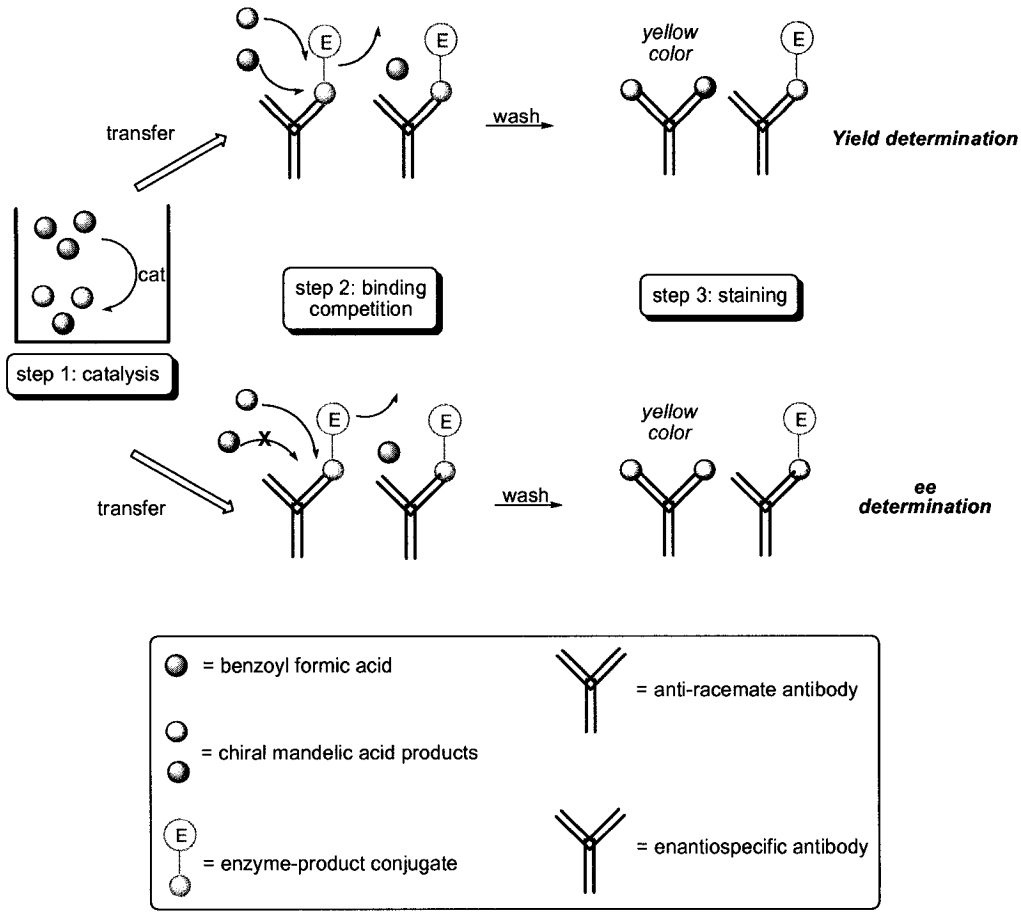

Figure 6: Depiction of the competitive immunoassay. (cat-EIA)

[32] Taran F.; Gauchet C.; Mohar B.; Meunier S.; Valleix A.; Renard P.Y.; Créminon C.; Grassi J.; Wagner A.; Mioskowski C. *Angew. Chem. Int. Ed.*, **2002**, *41*, 124.
[33] Taran F.; Renard P.Y.; Créminon C.; Valleix A.; Frobert Y.; Pradelles P.; Grassi J.; Mioskowski C. *Terahedron. Lett.*, **1999**, *20*, 1891.

After the reaction had occurred (step 1), two EIA runs were performed. One of the assays was the determination of the yield of the reaction. So, to the crude reaction mixture was added a specific anti-racemate antibody linked to a solid support which contained also an enzyme-product conjugate. Since this antibody was not stereoselective, the enzyme-product conjugate could be displaced by either of the enantiomers. Therefore, the yield of the reaction could be obtained by assessment of the decreasing absorbance which is related to the concentration of product in the reaction mixture. The absorbance decreased as more enzyme-product conjugate was released into solution. The difference between the absorbances was proportional to the concentration of product in the liquid phase. The other assay allowed the determination of the enantiomeric excess. This time, an enantiospecific antibody was used. Again, ee determination could be obtained by absorbance measurements. With this screening method, the enantioselective reduction of an α-ketoacid with chiral metal complexes was optimized. The hydrogen source, as well and the metal catalyst and ligands were varied. The calculated enantiomeric excesses were within 9% of the values obtained by HPLC. The choice of antibody required to have appropriate binding specificity in a way to be inert in the presence of the reactants. In the described experiment, monoclonal antibodies raised against hapten H3 were used but this type of antibody would not suit every application and must be optimized for every new reaction.

1.2.2.5 Indicator-Displacement Assay (IDA)

Recently, Anslyn[34] reported a new high-throughput indicator-displacement assay (IDA) He exploited the binding of boronic acids to α-hydroxyacids and catechols (**Scheme 6**).

[34] Zhu L.; Anslyn E.V. *J. Am. Chem. Soc.*, **2004**, *126*, 3676.

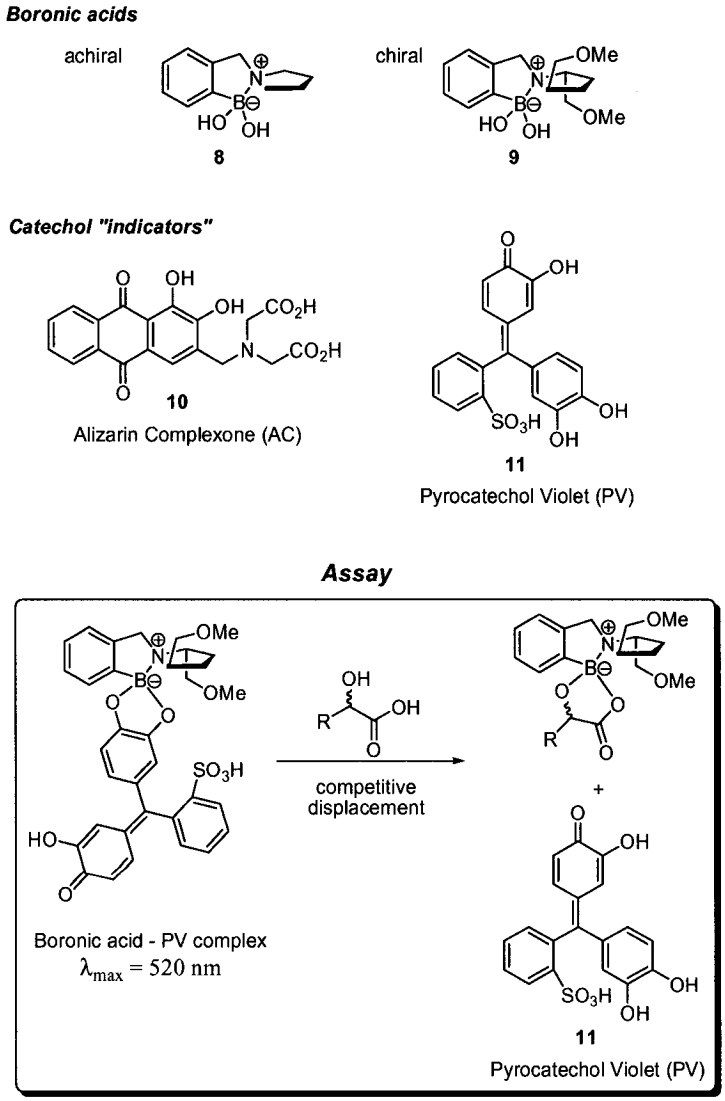

Scheme 6: Representation of IDA.

No selective binding of both enantiomers with the receptors was observed when achiral boronic acids were used. But, with a chiral boronic acid, D- and L-phenyllactic acids displaced the catechol indicators (AC and PV) enantioselectively. By monitoring of the absorbance the receptor-indicator complex at 520 nm for PV or 536 nm for AC, the selectivity could be measured. It was observed that the different displacements by D/L-phenyllactic acid, at a given concentration, resulted in distinct UV absorbances for pure

enantiomers. The difference in absorbance could be as large as 0.27. In solutions containing a mixture of the two enantiomers, the difference in absorbance could be correlated with the enantiomeric excess. Two independent measurements were necessary to obtain the concentration and ee of the products. First, an IDA was performed with an achiral receptor, a combination of PV and **8**, and the overall concentration of α-hydroxyacid could be calculated from the solution absorbance using the Lambert-Beer law. Then, a second IDA was done using a chiral receptor, PV and **9**. The enantiomeric excess could then be calculated, without generating an ee calibration curve. However, the accuracy of the overall concentration was within 10 % whereas the ee could be determined within 20 % error, which were not very precise.

1.2.2.6 Coupled Enzymatic Conversion

In 2001, a different strategy in the development of enzymatic high-throughput screening methods was developed by Bornscheuer[35]. The activity and enantiomeric selectivity of hydrolases (lipases and esterases) were measured using coupled enzymatic conversion (**Scheme 7**).

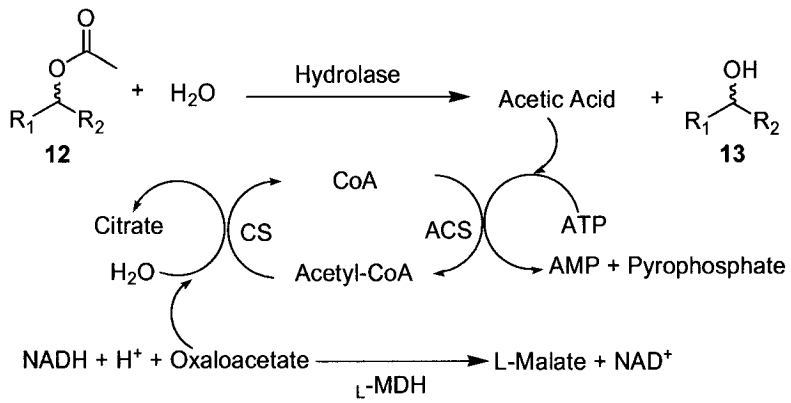

Scheme 7: Enzymatic reactions cascade monitoring acetic acid formation.

Acetic acid is released by lipase- or esterase-catalyzed hydrolysis from the corresponding chiral ester. Then, by a cascade of enzymatic reactions based on an available and cheap

[35] Baumann M.; Stürmer R.; Bornscheuer U.T. *Angew. Chem. Int. Ed.*, **2001**, *40*, 4201.

test-kit for food analysis. The rate of acetic acid formation is monitored by measuring the absorption at 340 nm caused by the increase in concentration of NADH. By performing this technique on a known enantioselective system, the enantiomeric ratio **E** for the enzymatic reaction could be determined. The ratio of their initial hydrolysis rates, obtained from absorbance measurements, was used to approximate the enantiomeric ratio of the enzyme, as in the method of Kazlauskas[28]. Comparison between the approximate enantiomeric ratios **E** calculated and the values measured by GC matched closely. The reading of a 96-well plate was done in 3 to 4 minutes, so up to 13,000 mutants could be screened every day. This technique can also be applied to other types of enzymes, such as proteases and amidases which also can produce acetic acid. Overall, the assay is rather cheap: less than a Canadian dollar per test-kit.

1.2.2.7 Enzymatic Method for Determining Enantiomeric Excess (EMDee)

An interesting enzymatic method was published by Seto[36] in the same year. In this one, enzyme is used to selectively process one enantiomer of a product from a catalytic reaction in which the direct relationship between the rate of the enzymatic reaction and the concentration of each enantiomer is provided by the Michaelis-Menten equation. The demonstration of the process was done with an addition of diethylzinc to benzaldehyde (**Scheme 8**).

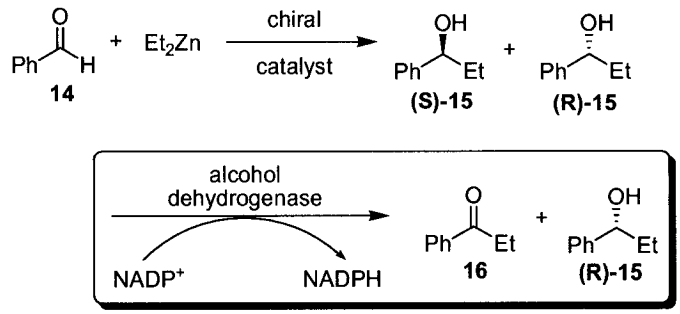

Scheme 8: Addition of diethylzinc to benzaldehyde.

[36] Abato P.; Seto C.T. *J. Am. Chem. Soc.*, **2001**, *123*, 9206.

The reaction gives a mixture of (R) and (S)-1-phenylpropanol **15** which once reacted with an alcohol dehydrogenase, oxidized selectively one of the enantiomers. Various combinations of samples were carried out where their correlation between the observed rates and known enantiomeric excesses was excellent. The reaction rates were obtained by monitoring the produced NADPH using UV/Fluorescence plate reader at 340 nm. 100 samples were analyzed in 30 minutes with an accuracy of ±10% compared to chiral GC values. Also, numerous other alcohol dehydrogenases exist that would be suitable for this method. The main drawback of EMDee is that there is no distinguishment between catalyzed reactions that proceed with low stereoselectivity but high conversion, and high stereoselectivity but low conversion. A second set of assays was analyzed using *Lactobacillus kefir*, an (R)-aromatic alcohol dehydrogenase, to quantify the amount of (R)-**15** present. Thus, the extent conversion can be calculated from the known amounts of (R) and (S)-**15**. A second approach to solve the problem involves the quantification of the residual benzaldehyde and reducing it to benzyl alcohol with an alcohol dehydrogenase in the presence of NADH or NADPH. These extra steps make the method more complicated. In general, EMDee is therefore suitable for screening large libraries of catalysts that are both highly active and selective. Despite this fact, it would be problematic to use it in the case of asymmetric catalyst design.

All those enzyme and antibody-based methods described above are efficient for the specific system that they were designed for. However, their applications in organic chemistry are limited because of the few existing types of reaction that could be screened. Moreover, extensive optimization was required in all cases.

1.2.3 Mass Spectrometry (MS)

Mass spectrometry is widely used, not only in everyday chemistry for characterization, but also in combinatorial chemistry. In the case of enantioselective reaction screening, mass spectroscopy, by itself, is useless because no chiral information is provided. Thus, the introduction of asymmetry must be done by forming diastereomeric complexes or adducts, thus adapting mass spectrometry to the determination of enantiomeric excess.

An example of a mass spectroscopic method in high-throughput screening was developed by Suizdak and Finn[37] using electrospray ionization mass spectrometry (ESI-MS), inspired by Horeau[38] for determination of the enantiomeric excess of alcohols and amines in a mixture.

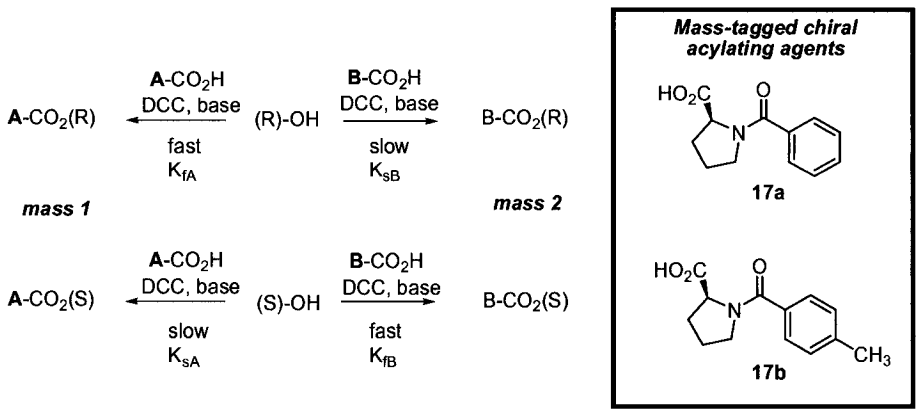

Scheme 9: Generalized reaction of chiral alcohols with mass-tagged chiral acids in the presence of DCC and base.

In the presence of DCC and a base, mixtures of chiral alcohols were reacted with chiral mass-tagged acids (**17a** and **17b**) (**Scheme 9**). The latter had different moieties that were not adjacent to the chiral centre, so that a correlation could be possible between the mass product and its configuration, thus making mass spectrometry useful to determine optical purity. Enantiomers differ in their reaction rates with chiral reagents, therefore kinetic resolution could be considered. Using the measured rates of esterification for each enantiomer (k) and the intensity of each peak (I), enantiomeric excess could be calculated from **Equation 6**. Precision and accuracy of this method were fairly good, with 1 to 3% standard deviation and 10% error.

[37] Guo J.; Wu J.; Siuzdak G.; Finn M.G. *Angew. Chem. Int. Ed.* **1999**, *38*, 1755.
[38] Horeau A.; Nouaille A. *Tetrahedron Lett.* **1990**, *31*, 2707.

$$\frac{I_{mass\ 1}}{I_{mass\ 2}} = y \bullet q$$

$$\%ee = \left[\frac{(y-1)(s+1)}{(y+1)(s-1)}\right] \bullet 100 \qquad \text{where} \begin{cases} s = \dfrac{k_{fast}}{k_{slow}} \\ y = \text{corrected intensity ratio} \end{cases} \qquad (6)$$

Reetz[39] has developed a similar strategy using slightly a different tactic. The principle was based on the use of isotopically labeled (deuterium) substrates in the form of pseudo-enantiomers or pseudo-prochiral compounds (**Scheme 10**).

a) Involving cleavage of the functional groups FG and labeled functional groups FG*.

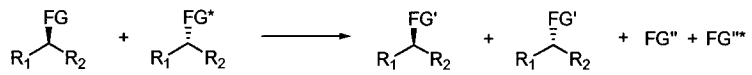

b) Involving either cleavage or bond formation at the functional group FG (isotopic labelling at R_2).

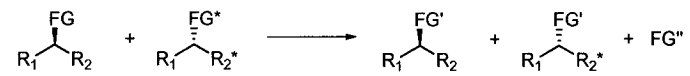

c) *Pseudo*-meso substrate: involving cleavage of the functional groups FG and labeled functional group FG*.

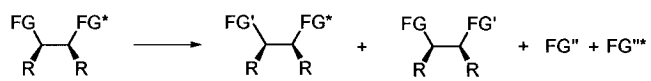

d) *Pseudo*-prochiral substrate: involving cleavage of the functional group FG and labeld functional group FG*.

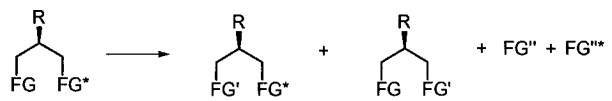

Scheme 10: Asymmetric transformation of a mixture of pseudo-enantiomers

All the mixtures underwent an asymmetric functional group (lipase-catalyzed) transformation and kinetic resolution. Detection of molecular mass difference was possible due to the fact that one of the products was deuterium labeled, while the other

[39] Reetz M.T.; Becker M.H.; Klein H.W.; Stöckigt D. *Angew. Chem. Int. Ed.* **1999**, *38*, 1758.

was not. Therefore, mass spectrometry could be used to identify these products, using electrospray ionization (ESI-MS) or matrix-assisted laser desorption/ionization (MALDI). The enantiomeric excess of the conversion was compared to GC analysis with a general agreement of ± 5%. In addition, this method could also be applied in monitoring the asymmetric transfer of prochiral substituants, but was not applicable to systems without enantiotopic faces. Also, the preparation of the labeled compounds was required as well as kinetic studies to identify the possibility of secondary isotopic effects. Application of this method to high-throughput screening was made by combining an automated liquid autosampler for microtiter plates with the ESI-MS system. A parallel eight-channel multiplexed ESI-MS system[40] considerably increased the speed of analysis. Using this equipment, analysis took approximately 9 seconds per sample. The additional equipment was expensive along with the cost of implementing this technology.

Mass spectrometry enabled the direct probing of the mixtures for identification. Similar to GC and HPLC methods, it is still considered as a low throughput technique despite its significant improvements in terms of rapidity.

1.2.4 Nuclear Magnetic Resonance (NMR)

The main advantages of NMR lie in its generality and the possibility of structure identification, where the previous discussed methods, except mass spectroscopy, do not allow this feature. In contrast to MS, the analysis conditions are very mild and the detection of compounds is made without destruction of the sample.

1.2.4.1 NMR spectroscopy in high-throughput screening of library compounds

In an example using ^{1}H NMR as a high-throughput characterization method to screen malonyl derivatives of penicillanic acids, Hamper[41] was able to design a technique for moderate-sized libraries. With the introduction of a flow-through probe interfaced with a sample injector and a flow cell, the automated analysis of a sample could run a sample in

[40] Schrader W.; Eipper A.; Pugh D.J.; Reetz M.T. *Can. J. Chem.* **2002**, *80*, 626.
[41] Hamper B.C.; Snyderman D.M.; Owen T.J.; Scates A.M.; Owsley D.C.; Kesselring A.S.; Chott R.C. *J. Comb. Chem.* **1999**, *1*, 140.

about 11 minutes, meaning that automated NMR instrument along with evaluation of the spectra would not significantly reduce the analysis time.

A drawback of NMR spectroscopy as a high-throughput method is the low sensitivity of ^{13}C NMR spectroscopy and the lack of reliable proton-based automated structure verification methods. In 2000, Schröder[42] reported a novel approach for the structure verification of a substituted 4-phenylbenzopyran library by using the experimental data from 2D ^{1}H-^{13}C-correlated (HSQC) NMR spectra, with automated pattern recognition[43]. Molecules from a library were viewed as combinations of different substructures that could be decomposed into a common central core. All those combinations were coded based on their structures and analyzed by 2D HSQC NMR as a sum of spectra of substructures. An internal reference integral from the central core spectrum, present in the library, was used to calculate a ratio of integrals of all the reference spectral patterns of each structural fragment (substructures). Then, those ratios were compared to the ratio of the NMR spectrum analyzed. This comparison allowed discrimination between correct and incorrect structures. Each sample could be analyzed in 10 minutes. The method developed by Schröder was used for qualitative purpose, but it would also be possible for quantitative analysis if the exact amount of compound was known.

1.2.4.2 NMR spectroscopy in high-throughput screening of enantioselective catalysis

Reetz[44] has taken a more rapid method for high-throughput NMR analysis and two similar methods were reported. ^{13}C-labeling was the first one, similar to that previously shown in mass spectroscopy (**1.2.3, Scheme 10**). A ^{13}C-labeled methyl group was used, whose proton signals would not split by $^{1}H,^{1}H$ coupling. Experimentally, the non-labeled enantiomer gave a singlet for that methyl group on the ^{1}H spectrum while the labeled enantiomer appeared as a doublet. This procedure was suitable for chiral alcohols and amines since acetylation can be performed with commercially available ^{13}C-labelled acetyl chloride and non-labeled acetyl chloride. To determine the catalyst activity along

[42] Schröder H., Neiding P., Rossé G., *Angew. Chem. Int. Ed.* **2000**, *39*, 3816.
[43] Schröder H., Neiding P., *Bruker Report,* **1999**, *147*, 18.
[44] Reetz M.T., Eipper A., Tielmann P., Mynott R., *Adv. Synth. Catal.* **2002**, *344*, 1008.

with enantiomeric excess, labeled and non-labeled enantiomer (pseudo-racemic) mixtures were prepared. Integration of the singlet and the doublet signals allowed the calculation of the selectivity factor E[35,45] (enantiomeric excess. Similarly, the conversion could also be measured by integrating the corresponding characteristic signal of the unreacted ester and the alcohol product. Compared to GC measurements, the values obtained were within 2%. By the automated method, 1 minute was required to analyze each sample. The same disadvantage of his mass spectrometric method[31] remained for reactions of prochiral compounds without enantiotopic faces.

To resolve the problems of these types of compounds, a second method was established. Using chiral reagents, such as Mosher's reagent, diastereomers could be prepared and differentiated by NMR. The enantiomeric excess would be calculated by integrating the desired peaks. In 1 minute, a sample could be analyzed and the resulting ee values were within 5% of GC data. Compared to the mass spectrometry method described previously, The NMR technique had demonstrated substantial precision over the rapidity of the MS method.

Generally, NMR screening provides precise structure identification but is still a low-throughput method along with expensive equipment requirements. Also, the flow-cells necessitate a large amount of product which goes against the goals of combinatorial synthesis. When organometallic reagents are screened, a pre-purification is required to avoid the presence of paramagnetic compounds.

1.2.5 Capillary Array Electrophoresis

For nearly two decades, enantiomeric purity has been determined by capillary electrophoresis (CE) with chiral stationary phases[46]. An important field of application of CE is DNA analysis and sequencing. Particularly for the human-genome project, many

[45] Chen C.S.; Fujimoto Y.; Girdaukus G.; Sih C.J. *J. Am. Chem. Soc.* **1982**, *104*, 7294; Kagan H.B.; Fiaud J.C. *Top. Stereochem* **1988**, *18*, 249.
[46] Gassman E.; Kuo J.E.; Zare R.N. *Science* **1985**, *230*, 813-814.

techniques have emerged to increase throughput considerably, among them, capillary array electrophoresis (CAE) in which a high number of capillaries operate in a parallel manner. High efficiency in DNA sequencing gave hope for the potential use of this method in the high-throughput screening of organic reactions.

Yeung[47] demonstrated the first example of HTS with CAE for measurements of organic reaction yields with a homebuilt prototype combining a commercial 96-capillary system with a UV detector. The model reaction studied with this method is a new palladium-catalyzed annulation reaction (**Scheme 11**).

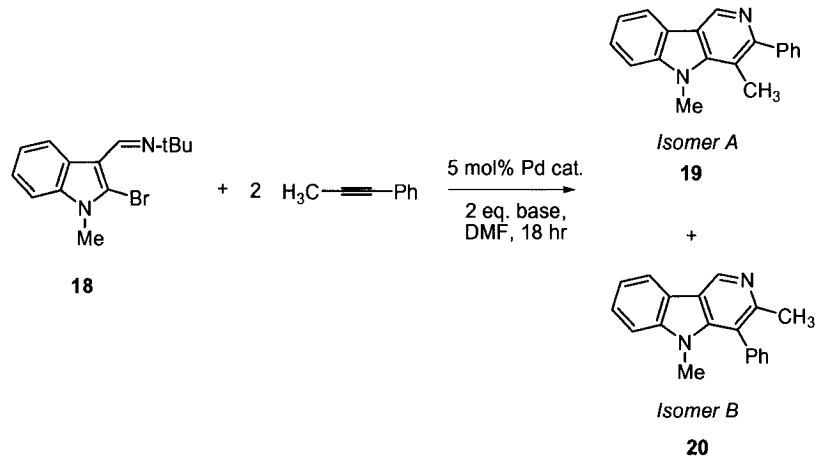

Scheme 11: Formation of a γ-carboline via a Pd-catalyzed annulation.

The analyses were carried out in organic-based buffers which were more adequate for organic synthesis, in contrast to aqueous media where the low solubility of the products could pose problems. At the same time, this meant that the sample could be directly injected without any purification, dilution or quenching before analysis. The reaction block containing the crude mixtures was put directly under the injection ends of the capillary array, in a way to avoid errors from transfers while pipetting. Different palladium catalysts were tested. The reading of the 96-capillary instrument took 90 minutes, including 30 minutes of capillary cleaning, which translates to almost one minute per sample. However, it was discovered that the length of the capillaries could be

[47] Zhang Y.; Gong X.; Zhang H.; Larock R.C.; Yeung E.S. *J. Comb. Chem.*, **2000**, *2*, 450.

shorted by 75% while still affording good resolution and at the same time, reducing the analysis to 15 minutes, plus cleaning time.

Soon after this published work, Reetz[48] reported a different way to screen enantioselective catalysts with CAE. His adaptation was based on the use of chirally modified electrolytes in the ee determination of chiral amines. By using commercially available cyclodextrins as chiral selectors, the measure of the enantiomeric excess would be possible. These selectors interact with the enantiomers to form reversible diastereomeric complexes that have different electrophoretic mobilities, thus allowing an enantiodifferentiation.

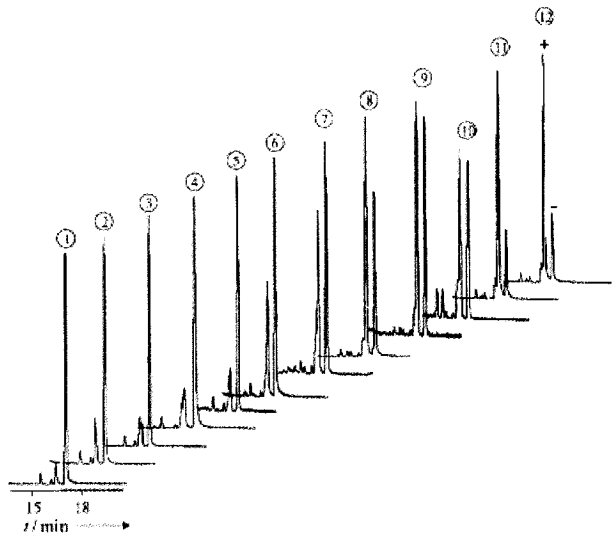

Figure 7: Example of a CAE separation of different (+)/(-) mixtures. (chiral amines + FTIC and cyclodextrin chiral selector)

Capillary array electrophoresis did not behave like single-capillary systems and several parameters had to be optimized in order to obtain reproducible results. For example, the column coatings, the electrolytes, the voltage and the pHs are all parameters that need optimization in a way to obtain comparable results with those from the GC analysis. A typical run took 19 minutes per plate, therefore more than 7000 ee determinations per day. Products were detected after separation by laser induced fluorescence (LIF).

[48] Reetz M.T.; Kühling J.M.; Deege A.; Hinrichs H.; Belder D. *Angew. Chem. Intl Ed.*, **2000**, *39*, 3891.

Therefore, a fluorescent tag (such as fluorescein isothiocyanate, FITC) had to be attached to the substrate to permit detection, necessitating an additional processing step.

The advantage of capillary array electrophoresis was the fact that it required a very small amount of product, barely any solvent and no high pressure pumps or valves. The columns were quite durable and the chiral phases were cheap to produce. Unfortunately, the instrumentation was expensive and very bulky. The extensive optimization required for the analysis represented the main disadvantage. Chiral separation by capillary electrophoresis has been well reviewed by Rizzi[49], which covers its optimization process, without elaborating on the application of high throughput screening.

1.2.6 Infrared Spectrometry

Sofia[50] reported the first example the use of automated infrared spectroscopy for screening using diffuse reflectance infrared Fourier transform spectroscopy (DRIFTS) for solid-phase reactions. This method was ideally suited to satisfy specific requirements for high-throughput applications which are no sample preparation, short analysis time and simple automation. By monitoring the reduction of resin-bound azido monsaccharides into the corresponding resin-bound amino monosccharides in the presence of trimethylphosphine, it was found that the sample did not need to be diluted in KBr, by the simple presence of the polystyrene-based resin. Hence, the time and material-consuming sample preparation step was eliminated. The progress of the reaction was qualitatively monitored by the disappearance of the characteristic signal (**Scheme 12**).

[49] Rizzi A. *Electrophoresis* , **2001**, *22*, 3079.
[50] Chan T.Y.; Sofia M.J. *Tetrahedron Lett.*, **1997**, *38*, 2821.

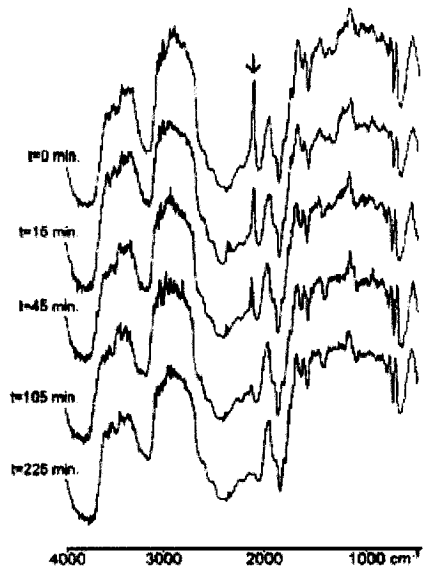

Scheme 12: Time resolved DRIFTS spectra of solid-phase reduction.

Each measurement took approximately 30 seconds. However, since spectra were evaluated manually, the actual analysis required longer and was not suited for large libraries.

Later, van Leeuwen[51] reported a novel technique for the rapid screening of enantioselective transfer-hydrogenation catalysts for the synthesis of chiral alcohols. In order to test their method, they used a known reaction: the reduction of acetophenone in propan-2-ol with a ruthenium(II) catalyst using (1R, 2S)-ephedrine **21** or (R)-phenylglycinol **22** as ligands (**Scheme 13**).

[51] Petra D.G.I; Reek J.N.H.; Kamer P.C.J.; Schoemaker H.E.; van Leeuwen P.W.N.M. *Chem. Commun.*, **2000**, 683-684.

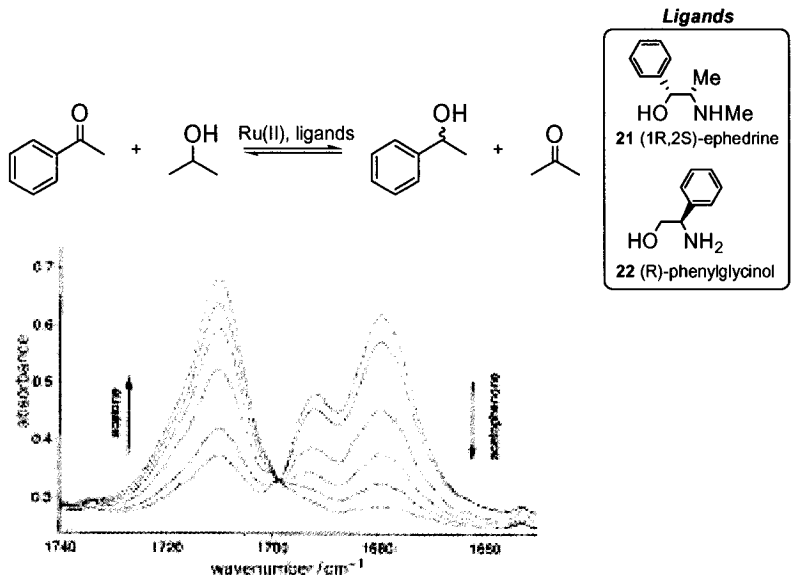

Scheme 13: The hydrogen transfer reaction followed by IR spectroscopy.

A single measurement was sufficient to calculate the enantiomeric excess of each mixture since a reference spectrum was subtracted from each sample spectrum. The resulting difference spectra gave flat lines for non-selective catalysts and large peaks for active or highly selective catalysts. Basically, this method can give a good estimation of the enantioselectivity and suggested that, with automation, near 100 IR spectra can be obtained per hour. In spite of this, the above method is problematic when signals of the starting material and the product are overlapping.

Shortly after this publication, a method for truly parallel screening using FTIR imaging was introduced by Caruthers and Lauterbach[52] The coupling of a focal plane array detector (FPA) and an FTIR spectrometer enabled the user to simultaneously obtain spectral and spatial information for multiple samples during a single experiment. The spectra were collected in 6 seconds and analyzed automatically by computer. Ultimately, the goal was to achieve automated development of a predictive pattern using chemistry

[52] Snively C.M.; Katzenberger S.; Oskarsdottir G.; Lauterbach J. *Opt. Lett.*, **1999**, *24*, 1841; Snively C.M; Oskarsdottir G.; Lauterbach J. *J. Comb. Chem.*, **2000**, *2*, 243; Lauterbach J.; Snively C.M.; Oskarsdottir G. *Angew. Chem. Int. Ed.*, **2001**, *40*, 3028; Caruthers J.M.; Lauterbach J.A.; Thomson K.T.; Venkatasubramanian V.; Snively C.M.; Bhan A.; Katare S.; Oskarsdottir G. *J. Catal.*, **2003**, *216*, 98.

models and experimental data. So far, this has not been fully realized because knowledge extraction required large amounts of high-quality data.

Reetz[53] elaborated a comparable method using an HTS-FTIR system (FTIR spectrometer connected to a HTS-XT system) and unlike the previous method, samples in standard 96, 384 or 1536 well microtiter plates in which each well could be read by the IR instrument. The spectra were then analyzed automatically according to a selected evaluation method, such as peak integration. This allowed direct calculation of the concentration of substrate using Beer-Lambert's law, once the molar coefficients of absorbance had been determined. This technology was adapted to the measurement of enantiomeric excess based on isotopic labeling leading to *pseudo*-enantiomers and *pseudo-meso*-compounds shown previously (**1.2.3, Scheme 10**). To illustrate the method, kinetic resolution of esters by catalytic action of lipases was considered (**Scheme 14**).

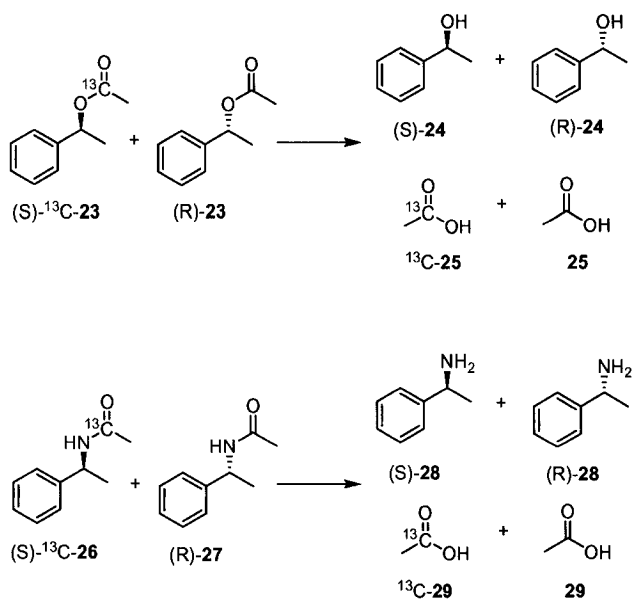

Scheme 14: Enzyme-catalyzed kinetic resolution of esters and amides by hydrolysis.

[53] Tielmann P.; Boese M.; Luft M.; Reetz M.T. *Chem. Eur. J.*, **2003**, *9*, 3882.

The carbonyl groups on the substrates were labeled with ^{13}C using commercially available reagents. The carbonyl functionality was chosen for labeling in part because it gives intense and characteristic vibrational bands in a region of the IR spectrum (1600-1800 cm^{-1}) where absorption from other functional groups is rare. The introduction of a ^{13}C-label shifts the carbonyl stretching vibration to lower frequencies by 40 to 50 wavenumbers. Mixtures containing various concentrations of the ^{13}C-labelled compound together with the non-labeled enantiomer were prepared and used as unknowns. The ee of these mixtures were measured on the FTIR set-up using a resolution of 8 cm^{-1} using 10 scans per sample. The values obtained corresponded, within 7 %, to the values obtained by GC. Each sample was analyzed in 8.9 seconds, meaning a range of 10,000 samples per day. One of the main advantages for this application is the fact that the samples do not need any workup and drying, unless there is interference with the solvent. On the other hand, a calibration curve must be compiled for every sample and the molar absorption coefficient ε has to be calculated for every enantiomer.

1.2.7 Infra-Red Thermography

Infra-red thermography screening methods are very interesting to researchers in terms of their rapidity and universality. Compared to other methods, the IR radiation measured comes from the desired compound itself or from its formation. Most chemical reactions proceed with a change in enthalpy which can be detected by a temperature increase or decrease. Therefore, assumption of change in heat detected relative to the product formation was made.

Morken[54] reported in 1998 a two-dimensional infrared thermography method that could measure the rates of an array of reactions. The temperature change in a catalytic reaction is proportional to the product of the turnover frequency and the enthalpy of reaction. If catalysts in a library are analyzed under the same reaction conditions, the most active catalysts will cause the largest temperature change. In this analysis, an IR camera was used to monitor the heat evolved by the reactions. The catalysts were attached to beads

[54] Taylor S.J.; Morken J.P. *Science*, **1998**, *280*, 267.

and placed together in solution. During the reaction, the more active catalyst beads exhibited a ~1 °C temperature increase relative to the solvent, which was easily distinguished from the inactive beads with the IR camera. Those beads could then be picked out and decoded. This technique is very general and could be applied to the screening of most libraries, but the manual picking of active catalysts could posed a problem, at least for industrial applications.

Reetz[55] brought some modifications to this potential screening method by introducing the reactions in microtiter plates. His first experiment was done with the enantioselective acylation of 1-phenylethanol with vinyl acetate, which is known to occur selectively (99%) in favor of the (R)-ester **30** (**Figure 8**).

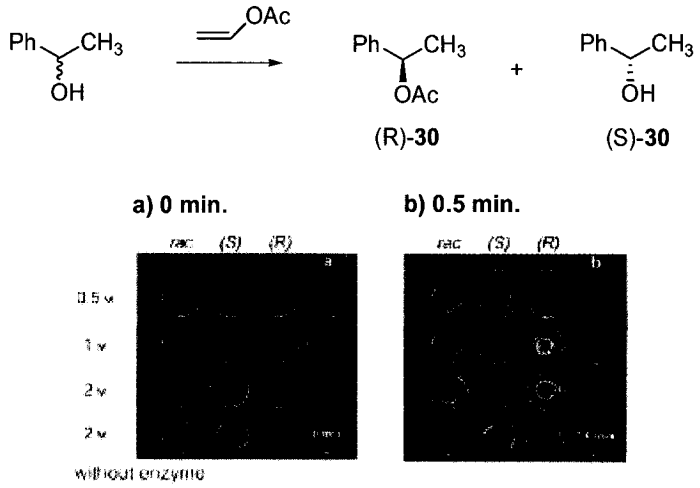

Figure 8: Time-resolved IR-thermographic imaging of lipase-catalyzed enantioselective synthesis of (R)-30 from a racemic mixture.

After the substrates were combined in each well, the plate was shaken for 5 seconds and detection was done for 5 seconds resulting in 250 recordings, from an IR camera, which were averaged to obtain **Figure 8a** and **8b**. The detection was carefully performed in the center of each well to avoid reflection from the top part of the vessel walls. Observing **Figure 8b**, it is clearly shown that (R)-**30** reacts preferentially by the appearance of red spots corresponding to a significant rise of temperature. Also, it was observed that (S)-**30**

[55] Reetz M.T.; Becker M.H.; Kühling K.M.; Holzwarth A. *Angew. Chem. Int. Ed.*, **1998**, *37*, 2647.

remained cool and that the racemic mixture lead to moderate rise of temperature. After the success of this experiment, the technique was then applied to an enantioselective transition metal catalysis of a ring-opening hydrolysis of epoxides using Jacobsen's salen catalysts (**Scheme 15**).

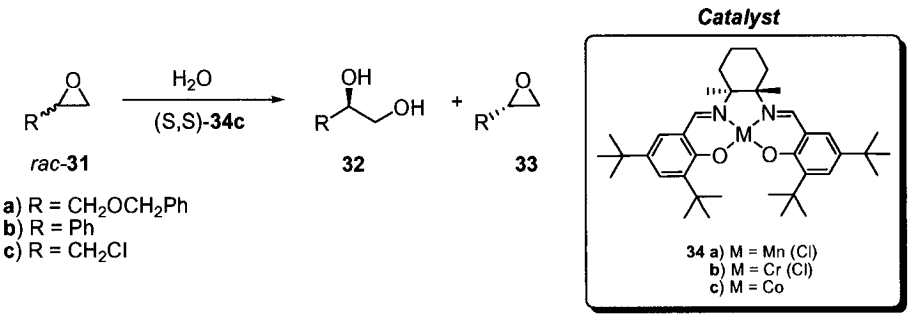

Scheme 15: Enantioselective epoxide opening.

It was found that (S,S)-**34c** was the most active catalyst and reacted selectively with (S)-**31c**. These observations corresponded to the results previously obtained by Jacobsen *et al.*[56] in laboratory-scale reactions. Overall, the IR-thermography screening in that case, demonstrated its feasibility on a qualitative basis. Further development, published in 2002, of the Reetz method was made by GlaxoSmithKline using the lipase-catalyzed acylation of the 1-phenylethanol system. They discovered that the enantiomeric excess was not only proportional to the initial rate of the reaction, but also to the area under the temperature curve[57].

The same methodology was later applied to a mildly endothermic reaction, olefin ring-closing metathesis, and proved to be just as reliable[58].

In IR thermography, several factors can cause problems while the image is recorded, even more when small differences of temperature have to be detected. If there are

---

[56] Larrow J.F.; Schaus S.E.; Jacobsen E.N. *J. Am. Chem. Soc.*, **1996**, *118*, 7420; Schaus S.E.; Jacobsen E.N. *Tet. Lett.*, **1996**, *37*, 7937; Jacobsen E.N.; Kakiuchi F.; Konsler R.G.; Larrow J.F.; Tokunaga M. *Tet. Lett.*, **1997**, *38*, 773; Tokunaga M.; Larrow J.F.; Kakiuchi F.; Jacobsen E.N. *Science*, **1997**, *277*, 936.
[57] Millot N.; Borman P.; Anson M.S.; Campbell I.B.; MacDonald S.J.F.; Mahmoudian M. *Org. Prod. R&D*, **2002**, *6*, 463.
[58] Reetz M.T.; Becker F.H.; Liebl M.; Fürstner A. *Angew. Chem. Int. Ed.*, **2000**, *39*, 1236.

secondary emissions or reflected radiations, the image may be disturbed and provide false information. To avoid these issues, Maier[59] recommended the use of a PtSi-based camera, instead of the usual focal plane array IR cameras (FPA). A linear correction was applied to the detector response and a reference spectrum was subtracted from all spectra in order to get the temperature differences caused by the catalytic activity. After this adjustment, IR thermography proved to be a powerful technique for the high-throughput screening of heterogeneous catalysts.

In 2001, Blackmond[60] reported a scale-transparent adaptation of infrared thermography. To avoid internal reflection and other undesirable interferences, the bottoms of the microtiter plates were replaced with IR-transparent materials. The radiations could therefore be detected directly from the well, not by reflection above the solutions.

This new feature was later used by Klein[61]. Since IR thermography is a very rapid technique that gave indirect information about reactivity, it was coupled to a slower but more precise analytical instrument, like MS, equipped with a positionable sampling capillary. The more active catalysts were detected by IR camera then picked up by a sampling capillary directed by a robotic system, and injected in a mass spectrometer. Therefore, only the most active and useful mixtures were thoroughly analyzed, providing both speed and quality.

Unfortunately, IR thermography had disadvantages. It suffers of relatively low resolution of temperature change (10 mK), required IR-transparent materials for visualization and inconvenient data analysis techniques (IR camera). To remedy to these drawbacks, Sutherland proposed an alternative such as the use of a multiplexed array of thermistors (**Figure 9**) to monitor reaction temperature in catalytic reactions[62].

---

[59] Holzwarth A.; Schmidt H.W.; Maier W.F. *Angew. Chem. Int. Ed.*, **1998**, *37*, 2644.
[60] Le Bars J.; Häußner T.; Lang J.; Pfaltz A.; Blackmond D.G. *Adv. Synth. Catal.*, **2001**, *343*, 207.
[61] Klein J.; Stichert W.; Strehlau W.; Brenner A.; Demuth D.; Schunk S.A.; Hibst H.; Storck S. *Catal. Today*, **2003**, *81*, 329.
[62] Connolly A.R.; Sutherland J.D. *Angew. Chem. Int. Ed.*, **2000**, *39*, 4268.

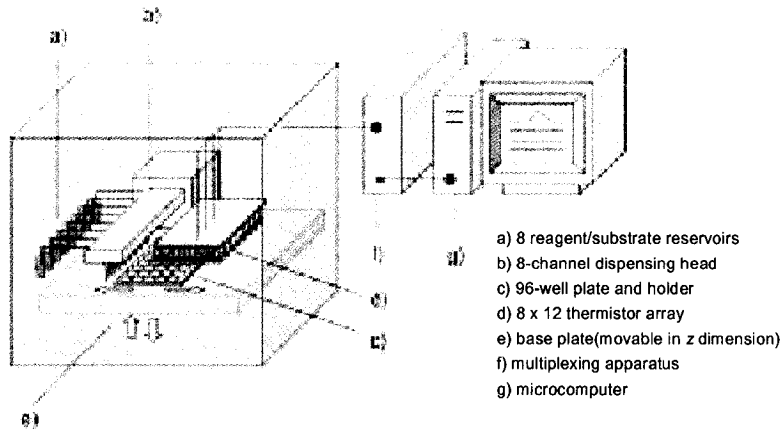

Figure 9: Thermistor apparatus.

The samples were placed in 96-well plates and their temperature was monitored for 10 seconds as a reference. The catalysts were then added and the plates were put in an incubator and shaken to mix the reagents. Mechanical rising of the plate permitted the immersion of the thermistors in the centre of each well. Temperature changes were monitored by the thermistors as resistance changes. When the reference was subtracted from the measurements, the more active catalysts could easily be detected visually. All the data were recorded in a numerical file and displayed on-screen during the reaction. To demonstrate the use of the thermistor arrays, the β-lactamase-catalyzed hydrolysis of penicillin G to penicilloate, known to be moderately exothermic, was studied. The wells were charged with a solution of β-lactamase in phosphate buffer. The plate was allowed to equilibrate at 37 °C before the addition of penicillin and mixing. Measurements of the maximum temperature attained in each well made quantification possible relative to the amount of enzyme. Another reaction was made with a β-lactamase inhibitor, potassium clavulanate. In this case, inhibition could be also observed by decrease of the maximum temperature as the amount of inhibitor increased. Thermistor arrays were an attractive alternative to IR thermography, because of its superior sensitivity (100 μK changes). However, in terms of rates and catalysts efficiency, the article did not cover these topics. Therefore, the thermistor arrays remained an uncertain alternative to screen for catalyst activity.

Unfortunately, IR thermography cannot indicate if the desired product is being formed, so it requires a coupled method, like MS, but it is a very rapid and efficient method for the approximation of catalytic activity for a particular target. IR thermography may not be the best option for catalyst discovery because the heat changes could result from side-reactions or unexpected reactivity. Therefore, it would be most likely useful in the high-throughput optimization of industrial processes rather than the screening of large, diversified catalyst libraries[60].

1.2.8 Thin-Layer Chromatography

Thin-layer chromatography (TLC) is omnipresent in organic chemistry, mostly because of its wide range of application. It can separate and compare a great number of compounds rapidly and efficiently. The high-throughput version of TLC offers the same advantages. Detection can be performed visually, with a UV lamp or even by mass spectroscopy, allowing its use for numerous choices of substrates.

In 1996, Reymond[63] described the first application in biocatalysis of TLC in high-throughput screening. He used acridone-tagged reagents for different enzyme-catalyzed reactions in 96-well microtiter plates. With an automated multichannel pipetter, small samples of the crude mixtures were applied on the TLC plate and dried under vacuum for 10 minutes. Pre-concentration is necessary before carrying out the elution, if a standard glass TLC plate was used. This was done by eluting the samples for 2.5 cm in polar solvents and drying again. This extra step can be avoided if HP-TLC plates with pre-concentration zone were used. The acridone moiety fluoresces under UV radiation (254 nm), so reagents and products could easily be detected on the TLC plate. All the substrates were identified visually by their retention factor (Rf). This method shows overall reliability, sensitivity and versatility, but did not show applications in enantioselective reactions.

[63] Reymond J.L.; Koch T.; Schröer J.; Tierney E. *Proc. Natl Acad. Sci. USA*, **1996**, *93*, 4251.

In 2003, Lavastre[64] demonstrated the versatility and the importance of TLC screening in cases where several elements were varied in an analysis. Different combinations of metal-containing reagents and ligands, both with and without metal salts and $N_2CHSiMe_3$, were tested as ring-closing metathesis catalysts (**Scheme 16**).

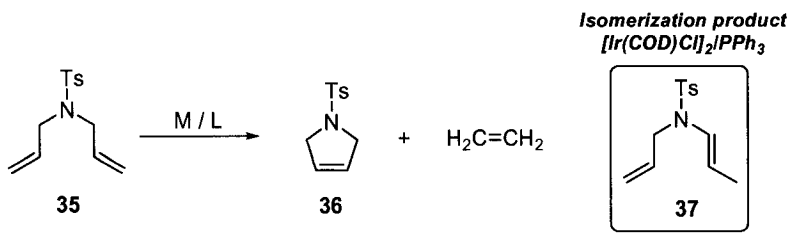

Scheme 16: Ring-closing metathesis of a diolefinic derivatives.

Once the reactions were completed, different colors were displayed in each well, Neither colorimetric nor UV-VIS spectroscopy would have been able to analyze these. A 1 μL aliquot of each well was taken by a 12-channel pipette and transferred to a TLC plate. After elution, the plates were analyzed visually and the products identified by their R_f. An interesting spot was discovered with $[Ir(COD)Cl]_2/PPh_3$ which was later identified as **37**, the product of isomerization of one of the double bonds on **35**. This would not have been noticed with most screening methods.

Particular contributions to TLC-based high-throughput screening were made by Salo[65] and Lavastre[66]. Salo first reported the use of various surface sampling probes coupled to mass-spectrometers for the quantitative analysis of TLC spots, but MS is a rather slow method and is very equipment intensive. On the other hand, Lavastre described a more cost-effective and convenient approach. Image analysis software was introduced to analyze the spots, which is commonly used in life sciences. This combination represented a potential alternative for quick qualitative and inexpensive separation of compounds, and quantification of corresponding spots. Images of the TLC plates were taken with an

[64] Lavastre O.; Touzani R.; Garbacia S. *Adv. Synth. Catal.*, **2003**, *345*, 974.
[65] Salo P.K.; Pertovaara A.M.; Salo V.-M.; Salomies H.E.M.; Kostiainen R.K. *J. Comb. Chem.*, **2003**, *5*, 223.
[66] Garbacia S.; Touzani R.; Lavastre O. *J. Comb. Chem.*, **2004**, *6*, 297.

office scanner or digital camera, and the image analysis software converted the 2D image into a 3D volume by integrating the area and intensity of the spots related to the amount of compound. Catalysts for the Sonogashira coupling reaction were screened to test the procedure (**Scheme 17**).

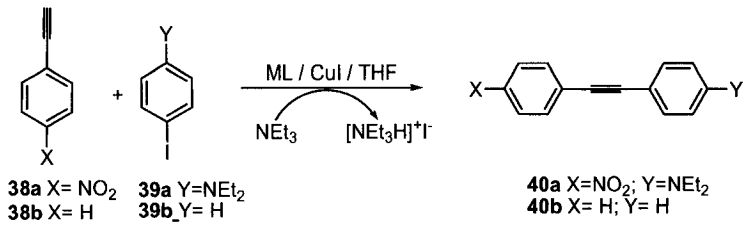

Scheme 17: Sonogashira Carbon-Carbon coupling reaction.

The reactions were carried out in 96-well microtiter plates then aliquots were taken with a 12-channel pipette and spotted on TLC plates. After elution, product **40a** was orange on the plate and therefore could be analyzed without a UV lamp or chemical staining. Calibration curves were established for **40a** in which correlation of the concentration versus the volume of each spot was performed. The colorless starting materials, **38a** and **39a** were not interfering with the image analysis. Colorimetric assay with a UV microplate reader could have been an option in that case, but the presence of a red side product in several vials eliminated this idea. The palladium catalysts were the most active, as expected. But also, this test revealed an unexpected activity for a ruthenium-based catalyst for the Sonogashira coupling, clearly illustrating the impact of combinatorial approaches by the fact that no reliable theory would have been able to predict this result.

In addition, detection and quantitative evaluation of colorless compounds, such as **38b**, **39b** and **40b**, can also be investigated using TLC-imaging analysis. After elution, images of the TLC plates under UV irradiation at 256 nm were taken and used for image analysis. The accuracy and reproducibility of these measurements were also very good, with less than 10% deviation from the calibration curve.

Thin-layer chromatography was a very promising method, especially for the high-throughput screening of organometallic compounds where these must undergo purification before analysis by GC, HPLC (in case of solid precipitation) and NMR (to remove paramagnetic compounds). But with TLC analysis, no pre-purification steps were required. The highlight of this method was its very broad application spectrum.

1.2.9 Colorimetric Assay

The use of dyes and other colored products have been reported in several methods for screening. Most of these assays require visual identification and even manual collecting of the most active compounds. Therefore, few techniques have been developed to improve their applications in high-throughput screening.

Resins have been extensively used in combinatorial syntheses and their importance in those processes encouraged their use in solid-phase enantioselective screening methods. Such a technique had been developed by Still and published in 1998[67]. His paper described a new approach to parallel synthesis and library screening of potential chiral selectors on polystyrene synthesis beads using enantiomeric probes labeled with colored dyes. In this case, they sought many chiral selectors, which are different chiral amines, by resolving amino acid derivatives using a Blue-labeled (L)-proline and a Red-labeled (D)-proline (**Scheme 18**).

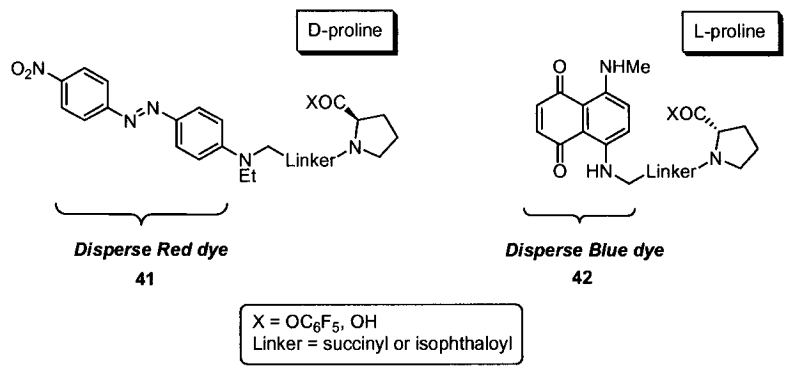

Scheme 18: Dye-labeled enantiomeric probes for the screening of chiral selectors.

[67] Weingarte M.D.; Sekanina K.; Still W.C. *J. Am. Chem. Soc.*, **1998**, *120*, 9112.

The chiral selectors could react or bind with the probes above either by acylating or salt formation, depending of the X substituent, but most of their work was focused on enantioselective acylation with the pentafluorophenyl ester of each probe. A 50:50 mixture of these substrates was treated with the various chiral sensors synthesized. After a predetermined amount of time, the reaction was stopped and the beads were washed with DMF. The recovered beads were either red or blue when the binding between the chiral selector and the probe was highly enantioselective. In the opposite case, the beads were brown if the binding was non-selective. All the beads showing selectivity were removed and screened under a low-power miscroscope.

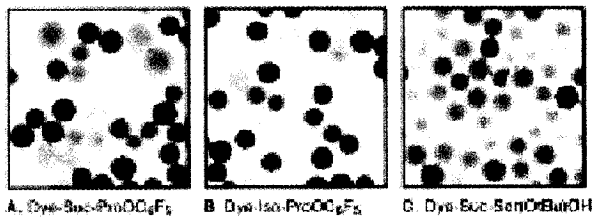

Figure 10: Chiral selector library beads screened for enantioselective binding by treatment with differentially labeled enantiomeric amino acid derivatives.

Analysis of the microscopic image of selected beads with a colour CCD camera provided the enantiomeric excess, with an accuracy of ±5%. The method has not yet been applied to a very large library, but its potency still to be studied and elaborate for larger libraries. The particular binding chemistry (irreversible acylation) used is obviously not ideal for practical resolution because the resolving resin is not recyclable, but reversible system can be developed.

Extended elaboration of the colorimetric assay using dyes has also been developed by Crabtree[68]. Reactive dyes composed of a donor (**D**) and an acceptor (**A**) group linked by a C=C or C=N functionality (**Scheme 19**) could undergo a color change (bleaching) if the electronic connection between the **D** and **A** groups was no longer existant. The choice of the **D** (ferrocenyl) and **A** (pyridinium) groups was made in function that none of them

[68] Cooper A.C.; McAlexander L.H.; Lee D.H.; Torres M.T.; Crabtree R.H. *J. Am. Chem. Soc.*, **1998**, *120*, 9971.

bared other oxidizable functionalities that could compete with the reactive site affinity with the catalyst. The global reaction used to study the principle was hydrosilation of alkene and amine where the saturation of the C=C or C=N bonds prevents the electron movement between the donor and the acceptor.

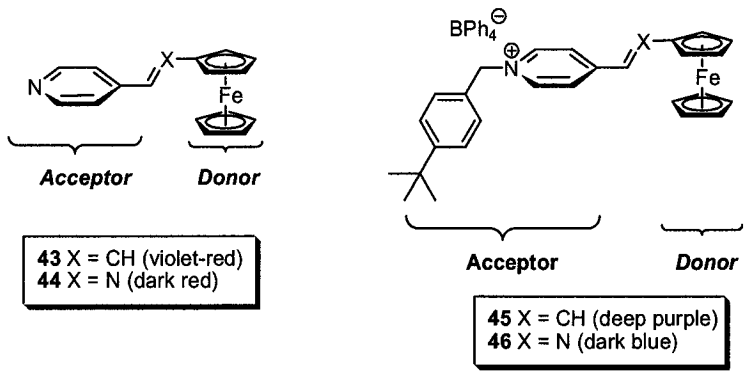

Scheme 19: Reactive dyes for the screening of catalyst activity in hydrosilation.

Upon reaction, the bright colors of the reactive dyes turned yellow. The rate of bleaching was recorded manually and images were taken by digital camera. An initial and final recording was done, corresponding to the first sign of bleaching and full bleaching which corresponded to 40 % and 95 % conversion respectively since it was a visual assay. Using their methodology, the Crabtree group discovered that $[Pd(Ar_2PC_6H_4CH_2)OAc]_2$, a new palladacyclic Heck reaction catalyst, was quite efficient in promoting hydrosilation. The accuracy of the method was restricted to the fact that visual assessments were made. Even if this technique could be adequate for monitoring a small number of reactions, it cannot logically be used to screen large libraries of potential catalysts. Therefore, an automated detection method should make it a very promising technique.

Another dye-based colorimetric screening assay was reported by Morken and Lavastre[69] in 1999 for the optimization of allylic alkylation catalysts (**Scheme 20**). The reaction principle relies on the fact that colorless 1-naphtol will undergo electrophilic aromatic substitution with Fast Red diazonium salt **49** to give a bright orange azo product **50**.

[69] Lavastre O.; Morken J.P. *Angew. Chem. Intl. Ed.*, **1999**, *38*, 3163.

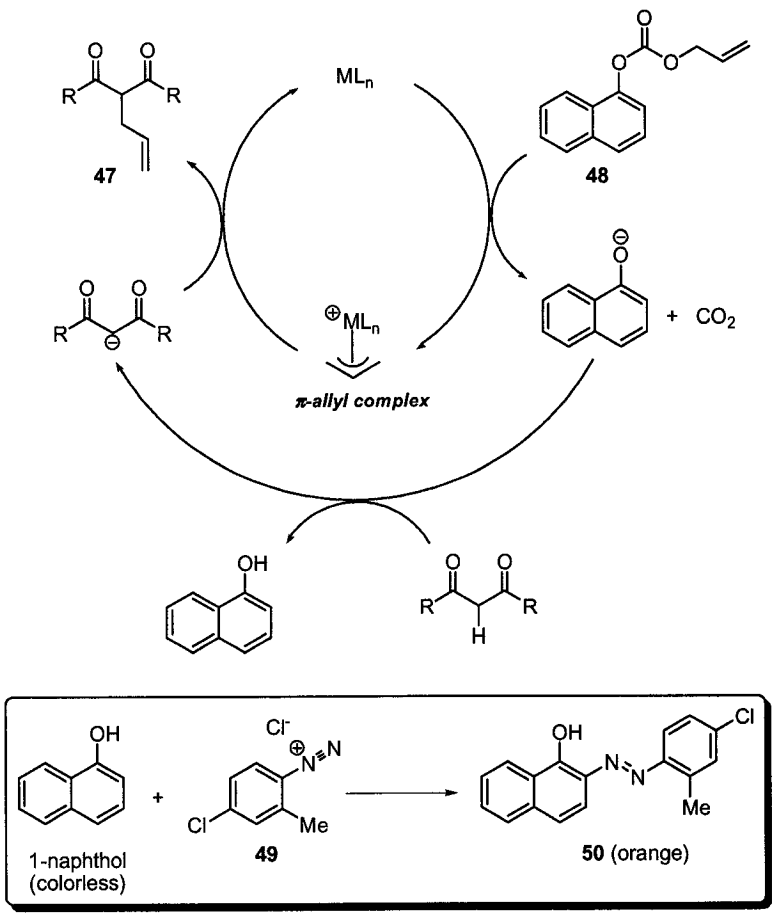

Scheme 20: Allylic alkylation using a catalyst ML$_n$ producing 1-naphtol monitored with Fast Red dye.

Studies of the reaction confirmed that the color formation on introduction of Fast Red dye is indicative only of the presence of 1-naphthol and therefore may be used as an indicator of the extent of allylic alkylation. Various metal salts and ligands were placed the 96 microtiter-well plates followed by addition of 1-naphthyl **48**. After 2 hours, Fast Red dye **49** was added to the solutions. Catalytic activity was assessed visually but to really differentiate catalysts with similar efficiency, parallel UV analysis may be used. With this screening, they discovered the first non-phosphane iridium catalyst for allylic alkylation. Generally, the technique is relatively simple and inexpensive, but so far, quite limited in applications.

In 2001, Hartwig reported two qualitative visual assays developed for the screening of transition metal catalysts promoting hydroamination. His first methodology aimed specifically at optimizing catalysts for the reaction of primary and secondary amines with acrylic acid derivatives[70] (**Scheme 21**).

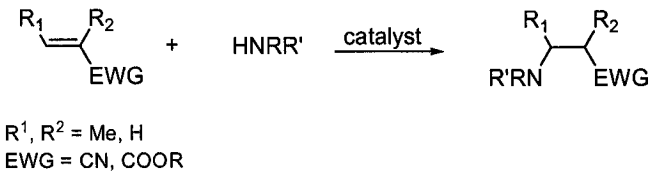

Scheme 21: General hydroamination reaction using catalysts.

Solutions of $[Na_2Fe(CN)_5NO{\bullet}2H_2O]$ and acetaldehyde became temporarily blue in the presence of secondary amines. The consumption of alkylamine reagents or formation of secondary amine products could therefore be followed visually with this indicator.

His second method was very similar but was designed for enantioselective hydroamination of aniline and dienes in the presence of a transition metal catalyst and TFA[71](**Scheme 22**).

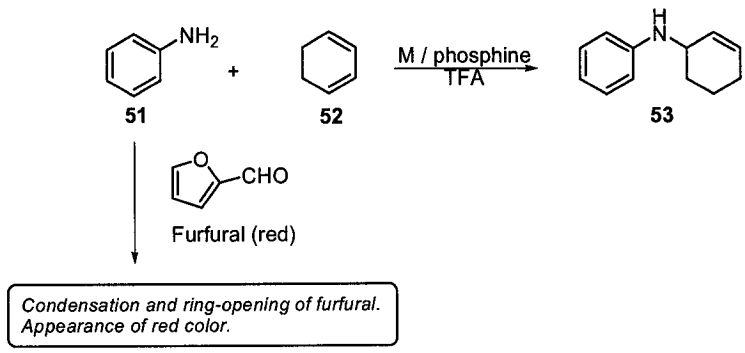

Scheme 22: Colorimetric monitoring of the presence of aniline in catalyzed hydroamination reaction.

[70] Kawatsura M.; Hartwig J.F. *Organometallics*, **2001**, *20*, 1960.
[71] Löber O.; Kawatsura M.; Hartwig J.F. *J. Am. Chem. Soc.*, **2001**, *123*, 4366.

In an acidic environment, furfural reacted with 2 equivalents of aniline to give a red product. Thus, the addition of furfural and acid to catalytic reactions will reveal the activity of each catalyst by evaluating the amount of aniline **51** consumed where the largest consumption will show absence of the red color.

Highly active and non-active catalysts could be sufficiently differentiated by these qualitative visual assays. So far, these methods have shown their applications on relatively small libraries, but they both could provide useful information about the optimal conditions for hydroaminations.

Colorimetric methods provided a rapid and reliable assay for very specific systems. Their range of applications in screening catalyst activity is so far limited to small libraries. The most important drawback would appeared when strong colored organometallic catalysts would be evaluated, since their interference would pose a challenge to distinguish chromophores.

1.2.10 Fluorescence

Fluorescence is one of the most versatile modes of detection. In addition, many methods use fluorescence because of its rapidity and efficiency. These assays have already proved their sensitivity and reliability. They have been applied mostly to DNA, enzyme and high-throughput screening. We have already discussed some of them in the Biological Methods section (**1.2.2**). In contrast, the screening of synthetic and organometallic catalysts will be the subject of the following section.

An example was reported in 2001, by Sames[72] for a high-throughput screening assay of new fluorogenic probes for atom transfer catalysis (oxygen, nitrogen, carbene, **Scheme 23**). The design is based on the change of fluorescent profile of these probes upon reaction which is a consequence of shortening or lengthening the extent of π-conjugation in terphenyl systems.

---

[72] Moreira R.; Havranek M.; Sames D. *J. Am. Chem. Soc.*, **2001**, *123*, 3927.

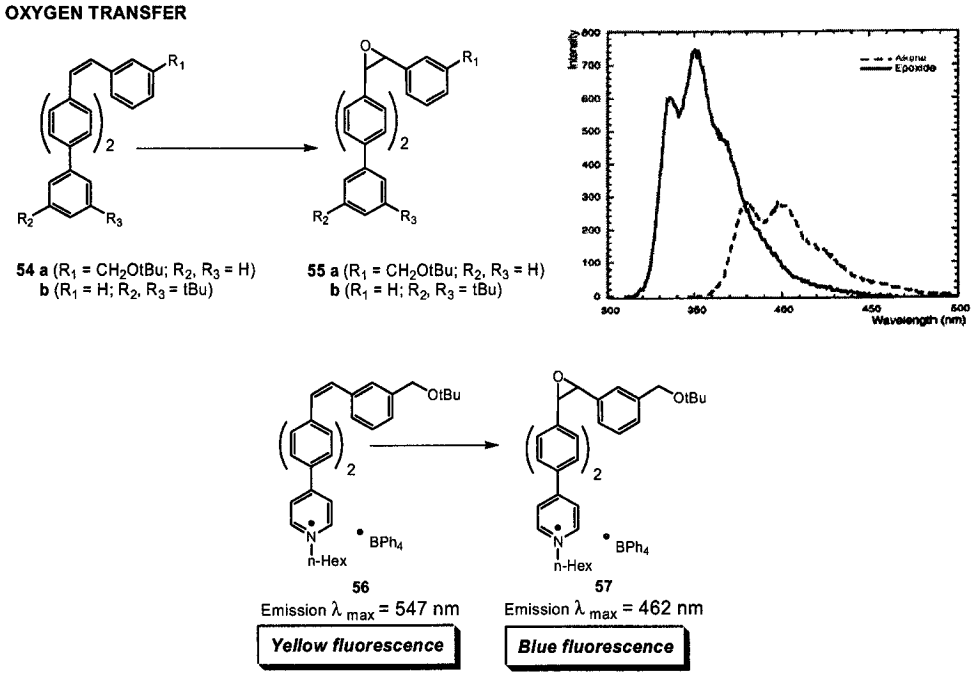

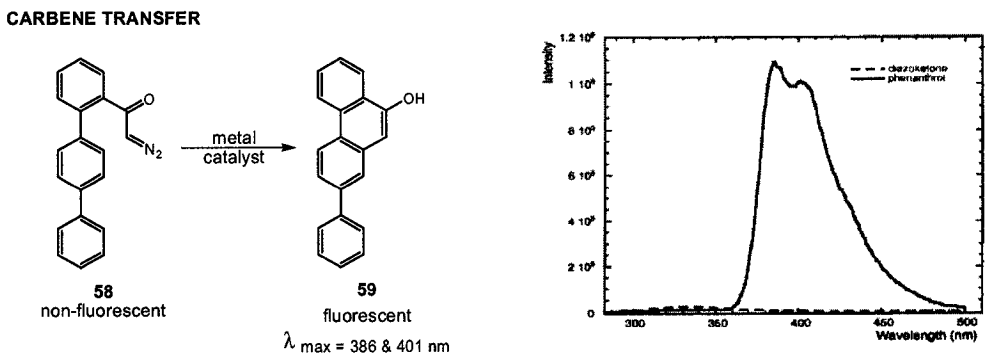

Scheme 23: Fluorescent probes for screening atom-transfer catalysis.

The readings of the experiment were done with a fluorescence plate reader. To study catalysts for epoxide formation, terphenyls **54a,b** and **56** were chosen. Other polycyclic arenes (e.g. pyrene, anthracene and phenanthracene) were degraded under these oxidative conditions and therefore were not suitable for the experiment. In the case of **54**, the reaction shortened the π-network, therefore resulting in a blue-shift in the emission maxima by 50 nm and an increase in the emission intensity by a factor of 2.5. In contrast, the use a pyridine moiety **56** increased the π-delocalization in the system, therefore, after

epoxide formation, displacing the emission maxima within the visible region. In general, the use of these probes provided detection for as low as 2-3 % conversion. In the case of carbene atom transfer, slightly different probes were designed. The terphenyl diazoketone **58** is a non-fluorescent probe which upon metal-catalyzed carbene insertion, is converted to the highly fluorescent phenanthrol **59**. This assay was very sensitive, detecting less than 1% conversion. Comparison of the measured yields using probe **58** corresponded within 5 % to those measured by NMR analysis. The probes were suitable to screen single beads supported catalysts. So, one bead was placed in each well of a 1536-microwell plate followed by addition of the probes and other reagents. The 1536-well plate could be scanned in 5 minutes, corresponding to 0.2 seconds per sample. The most time-consuming step was the manual distribution of beads on the plate but this could be automated.

In 1999, Hartwig reported one of the first fluorescence-based screening methods with applications in organic chemistry, for the optimization of coupling reactions[73]. To demonstrate this assay, the Heck coupling was chosen in order to develop ligands that could conduct the reaction with aryl chlorides and electron-rich bromides at low temperatures. The strategy includes one substrate (A) attached covalently to a fluorescent dye while the other substrate (B) would be linked to a solid support (**Scheme 24**).

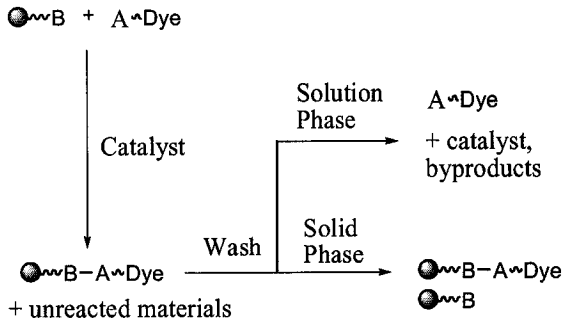

Scheme 24: Assay of solution and solid-phase coupling reaction.

The success of the coupling reaction was indicated by fluorescence on the solid support after washing and drying. Experimentally, the aryl halide reagent was attached to Wang

[73] Shaughnessy K.H.; Kim P.; Hartwig J.F. *J. Am. Chem. Soc.*, **1999**, *121*, 2123.

resin and acrylate was linked covalently to 4-methyl-7-hydroxycoumarin, a fluorescent tag (**Scheme 25**).

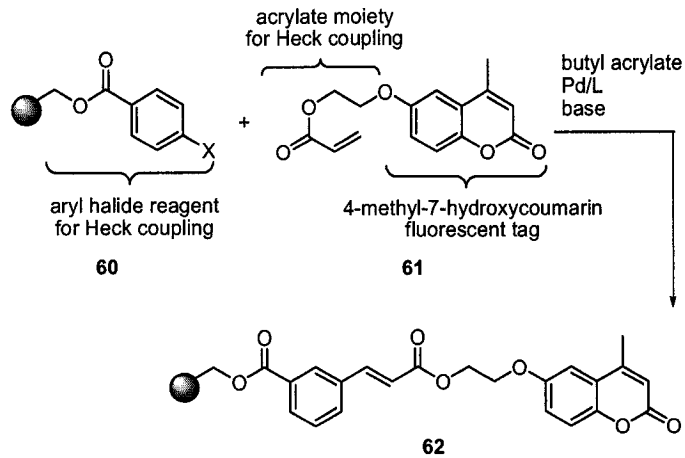

Scheme 25: Depiction of the Heck coupling reaction on solid support.

The reactions were carried out in vials placed in an aluminum heating block preheated to 100 °C. After workup and several solvent washes, the resins were dried and irradiated under a hand-held UV lamp. Pictures were recorded but the degree of fluorescence was evaluated visually. Because this method provides no information about selectivity, the ligands that appeared more reactive in the fluorescence screen were used in laboratory-scale experiments. This method was reliable and promoted the discovery of two ligands for the Heck coupling of aryl halides and aryl chlorides: di(tert-butylphosphino)ferrocene and tri(tert-butyl)-phosphine. It was also considerably faster than GC or HPLC analysis since each reaction mixture could be analyzed in 3 to 4.5 minutes but it was qualitative assay. The use of resins could also have been problematic with fluorescence detection since there was a risk of the resin altering the fluorescent properties of the dye.

In 1999, Miller[74] reported one of the most interesting and versatile screening methods for enantiomeric excess. During previous studies, the main highlight came from the observation that the most selective catalysts typically afforded the fastest reactions[75].

[74] Copeland G.T.; Miller S.J. *J. Am. Chem. Soc.*, **1999**, *121*, 4306.
[75] Miller S.J.; Copeland G.T.; Papaioannou N.; Horstmann T.E.; Ruel E.M., *J. Am. Chem. Soc.*, **1998**, *120*, 1629; Copeland G.T.; Jarvo E.R.; Miller S.J. *J. Org. Chem.*, **1998**, *63*, 6784.

Thus, this element became fundamental in the development of his screening assay in which the selectivity was expressed as k_{rel}, the ratio of reaction rates for the two enantiomers of a compound (k_{fast}/k_{slow}). Their studies were based on an enantioselective acyl transfer reaction, by peptide-based catalysts, which produced one equivalent of acetic acid per catalytic cycle. Thus, a direct method of detection for this product would provide an effective and accurate monitoring of the catalytic turnover. To detect production of acetic acid, a pH-sensitive fluorophore, aminomethylanthracene (AMA **63**, **Scheme 26**) was added to the solutions along with the reagents. AMA is well known to undergo photoinduced electron transfer process (PET), meaning that its free amine form is not fluorescent, but it become intensively fluorescent when protonated (**64**).

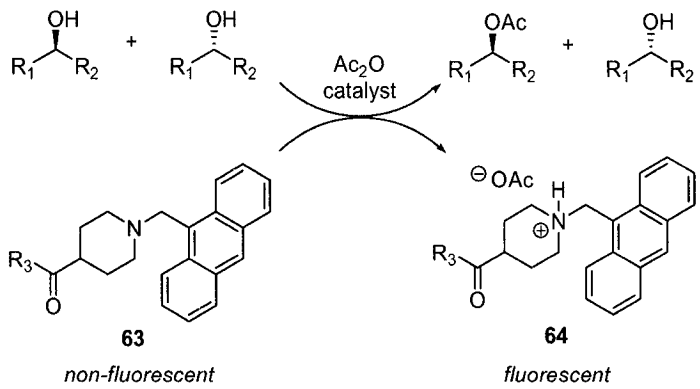

Scheme 26: Monitoring of enantioselective acyl transfer catalysts with a pH-sensitive fluorophore (AMA).

The emission intensity was then measured at regular intervals with a fluorescence plate reader and the resulting plot was interpreted as a direct readout of the evolution of acetic acid with time. Each catalyst was screened separately against both pure enantiomers of the starting material. The more selective catalyst was represented by a higher ratio of initial reaction rates, k_{fast}/k_{slow}, between enantiomers of a compound. The method could screen 1000 catalysts per hour. Unfortunately, pure enantiomers of the alcohols are necessary for the calculation of their indivual rate. This experiment was then adapted to identify highly effective catalysts during a simultaneous single-bead-single-catalyst

screening protocol[75,76]. The fluorescent sensor was covalently attached on solid support which was simultaneously functionalized with a potential peptide-based catalyst, as shown by **Figure 11**.

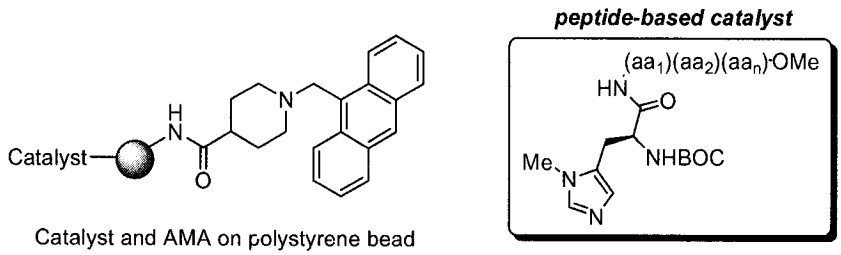

Figure 11: Solid support model used in the enantioselective acyl transfer catalysis.

The same reaction as previously described, was carried out with similar reliability. With this technique, Miller studied the use of small conformationally-constrained peptides as mimics of acylases. These oligopeptides, synthesized randomly by split-and-pool, were tested for the kinetic resolution of secondary[78] and tertiary[77] alcohols. After an initial screen, a new catalyst library was built to optimize the more selective candidates. The results obtained from single-bead assay and from the rescreening under optimized conditions were often quite different, but they were still a good approximation of selectivity. Several general and selective peptide catalysts were thus discovered for the kinetic resolution of alcohols.

Meanwhile, Miller elaborated his technique by introducing catalyst-functionalized beads placed in a polymer matrix allowing the diffusion of the substrates between the beads[78]. The fluorescent sensor is no longer bonded to the solid support, but incorporated in a gel. This feature would permit the speculation of the diffusion rate of reagents allowing efficient mass transport, such as real-time observation of the analyte migration would be possible. The reaction can be followed by the appearance of a fluorescent zone around the site of an active catalyst. The advantage of this method was the separation of the

[76] Copeland G.T.; Miller S.J. *J. Am. Chem. Soc.*, **2001**, *123*, 6496.
[77] Jarvo E.R.; Evans C.A.; Copeland G.T.; Miller S.J. *J. Org. Chem.*, **2001**, *66*, 5522.
[78] Harris R.F.; Nation A.J.; Copeland G.T.; Miller S.J. *J. Am. Chem. Soc.*, **2000**, *122*, 11270.

fluorescent sensor and the catalyst. This technique was not used as extensively as the previous one for catalyst screening.

So far, even if most of fluorescence applications are developed in biology and biochemistry, they are very promising, in organic chemistry, for the enantioselectivity and activity screening due to their excellent sensitivity and versatility. These methods, over the past few years, have been extensively used and considerably improved in rapidity, which, without a doubt, caught the attention of many recent experiments in the field.

1.2.11 Overall high throughput screening

Although innovative approaches, GC, HPLC, MS, NMR and CAE are still considered as low throughput methods that also required specific equipments. Despite their high quality to provide information about reaction mixtures, they demand more analysis time. Therefore, global approximations must be made in order to obtain results rapidly. Some may criticize the lack of accuracy in many of the more rapid techniques and defend the use of the more traditional instruments, which defeats the high-throughput screening purpose. However, these low-throughput techniques may be quite useful in secondary screening, after an initial more rapid evaluation of the library.

The most promising methods for high-throughput screening are probably IR thermography and fluorescence. IR thermography is quite rapid but does not give any indication as to whether the desired reaction is indeed occurring and it has not yet been adapted for enantioselectivity assays. Fluorescence methods, on the other hand, indicate clearly if the expected process is being monitored and can be used for enantioselective reactions.

There will most likely never be a general high-throughput screening methods for evaluating reactivity and stereoselectivity. But with so many techniques offered to the

chemists, it should be possible to screen most libraries very rapidly as considerably speed up the discovery and optimization of new reagents and catalysts.

The following chapters report our idea in the application of fluorescence in asymmetric reactions. Thus, we explore its use to design a screening method that could rapidly identify new catalysts and determine the enantioselectivity.

CHAPTER 2

Fluorescence Resonance Energy Transfer

Reviewing the different types of methods for the high-throughput screening of catalysts in enantioselective contexts suggested that fluorescence had great potential. Its advantages need to be exploited in a way to develop a more efficient and accurate method in this area. Recent applications in organic chemistry gave us the lead to further elaborate the concept. We decided to adapt the FRET method to the determination of enantioselectivity in a high throughput context.

Compared to other fluorescence methods described previously, in which chiral information could unfortunately not be determined precisely, another principle, called **F**luorescence **R**esonance **E**nergy **T**ransfer (FRET), would potentially be beneficial in providing this information.

2.1 Principle

Fluorescence is the emission of light caused by the electronic excitation and subsequent relaxation of a molecule. Upon absorption of light, a fluorophore is excited to some higher-energy electronic state. It can relax back to the ground state by several different processes (**Figure 12**).

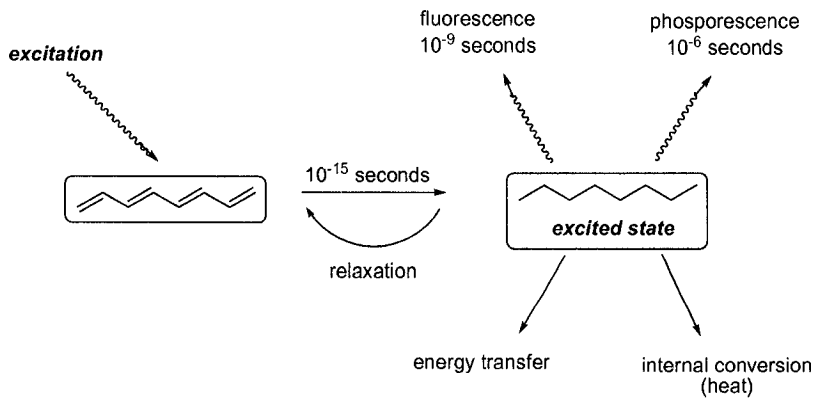

Figure 12: Different pathways of relaxation for photon excited state.

There are radiative processes, such as fast photon emission by fluorescence, or slower emissions by phosphorescence. Also, there are some non-radiative processes such as internal conversion of the energy into heat which is then released through rapid solvent relaxation. These processes are depicted in a model Jablonski diagram (**Figure 13**).

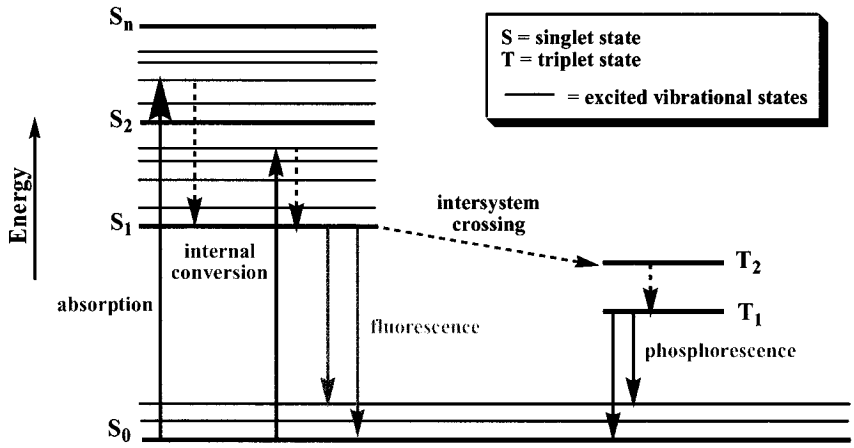

Figure 13: Jablonski Diagram.

As for the resonance energy transfer (FRET), it is the non-radiative transfer of energy between one fluorophore (the donor) to another (the acceptor). This transfer is due to a coupling of the donor and acceptor dipole moments, a mechanical analogy of which would be the resonance between two pendulums of similar length. FRET[1,2] is a distance-dependent excited state interaction that occurs when the emission band of one fluorophore overlaps the excitation band of an acceptor (**Figure 14**).

[1] Selvin P.R., *Nat. Struct. Biol.*, **2000**, *7*, 730.
[2] Knight C.G., *Method. Enzymol.*, **1995**, *248*, 18.

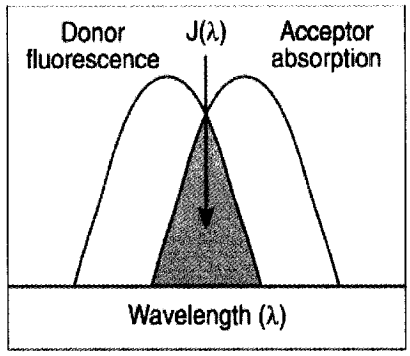

Figure 14: Emission band of a fluorophore overlaps the absorption band of an acceptor.

As long as the fluorophore (donor) and the acceptor are on the same molecule and within 10 to 100 Angstroms of each other, the characteristic emission of the donor is suppressed. The transfer of energy from a donor's excited state into an acceptor molecule, as mentioned, is the most important for the following studies. Measurements of energy transfer are often used in structural investigations in complex biological molecules, such as proteins. These measurements can provide intra- or intermolecular distance data for proteins and their ligands within 10 to 100 Angstroms. Generally, fluorescence is detected with a spectrofluorometer which resembles closely a UV-spectrophotometer, but differs in the orthogonal placement of the detector and excitation source.

Even if FRET quenching is necessarily an intramolecular principle, energy transfer will take place between isolated molecules in solution as long as the concentration of the components is high enough to bring the average intermolecular distance within 50-60 Angstroms. Overall, FRET efficiency is concentration dependent.

2.2 Donor and Acceptor Pairs

In most applications, the donor and the acceptor dyes are different, in which case FRET can be detected by the appearance of the acceptor's emission (fluorescent acceptor) or by quenching of donor fluorescence (non-fluorescent acceptor). The use of non-fluorescent acceptors has particular advantages in eliminating the potential problem of background

fluorescence resulting from direct excitation. The intensity of emission of each donor can vary from weak to very strong, depending of the extinction coefficients and does not affect the quenching with an acceptor, as long as the overlap between the emission and absorption bands is adequate. Different pairs used in biological samples have been listed in reviews, such as that by Wu and Brand[3].

With the principle in hand, it is now a matter of adapting the concept to enantioselective reactions either by forming or cleaving a bond between two substrates containing donor and acceptor moieties and studying the FRET response.

2.3 Background

Since the method of high throughput scanning in reaction development is fairly new, only a few studies using FRET have been published. Described herein is the recent work of two major contributors that have adopted FRET or related methodology for monitoring their reactions. These provide a solid foundation for the project at hand.

Hartwig, as previously mentioned, extended his work with fluorescence by taking a slightly different direction and conceived a general, rapid and quantitative screening assay using FRET in 2001[4]. Again, Heck reactions were studied. This assay was perfectly suited to screen this type of reaction. The cleavage of the molecules resulted in the reappearance of the donor emission and was very strong. A coupling reaction proceeded, a drop in fluorescence due to the proximity of the donor and acceptor groups was observed, which induced quenching. A dansyl fluorophore was tethered covalently to a styrenyl group (**65**) and an azodye quencher was tethered to an aryl bromide (**66**) (**Scheme 27**).

[3] Wu P.; Brand L., *Anal. Biochem.*, **1994**, *218*, 1.
[4] Stambuli J.P.; Stauffer S.R.; Shaughnessy K.H.; Hartwig J.F., *J. Am. Chem. Soc.* **2001**, *123*, 2677.

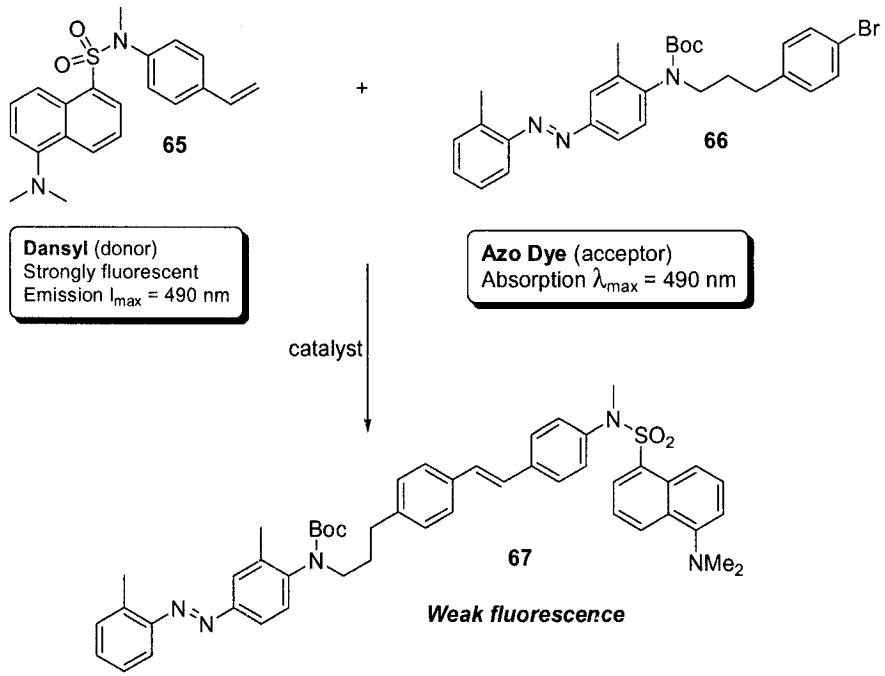

Scheme 27: Reagents for the FRET screening assay of Heck coupling catalysts.

The reactions were performed in an aluminum reaction block with a 96-well glass plate. After 15 hours at 70 °C, aliquots were taken, diluted and analyzed on a fluorescent plate reader. Each reaction could be analyzed in about 1 second, a significant improvement over the fluorescent bead method presented earlier. The emission intensity was converted to a reaction yield by using a linear plot correlating emission intensity to the mole fraction of coupled product. Yields determined by the FRET method differed at most by 10 % from the values obtained by HPLC. With this assay, two very active catalysts were discovered. At room temperature, 1-adamantyl-di-*tert*-butyl phosphine and $Ph_5FcP(t\text{-}Bu)_2$ with palladium complexes were found to catalyze the Heck coupling of aryl bromides. This method was also applied to other substrates for the Heck coupling, such as cyanoacetates[5] and amines[6].

FRET proved to be efficient and effective in this application. Reaction yields can be rapidly and accurately measured and it is far superior to the other methods, such as GC,

[5] Stauffer S.R.; Beare N.A.; Stambuli J.P.; Hartwig J.F., *J. Am. Chem. Soc.* **2001**, *123*, 4641.
[6] Stauffer S.R; Hartwig J.F., *J. Am. Chem. Soc.* **2003**, *125*, 6977.

HPLC, NMR, IR and colorimetric assays which cannot give any information about regio- and stereoselectivity. FRET is a perfect method for the discovery of highly active catalysts for coupling reactions, but unfortunately, still has disadvantages. In the case of chirality, FRET assays as demonstrated so far, are useless. In addition, the synthesis of the large fluorescent molecules can pose problems.

In the same year, Shair reported a very interesting method that is not directly related to FRET but should be considered for purposes of the present project. He adapted DNA microarray technology for the measurement of enantiomeric excess[7]. To evaluate the methodology, the composition of mixtures of α-amino acids was studied. As shown in **Scheme 28**, the N-Boc-protected amino acids were arrayed and covalently attached to an amino-functionalized glass slide by automated contact printing (**step 1**).

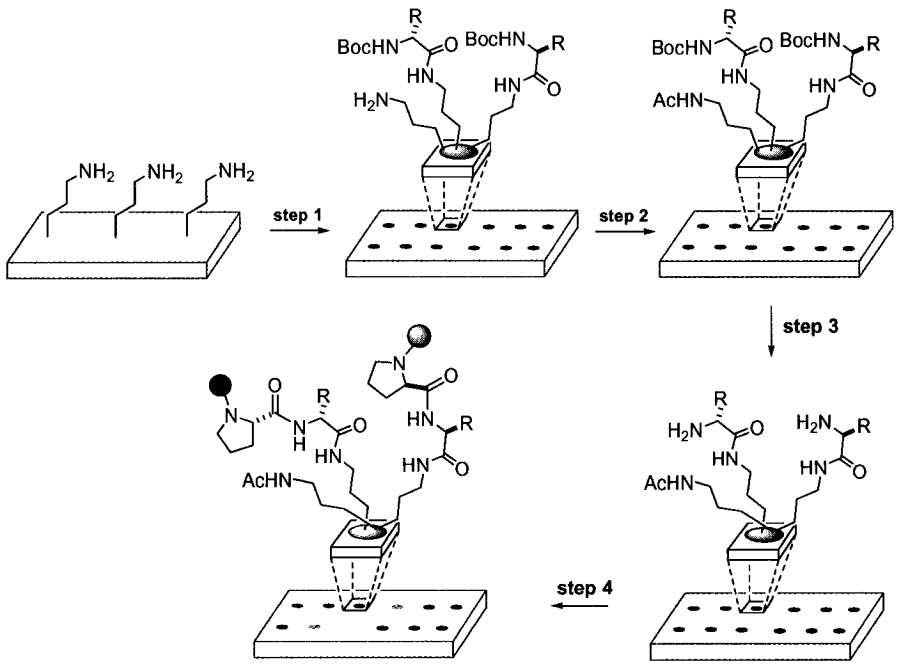

Scheme 28: DNA microarray technology adapted for the high throughput screening of enantiomeric excess.

[7] Korbel G.A.; Lalic G.; Shair M.D., *J. Am. Chem. Soc.* **2001**, *123*, 361.

Very small amounts of amino acid were required for each spot, less than 10^{-11} mole. The remaining uncoupled amine functionalities on the glass plate were then acetylated (**step 2**) and the amino acids were deprotected (**step 3**). The only free amines were therefore those of the amino acids. A 1:1 mixture of chiral fluorescent probes was then coupled with the free amines and, during the reaction, a parallel kinetic resolution occurred. The chiral fluorescent probes used were Cy3 and Cy5 fluorophores coupled to D- and L-proline respectively (**Figure 15**).

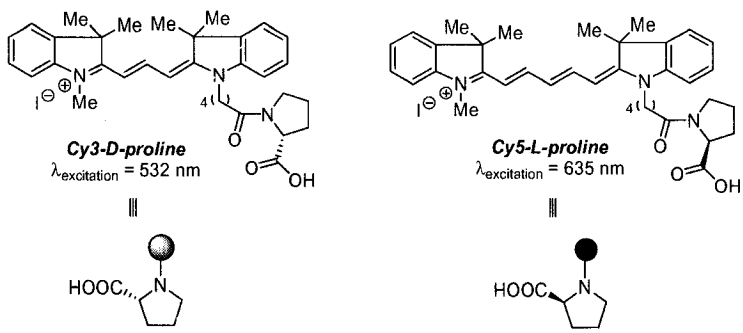

Figure 15: Pseudoenantiomeric fluorescent probes used in the microarray fluorescent assay.

Each of these fluorophores preferentially bound to one enantiomer of the α-amino acids and so, with kinetic resolution, the enantiomeric excess the original α-amino acid mixture could be expressed as a ratio of fluorescent intensities from pseudoenantiomeric fluorophores that emitted at different wavelengths. Irradiation with an automated laser scanner caused the excitation of Cy3 at 532 nm and Cy5 at 635 nm. The Cy3 fluorescence was seen as a green color, Cy5 as a red color and the equivalent mixture as yellow. The relation between enantiomeric excess and fluorescence intensity for each spot was expressed with equation (7).

$$\%\ ee = \left[\frac{(x-1)(s+1)}{(x+1)(s-1)}\right] \times 100\ \% \qquad (7)$$

$$x = \frac{I_{fluor,\ Cy5}}{I_{fluor,\ Cy3}} \times \frac{1}{z}$$

$$s = \frac{k_{fast}}{k_{slow}}$$

z = normalization factor

Many amino acids were tested with this method, up to 15 000 samples or more, depending on the diameter of the spots, could be tested on the same glass plate, requiring about 11 seconds per spots. The average measurements were within ±10 % of the real values. This method could be applied under various conditions. Unfortunately, any low gaseous reagents were not tolerated in this type of analysis.

In a manner to improve and extend the methodology, we propose a novel FRET assay which is designed to rapidly identify enantioselective catalysts.

2.4 Application of FRET in Amide Bond Formation

In an effort to test our methodology, our initial target reaction chosen was asymmetric amide bond formation. This reaction, well-known as a coupling reaction, is quite simple, but performing it on chiral substrates is often difficult. In general, three options are possible to carry out the reaction (**Scheme 29**).

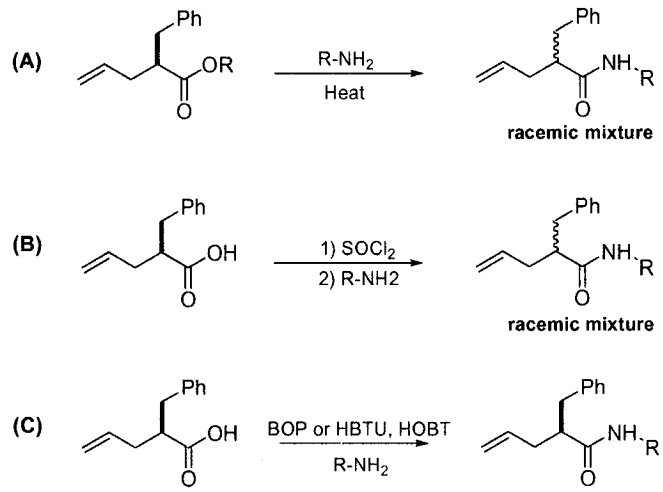

Scheme 29: Amide bond formation.

In (A), the conversion of esters to amides can be done by heating in the presence of amines, although simple and efficient, this process can potentially racemize a stereogenic centre which is α to the carbonyl group . Proceeding via and acid chloride (B), provides milder conditions, but the reaction conditions still can destroy the chiral information.

Therefore, expensive coupling agents (C), are often used, to avoid scrambling any chiral center adjacent to the carbonyl group.

In industry, this option has to be eliminated because of costs. Amide coupling on large scale can be extremely expensive due to the price of the coupling agents and the volumes of waste products. In order to solve this problem, a catalytic method would be favorable. An example of a potentially improved synthetic route using a catalyst would be the proposed synthesis of Indinavir (Crixivan), an HIV protease inhibitor[8] (**Scheme 30**).

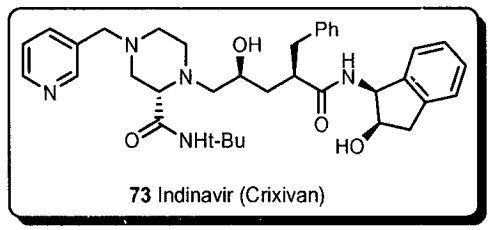

73 Indinavir (Crixivan)

Key step

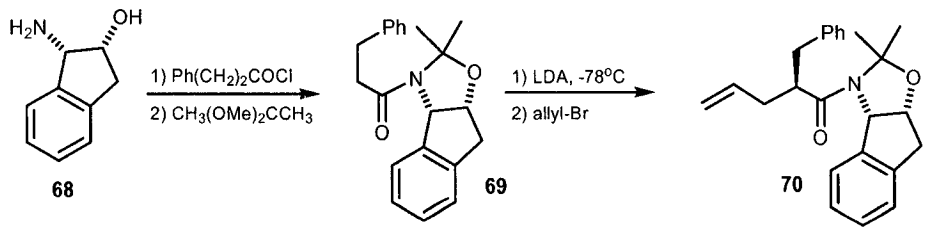

68 **69** **70**

Modified key step

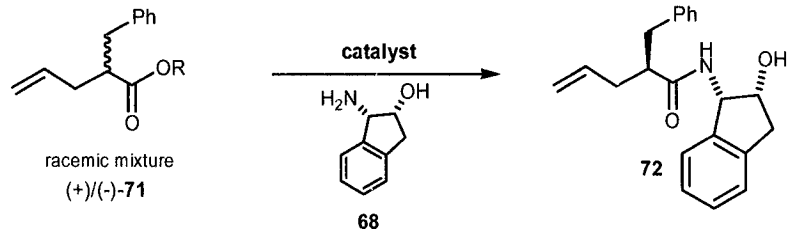

Scheme 30: Key steps of the synthesis of Indinavir (Crixivan).

[8] Rossen K.; Pye P.J.; DiMichele L.M.; Volante R.P.; Reider P.J. *Tetrahedron Lett.*, **1998**, *39*, 6823; Rossen K.; Reamer R.A.; Volante R.P.; Reider P.J., *Terahedron. Lett.*, **1996**, *37*, 6843; Maligres P.E.; Weissman S.A.; Upadhyay V.; Cianciosi S.J.; Reamer R.A.; Purick R.M.; Sager J.; Rossen K.; Eng K.K. *Tetrahedron*, **1996**, *52*, 3327; Maligres P.E.; Upadhyay V.; Rossen K.; Cianciosi S.J.; Purick R.M.; Eng K.K.; Reamer R.A.; Askin D.; Volante R.P.;Reider P.J. *Tetrahedron. Lett.*, **1995**, *36*, 2195; Askin D.; Eng K.K.; Rossen K.; Purick R.M.; Wells M.T.; Volante R.P.; Reider P.J. *Tetrahedron. Lett.*, **1994**, *35*, 673.

Currently, this drug is manufactured by a multi-step process which the key step is shown above. Compound **70** is formed from an amide formation via an acid chloride followed by the protection of the alcohol and the secondary amine with 1,1-dimethyl-1,1-dimethoxymethane. Then, allylation of the α position of the amide is carried out using LDA. The synthesis is elegant and practical but is somewhat linear, expensive and requires low temperature conditions. Modification to the key step by selectively coupling a previously formed amine **68** and racemic ester **71** in the presence of a catalyst would give the desired compound **72** in mild conditions. If an asymmetric catalyst is used, the resolution of the ester component could be possible. Since the starting ester is racemic, the uncoupled ester isomer can then be recycled or re-used. Overall, the catalytic option would definitely reduce the expense associated with amide coupling, and make possible a more convergent manufacturing scheme.

2.5 Novel Assay Development

To exploit this chemistry, we first needed to develop a method to rapidly screen enantioselectivity. Substrates containing a fluorophore (donor), a quencher (acceptor) and a recognition element are part of the assay (**Scheme 30**).

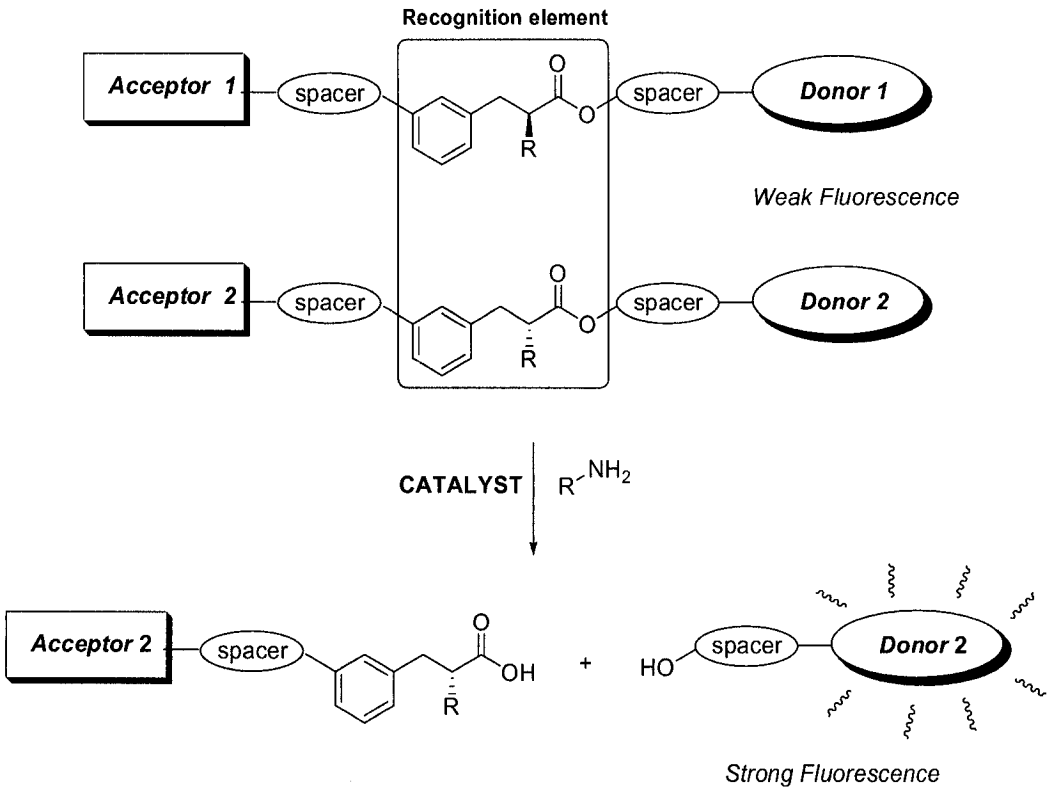

Scheme 31: Assay development using a novel FRET method.

As the principle of FRET was explained earlier, the fluorescence emission band of the donor should overlap with the absorption band of the acceptor. As long as both entities are on the same molecule, the fluorescence will be suppressed. The recognition element is the substrate of the reaction which is connected by spacer elements that ideally prevent any interference from the fluorescent groups (donor and acceptor) with the interaction of the catalyst and substrate. The screening would be performed with equimolar mixture of the two substrates. Coupling would result in the release of the acceptor moieties and the donor fragments would fluoresce strongly. Since the two donors will have different characteristic emission bands, four results are possible for such a reaction (**Figure 17**).

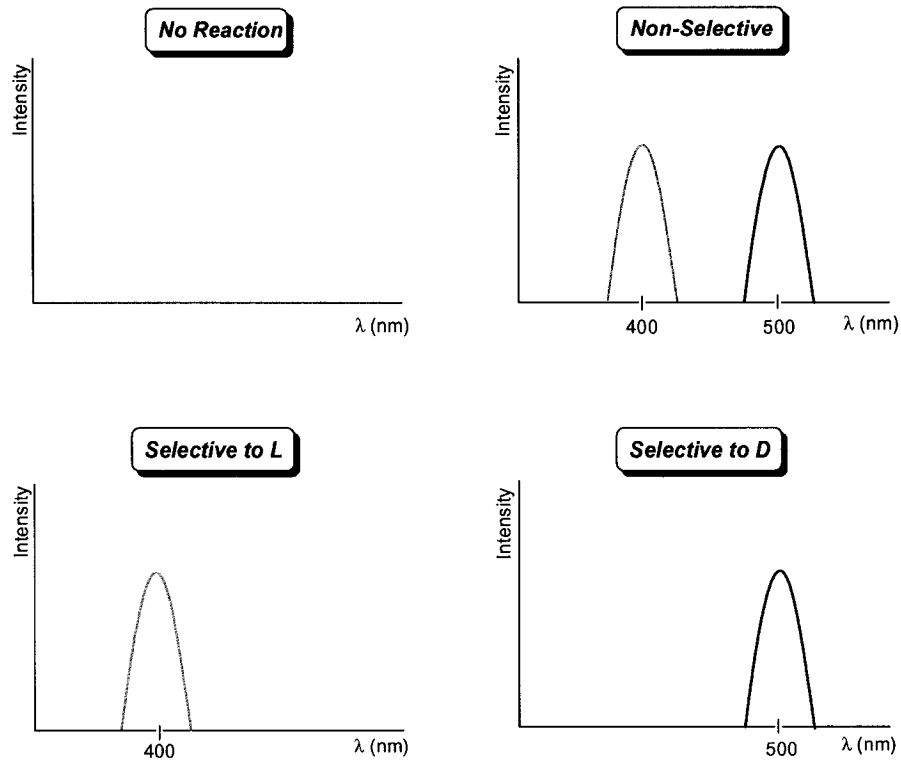

Figure 16: Possible results from the coupling using a catalyst.

Weak fluorescence will indicate no reaction while strong fluorescence at both characteristic wavelengths will illustrate a non-selective reaction. Otherwise, strong fluorescence at only one wavelength signifies an enatioselective coupling.

Therefore, substrates needed to be prepared and tested to ensure that proper fluorescence could be realized by evaluating the scope of the possible donor/acceptor pairs and then validation using a known enantioselective reaction would be carried out. The preparation of calibration curves would be required to normalize the response between the substrates. Eventually, the screening of designed catalysts will be performed using the novel methodology. The development and proof-of-principle studies are described in the following chapters.

CHAPTER 3

Proline-based system

Our first approach to the preparation of adequate substrates to validate the proposed FRET assay was launched from previous studies in which proline had been investigated for its potential in selective binding or coupling.

3.1 Background

In 1994, Still published an article on the binding of tripeptides including L-proline[87]. His research was based on new synthetic receptors that enabled the differentiation of closely related peptides in organic solvent, in a way to mimic the biological pathways. Highly stereoselective binding to a receptor mostly depends on the ability of the substrate to participate in intermolecular electrostatic interactions such as hydrogen bonds. He had shown that his new receptor exhibited high selectivity for binding tripeptides containing L-proline and in addition, it bound even more tightly with L-proline than other cyclic analogues. These results were supported by the fact the proline is the only amino acid having a secondary amine. This compound also possessed a constrained angle making its conformational preferences very different compared to the other naturally occurring amino acids. The five-membered ring of proline also did not allow any cyclic torsion[88].

As previously shown, studies from Shair[85] using proline-based fluorescent chiral probes demonstrated their potential selectivity (see **2.3**).

An additional feature in the choice of a proline substrate was the introduction of an activated ester that would enhance the reactivity of the proline substrate in coupling. In 2002, Chang[89] reported this feature in a fluorescence aminolysis kinetic study on solid phase. He used a tetrafluorophenol-activated ester which was easily displaced by benzylamine in 90 minutes to give a highly fluorescent product (**Scheme 32**).

---

[87] Still W.C.; Borchardt A., *J. Am. Chem. Soc.* **1994**, *116*, 7467.
[88] Still W.C.; MacDonald D.Q., *J. Org. Chem.* **1996**, *61*, 1385.
[89] Walsh D.P; Pang C.; Parikh P.B.; Kim Y.S.; Chang Y.T., *J. Comb. Chem.*, **2002**, *4*, 204.

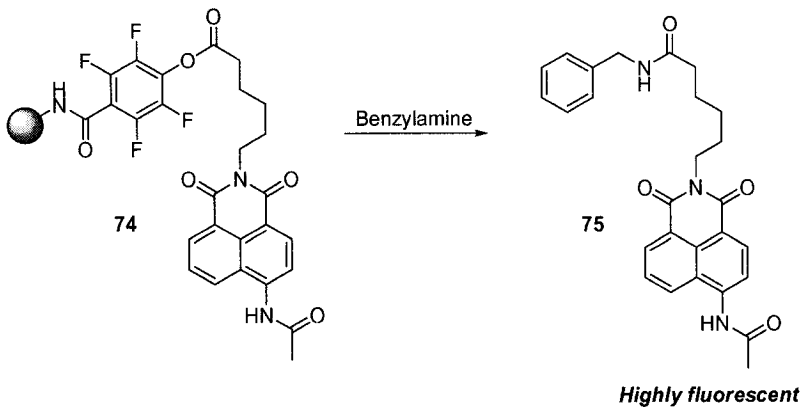

Scheme 32: Cleavage of an activated-ester with benzylamine.

3.2 Probes Synthesis

Putting every piece together, we ended up with a potential recognition element. But before preparing our substrate, the selection of donor/acceptor pairs had to be considered. Our starting choice was a combination of the dansyl **76** (donor) and diazo dye **77** (non-fluorescent acceptor). This FRET pair had proved to be reliable and easy to handle in Hartwig's experiments[83,84] as previously described. For the other pseudoenantiomer, it was necessary that the donor had a distinguishable emission wavelength different than the dansyl. Literature search indicated that the donor pyrene **78** and a benzofurazan acceptor **79** would potentially be a suitable pair.

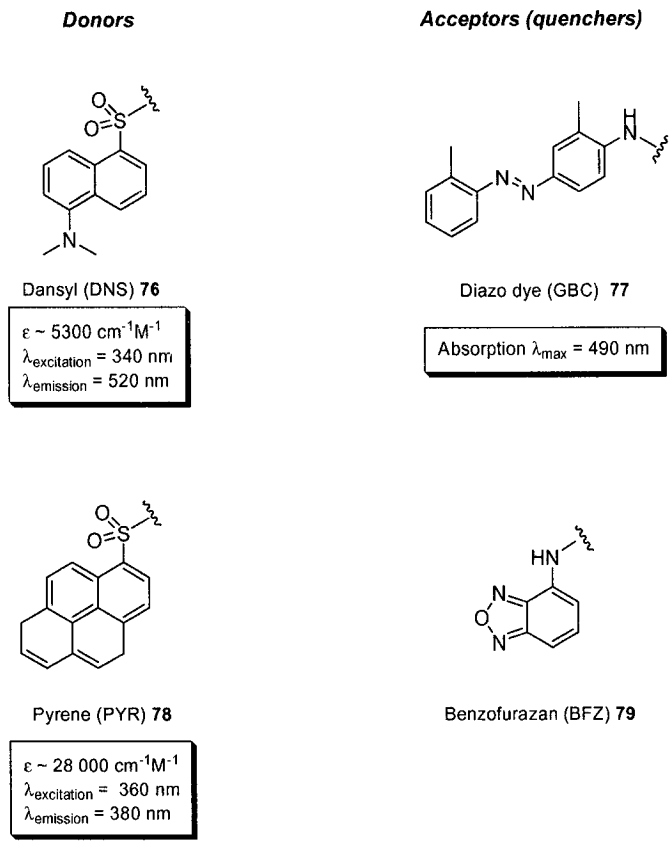

Figure 17: Donor/acceptors pairs for the FRET assay.

Aliphatic spacers, of at least 4 carbons long, would be installed between the recognition element and the fluorescent groups to avoid any interference from the latter. This seemed to be a wise choice because of simplicity and inertness compared to other functionalities that could interfere with the catalyst action, e.g. H-bonding or π-stacking from any heteroatom or alkenes respectively. We decided to use flexible spacers in the initial work in order to avoid problems of a physico-chemical nature such as insolubility. In doing so, we realized that this might cause problems with the recognition element. The assignment of each donor/acceptor pair to each substrate, L- and D-proline, was made arbitrarily.

The synthesis of the first probe with L-proline is depicted in the following schemes. Since the activated-ester was more reactive, the synthesis should save its formation for the last step to prevent cleavage during the other transformations. Therefore, a convergent

route was elaborated which involved the preparation of the acceptor and the donor moieties separately.

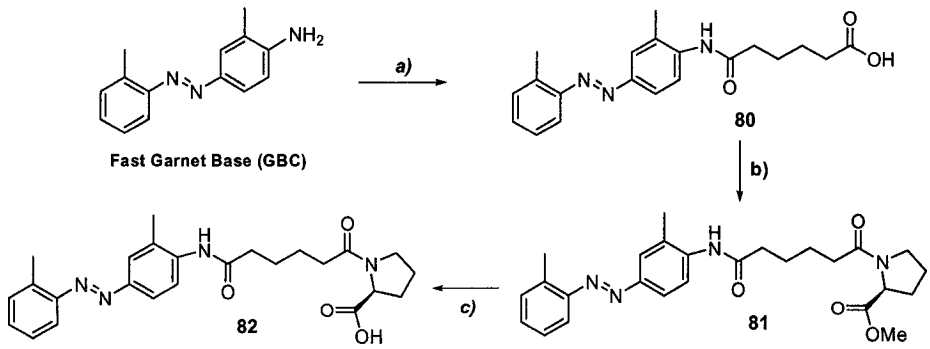

Reagents ***a)*** adipic anhydride, benzene, reflux, *87%*. ***b)*** L-proline methyl ester, EDC, HOBT, DIPEA, rt, *46%*. ***c)*** LiOH, THF/MeOH/H_2O, rt, *>99%*.

Scheme 33: Synthesis of the acceptor moiety 82 for the L-proline substrate.

First the acceptor moiety was prepared by condensing commercially available Fast Garnet Base (GBC) and adipic anhydride. The reaction required heat since the amine was poorly nucleophilic. After introduction of the proline substrate by a standard peptide coupling, we hydrolyzed the methyl ester in **81**. Hydrolysis of such ester is not normally the best choice when the preservation of chirality is concerned. The formation of the intermediate orthoester makes the chiral proton more acidic and subsequent deprotonation leading to epimerization of the center is possible. To evaluate this possibility, the coupling of **82** with (R)-methylbenzylamine was performed to obtain diastereoisomers that would be detectable by characteristic signals in the ^{1}HNMR spectra. **(Figure 18)**.

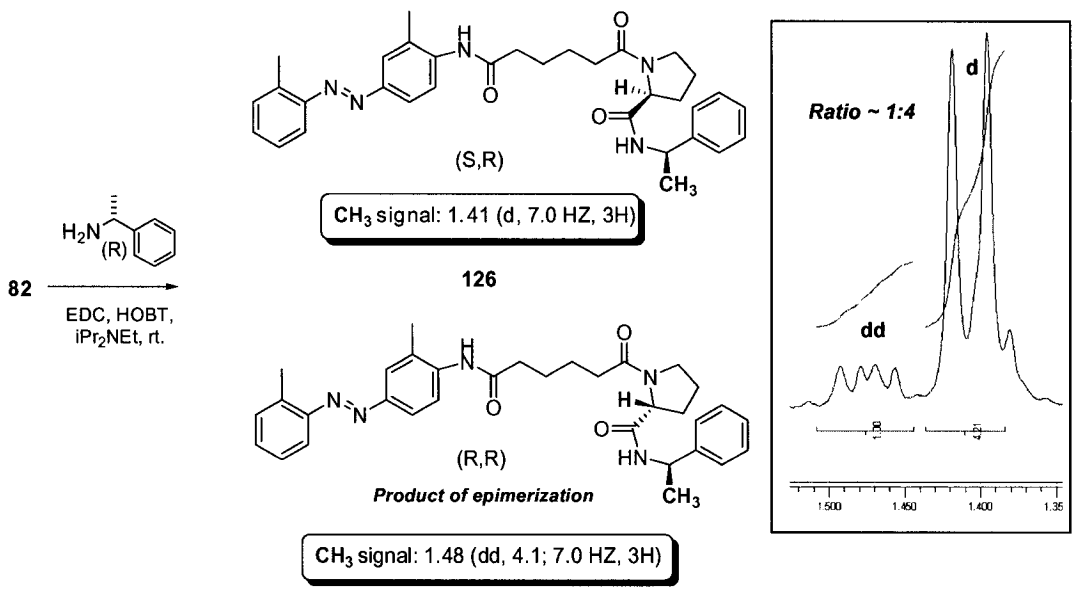

Figure 18: 1HNMR experiment in the investigation of epimerization possibility during hydrolysis.

The different signals result from the proton couplings with the chiral methyl group. The environment of this group differs depending of the configuration of the proline moiety. As expected, the (R,R) product showed an additional set of signals (doublet of doublet) due to the proximity of the proline's chiral proton. A ratio of approximately 4:1 of the desired (S)-configuration, calculated from the integration of each signal, was found. So, it can be concluded that the hydrolysis of L-proline methyl ester acceptor moiety did cause a significant amount of epimerization.

The preparation of the donor moiety was more straightforward because no chiral substrates were included (**Scheme 34**).

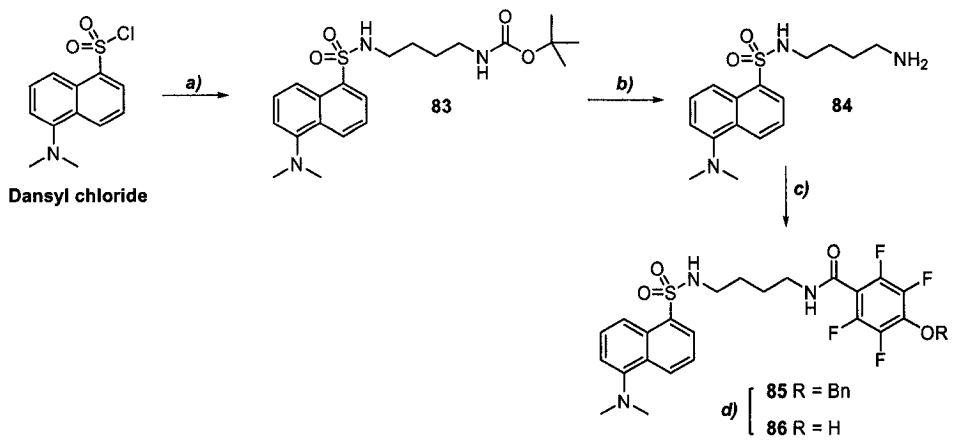

Reagents ***a)*** (4-Amino-butyl)-carbamic acid tert-butyl ester, Et_3N, 0°C, *51%*. ***b)*** Trifluoroacetic acid, CH_2Cl_2, rt, *>99%*. ***c)*** 2,3,5,6-tetrafluoro-4-benzyloxybenzoic acid, EDC, HOBT, DIPEA, rt, *74%*. ***d)*** H_2, Pd/C 10%, MeOH, rt, *79%*.

Scheme 34: Synthesis of the donor moiety 86 for the L-proline probe.

The last step of the synthesis of the first probe, using L-proline as the recognition element, relied on coupling to form the tetrafluorophenol-activated ester under usual coupling conditions (**Scheme 35**).

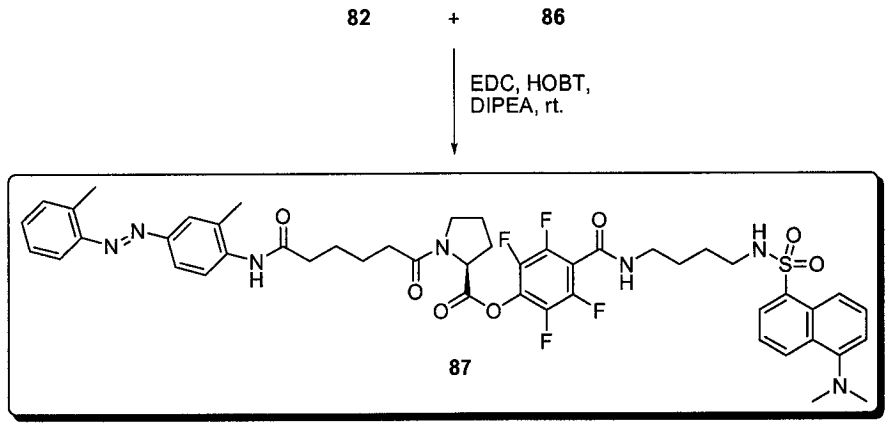

Scheme 35: Convergent synthesis of L-proline probe 87 by forming a tetrafluorophenol-activated ester.

Unfortunately, the isolation and purification of the probe was very difficult. Cleavage of the molecule was observed upon silica chromatography with the reappearance of a fluorescent band. Therefore, further preparation of the proposed system with an activated-ester was aborted, in part because of the aforementioned isolation problem, but also due to the epimerization found in the hydrolysis step. Other ways around the epimerization have been possible such as replacing the methyl ester by an allyl ester whose cleavage is carried out in very mild conditions with a Rhodium catalyst, but these avenues were not pursued.

We then based our research on finding a known and effective system using a catalyst that would allow us to validate our FRET principle.

CHAPTER 4

Leucine-based system

To our delight, we found a recent publication describing an enantioselective ester hydrolysis, which would be similar to our desired amide bond formation from esters. More importantly, it used a metal-free catalyst (homogeneous), eventually the catalyst' type we want to design and that their efficiency will be assessed by our novel FRET technology once validated.

4.1 System from Literature

In 2002, Snyder and Pirkle[90] described an (S)-proline-derived organocatalyst **90** that was effective for the enantioselective hydrolysis of N-acylated α–amino esters. Their system consisted of a chiral complexing agent that differentially affected the reactivity of the enantiomers of amino acid esters. Reactions were performed in a biphasic solvent and studied for kinetic resolution.

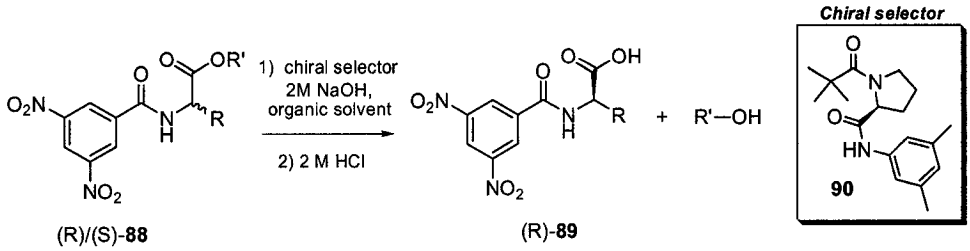

Scheme 36: Enantioselective biphasic hydrolysis of N-acylated α–amino acids esters.

The enantioselective hydrolysis was tested with various DNB-protected racemic esters **88** in nonpolar solvent with a solution of sodium hydroxide. Several experiments were carried out varying several conditions: the effects of the chiral selector concentrations, the temperature and the organic solvent used were all examined. The experiments showed best results with leucine methyl and ethyl esters in hexane/dichloromethane at 0 °C with

[90] Snyder S.E; Pirkle W.H., *Org. Lett.*, **2002**, *4*, 3283.

2 equivalents of chiral selector. Using these conditions, after the selective hydrolysis, the residual (S)-ester gave 92 % ee.

Snyder also studied the enantioselective formation of esters using the same chiral selector and conditions, and obtained 100 % ee. They also extended their studies to other hydrolytically labile compounds such as racemic phosphonate esters and lactams. Overall, this method appeared to provide an ideal test reaction for our proof of principle experiment.

4.2 System Testing

Before preparing probes based on Snyder's system, we decided to test it. We needed to modify the substrates in such a way to make the future synthesis of our probes simpler using the available reagents. So, the dinitrobenzene amide moiety was replaced by a para-tolyl group in which there was the possibility to attach the acceptor moiety in the para-position. Also, since the leucine methyl and ethyl esters gave the best results and similar stereoselectivities, they seemed to be appropriate for this application. Using methyl and ethyl esters would potentially provide a convergent way to test enantioselectivity by acting as pseudoenantiomeric labels.

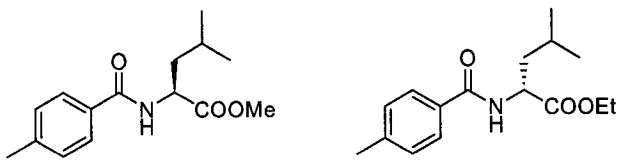

(D)-**91** (L)-**92**

Scheme 37: Modified leucine-based substrates.

The preparation of the required substrates was a one step coupling from para-toluic acid and the respective leucine esters available in our inventory. Carrying out the hydrolysis with the same conditions as described[91] for these substrates, the reaction was easily followed by TLC (see 7.3.1.1).

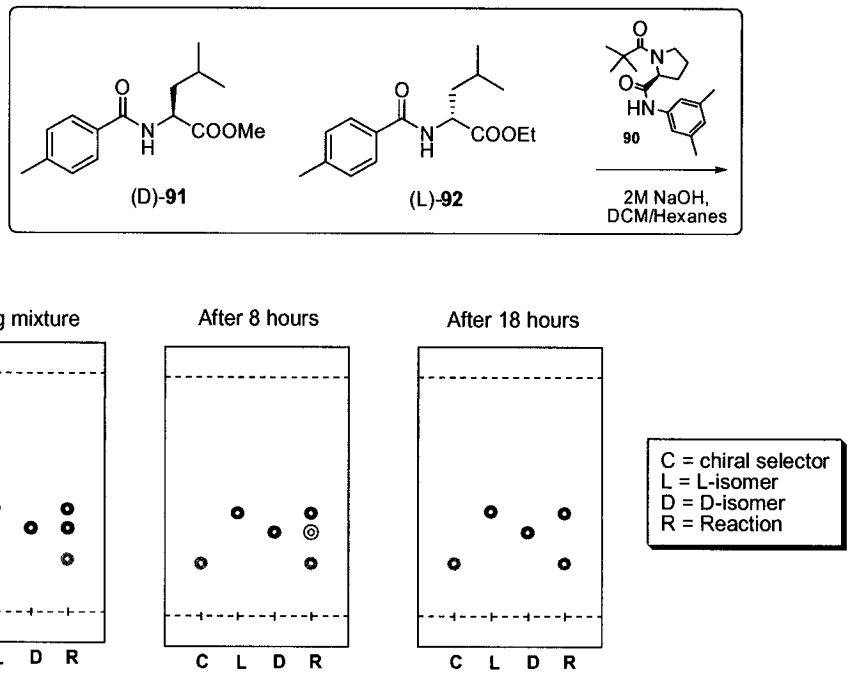

Figure 19: TLC experiment with leucine-based substrates 91 and 92 with chiral selector 90.

As predicted by the experiments described in the article, the D-isomer was selectively hydrolyzed with the L-proline-based chiral selector. After 18 hours of incubation, these experiments clearly showed that D-isomer **91** had been completely consumed. There was no indication that the L-isomer **92** had reacted. With this result in hand, we felt that the process was suited for further experimentation.

4.3 Probes Synthesis

Once again, the assignment of the donor/acceptor pairs to each pseudoenantiomer was done arbitrarily. With a test reaction identified and substrates selected, we proceeded to prepare our probes using the previously mentioned donor/acceptor pairs.

4.3.1 L-isomer probe

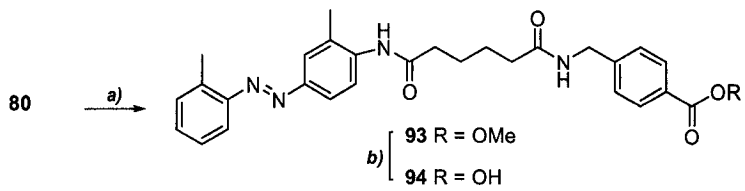

Reagents ***a)*** Methyl 4-(aminomethyl)benzoate, EDC, HOBT, DIPEA, rt, *36%*. ***b)*** LiOH, THF/MeOH/H_2O, rt, *>99%*.

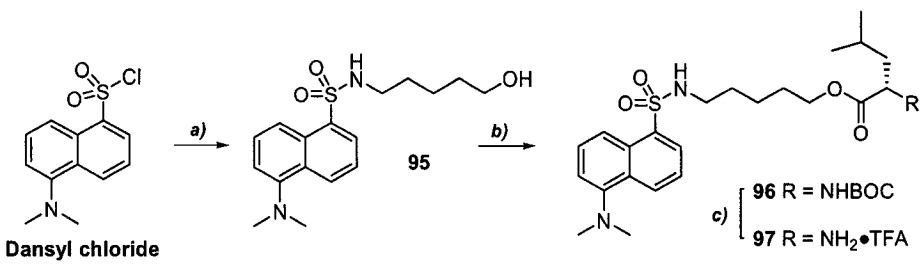

Reagents ***a)*** 5-aminopentanol, Et_3N, rt, *95%*. ***b)*** N-BOC-L-leucine, EDC, HOBT, DIPEA, rt, *46%*. ***c)*** TFA, rt.

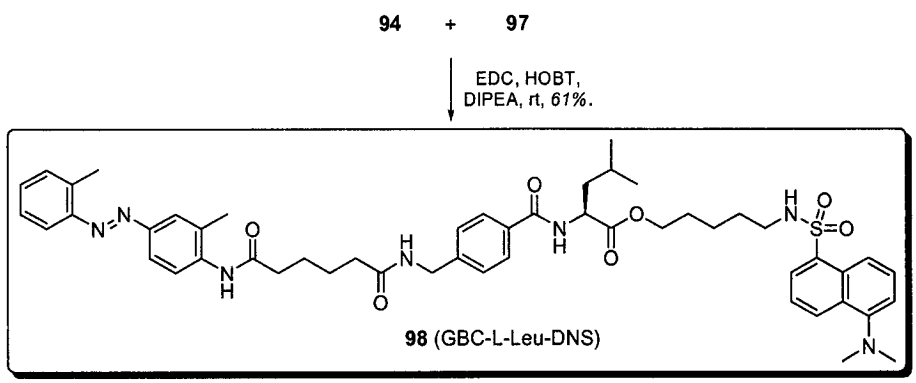

Scheme 38: Synthesis of the L-isomer probe.

The acceptor moiety was prepared from **80**, which had also been used in the previous synthesis. By a standard coupling reaction, the required phenyl moiety was introduced intended to mimic the para-tolyl group. As for the donor group, formation of the ester could be done in a straightforward manner to give the desired probe. Since it was not

activated, this ester was stable under many different conditions. The last step followed a deprotection of the BOC group with subsequent coupling of the resulting TFA salt **97** and the acceptor moiety **94** to obtain the desired probe **98**. In this order, no chiral information was lost.

A fluorescence spectrum of the donor **95** (DNS-OH) was taken since this would be the hydrolysis product that would eventually be detected. As shown on **Figure 20a**, this material displayed a clean fluorescence spectrum with a maximum wavelength of 483 nm. To show properly the quenching efficiency of the GBC moiety, a solution of the FRET substrate **98** was prepared and a fluorescence spectrum was obtained (see 7.3.1.2).

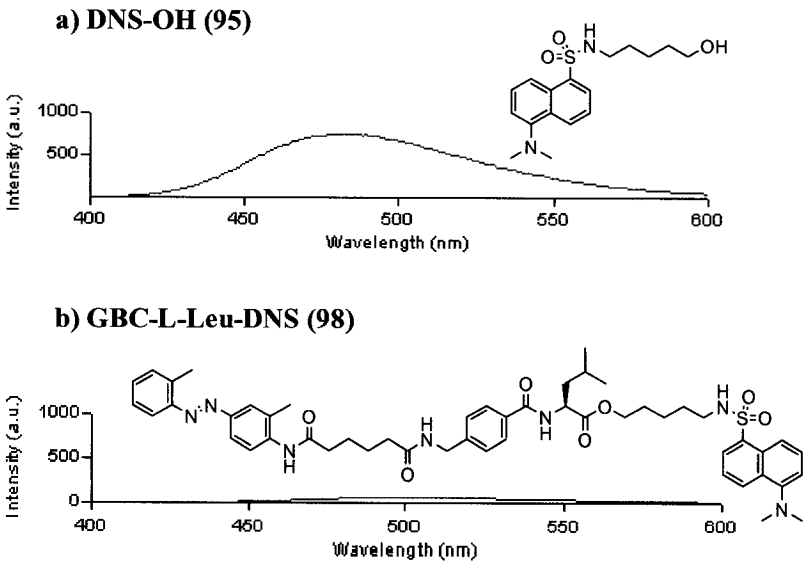

Figure 20:Fluorescence spectra for the L-isomer prob.

Happily, the DNS/GBC pair was suitable for FRET, as had been demonstrated also by Hartwig[82]. The disappearance of the fluorescence signal was clearly shown in the spectrum above (**Figure 20b**). As the GBC was a non-fluorescent group, no complicating emissions were observed on the spectrum of **98**.

4.3.2 D-isomer probe

As for the D-enantiomer, the BFZ/PYR pseudoenantiomer was selected. The synthesis of this substrates was done in a similar fashion to that of the L-enantiomer.

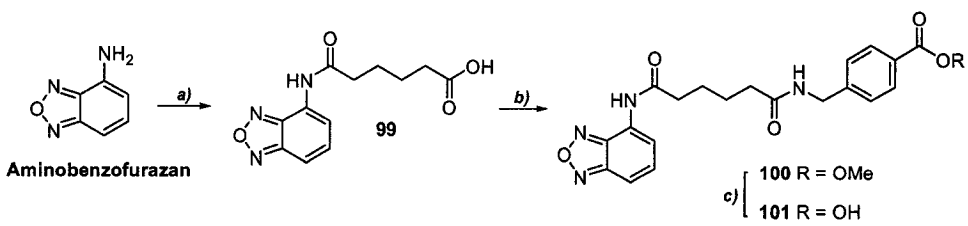

Reagents *a)* adipic anhydride, reflux, *65%*. ***b)*** Methyl 4-(aminomethyl)benzoate, EDC, HOBT, DIPEA, rt, *81%*. ***c)*** LiOH, THF/MeOH/H_2O, rt, *>99%*.

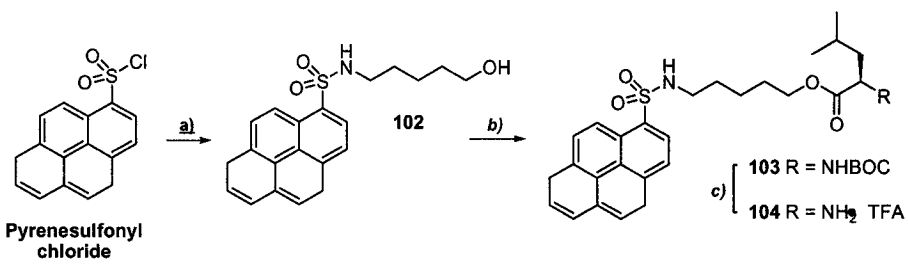

Reagents *a)* 5-aminopentanol, iPr_2NEt, rt, *43%*. ***b)*** N-BOC-D-Leucine, EDC, HOBT, DIPEA, rt, *50%*. c) TFA, rt.

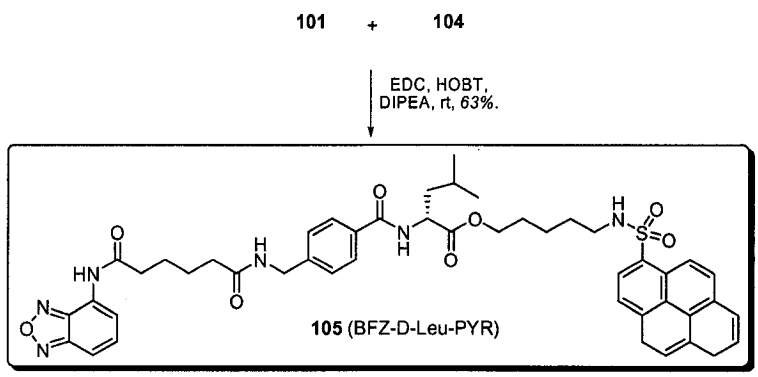

Scheme 39: Synthesis of D-isomer probe.

Condensation of aminobenzofurazan with adipic anhydride, followed by coupling with the benzylamine moiety and saponication of the methyl ester gave the BFZ moiety **101**. As for the donor moiety, aminopentanol was condensed with the pyrenesulfonyl chloride and coupling of the D-leucine ester was performed. Then, deprotection of the amine with subsequent coupling with the BFZ moiety gave the desired probe **105**.

Fluorescence spectra of donor **102** and probe **105** were recorded to evaluate the feasibility of this combination in our FRET assay (see 7.3.1.3).

a) PYR-OH (102)

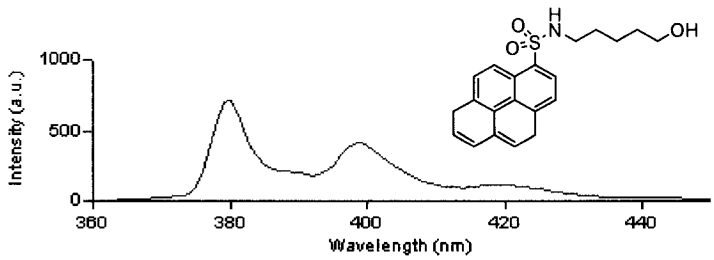

b) BFZ-D-Leu-PYR (105)

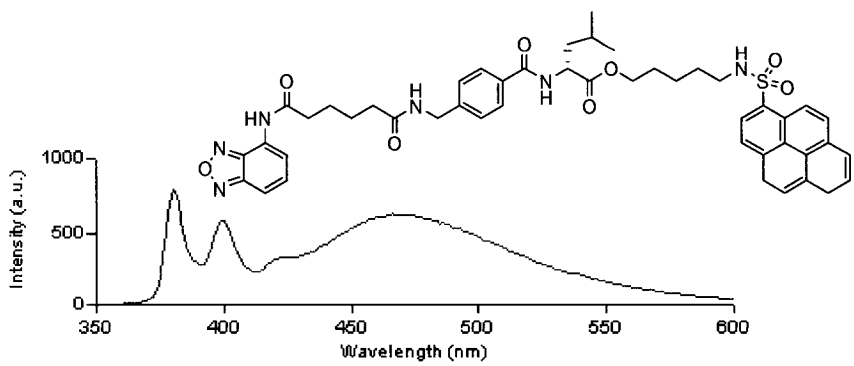

Figure 21: Fluorescence spectra for the D-isomer probe.

Unfortunately, for this combination of donor/acceptor, quenching of PYR by BFZ was not efficient as shown by the remaining presence of the characteristic emission bands of PYR-OH at 380 nm and 400 nm. In addition, the emission band of BFZ (λ_{max} = 466 nm)

was apparent, since this substance is a fluorescent acceptor. In any case, the emission of BFZ would mask the signal of DNS in our substrate mixture, and so this quencher would be unsuitable for our purposes. After reviewing articles that supported this combination, we found out that the structure of this acceptor was misidentified and that it was actually a nitrobenzofurazan that was used.

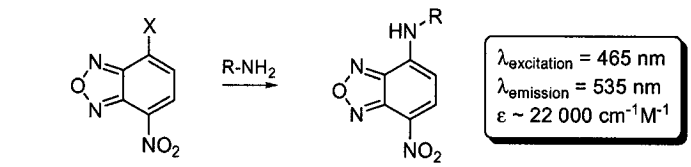

(X = Cl or F)

4-chloro-7-nitrobenzofurazan **NBD**

Scheme 40: Nitrobenzofurazan as an acceptor.

The NBD acceptor however is also fluorescent and would therefore present problems with a clear readout of the DNS signal. Also, the fact that the PYR-OH emission was much more intense than that of DNS-OH would have complicated screening, such that the slit of the apparatus would needed to be adjusted differently for each scan, in order to show both emission band in the same spectrum without over ranging data.

Those results led us to investigate other donor/acceptor pairs that would be suitable counterparts for the ideal situation of the GBC/DNS pair in the L-isomer probe. To keep the advantage of using the non-fluorescent GBC acceptor and because of its availability and low cost, we sought other donors that would be efficiently quenched by this acceptor and that would have distinguishable and reasonably intense emission bands. To help our search, the absorption spectrum of the GBC moiety that would result from the hydrolysis was taken to determine experimentally its absorption characteristics. The available GBC moiety contained the spacer and the terminal amino acid which for solubility reasons, the ester form was used (GBC-D-Phe-OEt **125**, see 7.3.1.4).

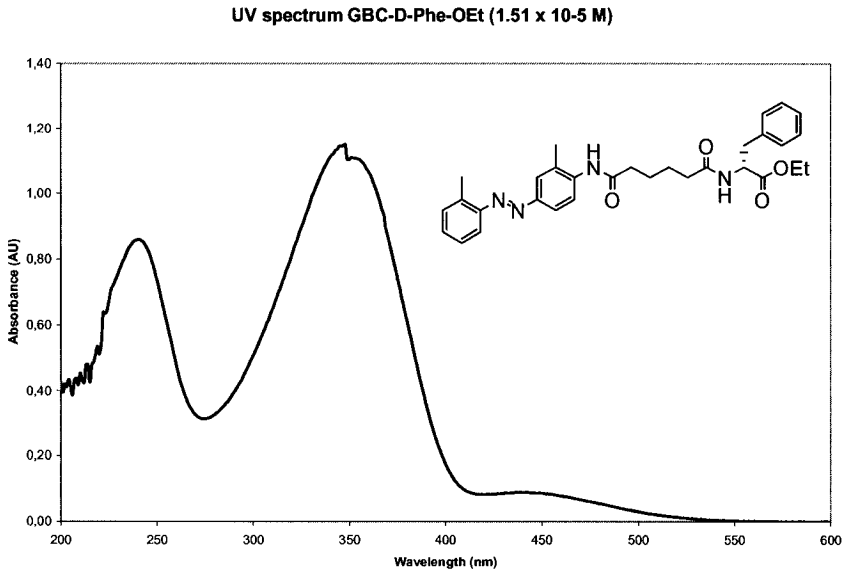

Figure 22: UV Absorption spectrum of GBC moiety.

The absorption maxima were found at 239, 348 and 442 nm and the entire absorption spectrum covered the range up to 520 nm. This data automatically eliminated any fluorophores available with emission bands over 520 nm. This was not a significant difficulty however, as most of these fluorophores contained charged species which were unsuitable for work in organic solvents.

4.3.2.1 2-dimethylaminonaphthalene-6-sulfonyl moiety (BRN)

The first donor considered was a dimethyl derivative of Bronner's acid (BRN). This moiety was appealing because it is an isomer of DNS with different fluorescence characteristics.

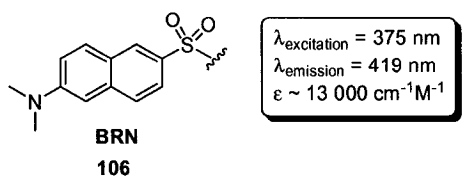

Figure 23: BRN donor group.

Based on spectral overlap, quenching with GBC would be expected and the fluorescence intensity would be comparable to that of DNS. The synthesis of the required probe was accomplished with the same reagents and conditions that were employed in the synthesis of GBC-L-Leu-DNS **98**, except for the use of 2-dimethylaminonaphthalene-6-sulfonyl chloride in place of the Dansyl chloride as we were preparing the pseudoenantiomer of **98**, N-BOC-D-Leucine was used.

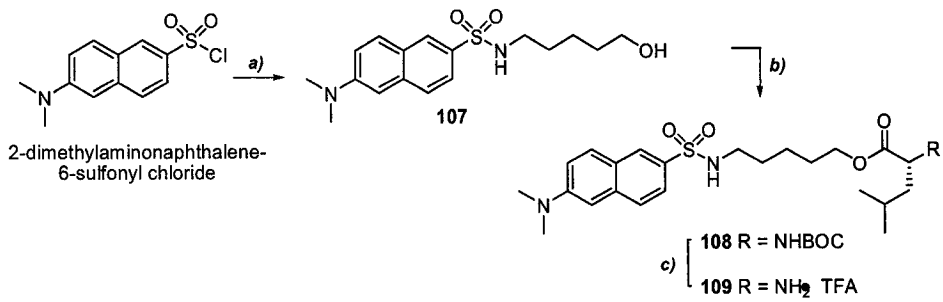

Reagents ***a)*** 5-aminopentanol, Et_3N, rt, *84%*. ***b)*** N-BOC-D-leucine, EDC, HOBT, DIPEA, rt, *74%*. ***c)*** TFA, rt.

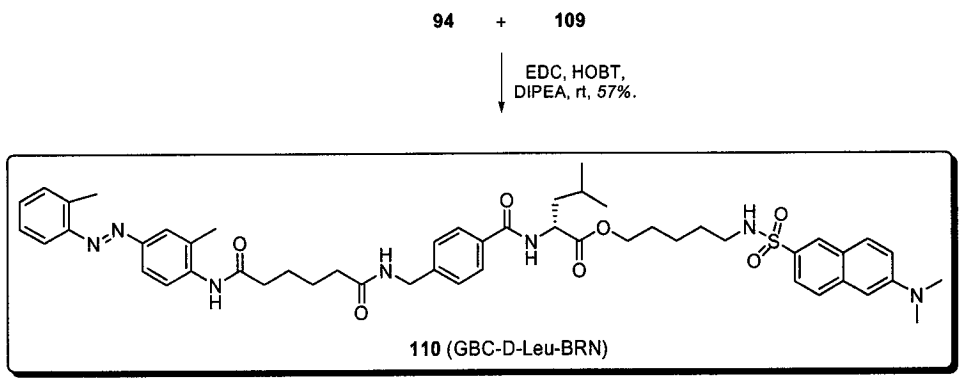

Scheme 41: D-isomer probe synthesis using BRN donor.

To test the possibility of using this FRET pair, the fluorescence spectra BRN-OH **107** and probe **110** were obtained with the fluorometer (see 7.3.1.5).

a) BRN-OH (107)

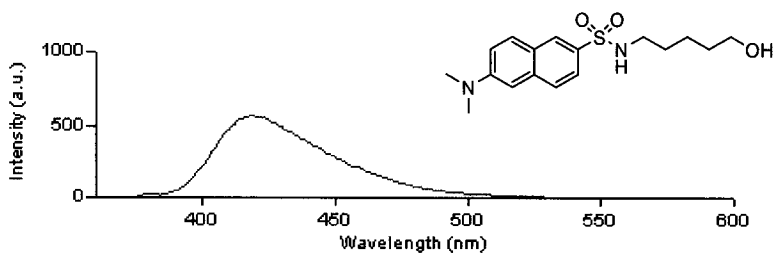

b) GBC-D-Leu-BRN (110)

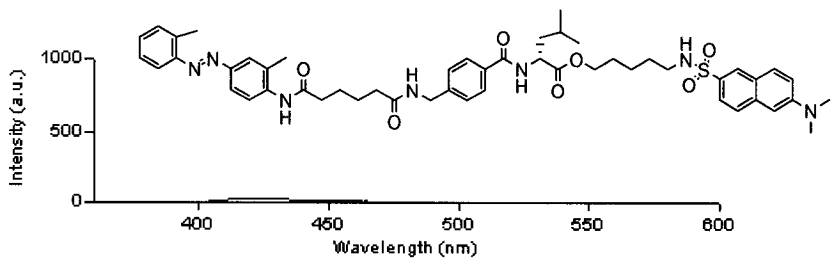

Figure 24: Fluorescence spectra for D-isomer probe with GBC/BRN pair.

Almost perfect quenching was obtained which was good news. To verify compatibility, a fluorescence spectrum of an equimolar mixture of DNS-OH **95** and BRN-OH **107** was obtained to evaluate the possible distinction between the characteristic emission bands of **95** and **107** (see 7.3.1.6).

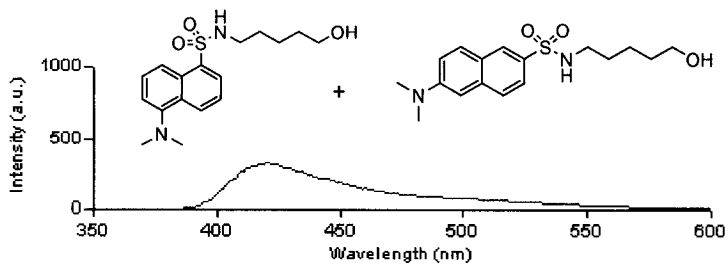

Figure 25: Fluorescence spectrum of equimolar mixture of DNS-OH and BRN-OH.

Unfortunately, as shown on the spectrum above, there was no observable distinction between their emission bands. Moreover, only the BRN-OH emission could be clearly identified whereas the DNS emission at 500 nm was completely undefined. Thus, BRN was not a suitable donor for the system.

4.3.2.2 N-phenyl-1-naphthylamine (NPN)

Another possibility was the use of NPN. As a fluorescence donor, this moiety emitted at 426 nm with an extinction coefficient of 8100 $cm^{-1}M^{-1}$ and so would make a suitable spectral pairing with DNS.

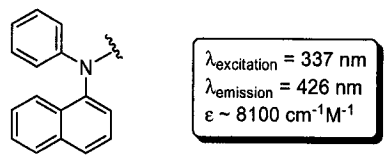

NPN
111

Figure 26: NPN donor group.

The synthesis of the probe including NPN was very similar to the synthesis of the other probes with a few small modifications. The synthesis of the donor fragment is shown in **Scheme 42**.

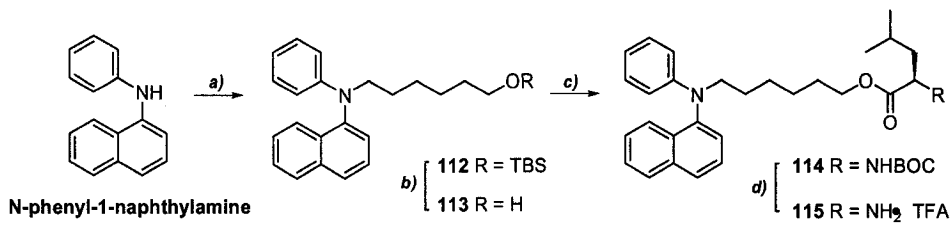

Reagents ***a)*** KH, $Br(CH_2)_6OTBS$, rt, *79%*. ***b)*** TBAF, rt, *88%*. ***c)*** N-BOC-D-Leucine, EDC, HOBT, DIPEA, rt, *35%*. ***d)*** TFA, rt.

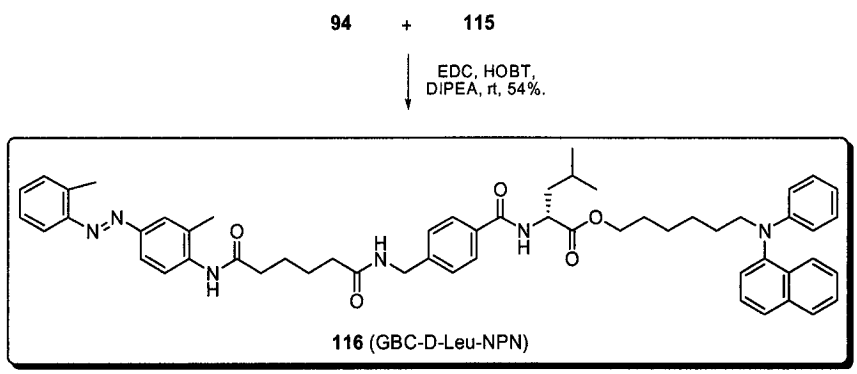

Scheme 42: D-isomer probe synthesis using NPN donor.

Alkylation of the secondary amine was carried out with deprotonation by KH followed by addition of the O-protected alkyl bromide. Deprotection of the alcohol and subsequent coupling of the N-BOC-D-Leu gave the donor moiety. Then, coupling between the required acceptor moiety and the donor moiety was accomplished with standard peptide coupling procedure to obtain the desired probe.

To evaluate the acceptor efficiency, fluorescence spectra of the NPN-OH **113** and probe **116** were taken (see 7.3.1.7).

a) NPN-OH (113)

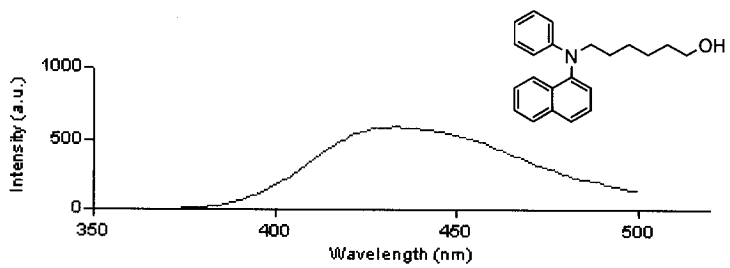

b) GBC-D-Leu-NPN (116)

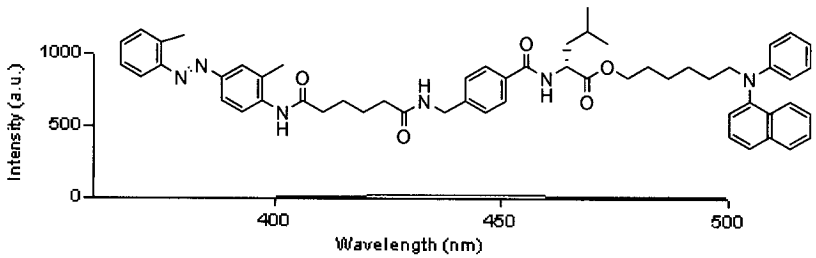

Figure 27: Fluorescence spectra for D-isomer probe with GBC/NPN pair.

Shown above, this NPN probe **116** gave a clean fluorescence spectrum with an emission wavelength at 434 nm and minimal spectral overlap at 500 nm. Successful FRET was observed for this moiety as shown in **Figure 27b**. In order to evaluate the potential of NPN in pseudoenantiomer applications, an equimolar mixture of DNS-OH **95** and NPN-OH **113** was prepared and the fluorescence spectrum was recorded (see 7.3.1.8).

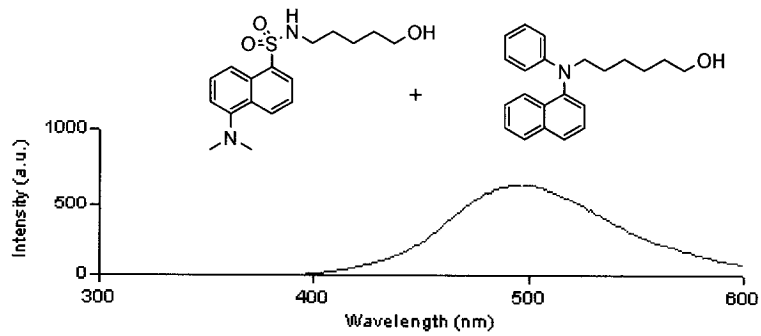

Figure 28: Fluorescence spectrum of equimolar mixture of DNS-OH and NPN-OH.

As shown in **Figure 28**, only fluorescence of the DNS moiety **95** was noted. The absence of the emission band of NPN-OH at 434 nm, together in solution with DNS-OH, was disappointing. Therefore, despite the efficient quenching of the NPN donor by the GBC acceptor, this FRET pair was not suitable for the assay with GBC/DNS pair.

4.3.2.3 Pyrenesulfonyl moiety (PYR)

Although previous experiments using PYR as a donor suggested that this moiety might not be appropriate due to its high fluorescence intensity and inadequate quenching, it occurred to us maybe this would be a good candidate for quenching with this GBC acceptor anyway. This was suggested by the observed spectral overlap between PYR and the GBC quencher. Because the PYR emission band was distinct from DNS, it would make a perfect situation for future detection. The use of the other characteristic PYR emission band at 400 nm, exciting at a different wavelength than the maximum one (340 nm) along with adjusting the excitation and emission slits would potentially solve the intensity problem. So, before making any adjustments to the scanning setup, the GBC/PYR probe was synthesized.

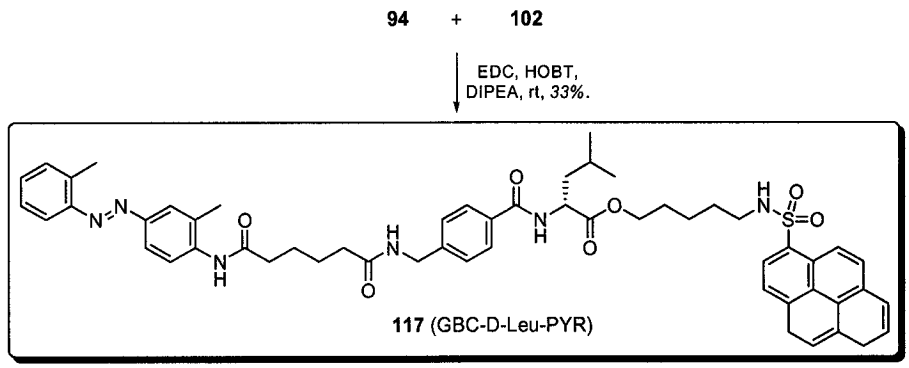

Scheme 43: D-isomer probe synthesis using PYR donor.

Its synthesis was done quickly since all the pieces were already built. A fluorescence spectrum of **117** was then taken to assess the GBC quenching efficiency (see 7.3.1.9).

GBC-D-Leu-PYR (117)

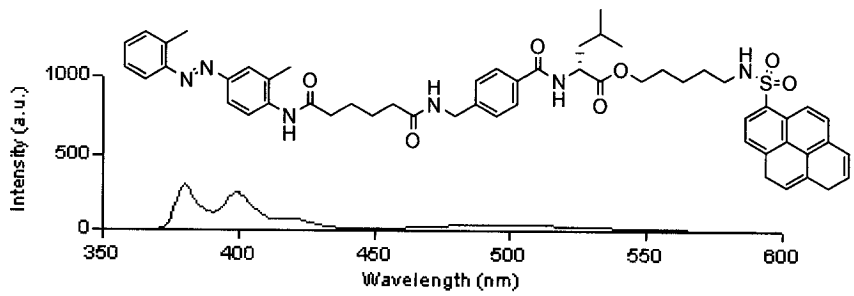

Figure 29: Fluorescence spectrum of D-isomer probe with GBC/PYR pair.

Although there still remained a small amount of fluorescence, quenching was considerably improved with GBC compared to the fluorescence spectra taken previously when BFZ was the acceptor. Assuming appropriate calibrations could be done, this would potentially be an acceptable FRET system. Thus, an equimolar mixture of DNS-OH **95** and PYR-OH **102** was prepared to make sure that the emission bands of each could be picked out (see 8.3.1.10). Our apprehension about this mixture was, that because of the intensity difference between PYR and DNS, that PYR-OH would be expected to give over ranged intensities.

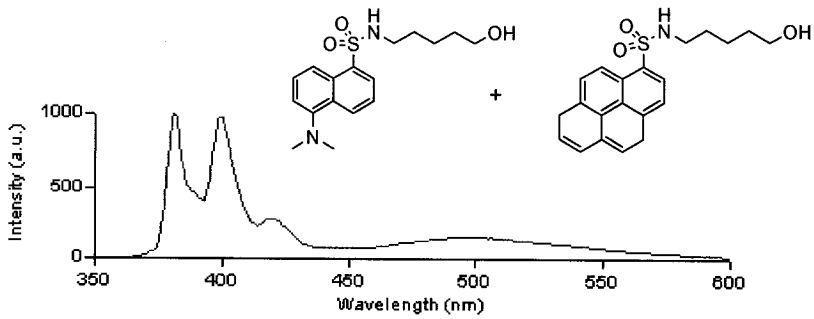

Figure 30: Fluorescence spectrum of equimolar mixture of DNS-OH and PYR-OH.

To our surprise, no over ranged data were obtained from the pyrene moiety, but lower intensities than expected were observed. In addition, a clear distinction between the emission bands of each donor was noted. In this case, PYR would be a suitable donor for the system when quenched by GBC.

4.4 Assay Development

Now that we had in hand the two probes, the L-proline-based chiral selector **90** was then put to the test.

4.4.1 Hydrolysis Reaction

Many reactions were performed to test the reported selective hydrolysis, even with probes that were not found to be ideal for the system. The following section describes our efforts in this area.

4.4.1.1 GBC-L-Leu-DNS and GBC-D-Leu-NPN

The first attempt was made while studying GBC/DNS and GBC/NPN pairs. Even though the donor's emissions were found to interfere, the reaction was carried out and followed by TLC, since each probe, and their hydrolysis products, had different Rf values and colors under UV light.

A first hydrolysis was done with an equimolar mixture of probes in the presence of LiOH under the reported biphasic conditions to study their hydrolytic ability (see 7.3.1.11). For the biphasic hydrolysis, 20:1 Hexanes/DCM was employed, but our probes were not soluble enough in this solvent system, so it was decided to carry out the reaction in DCM only. The reactions were followed by TLC and the results obtained are shown below.

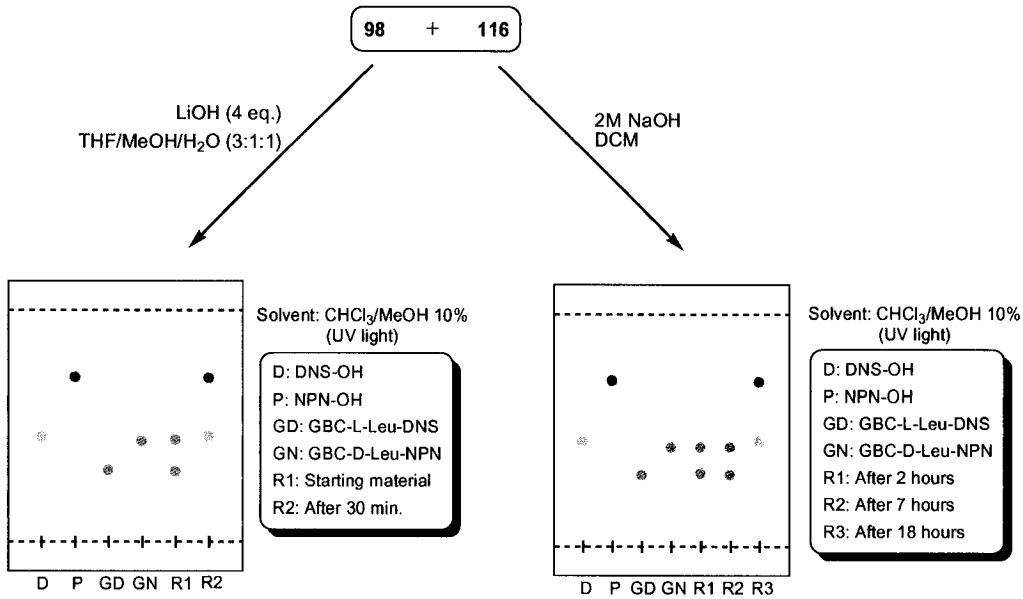

Figure 31: TLC of hydrolysis of equimolar mixture of GBC-L-Leu-DNS and GBC-D-Leu-NPN in different conditions.

These TLC experiments showed us that both probes were hydrolyzed in 30 minutes using LiOH, and that a much slower rate was observed in the biphasic system as expected. The enantioselective hydrolysis using the chiral selector was then performed and monitored over a longer period of time.

In order to verify that molecular recognition involved only the probe and the leucine moiety, both enantiomers of the proline-based catalyst were utilized. Again equimolar mixtures of probes were prepared and the reactions were followed by TLC (see 8.3.1.12).

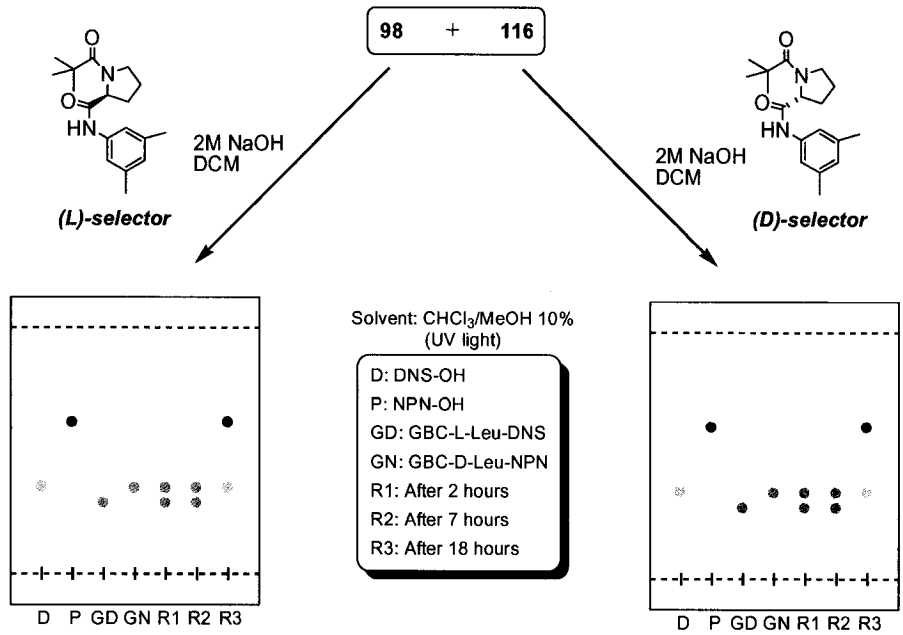

Figure 32: Enantioselective hydrolysis of equimolar mixture of GBC-L-Leu-DNS and GBC-D-Leu-NPN using (L) and (D)-selectors.

As shown above, no selectivity was observed with either of the selectors as the TLC showed spots corresponding to both hydrolysis products, DNS-OH and NPN-OH. The reliability of the results in the article was put in doubt at the time, but since our probes were different than the reported substrates, no conclusion could be made using these experiments.

4.4.1.2 GBC-L-Leu-DNS and GBC-D-Leu-PYR

The unsatisfying results obtained above gave us some experience in working with this donor/acceptor combination. So, the same process was applied to this system although, the reactions were monitored by the fluorescence method instead of TLC. The hydrolysis was carried out without the catalyst at first (see 7.3.1.13).

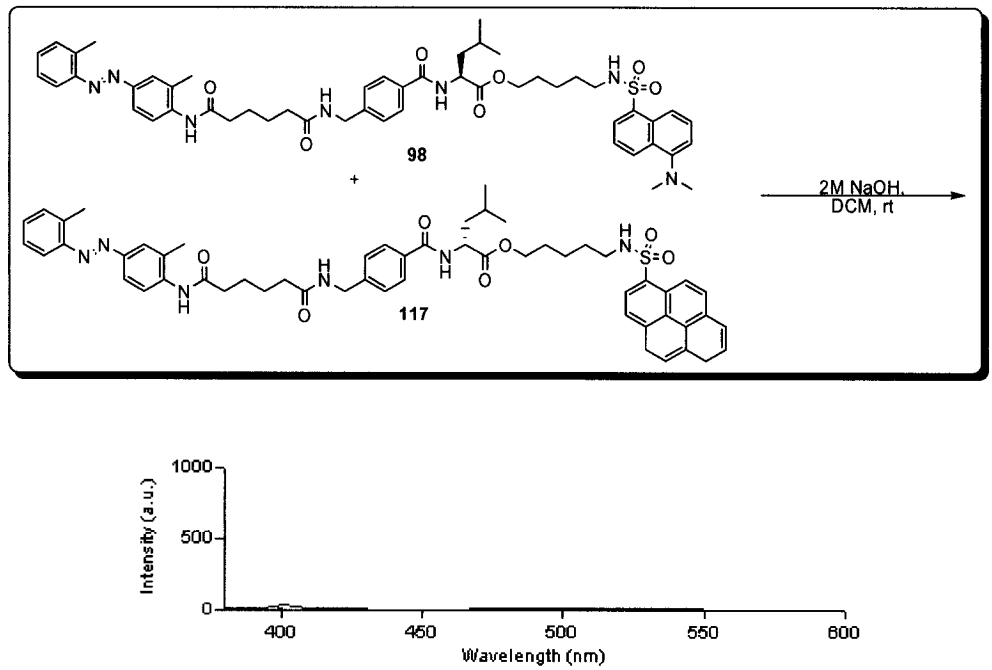

Figure 33: Hydrolysis of equimolar mixture of GBC-L-Leu-DNS 98 and GBC-D-Leu-PYR 117 without chiral selector after 2 days.

After 2 days, the spectrum did not show quantifiable hydrolysis of any of the probes. This situation left us perplexed, but we decide to go forward by carrying out the hydrolysis with the chiral selectors (see 7.3.1.14). Again, both (L)- and (D)-selectors were tried.

a) (L)-selector

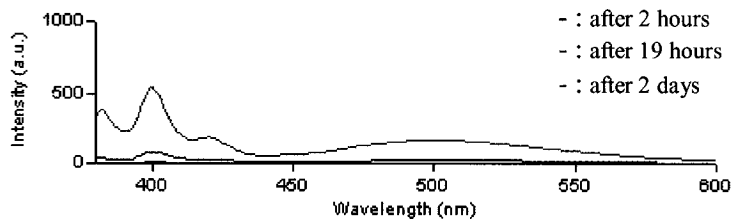

b) (D)-selector

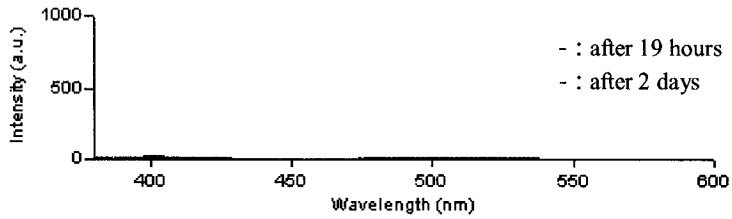

Figure 34: Hydrolysis of equimolar mixture of GBC-L-Leu-DNS and GBC-D-Leu-PYR with chiral selector.

No selectivity was observed with either of the chiral selectors which was confirmed by the spectra shown in **Figure 34a** that clearly show emission bands at 380, 400 and 500 nm corresponding to hydrolysis of both probes using the (L)-selector, and to no hydrolysis with the (D)-selector in **Figure 34b**. Also, inconsistent rates of hydrolysis did not make the study accurate. Therefore, reviewing the details of the published experiments was necessary.

4.4.2 Investigation of Results

Our previous TLC experiment was repeated using the modified substrates **91** and **92**, but this time we used the (D)-selector which was expected to hydrolyze the L-leucine substrates in preference to the (L)-selector. To our surprise, the (D)-selector hydrolyzed the D-leucine substrate (see 7.3.1.15), a result counter to our previous observation.

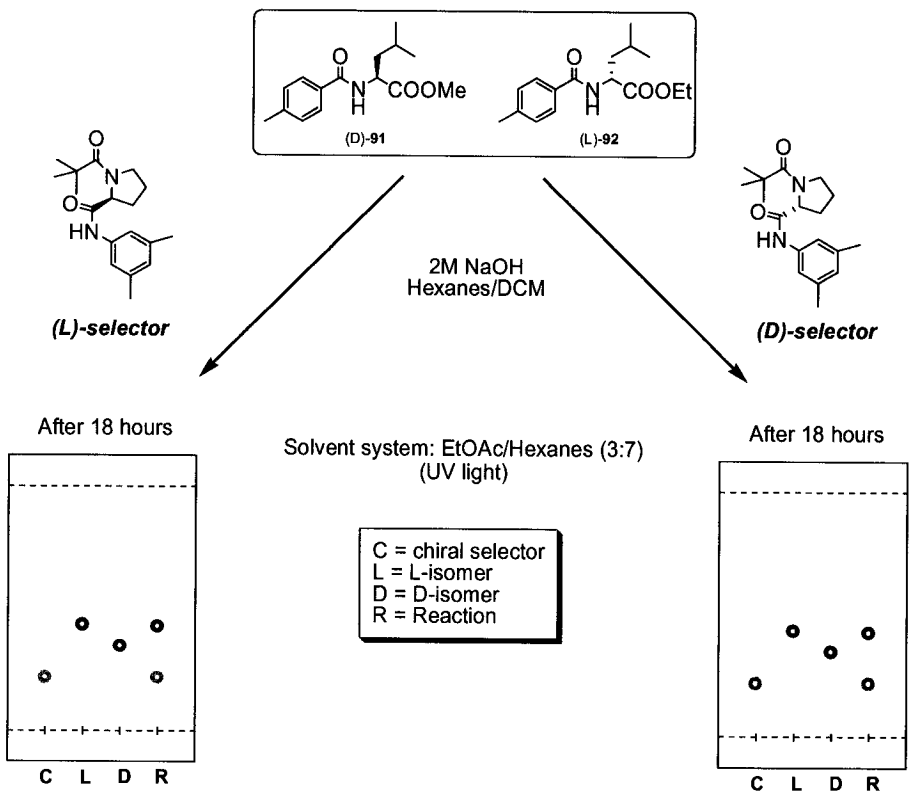

Figure 35: TLC experiments of hydrolysis of 91 and 92 with (L)- or (D)-selector.

The only difference between the substrates lay in the ester functionality: one was an ethyl ester and the other a methyl ester. So, the (D)-selectivity could have arisen from the fact that the rate of hydrolysis of a methyl ester is much faster than an ethyl ester and somehow, both chiral selectors had equal affinity with methyl esters. Therefore, the synthesis of both ethyl ester substrates was carried out and the experiment repeated, this time followed by chiral HPLC (see 7.3.1.16). By using the area under the curve (AUC) of the selector as an internal standard, the ratios of the substrates were calculated to assess their disappearance accurately.

Time (hours)	(L)-selector (AUC)		(D)-selector (AUC)	
	(L)-92	(D)-91	(L)-92	(D)-91
0	0.419	0.477	0.403	0.442
2	0.237	0.208	0.324	0.288
4	0.125	0.072	0.243	0.260

Table 1: AUC ratios obtained by chiral HPLC from hydrolysis of L- and D-leucine esters (91 and 92) with (L)- or (D)-selector.

The results showed that no apparent selectivity was obtained from either chiral selector. Thus, the hydrolysis using the exact system as reported in the article was attempted to verify the selectivity of the chiral selector.

The synthesis of both enantiomers was done following the procedures described and the hydrolyses were followed by chiral HPLC.

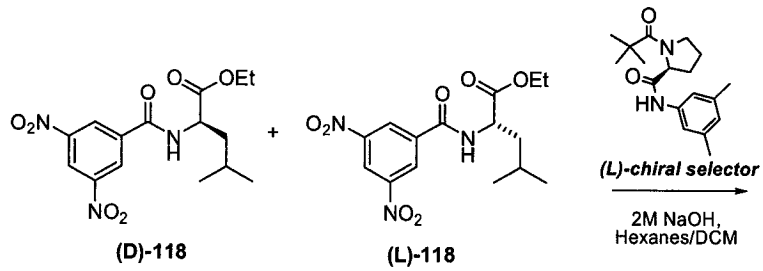

Scheme 44: Hydrolysis of DNB- leucine-based substrates with (L)-chiral selector.

Before performing the hydrolysis, an HPLC method to separate each component of the mixture had to be found. After trying different types of chiral columns available in the department and a variety of solvent systems, none were able to give an adequate separation. An alternative possibility to resolve the system was to condense the acids resulting from hydrolysis with a chiral amine to give diastereoisomers, which would be much easier to separate (see 7.3.1.17a). Our first idea was to hydrolyze the ethyl ester starting materials, since they were readily available, and then couple them with a chiral amine (see 7.3.1.17b). The hydrolysis step was unsuccessful and a red coloration of the mixture was observed. A similar observation was studied by Snyder and he published an article explaining a possible reason for this event.

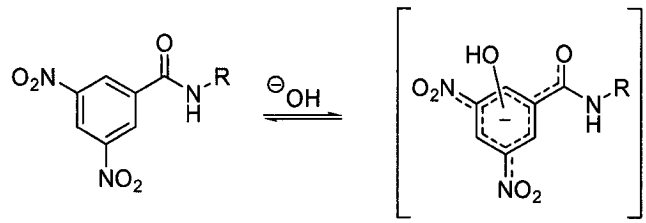

Scheme 45: Meisenheimer adduct.

He suspected the presence of the Meisenheimer adduct which is a cyclohexanedienyl derivative formed as a Lewis adduct from a nucleophile (Lewis base) and an aromatic compound[91]. We did not carry out any experiment to prove this explanation.

To get more details on the reaction, we communicated directly with the authors. It was found that the DNB protecting group was required to ensure selectivity and that the reaction was highly solvent dependent. In addition, their reactions were carried out in vials to maximize the surface between the solvents. So, these conditions were very specific to the substrates.

Therefore, with all these complications, the experiments were aborted. Too many parameters had to be changed in a way to adapt the conditions to our system. Because our chosen test reaction was not robust and repeatable, this reaction was abandoned. Before searching for a new test reaction, we decided to verify the linear response in our FRET pseudoenantiomers idealized system.

4.4.3 Calibration curves

With the collaboration of Ami J. Chin, the elaboration of calibration curves of different solutions, varying the ratio of DNS-OH and PYR-OH, was made.

[91] S.E. Snyder, A.B. Shvets, W.H. Pirkle, *Helv. Chem. Act.*, **2002**, *85*, 3605.

The excitation wavelength was chosen at 370 nm for both donors and slit adjustments were made so that the fluorescence of PYR-OH could be read in the same range as DNS-OH.

The first calibration curve was obtained from various mixture of the two donor moieties only (see 7.3.1.18). Fluorescence data were recorded under the parameters previously described.

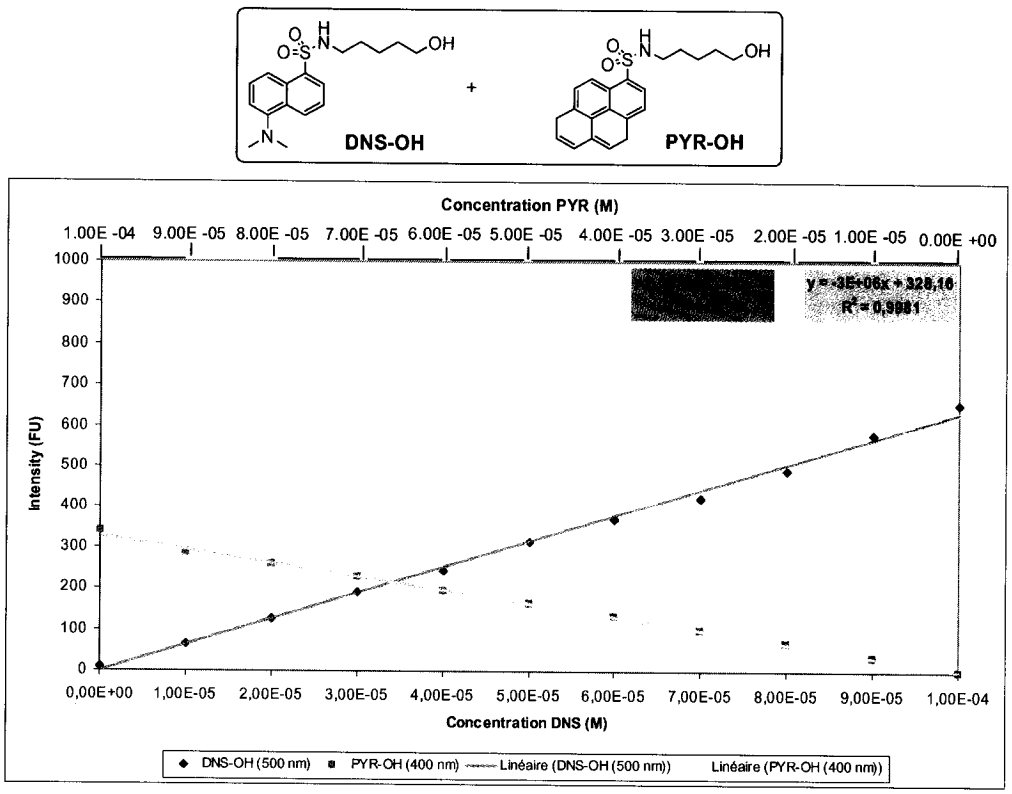

Figure 36: Calibration curve of various ratios of DNS-OH and PYR-OH mixtures.

As shown above, a linear dependence was obtained from the different samples. Also, the PYR fluorescence intensities were lower than those of DNS, possibly a result of the excitation wavelength chosen for the scans. Another calibration curve was then established considering the presence of the GBC moiety in solution after hydrolysis studying the effect of its presence on the donor's fluorescence intensity. For solubility

reasons, the GBC ester **93** was used (see 7.3.1.19). The GBC moiety was added to each solution in a manner to represent the hydrolysis course, so the same amount was added to each solution in that case. Then, fluorescence data were recorded.

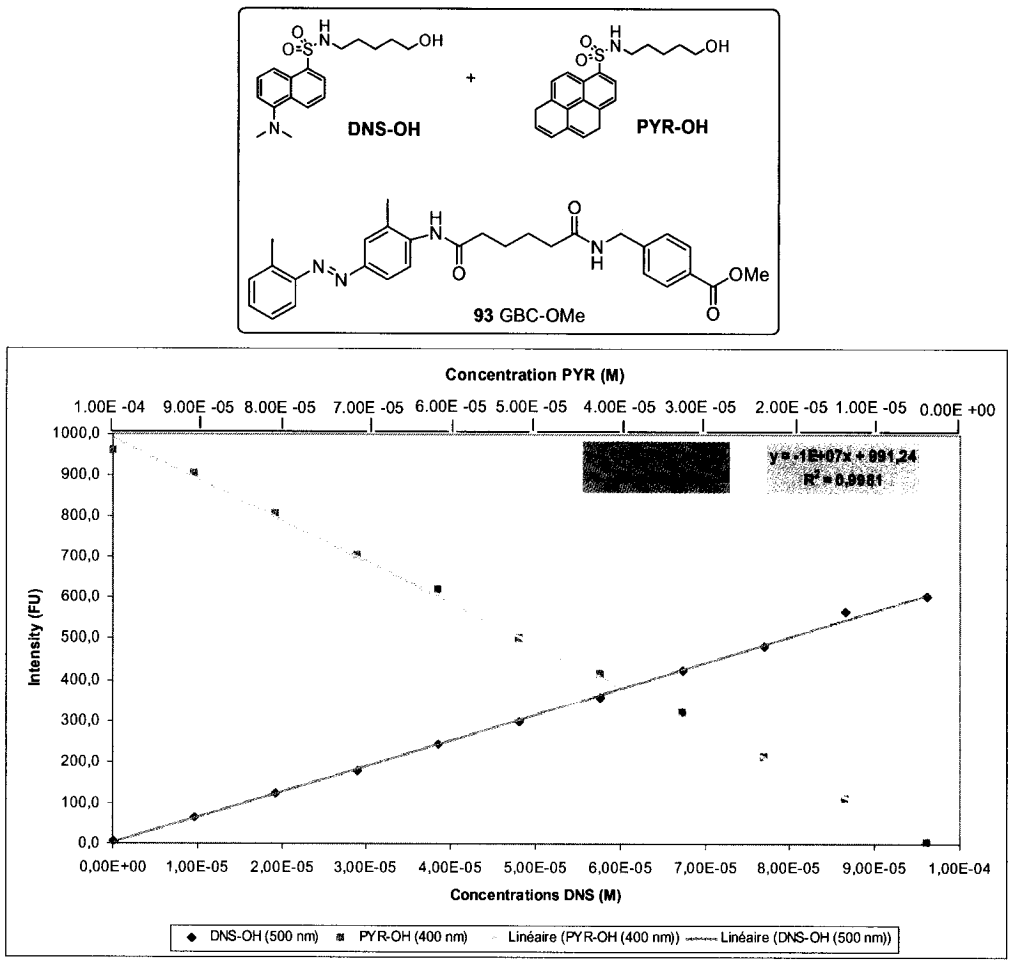

Figure 37: Calibration curve of various ratios of DNS-OH and PYR-OH mixtures with GBC ester 93.

Again, the trend was linear for both donors. The calibration experiments helped us to established standard parameters for this system in eventual scans. Thus, it was found that both donors would be excited at a wavelength of 370 nm and detection would be made at

400 nm for PYR-OH and 500 nm for DNS-OH. Depending of the concentration used the excitation and emission slits would be adjusted if necessary.

Overall, we were in need of finding a reliable enantioselective reaction to apply our concept, but this time we had in mind to keep it simple, meaning taking the substrates as they are.

CHAPTER 5

Alcalase® system

Since the number of examples of organocatalysts in enantioselective hydrolysis was limited, we turned our attention to biocatalysis. Aqueous enzymatic hydrolysis of a racemate to achieve the enantioselective preparation of chiral compounds is one of the most exploited fields in biocatalysis[92]. Therefore, we decided to find a reliable and efficient enzymatic system that would be readily adaptable to our purpose.

5.1 Biocatalysis with Alcalase®

Enzymes are attractive catalysts because of their chemo-, regio- and stereospecificity and their impressive catalytic efficiencies[93].

Alcalase® is known as a proteolytic enzyme prepared from *Bacillus Licheniformis*. Its major component is alkaline protease A (Substilisin Carlsberg), a serine protease. Alcalase is widely used as an additive in laundry detergents as a digesting enzyme. So far, its application in organic syntheses is limited, although it is an effective and inexpensive catalyst.

We focused on two reported enantioselective hydrolyses of esters using Alcalase® as an enzymatic catalyst.

The first one was reported in 1992[94] by Wang who described the use of Alcalase® to prepare amino acid derivatives, and for the selective hydrolysis of protected dipeptide esters. This procedure was able to resolve these compounds with high ee and yield. They prepared different N-protected amino acid esters by varying the protecting groups and

---

[92] Santaniello E.; Ferraboschi P.; Grisenti P.; Manzochi A. *Chem. Rev.*, **1992**, *5*, 1071.
[93] Yano Y.; Shimada K.; Okai J.; Goto K.; Matsumoto Y.; Ueoka R. *J. Org. Chem.*, **2003**, *68*, 1314.
[94] Chen S.T., Hsiao S.C., Chiou A.J., Wu S.H., Wang K.T., *J. Chin. Chem. Soc.*, **1992**, *39*, 91.

alkoxy groups on the ester. The Alcalase® was found to selectively hydrolyze the L-enantiomer.

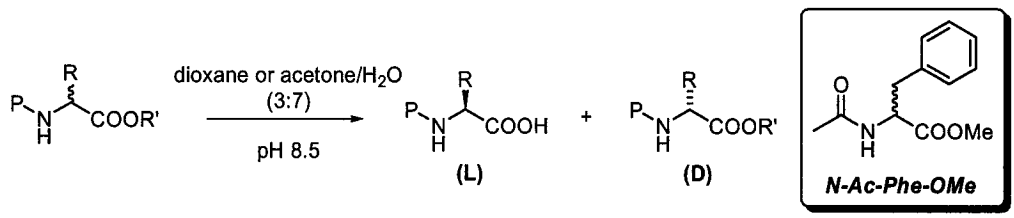

Scheme 46: Alcalase catalyzed enantioselective resolution of amino acids.

One of the best results in terms of reaction time, ee and yield was obtained by using N-acetylated phenylalanine methyl ester (N-Ac-Phe-OMe). They also extended the application for unnatural amino acids and studied the immobilization of the enzyme on Amberlite to prolong its duration of action and simplify the isolation of products.

A second reported application of Alcalase® was made in 1999 by Bailey[95]. In this report, Alcalase® was used to effect enantio- and regioselective monohydrolysis of a variety of (RS)-2-substituted succinate diesters.

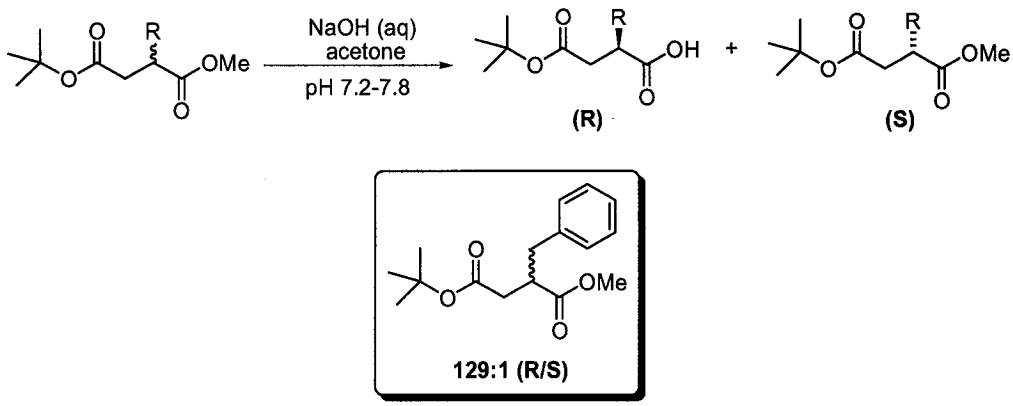

Scheme 47: Enantioselective hydrolysis with various succinate diesters.

[95] Bailey M.D., Halmos T., Adamson D., Bordeleau J., Grand-Maître C., *Tetrahedron Asymm.*, **1999**, *10*, 3285.

In that study, the R-enantiomer was selectively hydrolyzed. Different substituents α to the methyl ester were evaluated. Best results were obtained with 2-benzyl-substituted substrates. In addition, the rate of the enzymatic reaction was studied by varying the size of the ester. The rate of the reaction was influenced in this order: Me < Et < n-propyl < benzyl. It was also demonstrated that varying the temperature between 23 and 37 °C had no effect on the selectivity.

With these two applications in hand, the fact that the enzyme was strongly effective with a benzyl moiety led us to choose phenylalanine as the recognition element for our system. Moreover, the alkyl groups as spacers would seem to be appropriate.

5.2 Probes syntheses

The synthesis of both probes was straightforward since the donor and acceptor pieces were already available from our previous attempts. Donor and acceptor pairs were assigned arbitrarily to the chiral substrates. The synthesis was carried out as shown below.

5.2.1 L-isomer probe

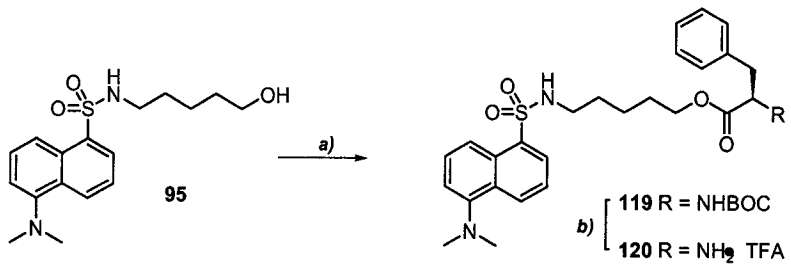

Reagents *a)* (L)-N-BOC-phenylalanine, EDC, HOBT, DIPEA, rt, *90%*. *b)* TFA, rt.

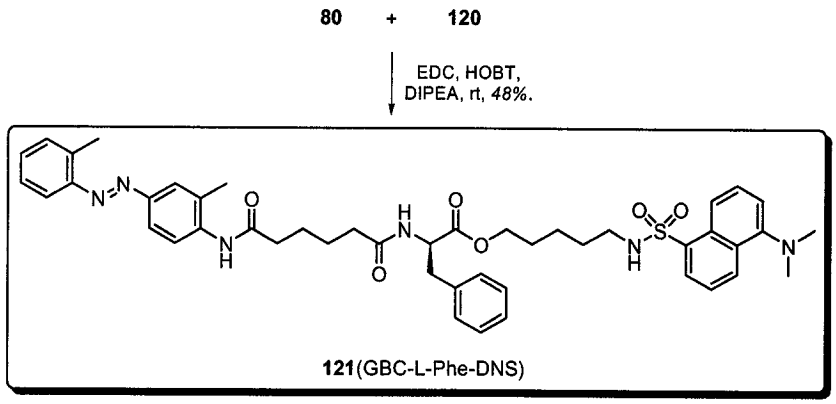

Scheme 48: Synthesis of L-isomer probe (GBC-L-Phe-DNS).

The amino acid was coupled to the donor moiety to form the carboxylate portion of the ester, followed by deprotection of the amine. Subsequent attachment of the acceptor moiety, from a crude GBC product **80**, gave the L-isomer probe **121** in reasonable yield.

5.2.2 D-isomer probe

Synthesis of the D-isomer probe was very similar to the L-isomer probe.

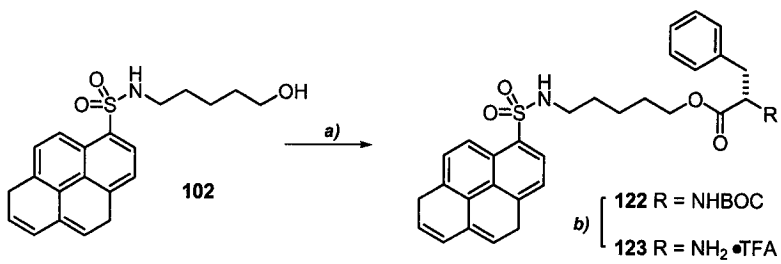

Reagents *a)* (D)-N-BOC-phenylalanine, EDC, HOBT, DIPEA, rt, *94%*. *b)* TFA, rt.

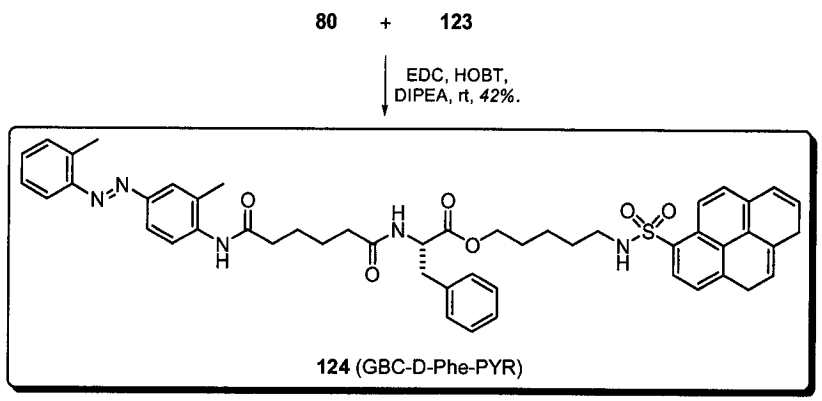

Scheme 49: Synthesis of D-isomer probe (GBC-D-Phe-PYR)

Again, the formation of the ester to be hydrolyzed was performed first followed by the attachment of the acceptor moiety to obtain the desired probe.

5.3 Hydrolysis assays

5.3.1 LiOH hydrolysis

With the two probes in hand, we first tested their hydrolytic ability with LiOH. An equimolar mixture of probes was used and aliquots were taken until complete hydrolysis. Each aliquot was washed with $NaHCO_3$ solution which removed the GBC acid product. Then, extraction with DCM was made to provide the samples so the reaction could be followed by fluorescence (see 7.3.2.1). Solvents commonly used in fluorescence are MeOH, H_2O and DMF, but in organocatalytic reactions, these are not generally used. We needed to verify fluorescence in less polar solvents such as THF and DCM. The use of

DCM seemed to be a proper solvent to recreate the organocatalyzed environment of future reactions. We were very happy to find out that DCM did not affect the fluorescence readings.

The necessity of performing such a work-up with each aliquot was due to the fact that direct reading, with proper dilution of the aliquot, gave very low fluorescence intensities. Hypothetically, this undesired effect could have been due to the enzyme coloration which would have altered the excitation beam, therefore considerably decreasing the emission intensity detection. Also, the GBC acid moiety (GBC-Phe-COOH) was known to be insoluble in DCM, so by removal of these components, we were able to recover those undesired effects and obtained adequate intensities.

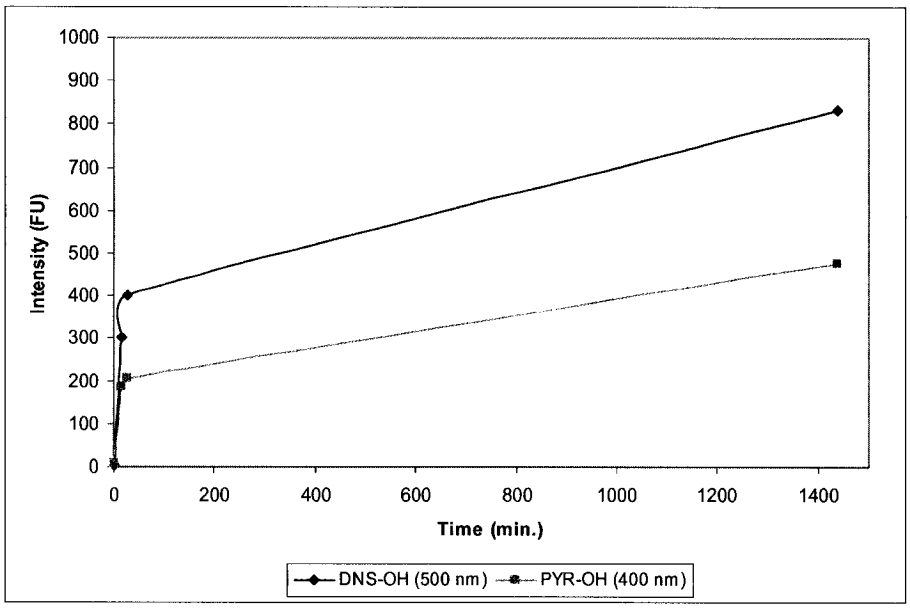

Figure 38: LiOH hydrolysis of equimolar mixture of GBC-L-Phe-DNS and GBC-D-Phe-PYR.

Readings were taken at 400 nm and 500 nm for PYR-OH and DNS-OH emission respectively with excitation at 370 nm in both cases. As is shown in **Figure 38**, both substrates were rapidly hydrolyzed in the first 25 minutes with complete hydrolysis

slowly occurring after a few hours. Since this assay was not made for kinetic studies, possible errors from the work-up step were not considered. Therefore, qualitative information cannot be drawn from this experiment. We could now pursue our experiments knowing that both probes were well hydrolyzing with distinguishable intensities.

5.3.2 Selective Hydrolysis

Using the Alcalase® this time, we set out to prove that it was possible to clearly show selectivity of a reaction by appearance of only one characteristic emission band.

5.3.2.1 Detergents

To proceed, similar conditions mentioned in the literature were used. Unfortunately, because of our bigger substrates, different solvent compositions of acetone/water or dioxane/water were not able to adequately solubilize the mixture. To solve this problem, we decided to use detergents commonly used in enzymatic reactions in water[96]. Triton x-100 (non-ionic detergent) and Zwittergent 3-12 (zwitterionic detergent) were readily available. Using an amount of each detergent above the critical micellar concentrations (CMC) in a phosphate buffer pH 7.3, the equimolar mixture of probes was tested. After stirring the mixtures for 24 hours, Zwittergent 3-12 gave the best solubility and therefore, was used for further experiments.

5.3.2.2 Alcalase® Hydrolysis

After testing probe hydrolytic abilities and finding the proper conditions, the selective enzymatic hydrolyses were performed. Before carrying out the reaction, we could predict that the L-isomer probe would be selectively hydrolyzed[94], so the appearance of the DNS-OH emission band at 500 nm would be observed.

---

[96] Srirama M. Bhairi, **A Guide to the Properties and Uses of Detergents in Biology and Biochemistry**, copyright Calbiochem-Novabiochem, 2001.

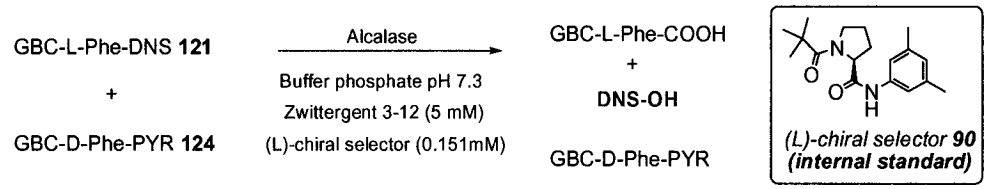

Scheme 50: Selective hydrolysis using Alcalase®.

We also added to the reaction an internal standard so as to normalize the fluorescence data by HPLC. The chosen internal standard was the readily available (L)-chiral selector **90** used in previous experiments, that was assumed to be inert under the reaction conditions and had a distinct retention time.

The mixture was prepared by dissolving an equimolar amount of each probe in phosphate buffer pH 7.3 containing Zwittergent 3-12 and stirring for 24 hours before adding the Alcalase® (see 7.3.2.2a). This pre-dissolution was found to be necessary to ensure the formation of a proper emulsion. Aliquots were taken regularly and washed with $NaHCO_3$ solution followed by extraction with DCM. The extracts were placed in a 5 mL volumetric flask. For the same reason as previously mentioned, this kind of work-up was necessary to obtain accurate results; moreover the aqueous mixture contained the detergent and the enzyme which amplified the intensity problem. Fluorescence readings were made at 400 nm (PYR-OH) and 500 nm (DNS-OH) with an excitation wavelength at 370 nm in both cases.

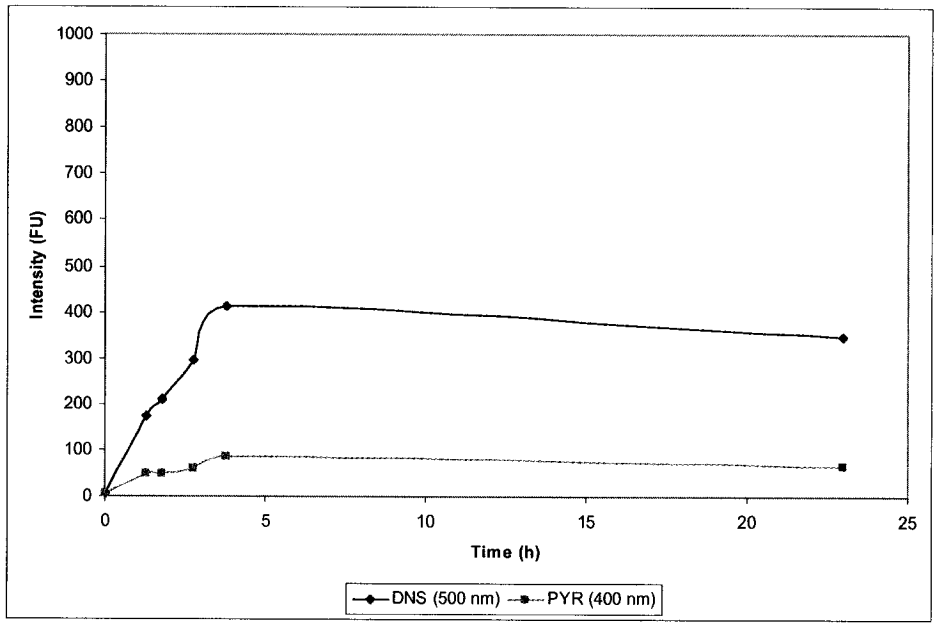

Figure 39: Fluorescence intensity versus time in the selective hydrolysis using Alcalase®.

We were glad to observe what might be a selective hydrolysis of the L-probe as demonstrated by the appearance of emission at 500 nm only. Little signal was observable at the pyrene emission wavelength (400 nm) which was possibly due to a small percentage of hydrolysis in these conditions. Again, because of the necessity of the work-up step, the curve obtained was not perfect. To verify these fluorescence data and their concentrations, we submitted all the samples onto the HPLC (see 7.3.2.2b).

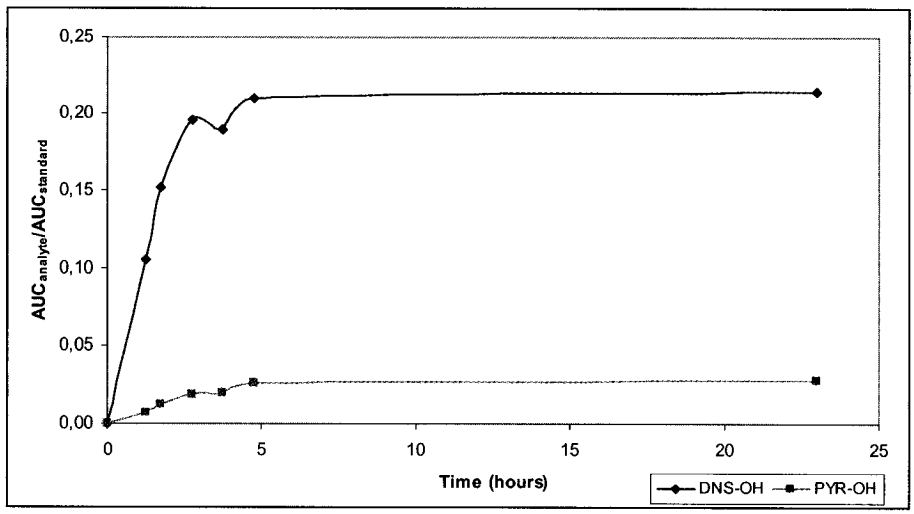

Figure 40: Selective hydrolysis using Alcalase® followed by HPLC.

A similar curve was obtained by HPLC, showing again the selectivity of the reaction for the L-probe. To validate the accuracy of the work-up step, the experimental concentrations of each donor part could be calculated with the AUC values (see 7.3.2.2b). With these HPLC data, we were able to determine the conversion and the enantiomeric excess which were respectively 57% and 89%. We did not push the reaction to completion which might have been necessary to really prove the selectivity of the reaction. In the next section, we established calibration curves of fluorescence intensities versus the calculated concentration. Therefore, it would be possible to compare the ee obtained by HPLC and fluorescence.

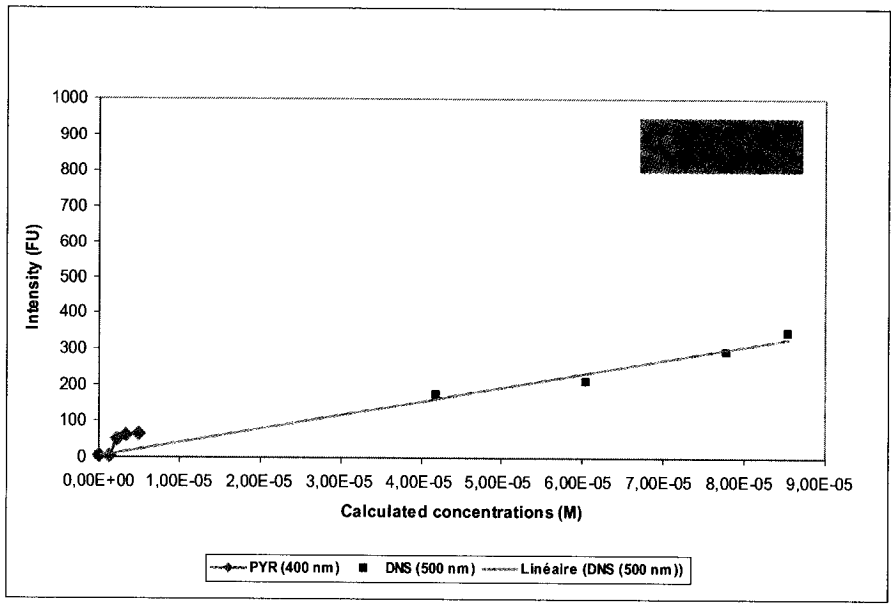

Figure 41: Fluorescence intensities versus calculated concentrations for the Alcalase® hydrolysis.

A linear relation was observed. The expected concentration of the donor moiety after completed hydrolysis was 1.51 x 10^{-4} M. We could see that the last aliquot taken had a lower concentration, meaning that the reaction may not have been totally completed, in contrast to the fluorescence data which suggested that the reaction was over. The work-up step could be the reason for this difference.

5.3.2.3 Overall

The experiments described above have shown the potential of our fluorescence method. Adjustments were of course to be made since the selective reaction chosen did not reflect perfectly the evolution of the hydrolysis, meaning that so far, our method could be use on a qualitative basis.

Therefore, we decided to pursue our experiments by establishing calibration curves that could mimic the eventual reaction in organic media. Consequently, quantitative information would be directly extracted from the fluorescence data.

5.3.3 Calibration curves

Solutions had to be prepared in a way to recreate a wide range of possible results. Since it was discovered that the GBC hydrolyzed product (GBC-Phe-COOH) had to be removed, we prepared solutions containing 4 components: GBC-L-Phe-DNS (L-probe), GBC-D-Phe-PYR (D-probe), DNS-OH and PYR-OH. Also, we added the same internal standard used previously to support the FRET data by HPLC data. The solutions were set up following 5 different situations: 1) Reaction selective to L-probe, 2) Reaction selective to D-probe, 3) Reaction non-selective: L-probe hydrolyzed in different ratios, while D-probe was kept constant at 50 % hydrolysis, 4) Reaction non-selective: D-probe hydrolyzed in different ratios, while L-probe was kept constant at 50 % hydrolysis and 5) Reaction non-selective: random ratios of hydrolysis for both probes. The concentration of each component in the solutions varied between 0 and 1.51 x 10^{-4} M which corresponded to a ratio of 0 to 10:1 (see 7.3.2.3).

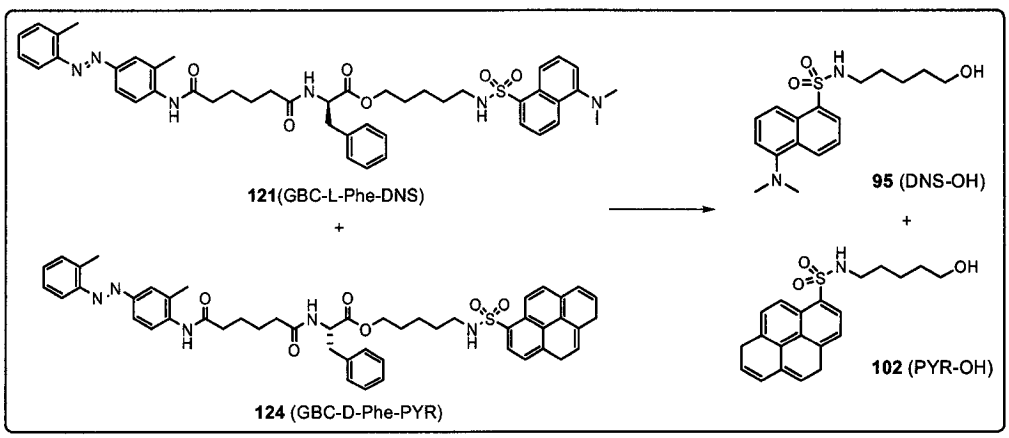

sln	GBC-L-Phe-DNS 121	DNS-OH 95	GBC-D-Phe-PYR 124	PYR-OH 102
	Selective to L-probe			
1	10	0	10	0
2	9	1	10	0
3	8	2	10	0
4	7	3	10	0
5	6	4	10	0
6	5	5	10	0
7	4	6	10	0
8	3	7	10	0
9	2	8	10	0
10	1	9	10	0
11	0	10	10	0
	Non-selective: D-probe constant at 50 % hydrolysis			
12	10	0	5	5
13	9	1	5	5
14	8	2	5	5
15	7	3	5	5
16	6	4	5	5
17	5	5	5	5
18	4	6	5	5
19	3	7	5	5
20	2	8	5	5
21	1	9	5	5
22	0	10	5	5
	Non-selective: L-probe constant at 50 % hydrolysis			
23	5	5	0	10
24	5	5	1	9
25	5	5	2	8
26	5	5	3	7
27	5	5	4	6
28	5	5	5	5
29	5	5	6	4
30	5	5	7	3
31	5	5	8	2
32	5	5	9	1
33	5	5	10	0
	Selective to D-probe			
34	10	0	10	0
35	10	0	9	1
36	10	0	8	2
37	10	0	7	3
38	10	0	6	4
39	10	0	5	5
40	10	0	4	6
41	10	0	3	7

42	10	0	2	8
43	10	0	1	9
44	10	0	0	10
	Random			
45	7	3	2	8
46	2	8	6	4
47	9	1	3	7
48	6	4	9	1
49	3	7	7	3
50	4	6	1	9
51	1	9	4	6
52	8	2	3	7
53	7	3	8	2
54	2	8	9	1
55	0	10	2	8

Table 2: 55 solutions for the calibration curves.

Table 2 summarizes the composition of each solution prepared. In all cases, the same amount of internal standard was added. Fluorescence acquisitions were made in the same fashion as described for earlier experiments, in which emissions detected at 400 nm and 500 nm for PYR-OH and DNS-OH respectively for the 55 solutions prepared. By establishing plots of fluorescence intensities versus concentration, we would eventually be able to directly convert these intensities to % ee.

Unfortunately, we had to use the cell holder which meant that each sample was read individually instead of using the plate reader, which would be considerably more efficient in terms of acquisition time (less than couple of minutes to read the whole plate). The reason for this was that the 96-well polystyrene plates available melted on contact with DCM. With the HPLC data, we were able to correct the concentrations of each component in the samples and plot these values with the intensities obtained. But first, plots of theoretical concentrations versus calculated concentrations were created to evaluate the precision of the prepared solutions.

a) Selective to L-probe (solutions 1-11)

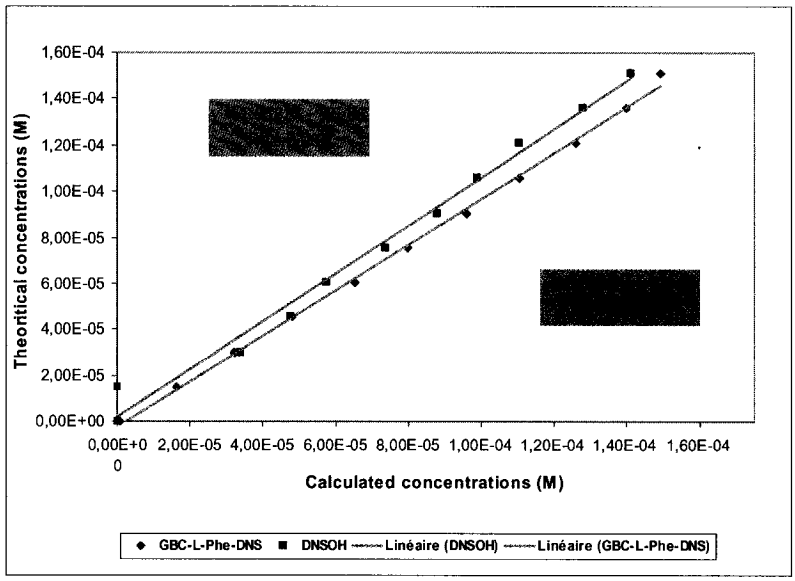

b) Selective to D-probe (solutions 34-44)

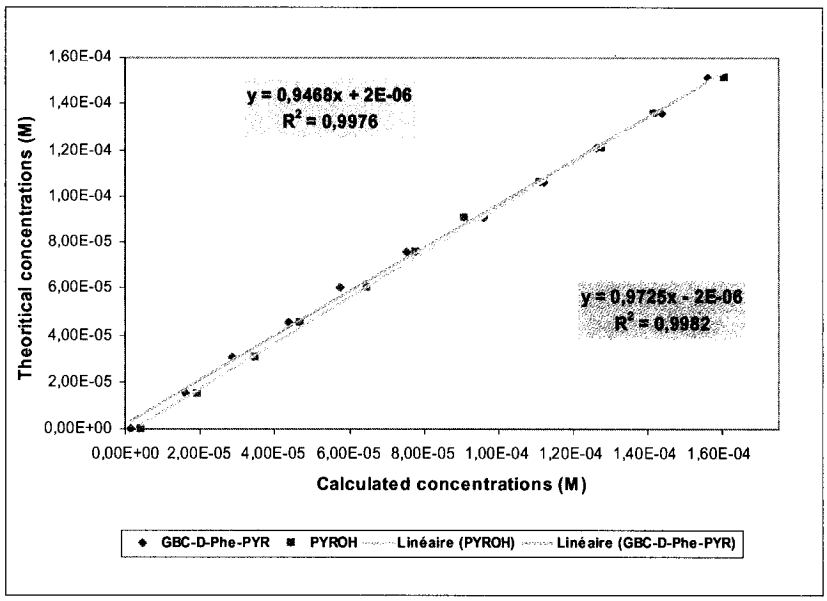

c) Non-selective: L-isomer varied while D-isomer constant at 7.55 x10^{-5} M (50 % hydrolysis, solutions 12-22)

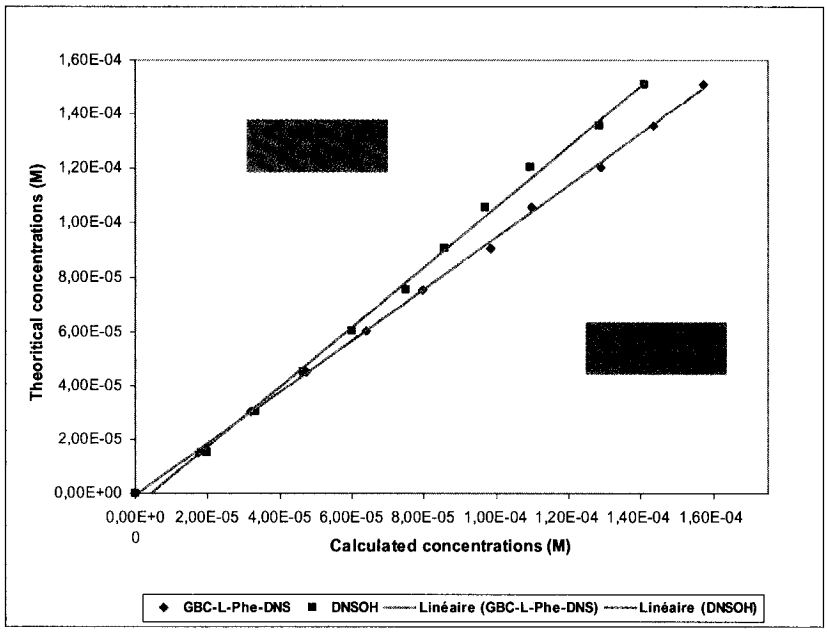

d) Non-selective: D-isomer varied while L-isomer constant at 7.55 x 10^{-5} M (50 % hydrolysis, solutions 23-33)

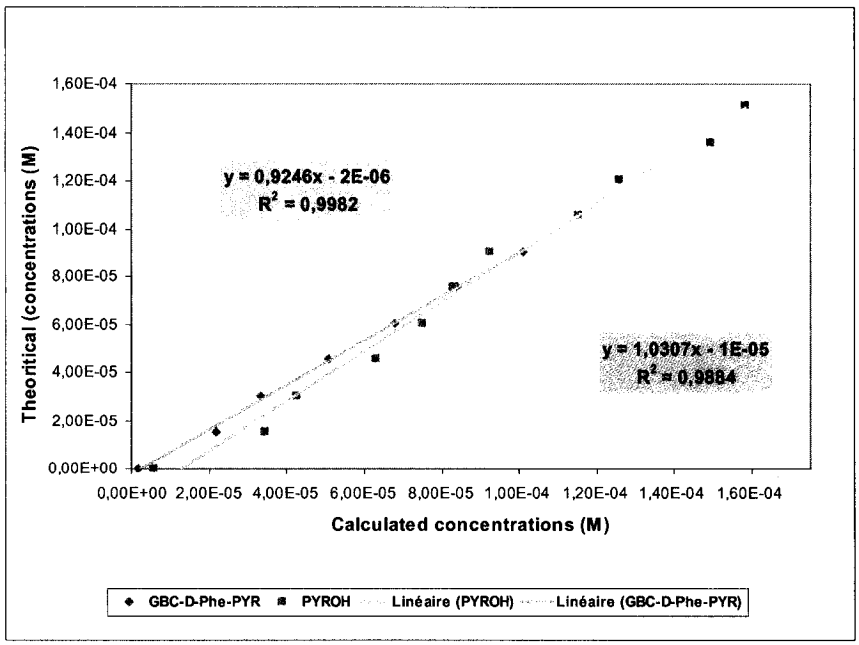

e) Random (solutions 45-55)

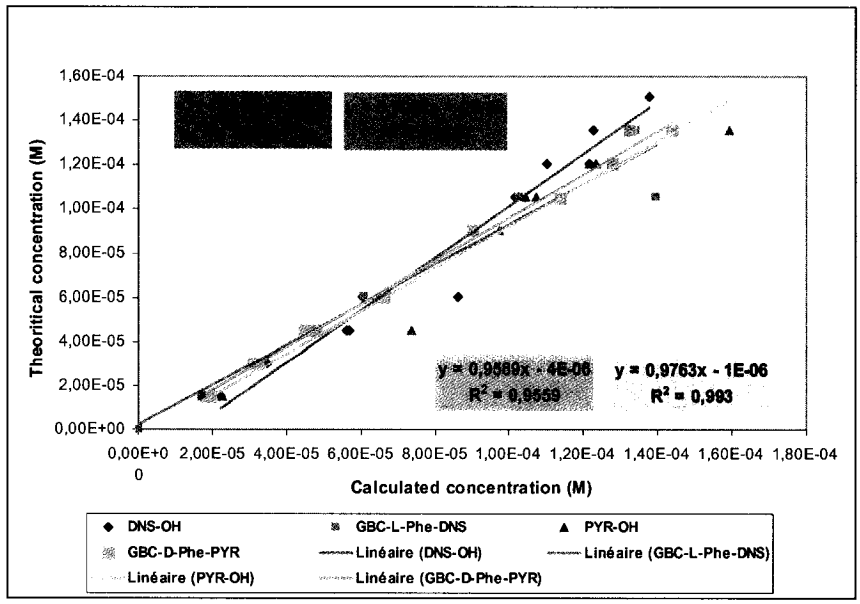

Figure 42: Theoretical concentrations versus calculated concentrations for the calibration solutions.

These plots showed a good precision in the preparation of the solutions in which a slope of 1 would mean a perfect correspondence between the amount of each component and their calculated concentrations. In all cases, a nearly 1:1 correspondence was observed, indicating that the concentrations used were accurate.

Knowing that our solutions were reliable, plots of fluorescence intensities versus calculated concentrations were then established.

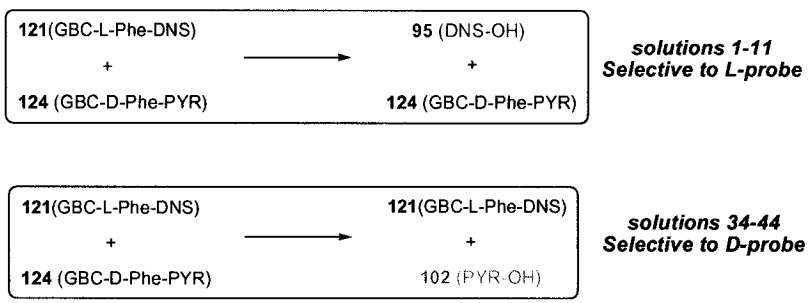

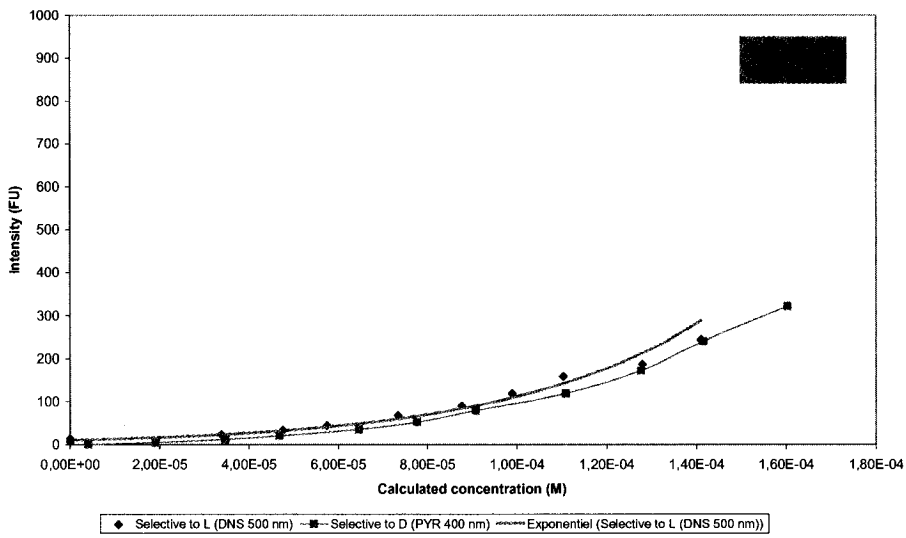

Figure 43: Fluorescence intensities versus calculated concentrations in a selective context (to L-probe: solutions 1-11; to D-probe: solutions 34-43)

For this first set of solutions, in a selective context, both curves showed an exponential relation. We were a bit surprised by these curves since we thought they should have been linear because of Beer-Lambert's law at low concentration.

121(GBC-L-Phe-DNS)
+
124 (GBC-D-Phe-PYR)

→

121(GBC-L-Phe-DNS) + **95** (DNS-OH)

124 (GBC-D-Phe-PYR) + 102 (PYR-OH)

constant at 50 % hydrolysis

solutions 12-22

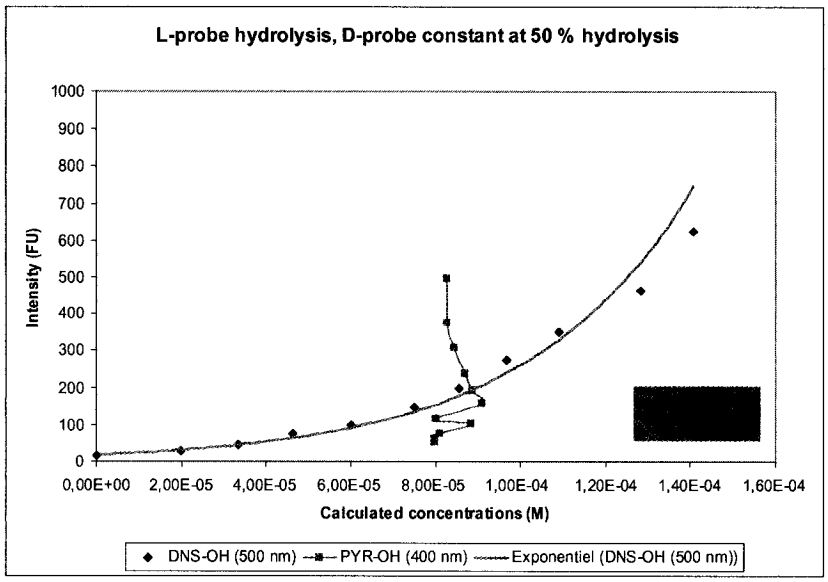

121(GBC-L-Phe-DNS)
+
124 (GBC-D-Phe-PYR)

→

121(GBC-L-Phe-DNS) + **95** (DNS-OH)
constant at 50 % hydrolysis
124 (GBC-D-Phe-PYR) + 102 (PYR-OH)

solutions 23-33

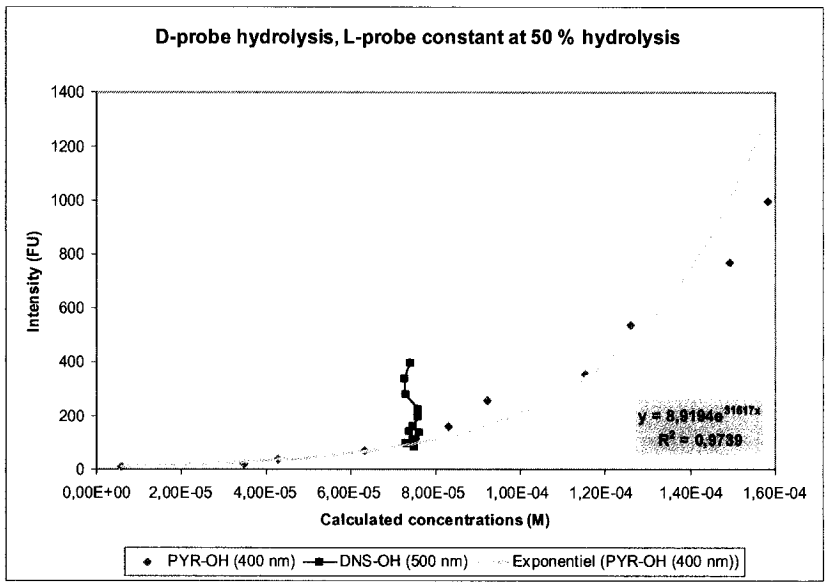

Figure 44: Fluorescence intensities versus calculated concentrations in a non-selective context (solutions 12-22 and solutions 23-33)

For the next sets, in a non-selective context, an exponential relation was again observed. Since in these sets one of the donors was maintained at a constant concentration corresponding at 50 % hydrolysis, we were expecting that the fluorescence intensity would be represented by a single spot on the graphic. Instead, an increase of the intensity was observed. Our only explanation for this situation would come from the fact that the GBC moiety in solution was not well represented. The GBC moiety, on the probes or as the hydrolysis product, should create intra- and intermolecular quenching respectively because of its absorbance. By excluding the GBC acid hydrolysis product, the intermolecular quenching was therefore absent which would affect the fluorescence emission of both donors. This hypothesis could be confirmed by the previous linear calibration curves made with the help of Ami J. Chin in which a proportional amount of GBC moiety was added to a mixture of DNS-OH and PYR-OH to account the probes and the hydrolysis product.

As we have mentioned previously, it would be possible to compare the conversion and the enantiomeric excess obtained by HPLC and fluorescence. But, because of the omission of the GBC moiety, the calibration curves established with the fluorescence intensities to represent the actual system was no longer acceptable and the comparison between these data would not be representative.

With the fluorescence data obtained from this experiment, we tried to establish a mathetical relation that could normalize this effect, but nothing simple and relevant was found.

We then reconsidered the process by preparing another set of solutions, this time carefully adding the correct amount of GBC hydrolysis product.

5.3.4 Calibration Curves (attempt #2)

We found out that the presence of the GBC acid hydrolysis product was an important component in the solutions. Since, as previously mentioned, the acid was not soluble in DCM, we used the ethyl ester instead (GBC-D-Phe-OEt **125**). In addition, we knew from

earlier tests that the presence of this component lowered significantly the fluorescence intensity.

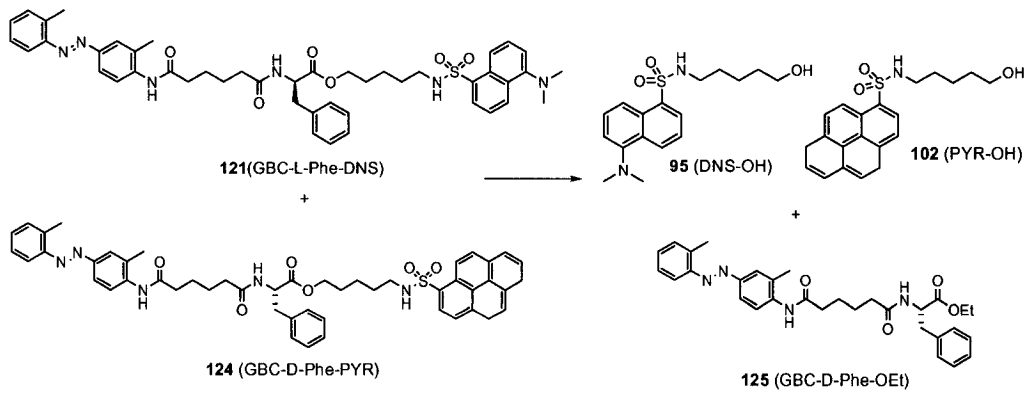

sln	GBC-L-Phe-DNS 121	DNS-OH 95	GBC-D-Phe-PYR 124	PYR-OH 102	GBC-D-Phe-OEt 125
	Selective to L-probe				
1	10	0	10	0	0
2	9	1	10	0	1
3	8	2	10	0	2
4	7	3	10	0	3
5	6	4	10	0	4
6	5	5	10	0	5
7	4	6	10	0	6
8	3	7	10	0	7
9	2	8	10	0	8
10	1	9	10	0	9
11	0	10	10	0	10
	Non-selective: D-probe constant at 50 % hydrolysis				
12	10	0	5	5	5
13	9	1	5	5	6
14	8	2	5	5	7
15	7	3	5	5	8
16	6	4	5	5	9
17	5	5	5	5	10
18	4	6	5	5	11
19	3	7	5	5	12
20	2	8	5	5	13
21	1	9	5	5	14
22	0	10	5	5	15
	Non-selective: L-probe constant at 50 % hydrolysis				

23	5	5	0	10	**15**
24	5	5	1	9	**14**
25	5	5	2	8	**13**
26	5	5	3	7	**12**
27	5	5	4	6	**11**
28	5	5	5	5	**10**
29	5	5	6	4	**9**
30	5	5	7	3	**8**
31	5	5	8	2	**7**
32	5	5	9	1	**6**
33	5	5	10	0	**5**
	Selective to D-probe				
34	10	0	10	0	**0**
35	10	0	9	1	**1**
36	10	0	8	2	**2**
37	10	0	7	3	**3**
38	10	0	6	4	**4**
39	10	0	5	5	**5**
40	10	0	4	6	**6**
41	10	0	3	7	**7**
42	10	0	2	8	**8**
43	10	0	1	9	**9**
44	10	0	0	10	**10**
	Random				
45	7	3	2	8	**11**
46	2	8	6	4	**12**
47	9	1	3	7	**8**
48	6	4	9	1	**5**
49	3	7	7	3	**10**
50	4	6	1	9	**15**
51	1	9	4	6	**15**
52	8	2	3	7	**9**
53	7	3	8	2	**5**
54	2	8	9	1	**9**
55	0	10	2	8	**18**

Table 3: 55 solutions for the calibration curves adding GBC-D-Phe-OEt 125

Once all these solutions were prepared, their fluorescence intensities were recorded one by one using a quartz cell. Again, each of the solution contained an equal amount of

internal standard, the (L)-chiral selector **90**, to obtain accurate concentrations by HPLC. Plots of theoretical concentrations versus calculated concentrations were created to evaluate the precision of the prepared solutions (see 7.3.2.4).

a) Selective to L-probe (sln 1-11)

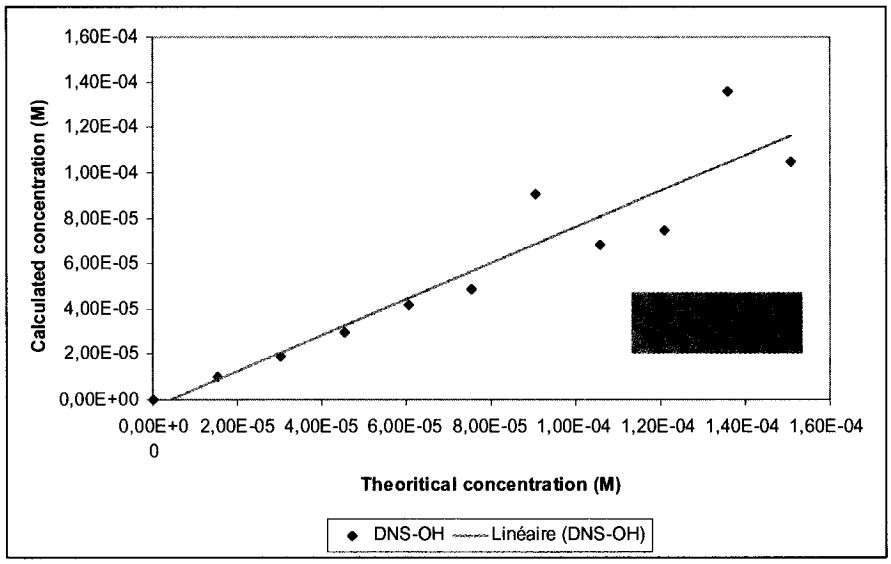

b) Selective to D-probe (sln 34-44)

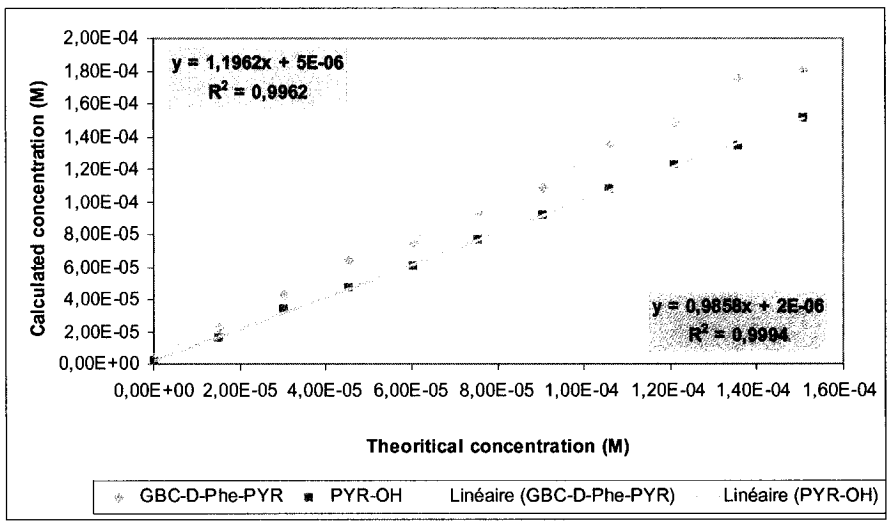

c) Non-selective: L-isomer varied while D-isomer constant at 7.55 x10^{-5} M (50 % hydrolysis, sln 12-22)

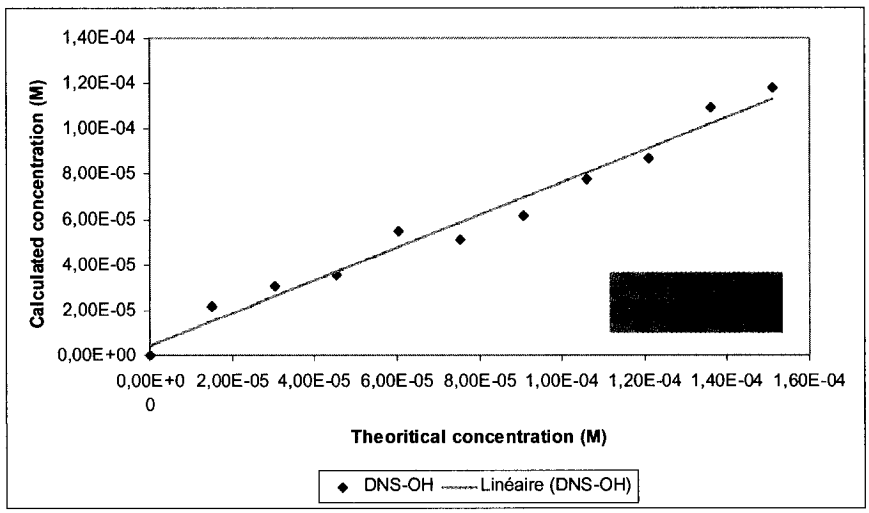

d) Non-selective: D-isomer varied while L-isomer constant at 7.55 x 10^{-5} M (50 % hydrolysis, sln 23-33)

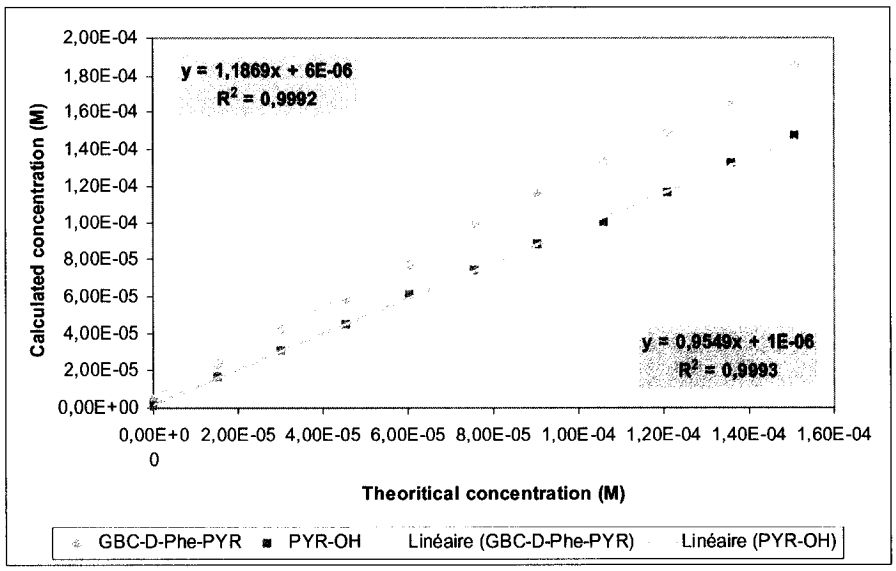

e) Random

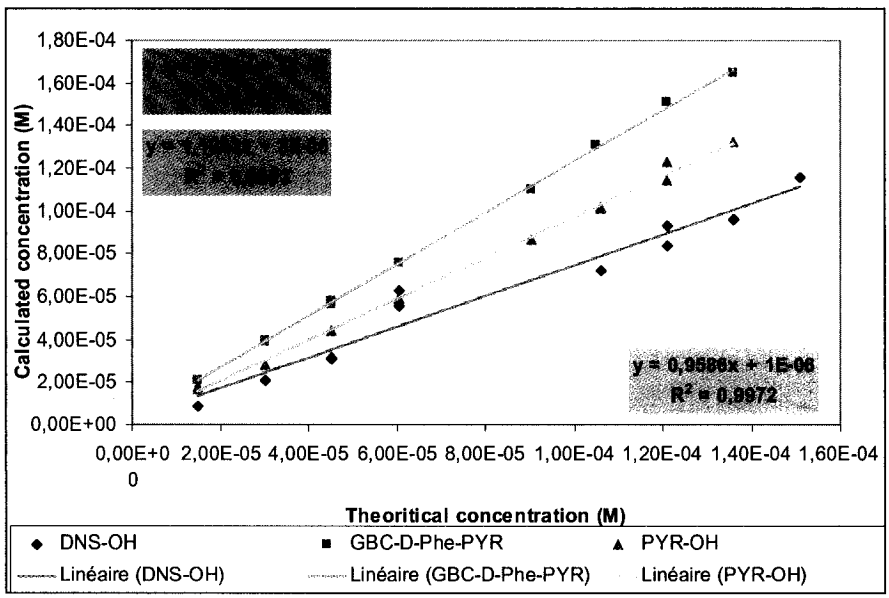

Figure 45: Theoretical concentrations versus calculated concentrations for the calibration solutions (attempt #2).

Unfortunately, separation of the GBC-L-Phe-DNS and the GBC-D-Phe-OEt could not be obtained; therefore we were not able to calculate their real concentrations. These plots however showed a good precision in the preparation of the solutions in which a slope of 1 would mean a perfect correspondence between the amount of each component and their calculated concentrations. An almost 1:1 correspondence was again found, indicating that our concentrations were accurate.

Before recording all the fluorescence data, we reevaluate the excitation wavelength at 370 nm and the slits at 5 nm used in previous experiment. We took both selective sets (solutions 1-11 and 34-44, **Table 3**) to have ideal results. The first screening was performed with these standard parameters, but unfortunately the range of the fluorescence intensities in both cases was very low, above 80 FU and even at the lowest concentration, it reached the negative scale. Therefore, we decided to increase the slits to 10 nm and at

the same time varied the excitation wavelength to assess the best parameters. The results obtained are shown in **Figure 46.**

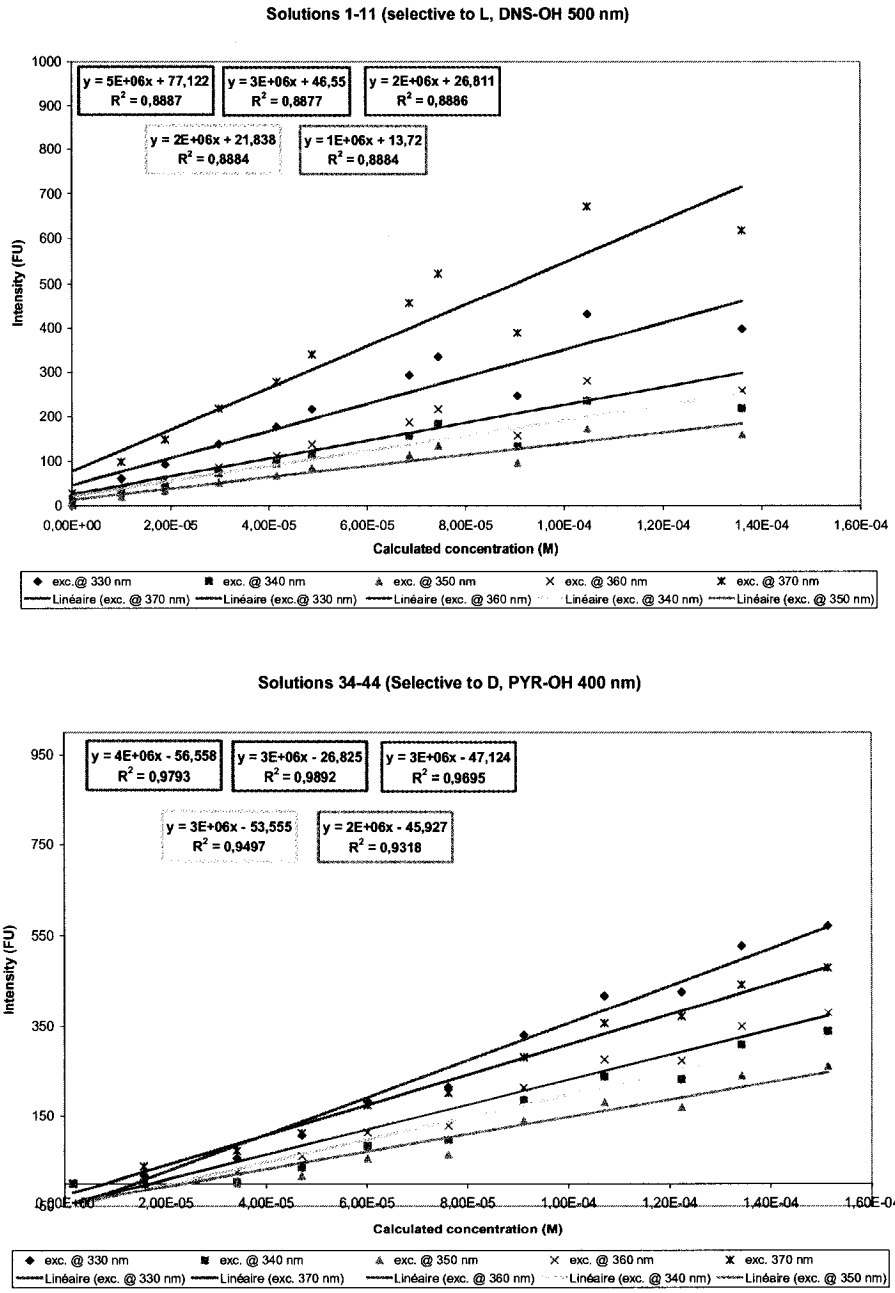

Figure 46: Calibration curves of solutions 1-11 and 34-44 while varying the excitation wavelength (slits at 10 nm)

The dansyl probe gave the highest intensity signal when excitation was done at 370 nm. As for the pyrene probe, it gave the best intensities when excited at either 330 or 370 nm. Happily, all the curves were linear and satisfying fluorescence intensities were obtained with the slits at 10 nm. Again, adjusting the excitation wavelength at 370 nm seemed to be a good choice for the detection of DNS-OH and PYR-OH. Considering these two parameters, fluorescence readings of the other sets of solutions were performed and plots of the calculated concentration, from the HPLC data, versus the fluorescence intensities was also established.

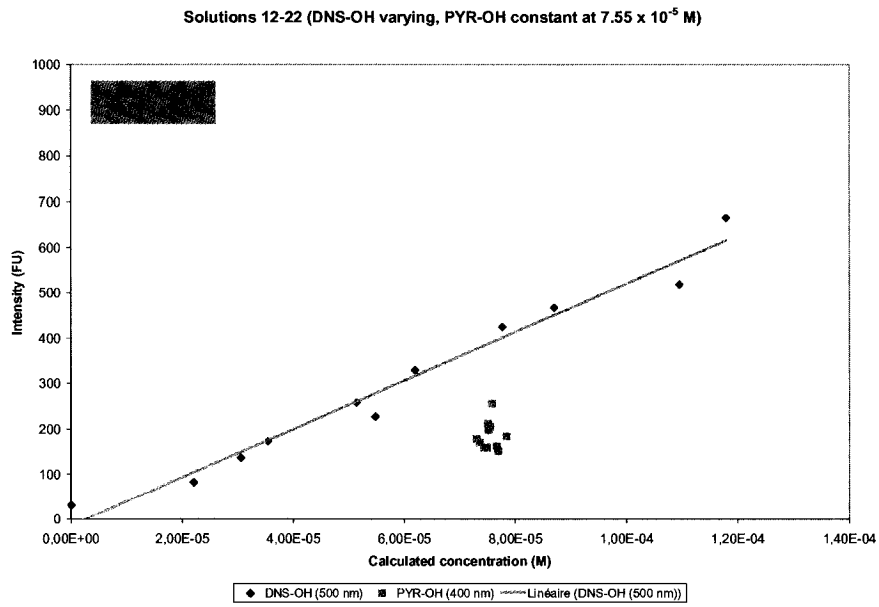

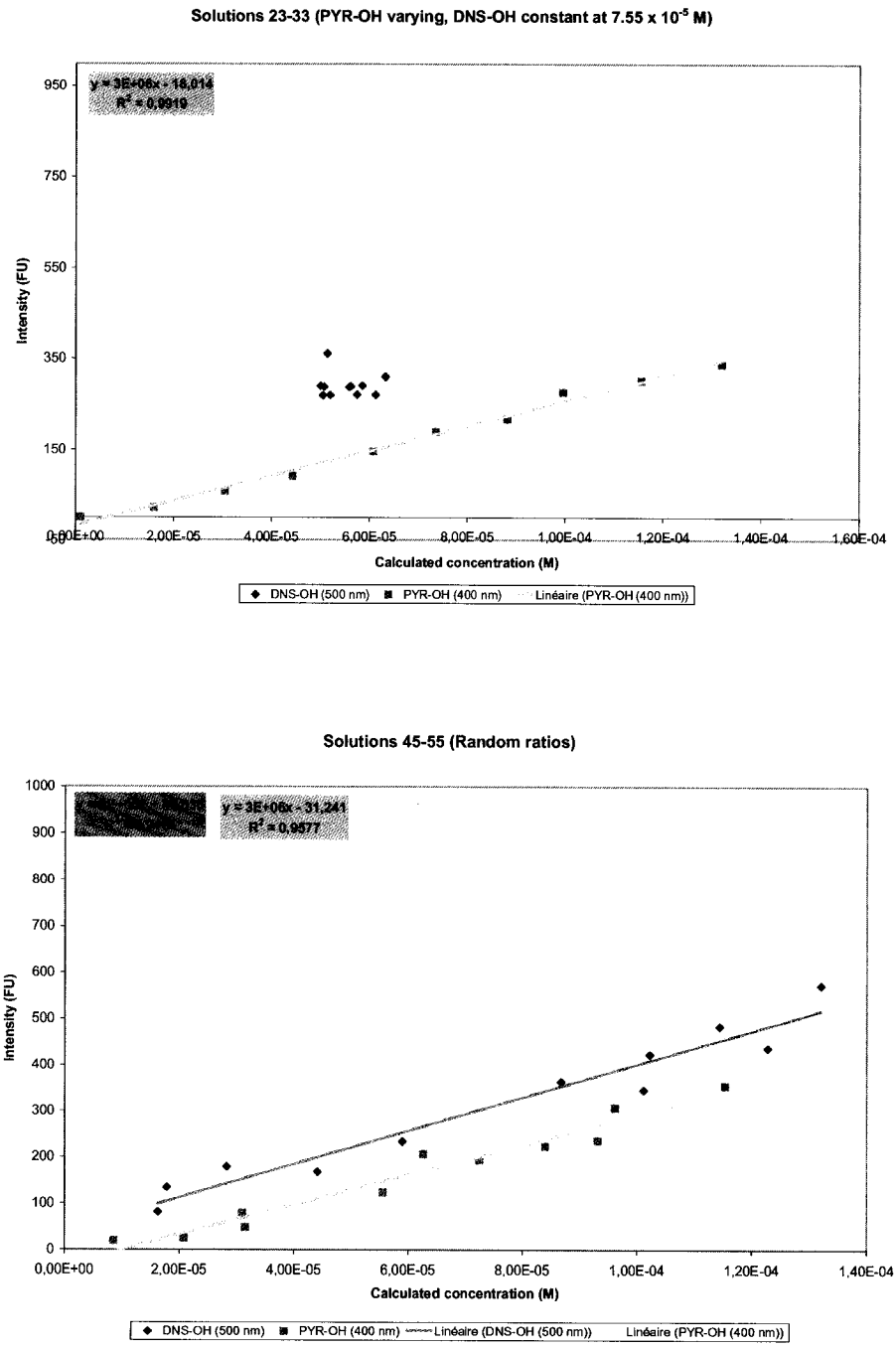

Figure 47: Calibration curves of solutions 12-22, 23-33 and 45-55.

As we can see above, the curves for each set were linear. In addition, from one set to another, the fluorescence intensities for each donor moiety were similar at a given concentration, meaning that direct reading of fluorescence emission could be converted in a precise quantity of substrate without being affected by the presence of the other components in the mixture. Of course, these values were not perfect since only one set of each solution have been prepared. Also, the presence of clusters in the plots of solutions 12-22 and 23-33 represented the fluorescence intensity of the donor kept at a constant concentration in each solution, which in an ideal situation would be represented by a single spot.

Having these satisfying results, we pursued our experiment by testing acquisition using a polypropylene 96-well plate which was resistant to DCM. By filling the wells with 300 µL of each solution, the plate was ready to be read by the fluorescence spectrophotometer.
The only problem encountered during this procedure was the fact that the DCM solutions quickly evaporated; therefore the fluorescence data collected was affected by this undesired effect. Even if the reading of the 55 wells took less than 3 minutes, the DCM was still a problem. To solve this issue, the DCM should be replaced by another solvent such as DMF, for example, in future experiments.

5.3.5 Conclusion

Despite these satisfying results, further experiments need to be accomplish to really ensure the precision of this method. Therefore, many sets of solutions have to be prepared to assess the reproducibility and subsequently, calculating an average fluorescence intensity that would be more accurate for each solution.

In terms of application of this FRET methodology, another enantioselective system from the literature should be considered in which direct aliquots could be taken from the reaction mixture and submit to the spectrofluorometer, therefore to establish a comparison with the calibration curve obtain from the 55 solutions. In this order, the use

of DCM as solvent would not be the best option even if its interference in fluorescence was negligible. Less volatile solvents are to be found.

CHAPTER 6

Claims to Original Research

1. Developed a novel high throughput screening using FRET technology to monitor an enantioselective reaction.

2. Surveyed different donor/acceptor pairs and discovered new ones such as NPN/GBC and BRN/GBC. These were found to be unsuitable when in the same mixture as DNS donor, but could be exploited otherwise.

3. Applied our novel methodology on already existent selective systems demonstrating its feasibility. Using phenylalanine-based probes, the enzyme Alcalase® hydrolyzed selectively the L-isomer probe which was observed by the appearance of a fluorescence emission at 500 nm (dansyl moiety). Establishment of calibration curves were made to prove possible quantification.

CHAPTER 7

Experimental

7.1 General

All reactions were performed under nitrogen atmosphere with oven-dried glasswares. All anhydrous solvents were distilled prior to use: tetrahydrofuran (THF) over sodium/benzophenone ketyl; benzene and dichloromethane were distilled over calcium hydride. Starting materials and reagents were obtained commercially and used as such. Column chromatographies were performed with silica gel 60 (230-400 mesh, Merck). ^{1}H NMR and ^{13}C NMR were recorded on Bruker AMX instruments at 300 MHz and 75 MHz, respectively. Chemical shifts are reported in ppm δ units relative to chloroform (7.26 ppm for ^{1}H NMR and 77.0 ppm for decoupled ^{13}C NMR) as internal standard unless noted otherwise. Melting points were uncorrected. IR spectra were recorded with a Bomen Michaelson 100 FTIR instrument. Mass spectra were recorded at The University of Ottawa Mass Spectrum Center. Fluorescence spectra were recorded with a fluorescence spectrophotometer Cary Eclipse Varian and UV spectra with a Varian Cary 1E spectrophotometer using a quartz cell (l = 1 cm), polystyrene microtiter plat 96-wells Microfluor® 2 white from Thermo Labsystems (No. 7905) and polypropylene 96-well plate white 300 µL from NUNC. Optical rotation ($[\alpha]_D$) were taken with a Perkin-Elmer 241 polarimeter in chloroform. HPLC data were recorded on a Varian Prostar equipped with a Varian Polaris C18 A-5u 250x046 mm (pumps Model PS210, PDA detector Model 330 and autosampler Prostar 430) and for chiral HPLC, a Waters 2690 equipped with a Chiralpak AS (4.6 x 250 mm) chiral column and Waters PDA detector 996.

7.2 Procedures and characterizations

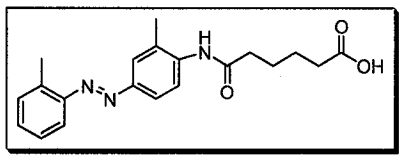

Compound 80: 6-[N-(2-methyl-4-(o-tolyldiazenyl)benzene)]amino-6-oxohexanoic acid

Fast Garnet Base GBC (1.42 g, 6.32 mmol) and adipic anhydride[97] (810.2 mg, 6.32 mmol) were dissolved in 30 mL benzene. The mixture was refluxed for 10 hours. The brown precipitate formed was filtered and washed with ether several times, until the filtrate became clear. No further purification of the product was done. 1.94 g (87 %) of crude brown product **80** was obtained. That was used without any further purification. For characterization, the crude was dissolved in MeOH and filtered. The filtrate was concentrated under reduced pressure, then dissolved in a saturated solution of $NaHCO_3$ and extracted with EtOAc. The aqueous layer was acidified with concentrated HCl and the precipitate formed was filtered washing with water and then hexanes. The beige solid was dried under vacuum. IR (film, cm^{-1}) 3293, 2952, 2876, 1694, 1660, 1530; ^1H NMR (300 MHz, DMSO-d_6) δ 12.10 (br, 1H), 9.40 (s, 1H), 7.75-7.69 (m, 3H), 7.53 (d, 7.8 Hz, 1H), 7.42-7.39 (m, 2H), 7.33-7.26 (m, 1H), 2.66 (s, 3H), 2,41 (t, 6.2 Hz, 2H), 2.32 (s, 3H), 2.26 (t, 6.3 Hz, 2H), 1.69-1.51 (m, 4H); ^{13}C NMR (75 MHz, DMSO-d_6) δ 173.3(s), 172.2(s), 150.9(s), 149.8(s), 140.4(s), 138.2(s), 132.5(s), 132.3(s), 131.9(d), 127.5(d), 125.5(d), 125.4(d), 121.4(d), 115.9(d), 36.5(t), 34.3(t), 25.7(t), 25.0(t), 18.9(q), 18.0(t); MS (EI) 353, 234, 106, 91, 55.

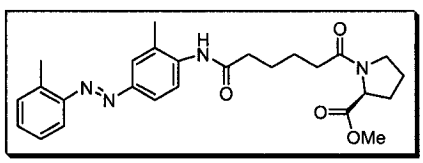

Compound 81: (S)-methyl 1-[6-(N-(2-methyl-4-(o-tolyldiazenyl)benzene))amino-6-oxohexanoyl]pyrrolidine-2-carboxylate

L-Proline methyl ester (49.4 mg, 0.18 mmol), DIPEA (0.10 mL, 0.56 mmol) and HOBT (28.6 mg, 0.21 mmol) were dissolved in 10 mL of dry DMF, followed by the addition of crude **80** (50.0 mg, 0.14 mmol) and EDC (32.8 mg, 0.21 mmol). The mixture was

[97] Hicks T.A.; Smith C.E.; Nigel Williamson W.R.; Day E.H. *J.Med.Chem.*, **1979**, *22*, 1460.

allowed to stir at room temperature for 12 hours. The clear solution was concentrated under reduced pressure and dissolved in EtOAc. Sequenced washes of the organic layer were done with 10 % HCl, saturated $NaHCO_3$ and brine. The organic layer was dried over $MgSO_4$, filtered and concentrated under reduced pressure to obtain a crude product that was purified on silica gel eluting with EtOAc: Hexanes. 30.3 mg (46 %) of product **81** was obtained as an orange oil. $[\alpha]_D$ ($CHCl_3$, c = 1) -39.6°; IR (film, cm^{-1}) 3279, 2954, 2876, 2356, 2340, 1747, 1652, 1529, 1194; ^1H NMR (300 MHz, $CDCl_3$) δ 8.11 (br s, 1H); 7.97 (m, 1H), 7.77-7.67 (m, 2H), 7.56 (d, 8.0 Hz, 1H), 7.34-7.15 (m, 3H), 4.46-4.33 (m, 1H), 3.63-3.52 (m, 4H), 3.50-3.37 (m, 1H), 2.66 (s, 3H), 2.47-2.22 (m, 7H), 2.22-1.61 (m, 8H); ^{13}C NMR (75 MHz, $CDCl_3$) δ 173.3 (s), 172.2 (s), 151.1 (s), 150.0 (s), 139.1 (s), 138.2 (s), 131.6 (d), 131.0 (d), 130.2 (d), 125.2 (s), 123.6 (d), 122.0 (d), 115.7 (d), 59.0 (q), 52.6 (d), 47.4 (t), 37.2 (t), 34.3 (t), 29.6 (t), 25.8 (t), 25.1 (t), 24.0 (t), 18.5 (q), 17.9 (q).; MS (EI) 464, 336, 240, 91, 70.

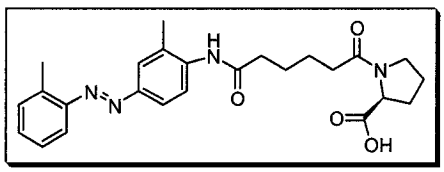

Compound 82: (S)-1-[6-(N-(2-methyl-4-(o-tolyldiazenyl)benzene))amino-6-oxohexanoyl]pyrrolidine-2-carboxylic acid

Compound 81 (56.5 mg, 0.09 mmol) was dissolved in 10 mL THF/MeOH/H_2O (3:1:1). LiOH (4.3 mg, 0.10 mmol) was added to the orange solution and the reaction was allowed to stir for 10 hours at room temperature. The mixture was concentrated under reduced pressure. The residue was diluted in EtOAc and 20 mL of NaOH 1M. The aqueous layer was separated and then acidified with 10 % HCl. The product was extracted twice with EtOAc. The combined organic extracts were dried over $MgSO_4$, filtered and concentrated under reduced pressure to give a quantitative yield of product **82** as an orange oil. $[\alpha]_D$ ($CHCl_3$, c = 1) -59.2°; IR (film, cm^{-1}) 3404, 3280, 2929, 2882, 1725, 1638; ^1H NMR (300 MHz, $CDCl_3$) δ 8.43 (br s, 1H), 7.96 (d, 8.2 Hz, 1H), 7.86-7.83 (m, 1H), 7.75-7.71 (m, 2H), 7.56 (d, 7.8 Hz, 1H), 7.32-7.28 (m, 2H), 7.22-7.18 (m, 1H), 4.52-4.48 (m, 1H), 3.64-3.53 (m, 1H), 3.50-3.39 (m, 1H), 2.67 (s, 3H), 2.48-2.35 (m, 4H), 2.32 (s, 3H), 2.29-2.17 (m, 2H), 2.09-1.92 (m, 2H), 1.82-1.66 (m, 4H); ^{13}C NMR (75 MHz, $CDCl_3$) δ 174.3(s), 174.0(s), 172.9(s), 172.8(s), 151.0(s), 150.2(s),

138.5(s), 138.3(s), 131.6(s), 130.9(s), 126.8(d), 125.3(d), 124.2(d), 121.9(d), 115.7(d), 59.8(d), 48.2(t), 37.2(t), 34.4(t), 29.0(t), 25.7(t), 25.1(t), 24.3(t), 18.7(q), 17.9(q) ; MS (EI) 450, 336, 91, 70.

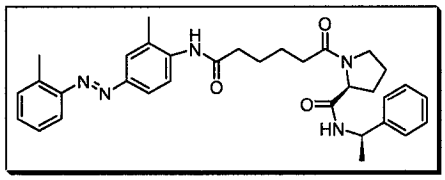

Compound 126: (S)-1-[(6-(N-(2-methyl-4-(o-tolyldiazenyl)benzene))amino-6-oxohexanoyl)-N-((S)-1-phenylethyl)]pyrrolidine-2-carboxamide

(R)-methylbenzylamine (0.01 mL, 0.08 mmol), HOBT (8.2 mg, 0.06 mmol) and DIPEA (0.03 mL, 0.16 mmol) were dissolved in 12 mL dry DCM, followed by the addition of **82** (20.0 mg, 0.04 mmol) and EDC (9.4 mg, 0.06 mmol). The mixture was allowed to stir for 12 hours at room temperature. The orange solution was concentrated under reduced pressure. Sequenced washes of the organic layer were done with HCl 10 %, saturated $NaHCO_3$ and brine. The organic layer was dried over MgSO4, filtered and concentrated under reduced pressure. No purification was done. Ratio (L:D) gave 4: 1 found by ^1H NMR. ^1H NMR (300 MHz, $CDCl_3$) δ 8.05 (br d, 8.8 Hz, 1H), 7.80-7.70 (m, 2H), 7.61-7.56 (m, 2H), 7.48-7.39 (m, 1H), 7.35-7.28 (m, 3H), 7.26-7.13 (m, 8H), 5.02-4.92 (m, 1H), 4.61-4.55 (m, 1H), 3.55-3.37 (m, 2H), 2.69 (s, 3H), 2.43-2.29 (m, 7H), 2.17-1.91 (m, 4H), 1.85-1.65 (m, 8H), 1.48 (dd, 4.1; 7.0 Hz, 3H), epimer 1.41 (d, 7.0 Hz, 3H).

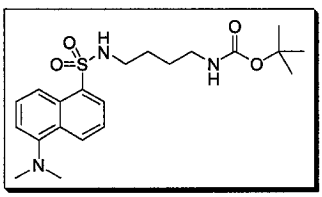

Compound 83: tert-butyl 4-(1-(dimethylamino)naphthalene-5-sulfonamido)butylcarbamate

(4-Amino-butyl)-carbamic acid tert-butyl ester[98] (1.52 g, 8.09 mmol) and triethylamine (0.89 mL, 8.90 mmol) were dissolved in 20 mL of dry DCM at 0 °C. A solution of dansyl chloride (1.98 g, 7.35 mmol) in 10 mL of dry DCM was added slowly to the mixture. The reaction proceeded during 60 minutes at room temperature. The yellow mixture was concentrated under reduced pressure and dissolved in EtOAc. The organic layer was then washed with 10 % HCl, saturated $NaHCO_3$ and brine, and dried over $MgSO_4$. The crude

[98] Krapcho, Kuell, *Synth. Commun.*, **1990**, *20*, 2559.

material was purified on silica gel by eluting with Hexanes: EtOAc 10% to 100% to obtain 1.574 g (51 %) of **83** as a thick fluorescent-yellow oil. IR (film, cm^{-1}) 3385, 2950, 2867, 2793, 2361, 2339, 1704, 1508, 1159; ^1H NMR (300 MHz, $CDCl_3$) δ 8.49 (d, 8.2 Hz, 1H), 8.29 (d, 8.0 Hz, 1H), 8.19 (d, 6.8 Hz, 1H), 7.48 (q, 8.2 Hz, 2H), 7.14 (d, 7.0 Hz, 1H), 5.43 (br s, 1H), 4.52 (br s, 1H), 2.96-2.78 (m, 10H), 1.45-1.24 (m, 13H); ^{13}C NMR (75 MHz, $CDCl_3$) δ 156.4 (s), 152.3 (s), 135.1 (s), 130.7 (d), 130.2 (s), 130.0 (s), 129.9 (d), 128.7 (d), 123.6 (d), 119.2 (d), 115.5 (d), 79.5 (s), 45.8 (q), 43.2 (t), 40.2 9t), 28.7 (q), 27.4 (t), 27.0 (t); MS (EI) 421, 347, 171.

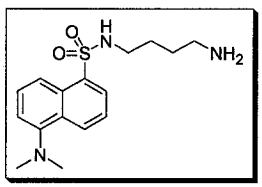

Compound 84: N-(4-aminobutyl)-5-(dimethylamino)naphthalene-1-sulfonamide

Compound 83 (1.07 g, 2.55 mmol) was dissolved in 20 mL of dry DCM under N_2 atmosphere. 5 mL of trifluoroacetic acid was added. The mixture was stirred for 1 hour at room temperature. The mixture was then concentrated under reduced pressure and repeated twice with the addition of benzene. The yellowish oil was dissolved in EtOAc and washed with saturated $NaHCO_3$ and brine. Then, dried over $MgSO_4$ to obtain quantitative yield of a fluorescent-yellow thick oil. IR (film, cm^{-1}) 3392, 2944, 2872, 2360, 2344, 1685, 1311, 1144; ^1H NMR (300 MHz, $CDCl_3$) δ 8.48 (d, 8.4 Hz, 1H), 8.19 (d, 6.8 Hz, 1H), 7.48 (m, 2H), 7.13 (d, 7.6 Hz, 1H), 4.08 (br s, 2H), 2.84 (m, 8H), 2.59 (m, 2H), 1.40 (m, 4H); ^{13}C NMR (75 MHz, $CDCl_3$) δ 152.2 (s), 135.4 (s), 130.5 (d), 130.2 (s), 130.0 (s), 129.8 (d), 128.5 (d), 123.6 (d), 119.3 (d), 115.5 (d), 45.8 9q), 43.3 (t), 41.2 (t), 29.8 (t), 27.6 (t); MS (EI) 321, 235, 171, 154, 70.

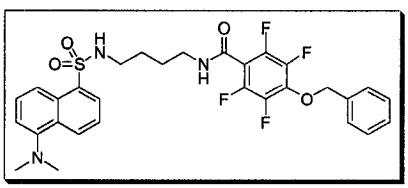

Compound 85: 4-(benzyloxy)-N-(4-(1-(dimethylamino)naphthalene-5-sulfonamido)butyl)-2,3,5,6-tetrafluorobenzamide

Compound 84 (398.9 mg, 1.24 mmol), DIPEA (0.55 mL, 8.14 mmol) and HOBT (159.4 mg, 1.18 mmol) were dissolved in 20 mL of dry THF, followed by the addition of 4-Benzyloxy-2,3,5,6-tetrafluoro-benzoic acid[99] (236.0 mg, 0.79 mmol) and EDC (183.0 mg, 1.18 mmol). The mixture was allowed to stir at room temperature for 12 hours. The yellowish solution was concentrated under reduced pressure and dissolved in EtOAc. Sequenced washes of the organic layer were done with HCl 10 %, saturated $NaHCO_3$ and brine. The organic layer was dried over $MgSO_4$, filtered and concentrated under reduced pressure. The crude product was purified on silica gel eluting with Hexanes: EtOAc 10% to 100%. 351.2 mg (74 %) of product **85** was obtained as a fluorescent-yellow foam. IR (film, cm^{-1}) 3372, 2952, 2365, 2342, 1652, 1559, 1319, 1141; ^1H NMR (300 MHz, $CDCl_3$) δ 8.49 (d, 8.9 Hz, 1H), 8.23 (d, 8.7 Hz, 1H), 7.48 (q, 7.5; 14.8 Hz, 2H), 7.44-7.32 (m, 5 H), 7.12 (d, 7.5 Hz, 2H), 6.45 (br s, 1H), 5.37 (br s, 1H), 5.19 (s, 2H), 3.25-3.21 (m, 2H), 2.93-2.77 (m, 8H), 1.58-1.35 (m, 4H); ^{13}C NMR (75 MHz, $CDCl_3$) δ 158.8 (s), 152.4 (s), 146.1 (s), 142.9 (s), 139.7 (s), 138.5 (s), 135.6 (s), 134.7 (s), 130.9 (d), 130.1 (s), 129.9 (d), 129.8 (s), 129.3 (s), 129.1 (d), 123.5 (d), 118.8 (d), 115.6 (d), 110.5 (s), 76.7 (t), 45.7 (q), 43.1 (t), 39.8 (t), 27.0 (t), 26.3 (t); MS (ESI, Na+) 626, 604, 211, 115, 83.

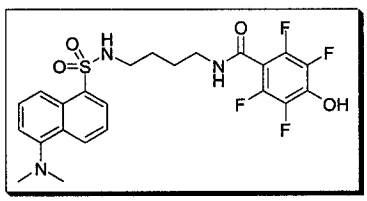

Compound 86: N-(4-(1-(dimethylamino)naphthalene-5-sulfonamido)butyl)-2,3,5,6-tetrafluoro-4-hydroxybenzamide

Compound 85 (237.2 mg, 0.39 mmol) was dissolved in 20 ml EtOAc under N_2 atmosphere. Then, 10% Palladium on activated carbon (≈ 20 mg) was added to the mixture and the atmosphere was changed under H_2 gas. The mixture was stirred for 12 hours at room temperature. The atmosphere was then changed for N_2 and the solution was filtered on celite with DCM. The filtrate was concentrated under reduced pressure and the crude was purified on silica gel eluting with Hexanes: EtOAC 30% to 100%. 159.3 mg (79 %) of product **86** was obtained as a fluorescent-yellow thick oil. IR (film,

[99] Cativiela C.; Serrano J.L.; Zurbano M.M. *J. Org. Chem.* **1995**, *60*, 3074.

cm^{-1}) 3435, 2931, 1650; ^1H NMR (300 MHz, $(CD_3)_2CO$) δ 8.54 (d, 8.1 Hz, 1H), 8.39 (d, 8.7 Hz, 1H), 8.20 (d, 6.8 Hz, 1H), 7.76 (br s, 1H), 7.66-7.24 (d, 7.4 Hz, 1H), 6.79 (br s, 1H), 3.38-3.19 (m, 2H), 3.02-2.89 (m, 2H), 2.85 (s, 6H), 1.65-1.43 (m, 4H); ^{13}C NMR (75 MHz, $(CD_3)_2CO$) δ 158.3 (s), 152.2 9s), 146.0 (s), 142.7 (s), 140.0 (s), 137.9 (s), 136.7 (s), 130.2 (s), 130.1 (d), 129.2 (d), 128.2 (d), 123.7 (d), 119.8 (d), 115.5 (d), 107.7 (s), 45.1 (q), 42.9 (t), 39.4 (t), 27.1 (t), 26.6 (t); MS (EI) 513, 262, 193, 171, 70.

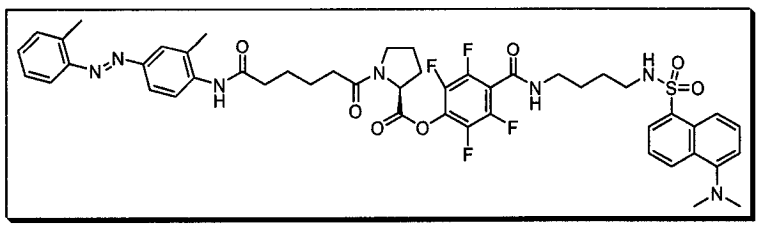

Compound 87: (S)-2,3,5,6-tetrafluoro-4-((1-(dimethylamino)naphthalene-5-sulfonamido)butylcarbamoyl)phenyl 1-[6-(N-(2-methyl-4-(o-tolyldiazenyl)benzene))amino-6-oxohexanoyl]pyrrolidine-2-carboxylate

Compound 86 (26.4 mg, 0.05 mmol), DIPEA (0.01 mL, 0.07 mmol) and HOBT (4.0 mg, 0.03 mmol) were dissolved in 20 mL of dry DMF, followed by the addition of **82** (7.7 mg, 0.02 mmol) and HBTU (11.2 mg, 0.03 mmol). The mixture was allowed to stir at room temperature for 12 hours. The mixture was washed three times with 30 mL of water adding EtOAc, then sequential washes of the organic layer was done with HCl 10 %, saturated $NaHCO_3$ and brine. The organic layer was dried over $MgSO_4$, filtered and concentrated under reduced pressure. The crude product could not be purified because of it cleaved on the silica gel.

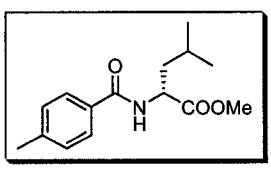

Compound 91: (R)-methyl 4-methyl-2-(4-methylbenzamido)pentanoate

D-leucine methyl ester (52.0 mg, 0.29 mmol), DIPEA (0.15 mL, 0.88 mmol) and HOBT (44.6 mg, 0.33 mmol) were dissolved in 6 mL of dry DCM, followed by the addition of para-toluic acid (30.0 mg, 0.22 mmol) and EDC (51.2 mg, 0.33 mmol). The mixture was

allowed to stir at room temperature for 18 hours. The clear solution was concentrated under reduced pressure and dissolved in EtOAc. Sequenced washes of the organic layer were done with 10 % HCl, saturated $NaHCO_3$ and brine. The organic layer was dried over $MgSO_4$, filtered and concentrated under reduced pressure. The crude product was purified on silica gel eluting with Hexanes: EtOAc 10% to 30%. 53.9 mg (93 %) of product **91** was obtained as a white solid. $[\alpha]_D$ ($CHCl_3$, c = 1) -21.3°; IR (film, cm^{-1}) 3368, 2960, 2869, 1746, 1638, 1540; ^1H NMR (300 MHz, $CDCl_3$) δ 7.67 (d, 8.1 Hz, 2H), 7.21 (d, 8.0 Hz, 2H), 6.47 (br d, 7.8 Hz, 1H), 4.87-4.80 (m, 1H), 3.74 (s, 3H), 2.37 (s, 3H), 1.76-1.60 (m, 3H), 0.96 (t, 6.0 Hz, 6H); ^{13}C NMR (75 MHz, CDCl3) δ 174.1(s), 167.4(s), 142.6(s), 131.5(s), 129.6(d), 127.4(d), 52.8(q), 51.5(d), 42.4(t), 25.4(q), 23.2(d), 22.5(q), 21.9(d); MS (EI) 263, 207, 119, 91.

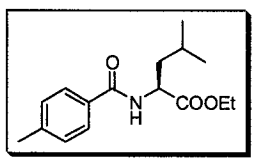

Compound 92: (S)-ethyl 4-methyl-2-(4-methylbenzamido)pentanoate

L-leucine ethyl ester (56.0 mg, 0.29 mmol), DIPEA (0.15 mL, 0.88 mmol) and HOBT (44.6 mg, 0.33 mmol) were dissolved in 6 mL of dry DCM, followed by the addition of para-toluic acid (30.0 mg, 0.22 mmol) and EDC (51.2 mg, 0.33 mmol). The mixture was allowed to stir at room temperature for 18 hours. The clear solution was concentrated under reduced pressure and dissolved in EtOAc. A sequenced wash of the organic layer was done with 10 % HCl, saturated $NaHCO_3$ and brine. The organic layer was dried over $MgSO_4$, filtered and concentrated under reduced pressure. The crude product was purified on silica gel eluting with Hexanes: EtOAc 10%. 60.0 mg (99 %) of product **92** was obtained as a white solid. $[\alpha]_D$ ($CHCl_3$, c = 1) + 24.8°; IR (film, cm^{-1}) 3358, 2956, 2876, 1747, 1640, 1504; ^1H NMR (300 MHz, $CDCl_3$) δ 7.67 (d, 8.0 Hz, 2H), 7.20 (d, 8.0 Hz, 2H), 6.49 (br d, 8.3 Hz, 1H), 4.86-4.78 (m, 1H), 4.19 (q, 7.1 Hz, 2H), 2.37 (s, 3H), 1.76-1.59 (m, 3H), 1.28 (t, 7.1 Hz, 3H), 0.96 (t, 6.1 Hz, 6H); ^{13}C NMR (75 MHz, $CDCl_3$) δ 173.7(s), 167.3(s), 142.5(s), 131.5(s), 129.6(d), 127.4(d), 61.8(t), 51.5(t), 42.4(q), 25.4(q), 23.2(q), 22.5(q), 21.9(d), 14.6(q); ; MS (EI) 278, 221, 204, 175, 119, 91, 65.

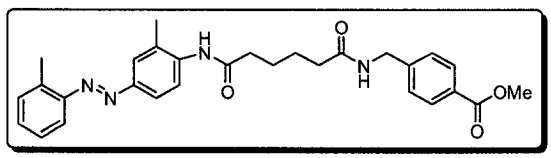

Compound 93: methyl 4-[6-(N-(2-methyl-4-(o-tolyldiazenyl)benzene))amino-6-oxohexanamido)methyl]benzoate

Methyl 4-(aminomethyl)benzoate hydrochloride (87.8 mg, 0.44 mmol), DIPEA (0.31 mL, 1.74 mmol) and HOBT (88.2 mg, 0.65 mmol) were dissolved in 8 mL of dry DMF, followed by the addition of crude **80** (200.0 mg, 0.57 mmol) and EDC (125.2 mg, 0.65 mmol). The mixture was allowed to stir at room temperature for 18 hours. The mixture was washed three times with 30 mL of water adding EtOAc, then sequential washes of the organic layer was done with 10 % HCl, saturated $NaHCO_3$ and brine. The organic layer was dried over $MgSO_4$, filtered and concentrated under reduced pressure. The crude product was purified on silica gel eluting with chloroform: MeOH 1%. 78.2 mg (36 %) of product **93** was obtained as an orange solid. IR (film, cm^{-1}) 3286, 2945, 2867, 1724, 1644, 1527, 1276; ^1H NMR (300 MHz, DMSO-d_6) δ 9.39 (br s, 1H), 8.45 (t, 5.8 Hz, 1 H), 7.90 (d, 8.1 Hz, 2H), 7.76-7.68 (m, 2H), 7.53 (d, 7.7 Hz, 1H), 7.43-7.27 (m, 6H), 4.33 (d, 6 Hz, 2H) 3.82 (s, 3H), 2.66 (s, 3H), 2.44-2.37 (m, 2H), 2.32 (s, 3H), 2.23-2.15 (m, 2H), 1.67-1.61 (m, 4H); ^{13}C NMR (75 MHz, DMSO-d_6) δ 173.0(s), 172.2(s), 171.0(s), 166.9(s), 150.9(s), 150.1(s), 146.4(s), 140.4(s), 138.2(s), 132.3(d), 132.0(d), 130.1(d), 128.9(s), 128.1(d), 127.5(d), 125.6(d), 121.4(d), 115.9(d), 52.9(q), 42.6(t), 36.6(t), 36.1(t), 25.9(t), 18.9(q), 18.0(q); MS (EI) 500, 381, 225, 149, 91.

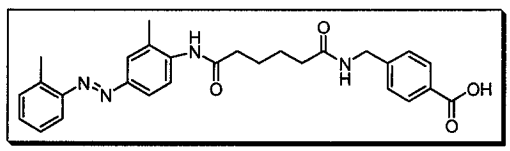

Compound 94: 4-[6-(N-(2-methyl-4-(o-tolyldiazenyl)benzene))amino-6-oxohexanamido)methyl]benzoic acid

Compound 81 (115.2 mg, 0.23 mmol) was dissolved in 20 mL THF/MeOH/H_2O (3:1:1). LiOH (29.0 mg, 0.69 mmol) was added to the solution and the reaction was allowed to stir for 10 hours at room temperature. The mixture was concentrated under reduced pressure. The residue was diluted in EtOAc and 20 mL of 1M NaOH. The aqueous layer

was acidified with concentrated HCl. The insoluble precipate was filtered and washed with water and then with hexanes. The product was dried under vacuum to give quantitative yield of product **94** as an orange solid. IR (film, cm^{-1}) 3412, 3279, 2928, 1688, 1637; ^1H NMR (300 MHz, DMSO-d_6) δ 12.96 (br s, 1H), 9.46 (br s, 1H), 8.51-8.43 (m, 1H), 7.88 (d, 7.9 Hz, 2H), 7.76-7.70 (m, 2H), 7.52 (d, 7.4 Hz, 1H), 7.41 (d, 4.1 Hz, 2H), 7.35-7.33 (m, 3H), 6.73 (br s, 1 H), 4.32 (d, 5.9 Hz, 2H), 2.66 (s, 3H), 2.44-2.32 (m, 2H), 2.31 (s, 3H), 2.24-2.18 (m, 2H), 1.66-1.57 (m, 4H); ^{13}C NMR (75 MHz, DMSO-d_6) δ 173.1(s), 171.9(s), 171.0(s), 166.7(s), 151.2(s), 150.3(s), 146.3(s), 139.9(s), 138.5(s), 132.2(d), 132.0(d), 129.8(d), 128.9(s), 128.1(d), 127.3(d), 124.9(d), 121.1(d), 115.7(d), 42.1(t), 36.4(t), 36.1(t), 25.7(t), 18.5(q), 17.9(q); MS (EI) 486, 225, 106, 91, 44.

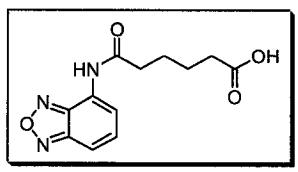

Compound 99: 6-(benzo[c][1,2,5]oxadiazol-4-ylamino)-6-oxohexanoic acid

1-aminobenzofurazan (Apollo Chemicals) (100.0 mg, 0.74 mmol) and adipic anhydride[100] (94.7 mg, 0.74 mmol) were dissolved in 10 mL benzene. The mixture was refluxed for 15 hours. The mixture was cooled and dissolved in EtOAc. Then, the solution washed with 10 % HCl and saturated $NaHCO_3$. The aqueous layer was acidified with concentrated HCl and extracted with EtOAc, followed by a brine wash. The organic layer was dried over $MgSO_4$, and concentrated under reduced pressure. To complete the crystallization, a portion of hexanes was added and the precipitate was filtered (Hirsch), and dried under vacuum. 118.0 mg (65 %) of product **99** was obtained as a yellow powder. IR (film, cm^{-1}) 3393, 2939, 2868, 1700, 1650; ^1H NMR (300 MHz, $(CD_3)_2CO$-d_6) δ 10.50 (br s, 1H), 9.62 (br s, 1H), 8.33-8.28 (m, 1H), 7.56-7.53 (m, 2H), 2.66 (t, 7.2 Hz, 2H), 2.35 (t, 7.1 Hz, 2H), 1.84-1.61 (m, 4H); ^{13}C NMR (75 MHz, $(CD_3)_2CO$-d_6) δ 173.9(s), 172.6(s), 150.0(s), 134.2(d), 127.6(s), 116.6(d), 116.5(d), 109.7(d), 36.6(t), 33.4(t), 25.1(t), 24.7(t); MS (EI) 263, 135, 55.

[100] Hicks T.A.; Smith C.E.; Nigel Williamson W.R.; Day E.H. *J.Med.Chem.*, **1979**, *22*, 1460.

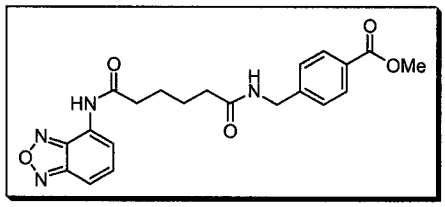

Compound 100: methyl 4-((6-(benzo[c][1,2,5]oxadiazol-4-ylamino)-6-oxohexanamido)methyl)benzoate

Methyl 4-(aminomethyl)benzoate hydrochloride (106.8 mg, 0.53 mmol), DIPEA (0.21 mL, 1.63 mmol) and HOBT (82.5 mg, 0.61 mmol) were dissolved in 7 mL of dry DCM, followed by the addition of **99** (100.0 mg, 0.41 mmol) and EDC (94.7 mg, 0.61 mmol). The mixture was allowed to stir at room temperature for 15 hours. The solution was concentrated under reduced pressure and dissolved in EtOAc. Sequenced washes of the organic layer were done with 10 % HCl, saturated $NaHCO_3$ and brine. The organic layer was dried over $MgSO_4$, filtered and concentrated under reduced pressure. The crude product was purified on silica gel eluting with Hexanes: EtOAc 30% to 100%. 128.9 mg (81 %) of product **100** was obtained as a pale yellow solid. IR (film, cm^{-1}) 3277, 2930, 2359, 2340, 1719, 1634, 1542, 1280, 1191, 1102; ^1H NMR (300 MHz, DMSO-d_6) δ 10.63 (br s, 1H), 8.43 (t, 5.8 Hz, 1H), 8.12 (d, 7.1 Hz, 1H), 7.87 (d, 8.1 Hz, 1H), 7.65 (d, 9.0 Hz, 1H), 7.58-7.52 (m, 1H), 7.35 (d, 8.1 Hz, 2H), 4.32 (d, 5.8 Hz, 2H), 3.81 (s, 3H), 2.55-2.51 (m, 2H), 2.22-2.17 (m, 2H), 1.65-1.50 (m, 4H); ^{13}C NMR (75 MHz, DMSO-d_6) δ 173.6(s), 172.9(s), 166.9(s), 150.2(s), 146.3(s), 145.6(s), 134.9(d), 130.0(d), 128.9(s), 128.1(d), 127.6(s), 118.3(d), 110.5(d), 52.9(q), 42.6(t), 36.6(t), 36.0(t), 25.8(t), 25.7(t); MS (EI) 410, 276, 207, 149, 106, 43.

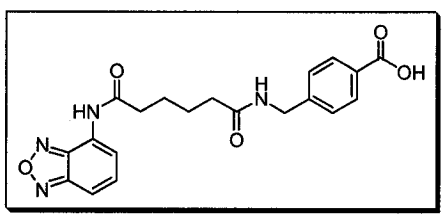

Compound 101: 4-((6-(benzo[c][1,2,5]oxadiazol-4-ylamino)-6-oxohexanamido)methyl)benzoic acid

Compound 100 (100.0 mg, 0.26 mmol) was dissolved in 10 ml THF/MeOH/H_2O (3:1:1) at 0°C. Hydrogen peroxide 30% (0.063 mL, 2.04 mmol) was added, followed by the addition of LiOH (23.1 mg, 0.51 mmol). The mixture was allowed to stir for 3 hours at 0°C. 10 mL of solution Na_2SO_3 1.5N was added to the mixture and stirred for 10 minutes.

The mixture was then concentrated under reduced pressure and extracted with EtOAc by adding saturated $NaHCO_3$.The aqueous layer was acidified with concentrated HCl and extracted with EtOAc, followed by a brine wash. The organic layer was dried over $MgSO_4$, filtered and concentrated under reduced pressure to give quantitative yield of product **101** as a white powder. IR (film, cm^{-1}) 3420, 3276, 2950, 2869, 1689, 1635, 1537; ^1H NMR (300 MHz, $CDCl_3$) δ 13.03 (br s, 1H), 10.65 (s, 1H), 8.48-8.42 (m, 1H), 8.12 (d, 7.1 Hz, 1H), 7.88-7.84 (m, 2H), 7.65 (d, 9 Hz, 1H), 7.58-7.52 (m, 1H), 7.33 (d, 8.1 Hz, 2H), 4.31 (d, 5.8 Hz, 2H), 2.67-2.50 (m, 2H), 2.22-2.13 (m, 2H), 1.67-1.49 (m, 4H); ^{13}C NMR (75 MHz, $CDCl_3$) δ 173.6(s), 173.0(s), 168.0(s), 150.2(s), 145.8(s), 145.7(s), 134.9(d), 130.2(d), 130.1(d), 128.0(d), 127.6(s), 118.4(d), 110.6(d), 42.6(t), 36.6(t), 36.0(t), 25.8(t), 25.7(t); MS (EI) 396, 262, 135.

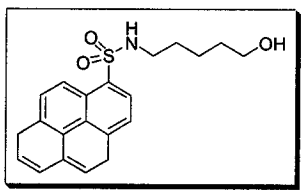

Compound 102: 4,8-Dihydro-pyrene-1-sulfonic acid (5-hydroxy-pentyl)-amide

1-pyrenesulfonic acid (3.00 g, 10.6 mmol) was dissolved in 30 mL benzene and 2 drops of DMF. Oxalyl chloride (4.67 mL, 53.1 mmol) was slowly added and the mixture was refluxed for 4 hours. The brown mixture was then cooled at room temperature and the benzene was evaporated under reduced pressure. The crude product was added slowly added to a solution of 1-aminopentanol (1.20 g, 11.7 mmol) and DIPEA (5.54 mL, 31.8 mmol) in 20 mL DCM at 0 °C. The mixture was allowed to stir for 10 hours at room temperature. The mixture was then concentrated under reduced pressure and dissolved in EtOAc. Sequenced washes of the organic layer were done with 10 % citric acid, saturated $NaHCO_3$ and brine. The organic layer was dried over $MgSO_4$, filtered and concentrated under reduced pressure. The crude product was purified on silica gel eluting with EtOAc: Hexanes 1:1 to 2:1. 1.36 g (43 %) of product **102** was obtained as a clear oil. IR (film, cm^{-1}) 3383, 2945, 2359, 2338, 1655, 1315, 1161; ^1H NMR (300 MHz, $(CD_3)_2CO$) δ 9.09 (d, 9.3 Hz, 1H), 8.68 (d, 8.7 Hz, 1H), 8.40-8.22 (m, 4H), 8.21-8.03 (m, 3H), 6.95 (br s, 1H), 3.44 (br t, 5.0 Hz, 1H), 3.31 (dd, 5.6; 11.2 Hz, 2H), 2.92 (dd, 6.6, 13.3 Hz, 2H),

1.47-1.33 (m, 2H), 1.33-1.12 (m, 4H); ^{13}C NMR (75 MHz, $(CD_3)_2CO$) δ 134.8 (s), 133.3 (s), 130.5 (s), 130.2 (d), 129.8 (d), 128.2 (s), 127.5 (d), 127.4 (d), 127.3 (d), 127.2 (d), 127.1 (d), 125.3 (s), 124.4 (d), 124.1 (s), 124.0 (d), 61.6 (t), 43.4 (t), 32.5 (t), 29.7 (t), 23.1 (t).; MS (EI) 367, 217, 201, 43.

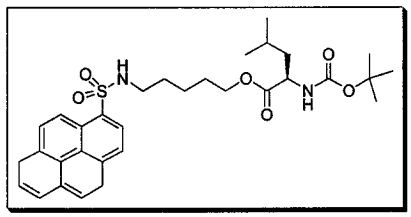

Compound 103: (R)-5-(1,5-dihydropyrene-8-sulfonamido)pentyl 2-(tert-butoxycarbonyl)-4-methylpentanoate

Compound 102 (36.1 mg, 0.10 mmol), DIPEA (0.07 mL, 0.39 mmol) and HOBT (19.9 mg, 0.15 mmol) were dissolved in 6 mL of dry DCM, followed by the addition of N-BOC-D-leucine (26.8 mg, 0.11 mmol) and EDC (22.8 mg, 0.15 mmol). The mixture was allowed to stir at room temperature for 18 hours. The solution was concentrated under reduced pressure and dissolved in EtOAc. Sequenced washes of the organic layer were done with HCl 10 %, saturated $NaHCO_3$ and brine. The organic layer was dried over $MgSO_4$, filtered and concentrated under reduced pressure. The crude product was purified on silica gel eluting with $CHCl_3$: MeOH 1 %. 28.5 mg (50 %) of product **103** was obtained as a pale yellow foam. $[\alpha]_D$ ($CHCl_3$, c = 1) + 10.0°; IR (film, cm^{-1}) 2999, 2093, 2073, 1506, 1366; ^1H NMR (300 MHz, $CDCl_3$) δ 8.95 (d, 9.4 Hz, 1H), 8.63 (d, 8.2 Hz, 1H), 8.21-8.17 (m, 3H), 8.09 (dd, 4.0; 8.2 Hz, 2H), 8.03-7.94 (m, 2H), 5.49 (t, 5.7 Hz, 1H), 4.90 (d, 8.6 Hz, 1H), 4.22-4.12 (m, 1H), 3.84 (t, 6.2 Hz, 2H), 2.87 (q, 6.6 Hz, 2H), 1.65-1.52 (m, 1H), 1.47-1.28 (m, 15H), 1.24-1.10 (m, 2H), 0.87-0.82 (m, 6H); ^{13}C NMR (75 MHz, $CDCl_3$) δ 173.9(s), 155.8(s), 135.0(s), 131.7(s), 131.2(s), 130.4(d), 130.3(d), 128.3(s), 127.7(d), 127.3(d), 127.2(d), 127.1(d), 125.5(s), 124.3(s), 124.2(s), 123.5(d), 80.2(s), 65.0(t), 52.5(d), 43.4(t), 41.9(t), 29.4(t), 28.7(t), 28.2(t), 25.1(q), 23.2(q), 23.1(t), 22.3(q); MS (EI) 580, 506, 217, 201, 86, 41.

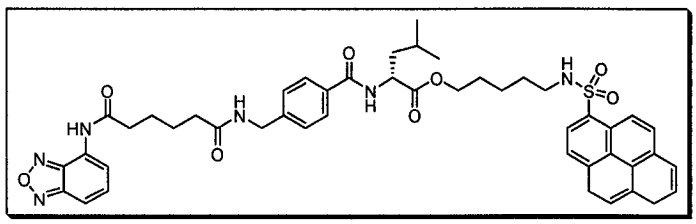

Compound 105: (R)-5-(1,9-dihydropyrene-6-sulfonamido)pentyl 2-(4-((6-(benzo[c][1,2,5]oxadiazol-4-ylamino)-6-oxohexanamido)methyl)benzamido)-4-methylpentanoate

Compound 103 (76.0 mg, 0.16 mmol) was dissolved in 8 mL DCM, followed by the addition of 2 mL of trifluoroacetic acid. The mixture was allowed to stir for one hour at room temperature. The solution was then concentrated under reduced pressure and dissolved in benzene and again concentrated under reduced pressure. This sequence was repeated twice to afford the desired product as a crude TFA salt **104**. The crude TFA salt, DIPEA (0.11 mL, 0.63 mmol) and HOBT (32.0 mg, 0.24 mmol) were dissolved in 8 mL of dry DMF, followed by the addition of **101** (71.8 mg, 0.19 mmol) and EDC (36.8 mg, 0.24 mmol). The mixture was allowed to stir at room temperature for 18 hours. The mixture was washed three times with 30 mL of water adding EtOAc, then sequential washes of the organic layer was done with HCl 10 %, saturated $NaHCO_3$ and brine. The organic layer was dried over $MgSO_4$, filtered and concentrated under reduced pressure. The crude product was purified on silica gel eluting with chloroform: MeOH 1% to 2%. 85.3 mg (63 %) of product **105** was obtained as an orange foam. $[\alpha]_D$ ($CHCl_3$, c = 1) + 1.4°; IR (film, cm^{-1}) 3374, 2953, 2366, 2336, 1655, 1559, 1265; ^1H NMR (300 MHz, $CDCl_3$) δ 8.92 (d, 9.4 Hz, 1H), 8.66 (br s, 1H), 8.57 (d, 8.2 Hz, 1H), 8.23-8.17 (m, 2H), 8.13-8.09 (m, 3H), 8.07-7.98 (m, 3H), 7.67 (d, 8.1 Hz, 2H), 7.34-7.30 (m, 1H), 7.23-7.16 (m, 2H), 6.97 (d, 7.9 Hz, 1H), 6.84 (br t, 5.8 Hz, 1 H), 5.92 (br t, 5.9 Hz, 1H), 4.66 (dd, 7.4; 14.7 Hz, 1H), 4.35 (d, 5.6 Hz, 2H), 4.02-3.83 (m, 2H), 2.85-2.77 (m, 2H), 2.48-2.40 (m, 2H), 2.37-2.20 (m, 2H), 1.72-1.60 (m, 6H), 1.44-1.10 (m, 6H), 0.89 (d, 5.8 Hz, 6H); ^{13}C NMR (75 MHz, $CDCl_3$) δ 173.7(s), 173.5(s), 172.7(), 167.7(s), 149.6(s), 144.99s), 143.0(s), 135.1(s), 133.6(s), 132.9(s), 131.6(d), 131.2(s), 130.5(s), 130.4(d), 130.3(d), 128.3(s), 128.09d), 127.9(d), 127.6(d), 127.4(d), 127.3(d), 127.2(d), 127.1(d), 126.6(s),

125.4(s), 124.3(s), 123.5(s), 116.9(d), 110.4(d), 65.3(t), 52.1(d), 43.3(t), 41.2(t), 37.0(t), 36.2(t), 29.3(t), 28.1(t), 25.4(d), 25.3(t), 25.1(t), 23.2(q), 23.1(t), 22.2(q); MS (ESI, Na+) 882, 115, 83.

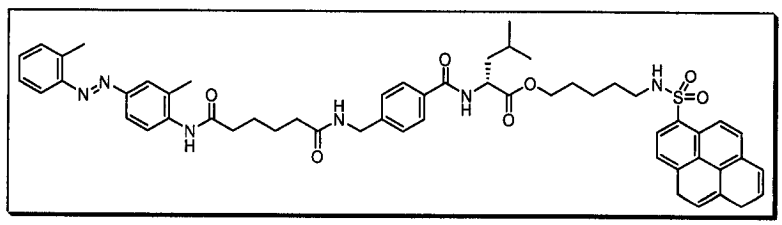

Compound 117: (R)-5-(1,9-dihydropyrene-6-sulfonamido)pentyl 4-methyl-2-[4-((6-(N-(2-methyl-4-(o-tolyldiazenyl)benzene)amino)-6-oxohexanamido)methyl)benzamido]pentanoate

103 (119.0 mg, 0.25 mmol) was dissolved in 8 mL DCM, followed by the addition of 2 mL of trifluoroacetic acid. The mixture was allowed to stir for one hour at room temperature. The solution was then concentrated under reduced pressure and dissolved in benzene and again concentrated under reduced pressure. This sequence was repeated twice to afford the desired product as a crude TFA salt **104**. The crude TFA salt, DIPEA (0.14 mL, 0.82 mmol) and HOBT (41.7 mg, 0.31 mmol) were dissolved in 12 mL of dry DMF, followed by the addition of **94** (100.0 mg, 0.21 mmol) and EDC (59.2 mg, 0.31 mmol). The mixture was allowed to stir at room temperature for 18 hours. The mixture was washed three times with 30 mL of water adding EtOAc, then sequential washes of the organic layer was done with 10 % HCl, saturated $NaHCO_3$ and brine. The organic layer was dried over $MgSO_4$, filtered and concentrated under reduced pressure. The crude product was purified on silica gel eluting with chloroform: MeOH 2%. 65.5 mg (33 %) of product **117** was obtained as an orange solid. IR (film, cm^{-1}) 3446, 3307, 3054, 2960, 2874, 2363, 2339, 1750, 1648, 1541, 1263; ^1H NMR (300 MHz, DMSO-d_6) δ 9.38 (br s, 1H), 8.97 (d, 9.4 Hz, 1H), 8.60-8.55 (m, 2H), 8.48-8.35 (m, 7H), 8.29-8.25 (m, 1H), 8.22-8.16 (m, 1H), 8.12-8.07 (m, 1H), 7.81-7.67 (m, 5H), 7.51 (, d 7.9 Hz, 1H), 7.40 (d, 4.2 Hz, 2H), 7.34-7.24 (m, 2H), 4.41-4.24 (m, 3H), 3.83-3.74 (m, 2H), 2.80-2.69 (m, 2H), 2.65 (s, 3H), 2.46-2.35 (m, 2H), 2.31 (s, 3H), 2.24-2.16 (m, 2H), 1.67-1.54 (m, 6H), 1.35-1.19 (m, 4H), 1.18-1.06 (m, 2H), 0.85 (d, 6.1 Hz, 3H), 0.80 (d, 6.1 Hz, 3H); ^{13}C NMR (75

MHz, DMSO-d_6) δ 173.4(s), 172.9(s), 167.2(s), 150.8(s), 149.8(s), 144.2(s), 140.3(s), 138.2(s), 134.7(s), 133.5(d), 133.1(d), 132.3(s), 131.9(s), 131.4(s), 130.8(d), 130.6(s), 130.3(d), 128.3(d), 128.1(d), 127.8(d), 127.6(d), 127.5(d), 127.4(d), 125.5(d), 125.0(s), 124.3(s), 124.0(d), 121.3(d), 115.4(d), 64.9(t), 51.9(d), 43.0(t), 42.5(t), 36.1(t), 29.3(t), 28.2(t), 25.8(t), 25.3(d), 23.6(q), 23.0(t), 22.1(q), 18.9(q), 18.0(q); MS (ESI, Na+) 971, 115, 83.

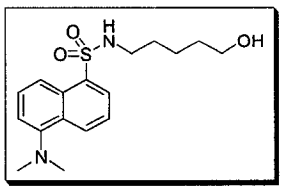

Compound 95: 5-Dimethylamino-naphthalene-1-sulfonyl (5-hydroxy-pentyl)-amide

1-aminopentanol (1.00 g, 9.69 mmol), triethylamine (3.68 mL, 26.4 mmol) were dissolved in 10 mL of dry DCM at 0°C followed by the addition of a solution of dansyl chloride in 5 mL DCM (2.38 g, 8.81 mmol). The mixture was allowed to stir at room temperature for 1 hour. The solution was concentrated under reduced pressure and dissolved in EtOAc. Sequenced washes of the organic layer were done with 10 % citric acid, saturated $NaHCO_3$ and brine. The organic layer was dried over $MgSO_4$, filtered and concentrated under reduced pressure. The crude product was purified on silica gel eluting with $CHCl_3$: MeOH 1%. 2.85 g (95 %) of product **95** was obtained as a fluorescent-yellow oil. IR (film, cm^{-1}) 3499, 3308, 2941, 2873, 2789, 2361, 2342, 1573, 1457, 1313, 1142, 1074; ^1H NMR (300 MHz, $CDCl_3$) δ 8.47 (d, 8.1 Hz, 1H), 8.30 (d, 8.1 Hz, 1H), 8.18 (d, 6.2 Hz, 1H), 7.46 (dt, 3.7; 8.1; 11.8 Hz, 2H), 7.11 (d, 7.4 Hz, 1H), 5.64 (br t, 6.2 Hz, 1H), 3.39 (t, 6.2 Hz, 2H), 2.90-2.75 (m, 8H), 2.52 (br s, 1H), 1.39-1.23 (m, 4H), 1.23-1.08 (m, 2H); ^{13}C NMR (75 MHz, $CDCl_3$) δ 152.2 (s), 135.3 (s), 130.6 (s), 130.2 (d), 130.0 (s), 129.8 (d), 128.7 (d), 123.6 (d), 119.3 (d), 115.6 (d), 62.6 (t), 45.8 (q), 43.4 (t), 32.2 (t), 29.5 (t), 22.9 (t); MS (EI) 336, 171, 154, 127, 40.

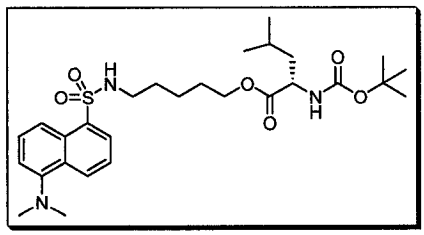

Compound 96: (S)-5-(1-(dimethylamino)naphthalene-5-sulfonamido)pentyl 2-(tert-butoxycarbonyl)-4-methylpentanoate

Compound 95 (1.00 g, 3.10 mmol), DIPEA (2.16 mL, 12.4 mmol) and HOBT (628.2 mg, 4.65 mmol) were dissolved in 20 mL of dry DCM, followed by the addition of N-BOC-L-leucine (1.005g, 4.03 mmol) and EDC (721.9 mg, 4.65 mmol). The mixture was allowed to stir at room temperature for 18 hours. The solution was concentrated under reduced pressure and dissolved in EtOAc. Sequenced washes of the organic layer were done with 10 % HCl, saturated $NaHCO_3$ and brine. The organic layer was dried over $MgSO_4$, filtered and concentrated under reduced pressure. The crude product was purified on silica gel eluting with chloroform: MeOH 1 %. 769.4 mg (46 %) of product **96** was obtained as a fluorescent-yellow foam. $[\alpha]_D$ ($CHCl_3$, c = 1) -5.4°; ^1H NMR (300 MHz, $CDCl_3$) δ 8.50 (d, 8.1 Hz, 1H), 8.28 (d, 6.7 Hz, 1H), 8.21 (d, 6.8 Hz, 1H), 7.50 (dd, 8.1; 17.4 Hz, 2H), 7.15 (d, 6.8 Hz, 1H), 5.06 (br t, 6.0 Hz, 1H), 4.90 (br d, 8.7 Hz, 1H), 4.21 (dd, 9.3; 14.3 Hz, 1H), 3.91 (t, 6.5 Hz, 2H), 2.91-2.79 (m, 8H), 1.72-1.28 (m, 16H), 1.26-1.10 (m, 2H), 0.90 (d, 3.0 Hz, 3H), 0.87 (d, 3.0 Hz, 3H); ^{13}C NMR (75 MHz, $CDCl_3$) δ 173.9(s), 155.8(s), 152.3(s), 135.2(s), 130.7(s), 130.2(s), 130.0(d), 129.9(d), 128.7(d), 123.6(d), 119.1(d), 115.5(d), 80.2(s), 65.1(t), 52.5(d), 45.7(q), 43.3(t), 42.0(t), 29.4(t), 28.7(q), 28.2(t), 25.1(q), 23.2(q), 23.0(t), 22.3(q); MS (EI) 549, 475, 172, 86.

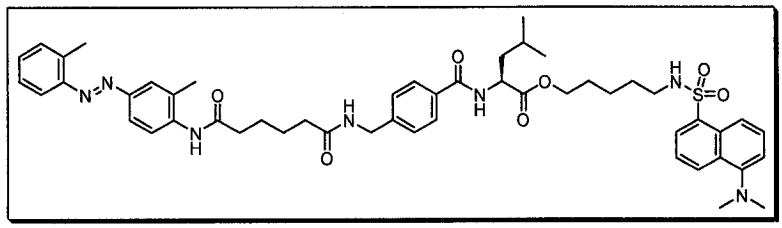

Compound 98: (S)-5-(1-(dimethylamino)naphthalene-5-sulfonamido)pentyl 4-methyl-2-[4-((6-(N-(2-methyl-4-(o-tolyldiazenyl)benzene)amino)-6-oxohexanamido)methyl)benzamido]pentanoate

Compound 96 (277.2 mg, 0.62 mmol) was dissolved in 8 mL DCM, followed by the addition of 2 mL of trifluoroacetic acid. The mixture was allowed to stir for one hour at room temperature. The solution was then concentrated under reduced pressure and dissolved in benzene and again concentrated under reduced pressure. This sequence was repeated twice to afford the desired product as a crude TFA salt **97**. The crude TFA salt, DIPEA (0.36 mL, 2.06 mmol) and HOBT (104.2 mg, 0.77 mmol) were dissolved in 15 mL of dry DMF, followed by the addition of **94** (250.0 mg, 0.51 mmol) and EDC (119.7 mg, 0.77 mmol). The mixture was allowed to stir at room temperature for 18 hours. The mixture was washed three times with 30 mL of water adding EtOAc, then sequential washes of the organic layer was done with 10 % HCl, saturated $NaHCO_3$ and brine. The organic layer was dried over $MgSO_4$, filtered and concentrated under reduced pressure. The crude product was purified on silica gel eluting with chloroform: MeOH 1 %. 285.8 mg (61 %) of product **98** was obtained as an orange foam. $[\alpha]_D$ ($CHCl_3$, c = 1) -4.4°; IR (film, cm^{-1}) 3292, 3061, 2947, 2869, 2367, 2332, 1734, 1651, 1525, 1265, 1145; ^1H NMR (300 MHz, $CDCl_3$) δ 8.47 (d, 8.7 Hz, 1H), 8.26 (d, 8.7 Hz, 1H), 8.14 (d, 6.8 Hz, 1H), 7.99-7.78 (m, 2H), 7.76-7.59 (m, 4H), 7.54 (d, 8.1 Hz, 1H), 7.43 (dd, 7.4; 14.9 Hz, 2H), 7.35-6.97 (m, 8H), 5.72 (br s, 1H), 4.65 (dd, 6.8; 13.6 Hz, 1H), 4.43-4.25 (m, 2H), 4.10-3.81 (m, 2H), 2.90-2.69 (m, 8H), 2.65 (s, 3H), 2.43-2.29 (m, 2H), 2.29-2.16 (m, 5H), 2.16-2.08 (m, 1H), 1.79-1.51 (m, 6H), 1.51-1.05 (m, 6H), 0.90 (d, 5.0 Hz, 6H); ^{13}C NMR (75 MHz, $CDCl_3$) δ 173.7(s), 172.2(s), 167.8(s), 152.3(s), 151.1(s), 150.1(s), 143.1(s), 138.7(s), 138.3(s), 135.2(s), 132.9(s), 131.6(d), 131.1(d), 130.7(d), 130.4(d), 130.2(s), 129.9(d), 129.7(s), 128.6(d), 127.9(d), 125.2(d), 123.7(d), 123.5(d), 122.0(d), 119.2(d), 115.7(d), 115.5(d), 65.3(t), 53.9(t), 52.1(d), 45.7(q), 43.3(t), 41.2(t), 37.1(t), 36.3(t),

29.3(t), 28.2(t), 25.5(t), 25.4(d), 23.2(q), 23.1(t), 22.2(q), 18.4(q), 17.9(q); MS (ESI, Na+) 940, 115, 83.

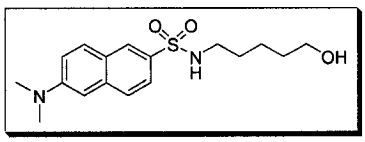

Compound 107: 6-(dimethylamino)-N-(5-hydroxypentyl)naphthalene-2-sulfonamide

1-aminopentanol (22.9 mg, 0.22 mmol), DIPEA (0.10 mL, 0.56 mmol) were dissolved in 5 mL of dry DCM at 0°C followed by the addition of a solution of 6-N,N-dimethylnaphthalene-2-sulfonyl chloride in 5 mL DCM (50.0 mg, 0.19 mmol). The mixture was allowed to stir at room temperature for 1 hour. The solution was concentrated under reduced pressure and dissolved in EtOAc. Sequenced washes of the organic layer were done with 10 % citric acid, saturated $NaHCO_3$ and brine. The organic layer was dried over $MgSO_4$, filtered and concentrated under reduced pressure. The crude product was purified on silica gel eluting with $CHCl_3$: MeOH 0% to 1%. 52.0 mg (84 %) of product **107** was obtained as a white solid. IR (film, cm^{-1}) 3468, 3133, 2936, 2854, 2361, 2340, 1653, 1267, 1135; ^1H NMR (300 MHz, $CDCl_3$) δ 8.22 (s, 1H), 7.76 (d, 9.3 Hz, 1H), 7.70-7.62 (m, 2H), 7.19 (d, 9.3Hz, 1H), 6.85 (s, 1H), 4.68 (br t, 6.2 Hz, 1H), 3.52 (t, 6.2 Hz, 2H), 3.08 (s, 6H), 2.91 (dd, 6.8; 13.0 Hz, 2H), 1.53-1.37 (m, 5H), 1.37-1.21 (m, 2H); ^{13}C NMR (75 MHz, $CDCl_3$) δ 150.7 (s), 137.2 (s), 131.8 (s), 130.5 (d), 128.8 (d), 127.5 (d), 124.9 (s), 123.2 (d), 117.3 (d), 105.5 (d), 62.9 (t), 43.4 (t), 40.8 (q), 32.3 (t), 29.6 (t), 23.1 (t); MS (EI) 336, 316, 186, 170, 40.

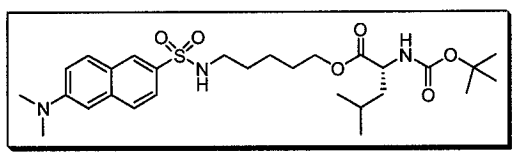

Compound 108: 2-tert-(R)-5-(2-(dimethylamino)naphthalene-6-sulfonamido)pentyl 2-(tert-butoxycarbonyl)-4-methylpentanoate

Compound 107 (49.5 mg, 0.15 mmol), DIPEA (0.10 mL, 0.59 mmol) and HOBT (29.8 mg, 0.22 mmol) were dissolved in 8 mL of dry DCM, followed by the addition of N-BOC-D-leucine (47.7 mg, 0.19 mmol) and HBTU (83.6 mg, 0.22 mmol). The mixture was allowed to stir at room temperature for 18 hours. The solution was concentrated

under reduced pressure and dissolved in EtOAc. Sequenced washes of the organic layer were done with H_2O twice then with 10 % HCl, saturated $NaHCO_3$ and brine. The organic layer was dried over $MgSO_4$, filtered and concentrated under reduced pressure. The crude product was purified on silica gel eluting with chloroform: MeOH 0 to 1%. 59.7 mg (74 %) of product **108** was obtained as a white foam. $[\alpha]_D$ ($CHCl_3$, c = 1) -2.9°; ^1H NMR (300 MHz, $CDCl_3$) δ 8.22 (s, 1H), 7.76 (d, 9.3 Hz, 1H), 7.69-7.63 (m, 2H), 7.18 (d, 9.3 Hz, 1H), 6.86 (s, 1H), 4.96-4.79 (m, 2H), 4.22 (dd, 8.6; 14.3 Hz, 1H), 4.01 (t, 6.2 Hz, 2H), 3.07 (s, 6H), 2.91 (dd, 6.2; 13.0 Hz, 2H), 1.70-1.41 (m, 7H), 1.39 (s, 9H), 1.37-1.16 (m, 2H), 0.89 (d, 6.8 Hz, 6H); ^{13}C NMR (75 MHz, $CDCl_3$) δ 173.9(s), 155.8(s), 150.6(s), 137.2(s), 132.0(s), 130.6(d), 128.8(d), 127.5(d), 125.0(s), 123.2(d), 117.3(d), 80.2(s), 65.1(t), 52.5(d), 43.3(t), 42.1(t), 40.9(q), 29.5(t), 28.7(t), 25.2(q), 23.2(q), 22.3(q); MS (EI) 549, 450, 170, 97, 86.

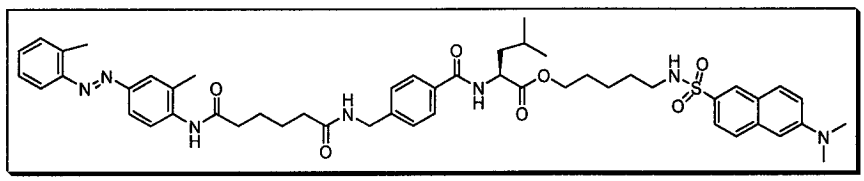

Compound 110: (R)-5-(2-(dimethylamino)naphthalene-6-sulfonamido)pentyl 4-methyl-2-[4-((6-(N-(2-methyl-4-(o-tolyldiazenyl)benzene)amino)-6-oxohexanamido)methyl)benzamido]pentanoate

Compound 108 (48.2 mg, 0.11 mmol) was dissolved in 8 mL DCM, followed by the addition of 2 mL of trifluoroacetic acid. The mixture was allowed to stir for one hour at room temperature. The solution was then concentrated under reduced pressure and dissolved in benzene and again concentrated under reduced pressure. This sequence was repeated twice to afford the desired product as a crude TFA salt **109**. The crude TFA salt, DIPEA (0.09 mL, 0.54 mmol), HOBT (21.8 mg, 0.16 mmol) and CSA (74.6 mg, 0.32 mmol) were dissolved in 8 mL of dry DMF, followed by the addition of **94** (69.6 mg, 0.14 mmol) and HBTU (60.9 mg, 0.16 mmol). The mixture was allowed to stir at room temperature for 18 hours. The mixture was washed three times with 30 mL of water adding EtOAc, then sequential washes of the organic layer was done with 10 % HCl, saturated $NaHCO_3$ and brine. The organic layer was dried over $MgSO_4$, filtered and

concentrated under reduced pressure. The crude product was purified on silica gel eluting with chloroform: MeOH 1% to 2%. 56.9 mg (57 %) of product **110** was obtained as an orange solid. $[\alpha]_D$ ($CHCl_3$, c = 1) -4.2°; IR (film, cm^{-1}) 3423, 3293, 2939, 2872, 1742, 1641, 1526, 1265, 1148; ^1H NMR (300 MHz, $CDCl_3$) δ 8.13 (s, 1H), 7.96-7.80 (m, 1H), 7.75-7.64 (m, 4H), 7.63-7.49 (m, 3H), 7.36-7.26 (m, 1H), 7.26-7.16 (m, 3H), 7.09 (dd, 9.3; 18.6 Hz, 2H), 7.02-6.91 (m, 1H), 6.80 (s, 1H), 5.42 (br t, 6.0 Hz, 1H), 4.65 (dd, 6.8; 14.3 Hz, 1H), 4.37 (d, 5.6 Hz, 2H), 4.14-3.93 (m, 2H), 3.03 (s, 6H), 2.79 (dd, 6.2; 12.4 Hz, 2H), 2.66 (s, 3H), 2.42-2.32 (m, 2H), 2.31-2.17 (m, 5H), 1.79-1.58 (m, 6H), 1.57-1.43 (m, 2H), 1.43-1.18 (m, 4H), 0.91 (d, 5.0 Hz, 6H); ^{13}C NMR (75 MHz, $CDCl_3$) δ; 173.7(s), 172.1(s), 167.8(s), 151.1(s), 150.6 (s), 150.0(s), 143.1(s), 138.7(s), 138.3(s), 137.2(s), 132.9(s), 131.8(s), 131.6(d), 131.0(d), 130.1(s), 128.6(d), 128.0(d), 127.9(d), 127.5(d), 126.7(d), 125.2(d), 124.9(s), 123.6(d), 122.0(d), 117.3(d), 115.7(d), 105.5(d), 65.4 (t), 52.1(d), 43.3(t), 41.1(t), 40.7(q), 37.1(t), 36.3(t), 29.3(t), 28.3(t), 25.5(t), 25.4(t), 23.3(t), 23.2(q), 22.2(q), 18.4(q), 17.9(q); MS (ESI, Na+) 940, 919, 179, 115, 83.

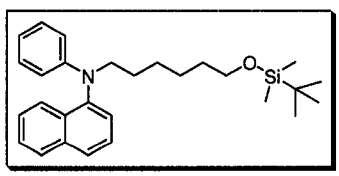

Compound 112: N-(6-(tert-butyldimethylsilyloxy)hexyl)-N-phenylnaphthalen-1-amine

Potassium hydride (30% wt) (152.6 mg, 3.80 mmol) was dissolved in 10 mL THF. A solution of N-phenylnaphthalen-1-amine (555.5 mg, 2.53 mmol) in 5 mL THF was slowly added. The mixture was allowed to stir for 2 hours at room temperature. Then, a solution of (6-bromohexyloxy)-tert-butyldimethylsilane (Aldrich No. 513148) (1.12 g, 3.80 mmol) in 5 mL THF and 20 mg of tetrabutylammonium fluoride was added. The mixture was stirred for 12 hours at room temperature. The mixture was cooled at 0°C and 20 mL of water was added. The mixture was extracted three times with Et_2O. The crude product was purified on silica gel eluting with Hexanes: EtOAc 1%. 869.7 mg (79 %) of product **112** was obtained as a clear oil. ^1H NMR (300 MHz, $CDCl_3$) δ 7.90 (d, 8.0 Hz, 1H), 7.82 (t, 7.8 Hz, 2H), 7.55-7.46 (m, 2H), 7.43-7.36 (m, 2H), 7.15-7.09 (m, 2H), 6.67 (t, 7.3 Hz, 1H), 6.53 (d, 8.2 Hz, 2H), 3.73 9t, 8.0 Hz, 2H), 3.57 (t, 6.5 Hz, 2H), 1.82-1.66

(m, 2H), 1.51-1.44 (m, 2H), 1.36-1.30 (m, 4H), 0.88 (s, 9H), 0.03 (s, 6H); ^{13}C NMR (75 MHz, $CDCl_3$) δ 149.8(s), 144.0(s), 135.7(s), 132.1(s), 129.4(d), 128.9(d), 127.3(d), 127.2(d), 126.8(d), 126.6(d), 124.4(d), 117.0(d), 113.5(d), 63.6(t), 53.0(t), 33.2(t), 28.2(t), 27.3(t), 26.4(q), 26.1(t), 18.8(s), -4.85(q); MS (EI) 433, 376, 232.

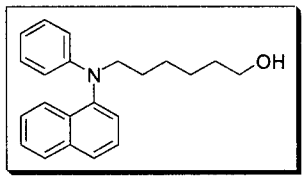

Compound 113: 6-(naphthalen-1-yl(phenyl)amino)hexan-1-ol

Compound 112 (859.3 mg, 1.98 mmol) was dissolved in 10 mL dry THF. A 1M solution in THF of TBAF (2.18 mL, 2.18 mmol) was added. The mixture was allowed to stir for 3 hours. The solution was concentrated under reduced pressure and dissolved in mixture of Et_2O/EtOAC (1:1). The organic layer was washed twice with water, dried over $MgSO_4$ and concentrated under reduced pressure. The crude product was purified on silica gel eluting with Hexanes: dichloromethane 10% to 100%. 556.3 mg (88%) of product **113** was obtained as a thick clear oil. IR (film, cm^{-1}) 3474, 2955, 2884, 2361, 2342, 1740, 1652, 1434, 1206; ^1H NMR (300 MHz, $CDCl_3$) δ 7.91 (d, 8.1 Hz, 1H), 7.82 (t, 8.0 Hz, 2H), 7.50 (dd, 8.1; 16.4 Hz, 2H), 7.44-7.34 (m, 2H), 7.12 (t, 8.0 Hz, 2H), 6.68 (t, 7.4 Hz, 1H), 6.54 (d, 8.1 Hz, 2H), 3.74 (t, 8.0 Hz, 2H), 3.58 (t, 6.4 Hz, 2H), 1.85-1.67 (m, 2H), 1.67-1.44 (m, 2H), 1.43-1.21 (m, 4H); ^{13}C NMR (75 MHz, $CDCl_3$) δ 149.8 (s), 143.9 (s), 135.7 (s), 132.0 (s), 129.4 (s), 128.9 (d), 127.3 (d), 126.8 (d), 126.7 (d), 126.6 (d), 124.3 (d), 117.0 (d), 113.5 (d), 63.2 (t), 52.9 (t), 33.1 (t), 28.2 (t), 27.3 (t), 26.0 (t); MS (EI) 319, 232, 104.

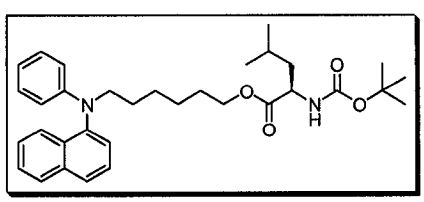

Compound 114: (R)-6-(naphthalen-1-yl(phenyl)amino)hexyl 2-(tert-butoxycarbonyl)-4-methylpentanoate

Compound 113 (41.4 mg, 0.13 mmol), DIPEA (0.09 mL, 0.52 mmol) and HOBT (26.3 mg, 0.20 mmol) were dissolved in 8 mL of dry DMF, followed by the addition of N-

BOC-D-phenylalanine (42.0 mg, 0.17 mmol) and EDC (37.4 mg, 0.20 mmol). The mixture was allowed to stir at room temperature for 18 hours. The mixture was washed three times with 20 mL of water adding EtOAc, then sequential washes of the organic layer were done with 10 % HCl, saturated $NaHCO_3$ and brine. The organic layer was dried over $MgSO_4$, filtered and concentrated under reduced pressure. The crude product was purified on silica gel eluting with Hexanes: EtOAc 10%. 24.4 mg (35 %) of product **114** was obtained as a white foamy solid. $[\alpha]_D$ ($CHCl_3$, c = 1) +3.2°; IR (film, cm^{-1}) 3380, 2933, 2859, 1741, 1499, 1160; ^1H NMR (300 MHz, $CDCl_3$) δ 7.90 (d, 8.1 Hz, 1H), 7.82 (d, 7.7 Hz, 2H), 7.52-7.36 (m, 4H), 7.12 (t, 7.8 Hz, 2H), 6.68 (t, 7.2 Hz, 1H), 6.54 (d, 8.3 Hz, 2H), 4.96 (br s, 1H), 4.30 (br s, 1H), 4.08 (t, 6.6 Hz, 2H), 3.74 (t, 7.8 Hz, 2H), 1.80-1.49 (m, 8H), 1.48-1.43 (m, 12H), 1.39-1.31 (m, 4H), 0.93 (d, 6.5 Hz, 6H); ^{13}C NMR (75 MHz, $CDCl_3$) δ 174.0(s), 155.9(s), 149.8(s), 143.9(s), 135.7(s), 132.0(s), 129.4(d), 128.9(d), 127.3(d), 127.1(d), 126.8(d), 126.6(d), 124.3(d), 117.1(d), 113.5(d), 80.3(d), 77.1(s), 65.6(t), 52.9(t), 52.5(d), 42.2(t), 28.9(t), 28.7(q), 28.7(t), 28.1(t), 27.1(t), 26.1(t), 25.2(d), 23.2(q), 22.4(q); MS (EI) 532, 458, 232, 130, 86, 57.

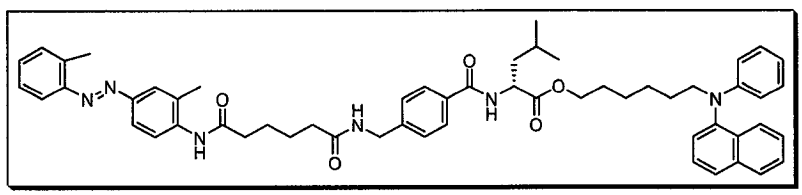

Compound 116: (R)-6-(naphthalen-1-yl(phenyl)amino)hexyl 4-methyl-2-[4-((6-(N-(2-methyl-4-(o-tolyldiazenyl)benzene)amino)-6-oxohexanamido)methyl)benzamido]pentanoate

114 (266.2 mg, 0.62 mmol) was dissolved in 8 mL DCM, followed by the addition of 2 mL of trifluoroacetic acid. The mixture was allowed to stir for one hour at room temperature. The solution was then concentrated under reduced pressure and dissolved in benzene and again concentrated under reduced pressure. This sequence was repeated twice to afford the desired product as a crude TFA salt **115**. The crude TFA salt, DIPEA (0.36 mL, 2.06 mmol) and HOBT (104.0 mg, 0.77 mmol) were dissolved in 15 mL of dry DMF, followed by the addition of **94** (250.0 mg, 0.51 mmol) and EDC (119.7 mg, 0.77 mmol). The mixture was allowed to stir at room temperature for 18 hours. The mixture

was washed three times with 30 mL of water adding EtOAc, then sequential washes of the organic layer was done with HCl 10 %, saturated $NaHCO_3$ and brine. The organic layer was dried over $MgSO_4$, filtered and concentrated under reduced pressure. The crude product was purified on silica gel eluting with chloroform: MeOH 1 %. 247.4 mg (54 %) of product **116** was obtained as an orange solid. $[\alpha]_D$ ($CHCl_3$, c = 1) -8.2°; IR (film, cm^{-1}) 3459, 3295, 3059, 2945, 2868, 2361, 2342, 1147, 1648, 1526, 1266; ^1H NMR (300 MHz, $CDCl_3$) δ 8.01-7.61 (m, 8H), 7.61-7.15 (m, 11H), 7.15-7.03 (m, 2H), 6.94-6.73 (m, 2H), 6.71-6.60 (m, 1H), 6.50 (d, 7.4 Hz, 2H), 5.26 (s, 2H), 4.83-4.68 (m, 1H), 4.44-4.28 (m, 2H), 4.15-3.99 (m, 2H), 3.69 (t, 7.4 Hz, 2H), 2.67 (s, 3H), 2.45-2.13 (m, 7H), 1.82-1.47 (m, 8H); ^{13}C NMR (75 MHz, $CDCl_3$) δ 173.7(s), 173.4(s), 171.9(s), 167.4(s), 151.1(s), 150.1(s), 149.7(s), 143.8(s0, 142.9(s), 138.6(s), 138.3(s), 135.6(s), 133.2(s), 132.0(s), 131.6(d), 131.1(d), 129.4(d), 128.9(d), 127.9(d), 127.8(d), 127.3(d), 127.1(d), 126.8(d), 126.6(d), 125.2(d), 124.2(d), 123.6(d), 122.1(d), 117.1(d), 115.7(d), 113.5(d), 65.8(t), 53.9(t), 52.8(t), 51,7(d), 43.3(t), 41.9(t), 37.2(t), 36.3(t), 28.9(t), 28.1(t), 27.1(t), 26.1(t), 25.5(t), 25.4(d), 25.3(t), 23.2(q), 22.4(q), 18.5(q), 17.9(q); MS (ESI, Na+) 924, 115.

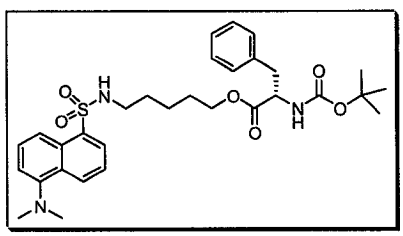

Compound 119: (S)-5-(1-(dimethylamino)naphthalene-5-sulfonamido)pentyl 2-(tert-butoxycarbonyl)-3-phenylpropanoate

Compound 95 (496.0 mg, 1.47 mmol), DIPEA (1.02 mL, 5.88 mmol) and HOBT (298.6 mg, 2.21 mmol) were dissolved in 20 mL of dry DCM, followed by the addition of N-BOC-L-phenylalanine (1.08 g, 2.95 mmol) and EDC (342.3 mg, 2.21 mmol). The mixture was allowed to stir at room temperature for 18 hours. The solution was concentrated under reduced pressure and dissolved in EtOAc. Sequenced washes of the organic layer were done with 10 % HCl, saturated $NaHCO_3$ and brine. The organic layer was dried over $MgSO_4$, filtered and concentrated under reduced pressure. The crude product was purified on silica gel eluting with Hexanes: EtOAc 30%. 768.9 mg (90 %) of product **119** was obtained as a fluorescent-yellow foam. $[\alpha]_D$ ($CHCl_3$, c = 1) +10.2°; IR

(film, cm^{-1}) 3335, 2944, 2867, 2361, 2336, 1718, 1700, 1505, 1166; ^1H NMR (300 MHz, $CDCl_3$) δ 8.52 (d, 8.5 Hz, 1H), 8.29 (d, 8.7 Hz, 1H), 8.22 (d, 7.3 Hz, 1H), 7.51 (dd, 7.9; 17.0 Hz, 2H), 7.25-7.13 (m, 4H), 7.08-7.06 (m, 2H), 4.99-4.94 (m, 2H), 4.48 (dd, 6.4; 14.2 Hz, 1H), 3.94-3.84 (m, 2H), 3.06-2.97 (m, 2H), 2.90-2.77 (m, 8H), 1.39-1.26 (m, 13H), 1.16-1.03 (m, 2H); ^{13}C NMR (75 MHz, $CDCl_3$) δ 172.3(s), 155.5(s), 152.4(s), 136.4(s), 135.1(s), 130.8(d), 130.2(s), 130.0(d), 129.7(d), 128.9(d), 128.8(d), 127.3(d), 123.6(d), 119.1(d), 115.6(d), 80.3(s), 65.3(t), 54.6(d), 45.8(q), 43.3(t), 38.8(t), 29.4(t), 28.7(q), 28.1(t), 23.1(t); MS (EI) 583, 392, 171, 56, 41.

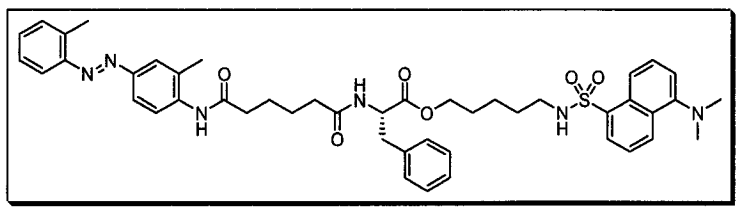

Compound 121: (S)-5-(1-(dimethylamino)naphthalene-5-sulfonamido)pentyl 2-[(6-(N-(2-methyl-4-(o-tolyldiazenyl)benzene)amino)-6-oxohexanamido]-3-phenylpropanoate

Compound 119 (312.2 mg, 0.54 mmol), was dissolved in 12 mL DCM, followed by the addition of 3 mL of trifluoroacetic acid. The mixture was allowed to stir for one hour at room temperature. The solution was then concentrated under reduced pressure and dissolved in benzene and again concentrated under reduced pressure. This sequence was repeated twice to afford the desired product as a crude TFA salt **120**. The crude TFA salt, DIPEA (0.37 mL, 2.15 mmol) and HOBT (181.0 mg, 1.34 mmol) were dissolved in 12 mL of dry DMF, followed by the addition of crude **80** (379.6 mg, 1.07 mmol) and EDC (208.4 mg, 1.34 mmol). The mixture was allowed to stir at room temperature for 18 hours. The mixture was washed three times with 30 mL of water adding EtOAc, then sequential washes of the organic layer was done with 10 % HCl, saturated $NaHCO_3$ and brine. The organic layer was dried over $MgSO_4$, filtered and concentrated under reduced pressure. The crude product was purified on silica gel eluting with chloroform: MeOH 1 %. 212.5 mg (48 %) of product **121** was obtained as an orange foam. $[\alpha]_D$ ($CHCl_3$, c = 1) +0.3°; IR (film, cm^{-1}) 3351, 2946, 2873, 2361, 2334, 1738, 1651, 1141; ^1H NMR (300 MHz, $CDCl_3$) δ 8.50 (d, 8.5 Hz, 1H), 8.28 (d, 8.7 Hz, 1H), 8.19 (d, 6.6 Hz, 1H), 8.02 (d,

8.4 Hz, 1H), 7.75-7.68 (m, 2H), 7.58-7.46 (m, 4H), 7.32-7.19 (m, 5H), 7.14-7.09 (m, 4H), 6.12 (d, 7.5 Hz, 1H), 5.44 (br t, 6.0 Hz, 1H), 4.10-3.88 (m, 2H), 3.15-2.99 (m, 4H), 2.89 (m, 5H), 2.68 (s, 3H), 2.41-2.36 (m, 2H), 2.27-2.22 (m, 5H), 1.80-1.64 (m, 4H), 1.46-1.30 (m, 4H), 1.25-1.16 (m, 2H); ^{13}C NMR (75 MHz, $CDCl_3$) δ 173.3(s), 172.2(s), 171.8(s), 152.3(s), 151.2(s), 149.9(s), 138.8(s), 138.2(s), 136.3(s), 135.2(s), 131.6(d), 131.0(d), 130.7(d), 130.2(s), 130.0(s), 129.8(d), 129.5(d), 129.0(d), 128.7(d), 127.5(d), 126.8(d), 125.1(d), 123.6(d), 123.0(d), 122.2(d), 119.1(d), 115.7(d), 115.6(d), 65.3(t), 53.9(d), 45.8(q), 43.2 (t), 38.0(t), 37.4(t), 36.1(t), 29.2(t), 28.1(t), 25.4(t), 25.0(t), 23.0(t), 18.4(q), 17.9(q); MS (ESI, Na+) 842, 445, 156, 115.

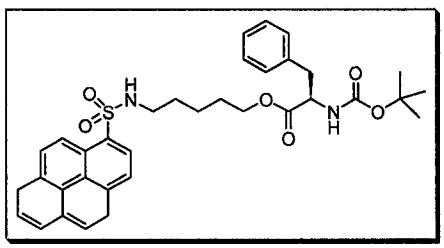

Compound 122: (R)-5-(1,5-dihydropyrene-8-sulfonamido)pentyl 2-(tert-butoxycarbonyl)-3-phenylpropanoate

Compound 102 (868.0 mg, 2.36 mmol), DIPEA (1.50 mL, 8.60 mmol) and HOBT (436.4 mg, 3.23 mmol) were dissolved in 40 mL of dry DCM, followed by the addition of N-BOC-D-phenylalanine (569.2 mg, 2.15 mmol) and EDC (618.3 mg, 3.23 mmol). The mixture was allowed to stir at room temperature for 18 hours. The solution was concentrated under reduced pressure and dissolved in EtOAc. A sequenced wash of the organic layer was done with 10 % HCl, saturated $NaHCO_3$ and brine. The organic layer was dried over $MgSO_4$, filtered and concentrated under reduced pressure. The crude product was purified on silica gel eluting with Hexanes: EtOAc 30% to 50%. 1.25 g (94 %) of product **122** was obtained as a fluorescent-yellow foam. $[\alpha]_D$ ($CHCl_3$, c = 2) -7.7°; IR (film, cm^{-1}) 3335, 2939, 2868, 2340, 1713, 1154; ^1H NMR (300 MHz, $CDCl_3$) δ 8.95 (d, 9.4 Hz, 1H), 8.68 (d, 8.2 Hz, 1H), 8.31-8.27 (m, 3H), 8.20 (d, 8.7 Hz, 2H), 8.12-8.07 (m, 2H), 7.22-7.13 (m, 3H), 7.05-7.02 (m, 2H), 4.92 (m, 2H), 4.42 (dd, 6.4; 13.6 Hz, 1H), 3.86-3.78 (m, 2H), 2.97-2.83 (m, 4H), 1.42-1.21 (m, 13H), 1.17-1.03 (m, 2H); ^{13}C NMR (75 MHz, $CDCl_3$) δ 172.3(s), 155.4(s), 136.4(s), 135.2(s), 131.5(s), 131.3(s), 130.6(s),

130.6(s), 130.5(s), 129.6(d), 128.9(d), 128.4(s), 127.9(d), 127.5(d), 127.3(d), 127.2(d), 125.6(s), 124.4(s), 124.3(d), 123.4(d), 80.3(s), 65.2(t), 54.8(d), 43.4(t), 38.7(t), 29.4(t), 28.7(q), 28.1(t), 23.1(t); MS (EI) 614, 201, 41.

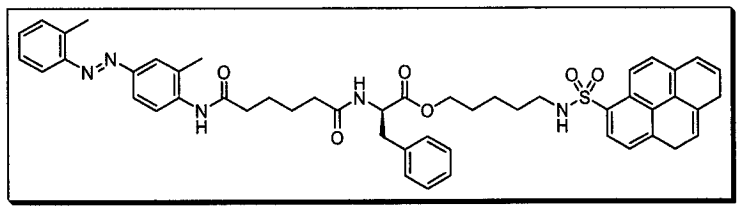

Compound 124: (R)-5-(1,5-dihydropyrene-8-sulfonamido)pentyl 2-[(6-(N-(2-methyl-4-(o-tolyldiazenyl)benzene)amino)-6-oxohexanamido]-3-phenylpropanoate

Compound 122 (219.7 mg, 0.36 mmol) was dissolved in 8 mL DCM, followed by the addition of 2 mL of trifluoroacetic acid. The mixture was allowed to stir for one hour at room temperature. The solution was then concentrated under reduced pressure and dissolved in benzene and again concentrated under reduced pressure. This sequence was repeated twice to afford the desired product as a crude TFA salt **123**. The crude TFA salt, DIPEA (0.25 mL, 1.42 mmol) and HOBT (72.1 mg, 0.53 mmol) were dissolved in 12 mL of dry DMF, followed by the addition of crude **80** (163.6 mg, 0.46 mmol) and EDC (102.4 mg, 0.53 mmol). The mixture was allowed to stir at room temperature for 18 hours. The mixture was washed three times with 30 mL of water adding EtOAc, then sequential washes of the organic layer was done with 10 % HCl, saturated $NaHCO_3$ and brine. The organic layer was dried over $MgSO_4$, filtered and concentrated under reduced pressure. The crude product was purified on silica gel eluting with $CHCl_3$: MeOH 0 to 1 %. 128.7 mg (42 %) of product **124** was obtained as an orange foam. $[\alpha]_D$ ($CHCl_3$, c = 1) +5.0°; IR (film, cm^{-1}) 3306, 2930, 2867, 2362, 2342, 1650, 1540, 1264, 1158; ^1H NMR (300 MHz, $CDCl_3$) δ 8.95 (d, 9.4 Hz, 1H), 8.64 (d, 8.2 Hz, 1H), 8.26-8.12 (m, 5H), 8.07-8.01 (m, 2H), 7.92 (d, 8.5 Hz, 1H), 7.60-7.52 (m, 4H), 7.33-7.18 (m, 6H), 7.12-7.08 (m, 2H), 6.11 (d, 7.3 Hz, 1H), 5.81 (t, 6.0 Hz, 1H), 4.70 (dd, 7.2; 13.3 Hz, 1H), 4.09-4.01 (m, 1H), 4.00-3.82 (m, 1H), 3.14-3.00 (m, 2H), 2.99-2.82 (m, 2H), 2.67 (s, 3H), 2.45-2.37 (m, 2H), 2.33-2.26 (m, 2H), 2.18 (s, 3H), 1.80-1.70 (m, 4H), 1.43-1.29 (m, 4H), 1.25-1.15 (m, 2H); ^{13}C NMR (75 MHz, $CDCl_3$) δ 173.4(s), 172.2(s), 171.8(s), 151.1(s), 149.7(s), 138.7(s), 138.3(s), 136.3(s), 135.1(s), 131.6(d), 131.3(s), 131.0(d), 130.5(d),

130.5(s), 130.4(d), 129.5(d), 129.3(s), 129.1(d), 128.3(s), 127.7(d), 127.6(d), 127.4(d), 127.3(d), 127.3(d), 127.2(d), 126.8(d), 125.5(s), 125.0(d), 124.4(s), 124.2(d), 123.4(d), 122.9(d), 122.0(d), 115.7(d), 66.2(t), 54.0(d), 43.2(t), 38.0(t), 37.3(t), 36.1(t), 29.1(t), 28.0(t), 25.4(t), 25.0(t), 23.0(t), 18.2(q), 18.0(q); MȘ (ESI, Na+) 873, 115, 83.

7.3 Procedures of Acquisition of Fluorescence Spectra and Hydrolysis

7.3.1 CHAPTER 4: Leucine-based system

7.3.1.1 TLC experiment with modified substrates (Figure 19)

Compounds 91 (1.9 mg, 0.0072 mmol) and **92** (2.0 mg, 0.0072 mmol) were dissolved in 0.1 mL DCM and 2 mL of Hexanes. L-proline chiral selector **90** (4.4 mg, 0.0144 mmol) was added, followed by the addition of solution 2M NaOH (2 mL). The reaction was vigorously stirred at room temperature. TLC samples from the organic layer were taken at 0, 8 and 18 hours and eluted with EtOAc/Hexanes 3:7 and revelated under UV light.

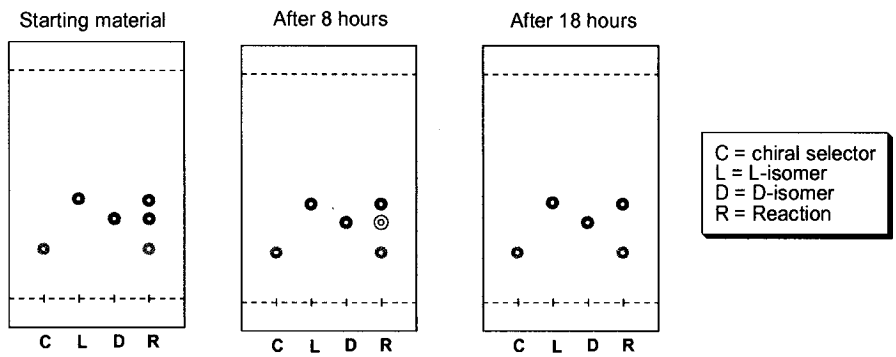

7.3.1.2 Fluorescence spectra of DNS-OH and GBC-L-Leu-DNS (Figure 20)

a) A quartz cell (l = 1 cm) was filled with a solution of DNS-OH **95** (1.51×10^{-4} M in DCM). By using a scan mode, maximum excitation and emission wavelengths were found to be 337 nm and 483 nm respectively. The excitation/emission slits were adjusted at 5/2.5 nm.

Excitation spectrum (Emission @ 530 nm)

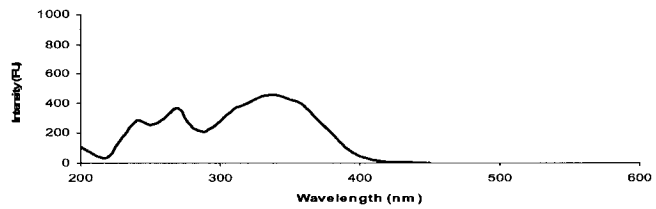

Emission spectrum (Excitation @ 360 nm)

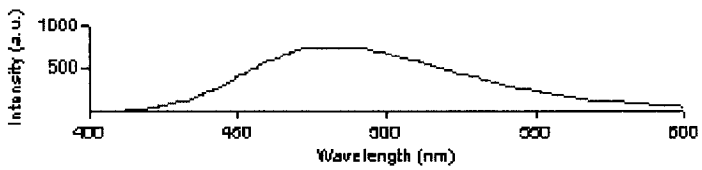

b) A quartz cell (l = 1 cm) was filled with a solution of GBC-L-Leu-DNS **98** (1.51 x 10^{-4} M in DCM). The excitation/emission slits were adjusted to 5 nm.

Emission spectrum (Excitation @ 337 nm)

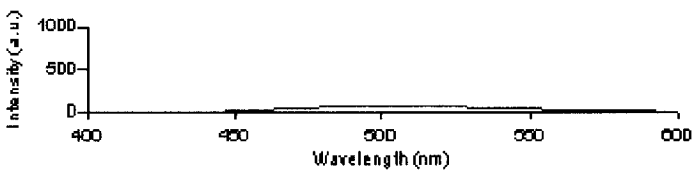

7.3.1.3 Fluorescence spectra of PYR-OH and BFZ-D-Leu-PYR (Figure 21)

a) A quartz cell (l = 1 cm) was filled with a solution of PYR-OH **102** (2.86 x 10^{-5} M in DCM). By using a scan mode, maximum excitation and emission wavelengths were found to be 340 nm and 380 nm respectively. A second emission band also appeared at 400 nm. The excitation/emission slits were adjusted at 5/2.5 nm.

Excitation spectrum (Emission @ 380 nm)

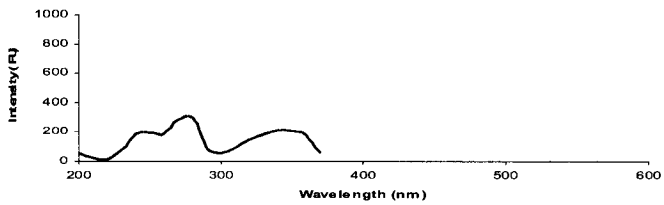

Emission spectrum (Excitation @ 340 nm)

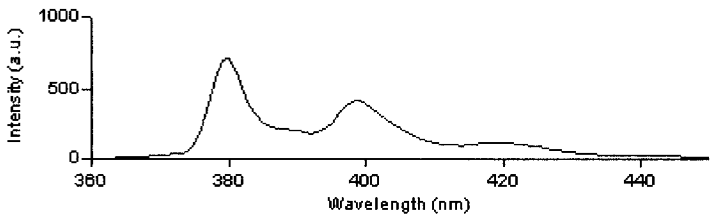

b) A quartz cell (l = 1 cm) was filled with a solution of BFZ-D-Leu-PYR **105** (2.86 x 10^{-5} M in DCM). The excitation/emission slits were adjusted at 5 nm. An additional emission appeared at 466 nm which correspond to BFZ emission band.

Emission spectrum (Excitation @ 340 nm)

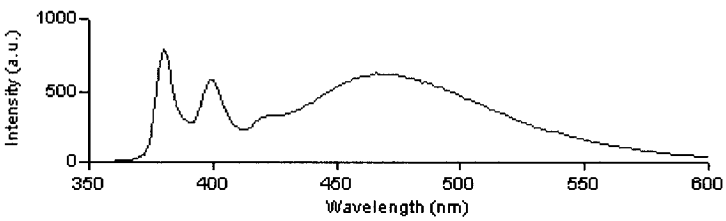

*7.3.1.4 UV absorption spectrum of GBC ester **125** (Figure 22)*

A quartz cell (l = 1 cm) was filled with a solution of GBC-D-Phe-OEt **125** (1.51 x 10^{-5} M in DCM). The $\lambda_{maximum}$ were found to be 239, 348 and 442 nm.

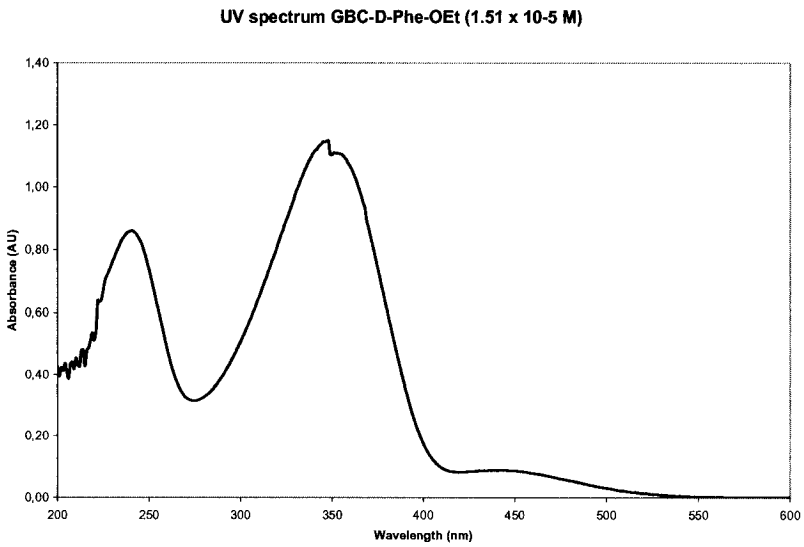

7.3.1.5 Fluorescence spectra of BRN-OH and GBC-D-Leu-BRN (Figure 24)

a) A quartz cell (l = 1 cm) was filled with a solution of BRN-OH **107** (6.15 x 10^{-5} M in DCM). By using a scan mode, maximum excitation and emission wavelengths were found to be 343 nm and 418 nm respectively. The excitation/emission silts were adjusted to 1.5/5 nm.

Excitation spectrum (Emission @ 419 nm)

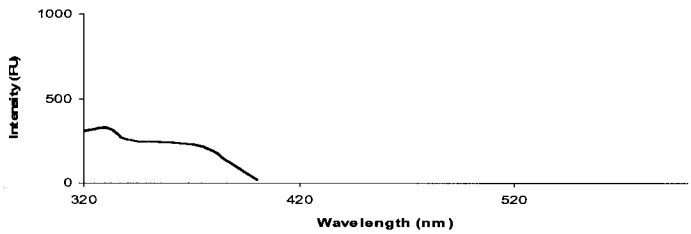

Emission spectrum (Excitation @ 330 nm)

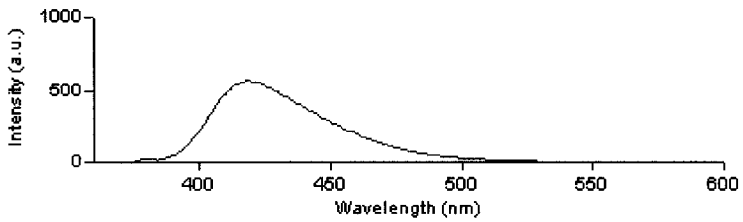

b) A quartz cell (l = 1 cm) was filled with a solution of GBC-D-Leu-BRN **110** (6.15 x 10^{-5} M in DCM). The excitation/emission slits were adjusted at 5 nm. Weak emission remained at 418 nm.

Emission spectrum (Excitation @ 343 nm)

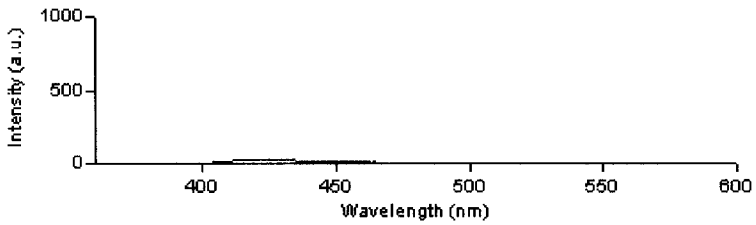

7.3.1.6 Fluorescence spectrum of equimolar mixture of DNS-OH and BRN-OH (Figure 25)

A quartz cell (l = 1 cm) was filled with an equimolar solution of **95** and **107** (1.01 x 10^{-4} M of each in DCM). Chosen $\lambda_{excitation}$ @ 350 nm. The excitation/emission slits were adjusted at 5 nm. Emission bands at 419 nm and 500 nm were expected. An emission maximum was observed at 420 nm only, no distinction between emission bands.

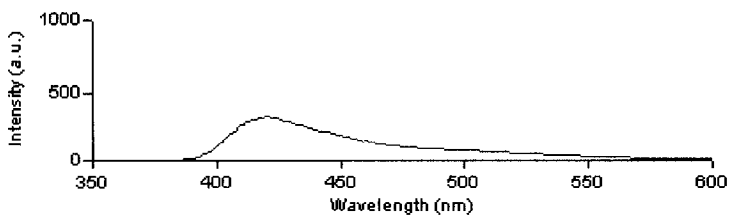

7.3.1.7 Fluorescence spectra of NPN-OH and GBC-D-Leu-NPN (Figure 27)

a) A quartz cell (l = 1 cm) was filled with a solution of NPN-OH **113** (6.51 x 10^{-5} M in DCM). By using a scan mode, maximum excitation and emission wavelengths were found to be 343 nm and 434 nm respectively. The excitation/emission slits were adjusted at 5 nm.

Excitation spectrum (Emission at 434 nm)

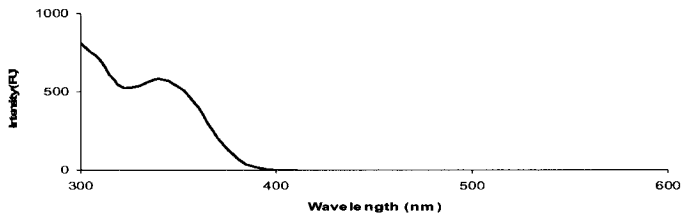

Emission spectrum (Excitation at 343 nm)

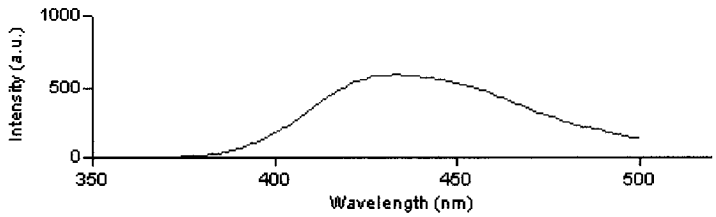

b) A quartz cell (l = 1 cm) was filled with a solution of GBC-D-Leu-NPN **116** (6.51 x 10^{-5} M in DCM). Chosen $\lambda_{excitation}$ was at 343 nm. The excitation/emission slits were adjusted at 5 nm.

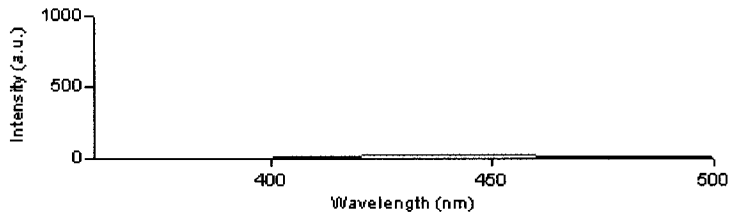

7.3.1.8 Fluorescence spectrum of equimolar mixture of DNS-OH and NPN-OH (Figure 28)

A quartz cell (l = 1 cm) was filled with an equimolar solution of DNS-OH **95** and NPN-OH **113** (1.01 x 10^{-4} M of each in DCM). Chosen $\lambda_{excitation}$ was at 343 nm. The excitation/emission slits were adjusted at 5 nm and 2.5 nm respectively. NPN emission band disappeared, only an emission at 500 nm was observed.

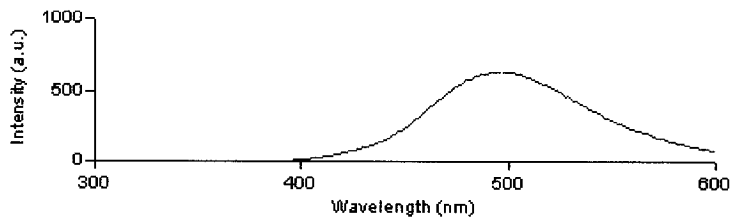

7.3.1.9 Fluorescence spectrum of GBC-D-Leu-PYR (Figure 28)

A quartz cell (l = 1cm) was filled with a solution of GBC-D-Leu-PYR **117** (2.86 x 10^{-5} M in DCM). Chosen $\lambda_{excitation}$ was at 340 nm. The excitation/emission slits were adjusted at 5 nm.

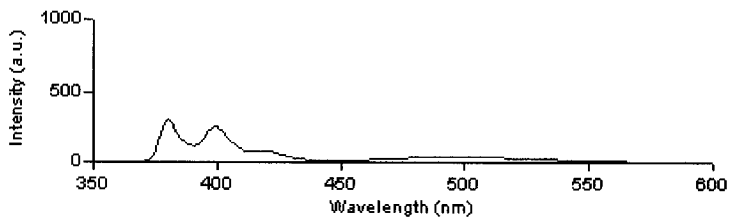

7.3.1.10 Fluorescence spectrum of equimolar mixture of DNS-OH and PYR-OH (Figure 30)

A quartz cell (l = 1 cm) was filled with an equimolar solution of DNS-OH **95** and PYR-OH **102** (1.01 x 10^{-4} M of each in DCM). Chosen $\lambda_{excitation}$ was at 370 nm. The

excitation/emission slits were adjusted at 5 nm. The spectrum showed a clear distinction of emission band of each donor.

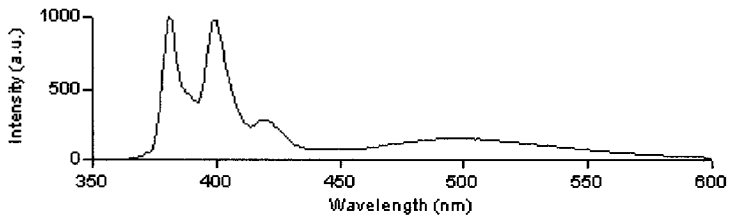

7.3.1.11 Hydrolysis of GBC-L-Leu-DNS and GBC-D-Leu-NPN followed by TLC (Figure31)

LiOH hydrolysis:

Compounds 98 (2 mg, 0.0022 mmol) and **116** (1.9 mg, 0.0022 mmol) were dissolved in 5 mL THF/MeOH/H_2O (3:1:1), followed by the addition of 1mg of LiOH. The mixture was allowed to stir at room temperature. TLC samples were taken at 0 and 30 minutes eluting with $CHCl_3$: MeOH 10% and revealed under UV light.

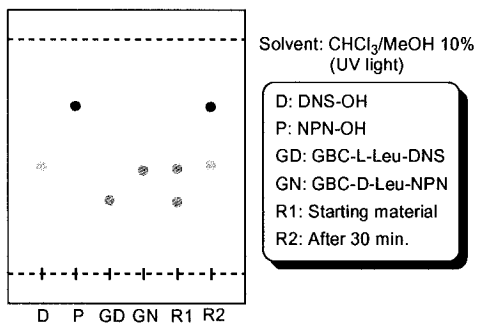

Biphasic Hydrolysis:

Compounds 98 (2 mg, 0.0022 mmol) and **116** (1.9 mg, 0.0022 mmol) were dissolved in 2 mL DCM, followed by the addition of 2 mL of solution 2M NaOH. The mixture was allowed to stir vigorously at room temperature. TLC samples were taken at 0, 2, 7 and 18 hours eluting with $CHCl_3$: MeOH 10% and revealed under UV light.

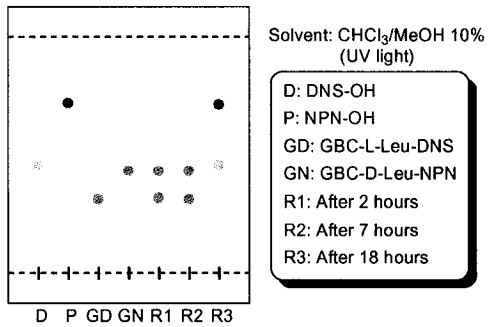

7.3.1.12 Hydrolysis of GBC-L-Leu-DNS and GBC-D-Leu-NPN followed by TLC using chiral selector (Figure 32)

Compounds 98 (2 mg, 0.0022 mmol) and **116** (1.9 mg, 0.0022 mmol) were dissolved in 2 mL DCM, followed by the addition of ~1 mg of (L)- or (D)-selector and 2 mL of solution 2M NaOH. The mixture was allowed to stir vigorously at room temperature. TLC samples were taken at 0, 2, 7 and 18 hours eluting with $CHCl_3$: MeOH 10% and revealed under UV light.

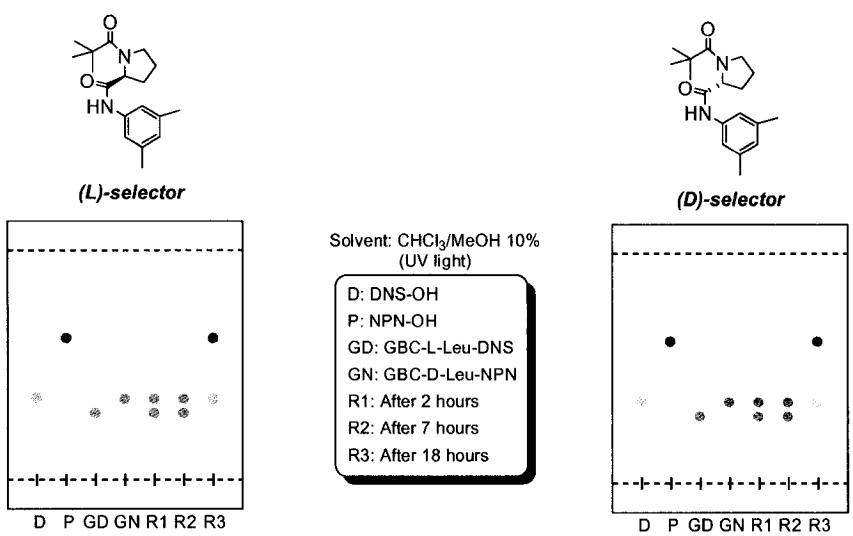

7.3.1.13 Hydrolysis of GBC-L-Leu-DNS and GBC-D-Leu-PYR followed by fluorescence (Figure33)

An equimolar mixture of **98** and **117** (1.01 x 10^{-4} M of each) was dissolved in 10 mL DCM, followed by the addition of 10 mL of solution 2M NaOH. The mixture was allowed to stir vigorously at room temperature. Fluorescence spectra were recorded at 0, 19 hours and 2 days using a quartz cell (l = 1 cm) filled with the DCM layer. Chosen $\lambda_{excitation}$ was at 370 nm and the excitation/emission slits were adjusted at 2.5 nm. After 2 days, there was no observable hydrolysis.

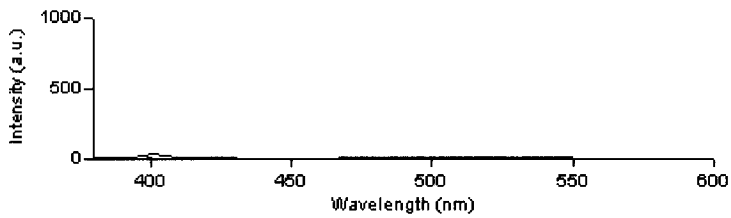

7.3.1.14 Hydrolysis of GBC-L-Leu-DNS and GBC-D-Leu-PYR followed by fluorescence (Figure34)

a) Equimolar solution of **98** and **117** (1.01 x 10^{-4} M of each) was dissolved in 10 mL DCM, followed by the addition of ~ 5 mg of (L)-selector and 10 mL of solution 2M NaOH. The mixture was allowed to stir vigorously at room temperature. Fluorescence spectra were recorded at 0, 2, 19 hours and 2 days using a quartz cell (l = 1 cm) filled with the DCM layer. Chosen $\lambda_{excitation}$ was at 370 nm. The excitation/emission slits were adjusted at 2.5 nm.

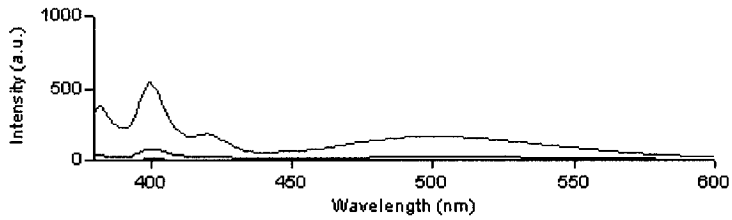

b) Same procedure as in a), but added (D)-selector.

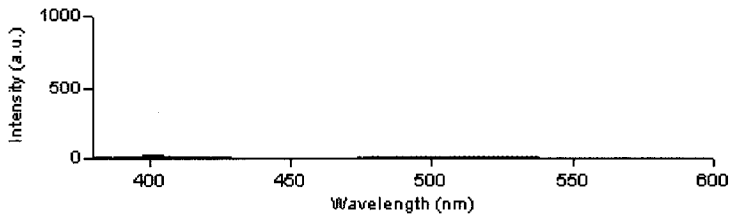

7.3.1.15 Investigation of results: TLC experiment on modified substrates (Figure 35)

(L)-selector

Compounds (D)-**91** (1.9 mg, 0.0072 mmol) and (L)-**92** (2.0 mg, 0.0072 mmol) were dissolved in 0.1 mL DCM and 2 mL Hexanes. L-proline chiral selector **90** (4.4 mg, 0.0144 mmol) was added, followed by the addition of 2 mL of solution 2M NaOH. The reaction was vigorously stirred at room temperature. TLC samples of the organic layer were taken at 0, 8 and 18 hours and eluted with EtOAc/Hexanes 3:7 and revelated under UV light.

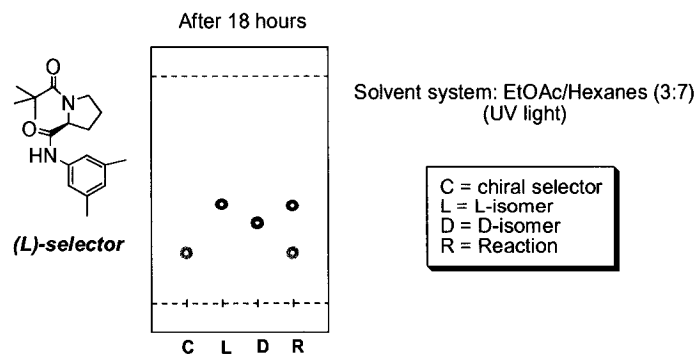

(D)-selector

Compounds (D)-**91** (2.1 mg, 0.0089 mmol) and (L)-**92** (2.5 mg, 0.0089 mmol) were dissolved in 0.1 mL DCM and 2 mL Hexanes. D-proline chiral selector **90** (5.4 mg, 0.0177 mmol) was added, followed by the addition of 2 mL of solution 2M NaOH. The reaction was vigorously stirred at room temperature. TLC samples of the organic layer were taken at 0, 8 and 18 hours and eluted with EtOAc/Hexanes 3:7 and revelated under UV light.

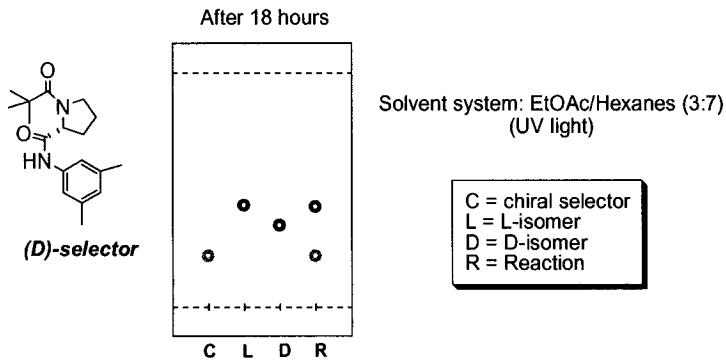

7.3.1.16 Investigation of results: chiral HPLC method on modified substrates. (Table 1)

Compounds (L)-**92** (9.3 mg, 0.038 mmol) and (D)-**91** (9.3 mg, 0.038 mmol) were dissolved in 10 mL Hexanes/DCM (20 :1). Then, (L)-selector **90** (45.6 mg, 0.15 mmol) and 10 mL of solution 2M NaOH were added. The mixture was stirred vigorously at room temperature. Aliquots were taken at 0, 2 and 4 hours and submitted on a chiral HPLC (Hexanes/isopropanol 98:2, isocratic). Same procedure was used for the (D)-selector.

Results

(L)-selector

Time (hours)	AUC selector	(L)-92		(D)-91	
		AUC	ratio	AUC	ratio
0	194216900	81342586	0,419	92635071	0,477
2	294602129	69920473	0,237	61182697	0,208
4	170883981	21352138	0,125	12379507	0,072

(D)-selector

Time (hours)	AUC selector	(L)-92		(D)-91	
		AUC	ratio	AUC	ratio
0	177975471	71773776	0,403	78604090	0,442
2	213703493	69227039	0,324	61506502	0,288
4	183775103	44572199	0,243	47772158	0,260

7.3.1.17 Dinitro compounds hydrolysis (Scheme 44)

a) Compounds (L)-**118** (20.0 mg, 0.057 mmol) and (D)-**118** (20.0 mg, 0.057 mmol) were dissolved in 10 mL DCM/Hexanes 3:7. (L)-selector **90** (68.5 mg, 0.23 mmol) was added, followed by the addition of 10 mL of solution 2M NaOH. The mixture was stirred vigorously at 0 °C. After 8 hours, the mixture was extracted three times with DCM. The aqueous layer was then acidified with 2M HCl and extracted with EtOAc. The organic layer was dried over $MgSO_4$ and concentrated under reduced pressure to give 6.1 mg of an unknown compound.

b) Compounds (L)-**118** (149.5 mg, 0.42 mmol) was dissolved in 10 mL THF/MeOH/H_2O (3:1:1). H_2O_2 (0.1 mL, 3.38 mmol) was added, followed by the addition of LiOH (53.3 mg, 1.27 mmol) at 0 °C. The mixture was stirred for 18 hours at 0 °C. A red coloration appeared. 5 mL of solution 1.5N Na_2SO_3 was added and the mixture was concentrated under reduced pressure, then extracted three times with DCM. The aqueous layer was acidified with 2M HCl and extracted three times with EtOAc. The organic layer was dried over $MgSO_4$ and concentrated under reduced pressure to give an unknown compound.

7.3.1.18 Calibration curve (Figure36)

All solutions were prepared from stock solutions in 10 mL volumetric flask.

Concentration of stock solution DNS-OH = 1.01 x 10^{-3} M (3.4 mg in 10 mL DCM)

Concentration of stock solution PYR-OH = 1.00 x 10^{-3} M (3.7 mg in 10 mL DCM)

Volumes taken from the stock solutions were measured with a 1 mL volumetric pipette and DCM was used as solvent.

solution #	volume stock sln DNS-OH (mL)	[DNS-OH] (M)	volume stock sln PYR-OH (mL)	[PYR-OH] (M)
1	1.0	1,00E-04	0.0	0,00E+00
2	0.9	9,00E-05	0.1	1,00E-05
3	0.8	8,00E-05	0.2	2,00E-05
4	0.7	7,00E-05	0.3	3,00E-05
5	0.6	6,00E-05	0.4	4,00E-05
6	0.5	5,00E-05	0.5	5,00E-05
7	0.4	4,00E-05	0.6	6,00E-05
8	0.3	3,00E-05	0.7	7,00E-05
9	0.2	2,00E-05	0.8	8,00E-05
10	0.1	1,00E-05	0.9	9,00E-05
11	0.0	0,00E+00	1.0	1,00E-04

Fluorescence spectra were recorded for each solution using a quartz cell (l = 1 cm). Chosen $\lambda_{excitation}$ was at 370 nm. Two scans were made per solution:

1) PYR-OH $\lambda_{emission}$ at 400 nm; excitation/emission slits = 2.5/2.5 nm.

2) DNS-OH $\lambda_{emission}$ at 500 nm; excitation/emission slits = 2.5/5 nm.

The experiment was repeated three times, so that an intensity average could be calculated.

1) Results for PYR-OH scans

Solution #	repeat 1	repeat 2	repeat 3	average
1	305,7	351,7	361,0	339,5
2	258,4	286,0	319,1	287,8
3	224,0	265,9	286,7	258,9
4	203,2	238,4	244,6	228,8
5	172,1	195,7	213,2	193,7
6	141,9	167,0	180,7	163,2

7	111,9	136,3	153,7	134,0
8	87,9	100,2	112,8	100,3
9	58,0	68,8	77,4	68,1
10	29,7	30,3	39,3	33,1
11	0,2	0,2	0,3	0,2

2) Results for DNS-OH scans

Solution #	repeat 1	repeat 2	repeat 3	average
1	8,2	9,3	7,9	8,5
2	71,4	63,3	64,1	66,3
3	138,1	122,0	122,6	127,6
4	207,4	185,5	177,4	190,1
5	265,6	235,8	230,7	244,0
6	320,8	309,6	314,9	315,1
7	387,9	364,4	359,1	370,5
8	447,0	398,1	420,2	421,8
9	512,2	464,1	491,8	489,4
10	615,3	549,4	578,6	581,1
11	695,5	638,7	626,6	653,6

Plot was established of concentrations versus the average fluorescence intensity at each characteristic wavelength.

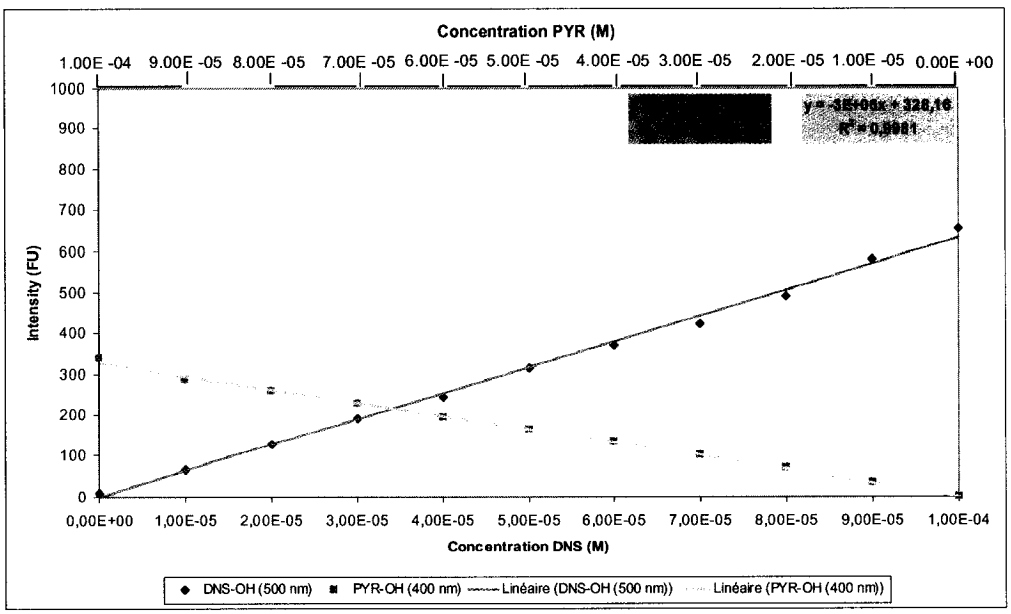

7.3.1.19 Calibration curve (Figure 37)

5 mL of each solution prepared in 7.3.1.18 was placed in separate vials. Then, 0.2 mL of a 2.50 x 10^{-3} M stock solution of **93** (25.0 mg in 20 mL DCM) was added to each vial which correspond to equivalent amount of GBC moiety that would be released in the case of a complete hydrolysis. A concentration correction was made to compensate this small dilution. The scans were repeated three times with the same parameters as used in 7.3.1.18.

solution #	[DNS-OH] (M)	[DNS-OH] (M) corrected	[PYR-OH] (M)	[PYR-OH] (M) corrected
1	1,00E-04	9,62E-05	0,00E+00	0,00E+00
2	9,00E-05	8,65E-05	1,00E-05	9,62E-06
3	8,00E-05	7,69E-05	2,00E-05	1,92E-05
4	7,00E-05	6,73E-05	3,00E-05	2,88E-05
5	6,00E-05	5,77E-05	4,00E-05	3,85E-05
6	5,00E-05	4,81E-05	5,00E-05	4,81E-05
7	4,00E-05	3,85E-05	6,00E-05	5,77E-05
8	3,00E-05	2,88E-05	7,00E-05	6,73E-05
9	2,00E-05	1,92E-05	8,00E-05	7,69E-05
10	1,00E-05	9,62E-06	9,00E-05	8,65E-05
11	0,00E+00	0,00E+00	1,00E-04	9,62E-05

1) Results for PYR-OH scans (Fluorescence intensities)

Solution #	repeat 1	repeat 2	repeat 3	average
1	879,7	998,3	1000,0	959,3
2	789,0	923,7	1000,0	904,2
3	713,6	828,2	872,9	804,9
4	602,5	714,1	787,2	701,3
5	512,7	641,7	704,6	619,6
6	407,6	524,5	574,8	502,3
7	362,7	409,7	473,0	415,1
8	272,2	313,7	380,5	322,2
9	184,1	205,7	255,2	215,0
10	93,9	109,1	129,3	110,7
11	1,3	2,6	1,2	1,7

2) Results for DNS-OH scans (Fluorescence intensities)

Solution #	repeat 1	repeat 2	repeat 3	average
1	2,8	7,5	10,4	6,9
2	65,1	65,4	64,7	65,1
3	132,6	120,5	120,0	124,4
4	187,2	173,6	178,6	179,8
5	249,3	242,7	241,4	244,5
6	294,3	295,8	308,2	299,4
7	383,0	344,5	346,5	358,0
8	439,0	409,6	422,8	423,8
9	500,3	460,0	488,0	482,8
10	600,9	524,6	576,5	567,3
11	627,9	581,9	600,8	603,5

Plot was established of concentrations versus the average fluorescence intensity at each characteristic wavelength.

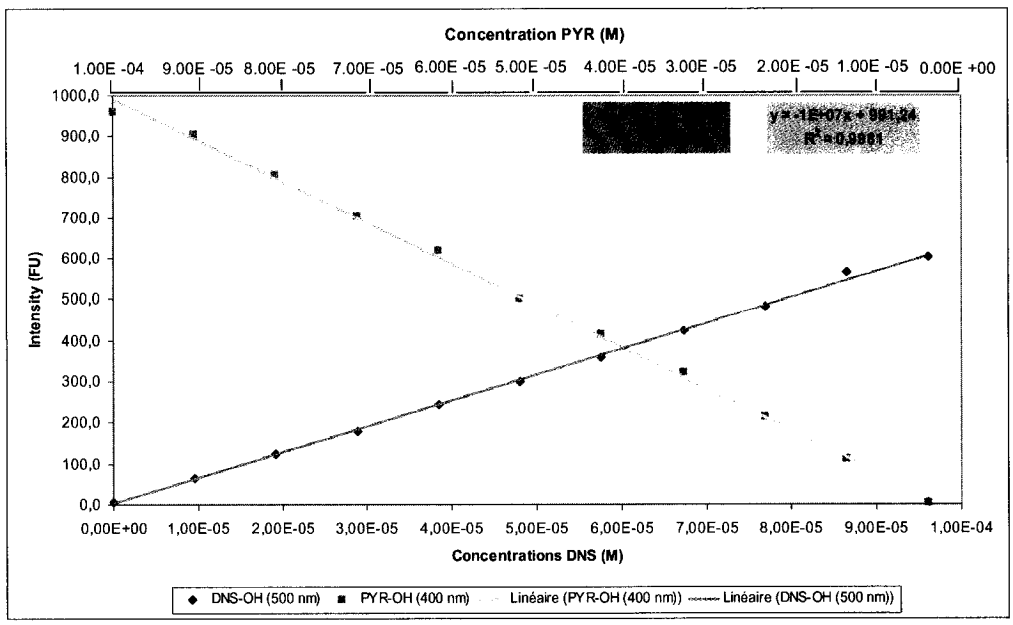

7.3.2 CHAPTER 6: Alcalase.

7.3.2.1 LiOH hydrolysis (Figure 38)

Reaction procedure

In a 25 mL round bottom flask, **121** (16.4 mg, 2.00 x 10^{-5} moles) and **124** (17.0 mg, 2.00 x 10^{-5} moles) were in dissolved in 20 mL THF/MeOH/H_2O (3:1:1). LiOH (2.5 mg, 6.00 x 10^{-5} moles) was added and the mixture was stirred at room temperature. Aliquots (0.76 mL) were taken at 0, 15, 25 and 1440 minutes and were placed in a separatory funnel where $NaHCO_3$ solution was added. Extraction with minimal DCM volumes was performed and the organic layer was poured into a 5 ml volumetric flask to give a 1.51 x 10^{-4} M solution of each donor in a hypothetical completed hydrolysis. Emission fluorescence readings (Advanced Reads program) were taken at 400 nm (PYR-OH) and 500 nm (DNS-OH) with excitation wavelength at 370 nm in both cases. The excitation/emission slits were adjusted at 5 nm.

Results

time (min)	400 nm	500 nm
0	5.81	4.26
15	185.02	300.6
25	205.76	399.41
1440	475.83	831.56

A plot of fluorescence intensities versus the time was established.

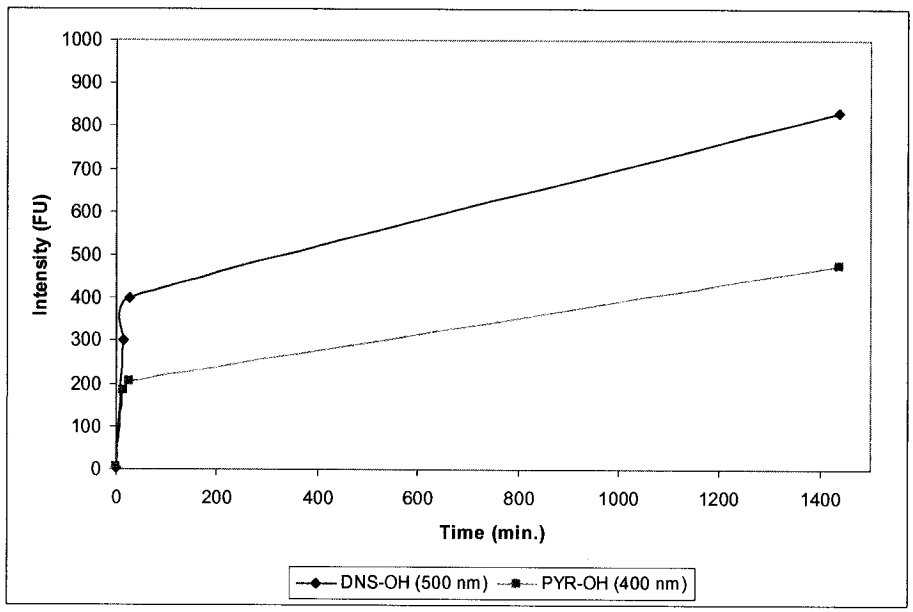

7.3.2.2 Alcalase® Hydrolysis (Figure 39, 40 and 41)

Reaction procedure

a) In a 50 mL round bottom flask, GBC-L-Phe-DNS **121** (16.4 mg. 2.00 x 10^{-5} moles) and GBC-D-Phe-PYR **124** (17.0 mg. 2.00 x 10^{-5} moles) were dissolved in 20 mL buffer phosphate 50 mM pH 7.3 containing 5mM Zwittergent 3-12 (33.6 mg, CMC ≈ 2-4 mM. Calbiochem) and (L)-selector **90** as an internal standard (1.51 x 10^{-4} M). The mixture was vigorously stirred at room temperature over 24 hours or until completed dissolution. Then, 10 drops of brown crude liquid Alcalase® was added to the mixture and gently stirred at room temperature. Aliquots (0.76 mL) were taken regularly and were placed in a separatory funnel where $NaHCO_3$ solution was added. Extraction with minimal DCM volumes was performed and the organic layer was poured into a 5 ml volumetric flask to give a 1.51 x 10^{-4} M solution of each donor in a hypothetical completed hydrolysis. Emission fluorescence readings (Advanced Reads program) were taken at 400 nm (PYR-OH) and 500 nm (DNS-OH) with excitation wavelength at 370 nm in both cases. The excitation /emission slits were adjusted at 5 nm.

Results by fluorescence

Time (h)	PYR (400nm)	DNS (500nm)
0	4,8384	4,7789
1,25	47,5397	173,9859
1,75	49,0861	211,1361
2,75	59,1839	294,98
3,75	85,7564	413,3461
23	64,4809	346,1938

A plot of the fluorescence intensities versus the time was established (***Figure 39***).

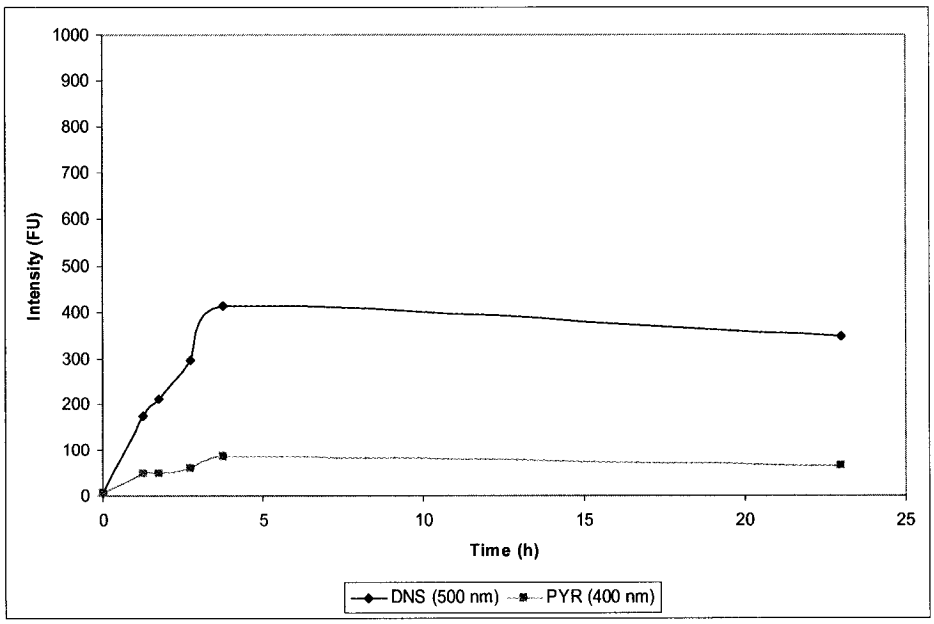

b) Certain amount of each sample was placed into a vial and let to evaporate. Redissolution in acetonitrile (HPLC grade) was done and all the samples were submitted onto the HPLC. 5 peaks were detected. Method: (A: H_2O; B: acetonitrile) gradient 30 to 100 % B for 20 minutes and hold 100 % B for 15 minutes.

Results by HPLC

	AUC				
Time (h)	Internal standard (≈ 14.00 min.)	GBC-L-Phe-DNS (≈ 24.00 min.)	DNS-OH (≈ 5.00 min.)	GBC-D-Phe-PYR (≈ 31.00 min.)	PYR-OH (≈ 16.00 min.)
0	17522374	12886471	0	16396338	0
1,25	16320566	4007569	1717363	8764775	111083
1,75	17603026	2643805	2674393	10813666	212420
2,75	16950318	894923	3316824	10494063	313309
3,75	15109334	636040	2858692	10035588	298832
4,75	15118677	700453	3179395	12579239	389950
23	16161875	424034	3469926	12551107	445872

A plot of the ratio of AUC of donors and AUC of the internal standard versus the time was established (***Figure 40***).

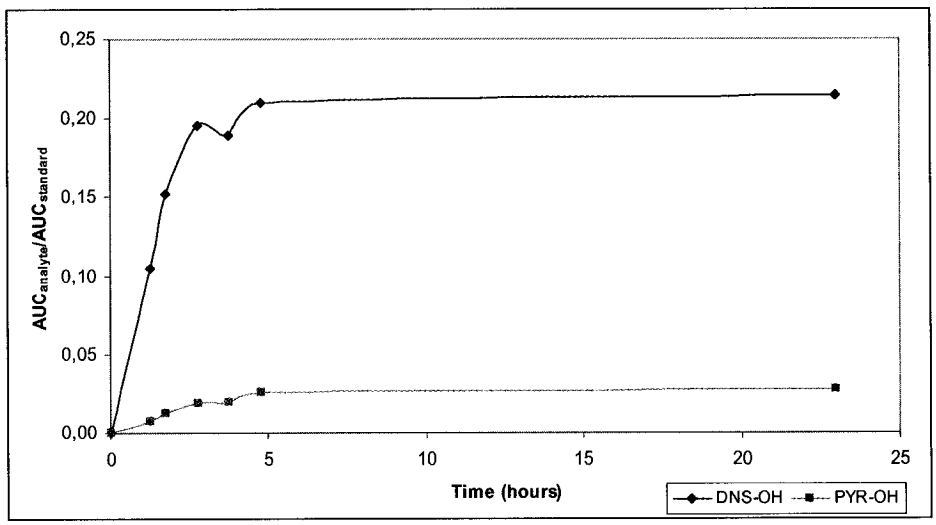

To obtain the calculated concentrations of each component in the sample, each analyte was placed in solution with the internal standard of known concentrations and submitted on the HPLC to calculate the signal ratio calculated. Each solution was prepared in a 5 mL volumetric flask containing 1.51 x 10^{-4} M of internal standard (L-chiral selector **90**) and 1.51 x 10^{-4} M of analyte as a 1:1 mixture.

	AUC analyte	AUC internal standard	Signal ratio calculated
GBC-L-Phe-DNS	13142119	16054871	0.8186
DNS-OH	5753030	15149971	0.3797
GBC-D-Phe-PYR	18764666	16304683	1.1509
PYR-OH	15962228	19185718	0.8320

Using these known values and the AUC obtained from the reaction, the real concentrations of each donor moiety in the sample could be calculated.

$$\text{Signal ratio analyte} = \frac{\text{AUC analyte}}{\text{AUC internal standard}} \qquad \text{Concentration ratio unknown} = \frac{\text{Signal ratio analyte}}{\text{Signal ratio calculated}}$$

$$\text{Calculated concentration} = 1.51 \times 10^{-4}\ \text{M} * \text{Concentration ratio unknown}$$

Time (h)	DNS-OH			PYR-OH		
	Signal ratio analyte	Concentration ratio unknown	Calculated concentration	Signal ratio analyte	Concentration ratio unknown	Calculated concentration
0	0,0000	0,0000	0	0	0	0
1,25	0,1052	0,2771	4,18E-05	0,0068	0,0082	1,24E-06
1,75	0,1519	0,4001	6,04E-05	0,0121	0,0145	2,19E-06
2,75	0,1957	0,5153	7,78E-05	0,0185	0,0222	3,35E-06
3,75	0,1892	0,4982	7,52E-05	0,0198	0,0238	3,59E-06
4,75	0,2103	0,5538	8,36E-05	0,0258	0,0310	4,68E-06
23	0,2147	0,5654	8,54E-05	0,0276	0,0332	5,01E-06

A plot of calculated concentration for the donors versus fluorescence intensity was established (***Figure 41***).

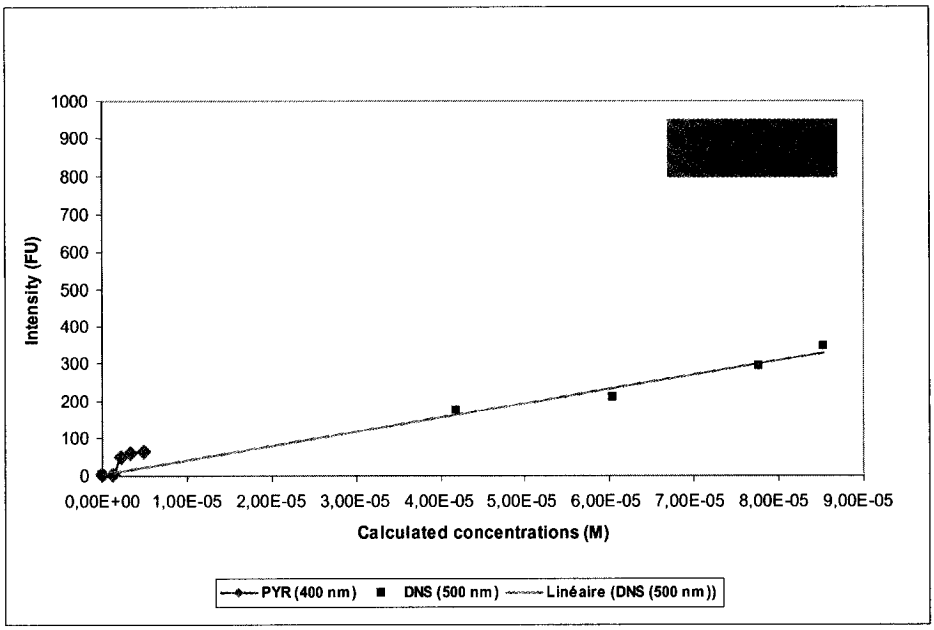

Conversion and enantiomerice excess determination

Calculated concentration GBC-L-Phe-DNS at 0 = 1.36×10^{-4} M
Calculated concentration DNS-OH at 23 h = 8.54×10^{-5} M
Calculated concentration PYR-OH at 23 h = 5.01×10^{-6} M

$$\% \text{ Conversion} = \frac{[\text{DNS-OH}]_{23h}}{[\text{GBC-L-Phe-DNS}]_0} \times 100 = \mathbf{57\ \%}$$

$$ee_L = \frac{L - D}{D + L} = \frac{8.54 \times 10^{-5} - 5.01 \times 10^{-6}}{8.54 \times 10^{-5} + 5.01 \times 10^{-6}} = 0.889 = \mathbf{89\ \%}$$

7.3.2.3 Calibration curves (Figure 42, 43 and 44)

55 solutions were prepared from stock solutions of each component with a 1 mL volumetric pipette and 5 mL volumetric flasks. All solutions were prepared in DCM.

GBC-L-Phe-DNS **121** = 1.346×10^{-3} M
GBC-D-Phe-PYR **124** = 1.229×10^{-3} M
DNS-OH **95** = 1.158×10^{-3} M
PYR-OH **102** = 1.284×10^{-3} M

Also, an internal standard, (L)-selector **90**, was added to each of them for HPLC measurements. (0.361 mL, 1.51 x 10^{-4} M; from a stock solution of 2.090 x 10^{-3} M)

The ratio of each component varied from 0 to 10 which correspond to a specific concentration:

10 ⇒ 1.51 x 10^{-4} M
9 ⇒ 1.359 x 10^{-4} M
8 ⇒ 1.208 x 10^{-4} M
7 ⇒ 1.057 x 10^{-4} M
6 ⇒ 9.06 x 10^{-5} M
5 ⇒ 7.55 x 10^{-5} M
4 ⇒ 6.04 x 10^{-5} M
3 ⇒ 4.53 x 10^{-5} M
2 ⇒ 3.02 x 10^{-5} M
1 ⇒ 1.51 x 10^{-5} M
0 ⇒ 0

Sln #	GBC-L-Phe-DNS	DNS-OH	GBC-D-Phe-PYR	PYR-OH
Selective to L				
1	10 (0,561 mL)	0 (-)	10 (0,614 mL)	0 (-)
2	9 (0,505 mL)	1 (0,065 mL)	10 (0,614 mL)	0 (-)
3	8 (0,449 mL)	2 (0,130 mL)	10 (0,614 mL)	0 (-)
4	7 (0,393 mL)	3 (0,196 mL)	10 (0,614 mL)	0 (-)
5	6 (0,337 mL)	4 (0,261 mL)	10 (0,614 mL)	0 (-)
6	5 (0,280 mL)	5 (0,326 mL)	10 (0,614 mL)	0 (-)
7	4 (0,224 mL)	6 (0,391 mL)	10 (0,614 mL)	0 (-)
8	3 (0,168 mL)	7 (0,456 mL)	10 (0,614 mL)	0 (-)
9	2 (0,112 mL)	8 (0,522 mL)	10 (0,614 mL)	0 (-)
10	1 (0,056 mL)	9 (0,587 mL)	10 (0,614 mL)	0 (-)
11	0 (-)	10 (0,652 mL)	10 (0,614 mL)	0 (-)
Non-Selective				
12	10 (0,561 mL)	0 (-)	5 (0,307 mL)	5 (0,294 mL)
13	9 (0,505 mL)	1 (0,065 mL)	5 (0,307 mL)	5 (0,294 mL)
14	8 (0,449 mL)	2 (0,130 mL)	5 (0,307 mL)	5 (0,294 mL)
15	7 (0,393 mL)	3 (0,196 mL)	5 (0,307 mL)	5 (0,294 mL)
16	6 (0,337 mL)	4 (0,261 mL)	5 (0,307 mL)	5 (0,294 mL)
17	5 (0,280 mL)	5 (0,326 mL)	5 (0,307 mL)	5 (0,294 mL)
18	4 (0,224 mL)	6 (0,391 mL)	5 (0,307 mL)	5 (0,294 mL)
19	3 (0,168 mL)	7 (0,456 mL)	5 (0,307 mL)	5 (0,294 mL)
20	2 (0,112 mL)	8 (0,522 mL)	5 (0,307 mL)	5 (0,294 mL)
21	1 (0,056 mL)	9 (0,587 mL)	5 (0,307 mL)	5 (0,294 mL)
22	0 (-)	10 (0,652 mL)	5 (0,307 mL)	5 (0,294 mL)

23	5 (0,280 mL)	5 (0,326 mL)	0 (-)	10 (0,588 mL)
24	5 (0,280 mL)	5 (0,326 mL)	1 (0,061 mL)	9 (0,529 mL)
25	5 (0,280 mL)	5 (0,326 mL)	2 (0,123 mL)	8 (0,470 mL)
26	5 (0,280 mL)	5 (0,326 mL)	3 (0,184 mL)	7 (0,412 mL)
27	5 (0,280 mL)	5 (0,326 mL)	4 (0,246 mL)	6 (0,353 mL)
28	5 (0,280 mL)	5 (0,326 mL)	5 (0,307 mL)	5 (0,294 mL)
29	5 (0,280 mL)	5 (0,326 mL)	6 (0,369 mL)	4 (0,235 mL)
30	5 (0,280 mL)	5 (0,326 mL)	7 (0,430 mL)	3 (0,176 mL)
31	5 (0,280 mL)	5 (0,326 mL)	8 (0,491 mL)	2 (0,118 mL)
32	5 (0,280 mL)	5 (0,326 mL)	9 (0,553 mL)	1 (0,059 mL)
33	5 (0,280 mL)	5 (0,326 mL)	10 (0,614 mL)	0 (-)
Selective to D				
34	10 (0,561 mL)	0 (-)	10 (0,614 mL)	0 (-)
35	10 (0,561 mL)	0 (-)	9 (0,553 mL)	1 (0,059 mL)
36	10 (0,561 mL)	0 (-)	8 (0,491 mL)	2 (0,118 mL)
37	10 (0,561 mL)	0 (-)	7 (0,430 mL)	3 (0,176 mL)
38	10 (0,561 mL)	0 (-)	6 (0,369 mL)	4 (0,235 mL)
39	10 (0,561 mL)	0 (-)	5 (0,307 mL)	5 (0,294 mL)
40	10 (0,561 mL)	0 (-)	4 (0,246 mL)	6 (0,353 mL)
41	10 (0,561 mL)	0 (-)	3 (0,184 mL)	7 (0,412 mL)
42	10 (0,561 mL)	0 (-)	2 (0,123 mL)	8 (0,470 mL)
43	10 (0,561 mL)	0 (-)	1 (0,061 mL)	9 (0,529 mL)
44	10 (0,561 mL)	0 (-)	0 (-)	10 (0,588 mL)
Random				
45	7 (0,393 mL)	3 (0,196 mL)	2 (0,123 mL)	8 (0,470mL)
46	2 (0,112 mL)	8 (0,522 mL)	6 (0,369 mL)	4 (0,235 mL)
47	9 (0,505 mL)	1 (0,065 mL)	3 (0,184 mL)	7 (0,412 mL)
48	6 (0,337 mL)	4 (0,261 mL)	9 (0,553 mL)	1 (0,059 mL)
49	3 (0,168 mL)	7 (0,456 mL)	7 (0,430 mL)	3 (0,176 mL)
50	4 (0,224 mL)	6 (0,391 mL)	1 (0,061 mL)	9 (0,529 mL)
51	1 (0,056 mL)	9 (0,587 mL)	4 (0,246 mL)	6 (0,353 mL)
52	8 (0,449 mL)	2 (0,130 mL)	3 (0,184 mL)	7 (0,412 mL)
53	7 (0,393 mL)	3 (0,196 mL)	8 (0,491 mL)	2 (0,118 mL)
54	2 (0,112 mL)	8 (0,522 mL)	9 (0,553 mL)	1 (0,059 mL)
55	0 (-)	10 (0,652 mL)	2 (0,123 mL)	8 (0,470 mL)

HPLC data

To measure the exact concentration of each component in the solutions, each of them was submitted on HPLC reverse phase (A: H2O, B: acetonitrile; 30 to 100 % B for 20 minutes and hold 100 % B for 15 minutes).

sln	Internal std	GBC-L-Phe-DNS	DNS-OH	GBC-D-Phe-PYR	L-PYR-OH
1	12926245	9025899	0	13299777	0
2	13231630	10038566	0	15171623	0
3	12848968	8788933	1091807	15143084	0
4	13627503	8167508	1630198	16189200	0
5	13224560	6881140	1911844	15736594	0
6	13933029	6013907	2574810	17415764	0
7	13214764	4665836	2913755	17025718	0
8	13415372	3497079	3340271	17163218	0
9	14179190	2467592	3936273	17423514	0
10	14182666	1258760	4566525	18131094	0
11	12672836	38806	4497613	16154387	2201634
12	14622676	12460096	0	9257514	6426123
13	13089477	10173384	653779	8388917	5768051
14	13192776	9215545	1101522	8389799	5891040
15	13301226	7899540	1551320	8818724	6492933
16	10536678	5618341	1587267	7591513	6199243
17	15701744	6778815	2962450	10163031	7877684
18	12330391	4260192	2656398	8028823	6036634
19	15531011	3976214	3786122	9831076	7459441
20	13006085	2256137	3574594	8323854	6048755
21	12752140	1195871	4115711	8255125	5817943
22	12746339	0	4512596	8128796	5813444
23	11978195	5096001	2232132	161607	10443017
24	11018658	4693923	2009937	1832878	9068331
25	11704891	4976445	2144714	2981861	8116621
26	11542608	4996898	2196743	4469914	7330349
27	11391424	4950667	2169154	5905483	5793335
28	12138039	5121380	2278888	7771790	5549061
29	9440185	4091425	1806512	7261211	3910437
30	11913988	5240493	2235153	13761623	4144986
31	14851852	6418164	2720259	15113130	3485632
32	9979110	4251013	1880210	11152152	1896984
33	11726941	5007819	2174270	9562977	374783
34	13451101	11705548	0	15995182	302938
35	13159176	11381581	0	14401415	1386336
36	11261248	9662010	0	10820169	2151839
37	16662481	14296527	0	14235252	4300579
38	12579711	10702714	0	9190365	4480481
39	10825527	8860638	0	6208756	4635086
40	14917181	11633049	0	6512599	7466362
41	8912902	7120528	0	2974335	5448169
42	12473324	9961861	0	2727404	8776888
43	12005736	9680473	0	1471363	9365763
44	10816432	8876470	0	124357	9559820
45	10498765	5839532	1500648	2448659	7137897
46	10220552	1725197	3129817	7017215	3740896
47	8982296	6530894	503766	3069225	5305251

48	10721636	5249392	1630306	10809940	1331257
49	7483546	1928550	1909998	6485455	3040956
50	8543827	2822451	1849338	1260679	7502644
51	10920536	1006821	3370388	5510931	5857173
52	10350504	7204367	906476	3774918	5966029
53	10010552	7578999	1417639	9753320	1798448
54	9887510	1733540	2742940	10826430	939408
55	11408291	0	3953402	2800872	7640548

With the same calculations shown previously in 8.3.2.2b, exact concentrations of each component in the solutions could be obtained.

	Theoretical	Calculated	Theoretical	Calculated	Theoretical	Calculated	Calculated	Calculated
1	1,51E-04	1,49E-04	0,00E+00	0,00E+00	1,51E-04	1,35E-04	0,00E+00	0,00E+00
2	1,36E-04	1,40E-04	1,51E-05	0,00E+00	1,51E-04	1,50E-04	0,00E+00	0,00E+00
3	1,21E-04	1,26E-04	3,02E-05	3,38E-05	1,51E-04	1,55E-04	0,00E+00	0,00E+00
4	1,06E-04	1,11E-04	4,53E-05	4,76E-05	1,51E-04	1,56E-04	0,00E+00	0,00E+00
5	9,06E-05	9,60E-05	6,04E-05	5,75E-05	1,51E-04	1,56E-04	0,00E+00	0,00E+00
6	7,55E-05	7,96E-05	7,55E-05	7,35E-05	1,51E-04	1,64E-04	0,00E+00	0,00E+00
7	6,04E-05	6,51E-05	9,06E-05	8,77E-05	1,51E-04	1,69E-04	0,00E+00	0,00E+00
8	4,53E-05	4,81E-05	1,06E-04	9,90E-05	1,51E-04	1,68E-04	0,00E+00	0,00E+00
9	3,02E-05	3,21E-05	1,21E-04	1,10E-04	1,51E-04	1,61E-04	0,00E+00	0,00E+00
10	1,51E-05	1,64E-05	1,36E-04	1,28E-04	1,51E-04	1,68E-04	0,00E+00	0,00E+00
11	0,00E+00	5,65E-07	1,51E-04	1,41E-04	1,51E-04	1,67E-04	0,00E+00	3,15E-05
12	1,51E-04	1,57E-04	0,00E+00	0,00E+00	7,55E-05	8,31E-05	7,55E-05	7,98E-05
13	1,36E-04	1,43E-04	1,51E-05	1,99E-05	7,55E-05	8,41E-05	7,55E-05	8,00E-05
14	1,21E-04	1,29E-04	3,02E-05	3,32E-05	7,55E-05	8,35E-05	7,55E-05	8,10E-05
15	1,06E-04	1,10E-04	4,53E-05	4,64E-05	7,55E-05	8,70E-05	7,55E-05	8,86E-05
16	9,06E-05	9,84E-05	6,04E-05	5,99E-05	7,55E-05	9,45E-05	7,55E-05	1,07E-04
17	7,55E-05	7,96E-05	7,55E-05	7,50E-05	7,55E-05	8,49E-05	7,55E-05	9,11E-05
18	6,04E-05	6,37E-05	9,06E-05	8,57E-05	7,55E-05	8,54E-05	7,55E-05	8,89E-05
19	4,53E-05	4,72E-05	1,06E-04	9,69E-05	7,55E-05	8,31E-05	7,55E-05	8,72E-05
20	3,02E-05	3,20E-05	1,21E-04	1,09E-04	7,55E-05	8,40E-05	7,55E-05	8,44E-05
21	1,51E-05	1,73E-05	1,36E-04	1,28E-04	7,55E-05	8,50E-05	7,55E-05	8,28E-05
22	0,00E+00	0,00E+00	1,51E-04	1,41E-04	7,55E-05	8,37E-05	7,55E-05	8,28E-05
23	7,55E-05	7,85E-05	7,55E-05	7,41E-05	0,00E+00	1,77E-06	1,51E-04	1,58E-04
24	7,55E-05	7,86E-05	7,55E-05	7,25E-05	1,51E-05	2,18E-05	1,36E-04	1,49E-04
25	7,55E-05	7,84E-05	7,55E-05	7,29E-05	3,02E-05	3,34E-05	1,21E-04	1,26E-04
26	7,55E-05	7,99E-05	7,55E-05	7,57E-05	4,53E-05	5,08E-05	1,06E-04	1,15E-04
27	7,55E-05	8,02E-05	7,55E-05	7,57E-05	6,04E-05	6,80E-05	9,06E-05	9,23E-05
28	7,55E-05	7,78E-05	7,55E-05	7,47E-05	7,55E-05	8,40E-05	7,55E-05	8,30E-05
29	7,55E-05	7,99E-05	7,55E-05	7,61E-05	9,06E-05	1,01E-04	6,04E-05	7,52E-05
30	7,55E-05	8,11E-05	7,55E-05	7,46E-05	1,06E-04	1,52E-04	4,53E-05	6,31E-05
31	7,55E-05	7,97E-05	7,55E-05	7,28E-05	1,21E-04	1,34E-04	3,02E-05	4,26E-05
32	7,55E-05	7,86E-05	7,55E-05	7,49E-05	1,36E-04	1,47E-04	1,51E-05	3,45E-05

33	7,55E-05	7,88E-05	7,55E-05	7,37E-05	1,51E-04	1,07E-04	0,00E+00	5,80E-06
34	1,51E-04	1,61E-04	0,00E+00	0,00E+00	1,51E-04	1,56E-04	0,00E+00	4,09E-06
35	1,51E-04	1,60E-04	0,00E+00	0,00E+00	1,36E-04	1,44E-04	1,51E-05	1,91E-05
36	1,51E-04	1,58E-04	0,00E+00	0,00E+00	1,21E-04	1,26E-04	3,02E-05	3,47E-05
37	1,51E-04	1,58E-04	0,00E+00	0,00E+00	1,06E-04	1,12E-04	4,53E-05	4,68E-05
38	1,51E-04	1,57E-04	0,00E+00	0,00E+00	9,06E-05	9,59E-05	6,04E-05	6,46E-05
39	1,51E-04	1,51E-04	0,00E+00	0,00E+00	7,55E-05	7,53E-05	7,55E-05	7,77E-05
40	1,51E-04	1,44E-04	0,00E+00	0,00E+00	6,04E-05	5,73E-05	9,06E-05	9,08E-05
41	1,51E-04	1,47E-04	0,00E+00	0,00E+00	4,53E-05	4,38E-05	1,06E-04	1,11E-04
42	1,51E-04	1,47E-04	0,00E+00	0,00E+00	3,02E-05	2,87E-05	1,21E-04	1,28E-04
43	1,51E-04	1,49E-04	0,00E+00	0,00E+00	1,51E-05	1,61E-05	1,36E-04	1,42E-04
44	1,51E-04	1,51E-04	0,00E+00	0,00E+00	0,00E+00	1,51E-06	1,51E-04	1,60E-04
45	1,06E-04	1,03E-04	4,53E-05	5,68E-05	3,02E-05	3,06E-05	1,21E-04	1,23E-04
46	3,02E-05	3,11E-05	1,21E-04	1,22E-04	9,06E-05	9,01E-05	6,04E-05	6,64E-05
47	1,36E-04	1,34E-04	1,51E-05	2,23E-05	4,53E-05	4,48E-05	1,06E-04	1,07E-04
48	9,06E-05	9,03E-05	6,04E-05	6,05E-05	1,36E-04	1,32E-04	1,51E-05	2,25E-05
49	4,53E-05	4,75E-05	1,06E-04	1,01E-04	1,05E-04	1,14E-04	4,53E-05	7,38E-05
50	6,04E-05	6,09E-05	6,04E-05	8,61E-05	1,51E-05	1,94E-05	1,36E-04	1,59E-04
51	1,51E-05	1,70E-05	1,36E-04	1,23E-04	6,04E-05	6,62E-05	9,06E-05	9,73E-05
52	1,21E-04	1,28E-04	3,02E-05	3,48E-05	4,53E-05	4,79E-05	1,06E-04	1,05E-04
53	1,06E-04	1,40E-04	4,53E-05	5,63E-05	1,21E-04	1,28E-04	3,02E-05	3,26E-05
54	3,02E-05	3,23E-05	1,21E-04	1,10E-04	1,36E-04	1,44E-04	1,51E-05	1,72E-05
55	0,00E+00	0,00E+00	1,51E-04	1,38E-04	3,02E-05	3,22E-05	1,21E-04	1,22E-04

Plots of the theoretical concentration versus calculated concentration were established for each situation (***Figure 42***).

a) Selective to L-probe (sln 1-11)

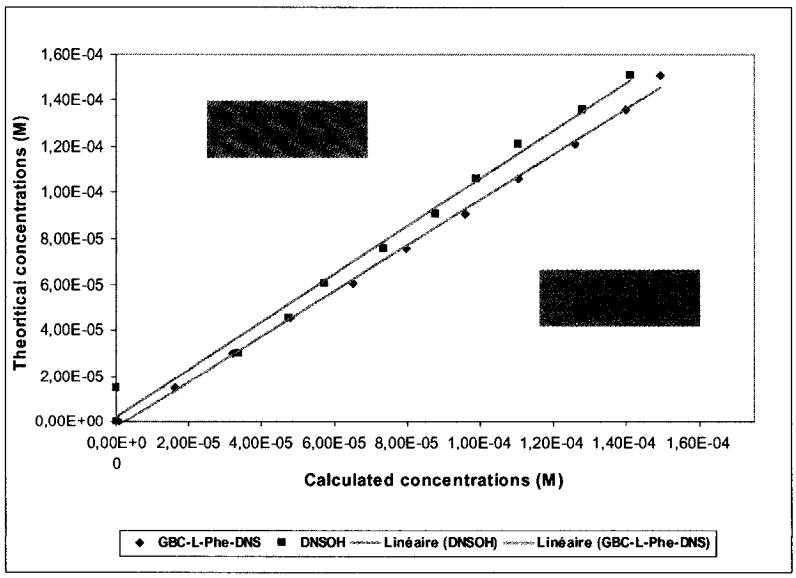

b) Selective to D-probe (sln 34-44)

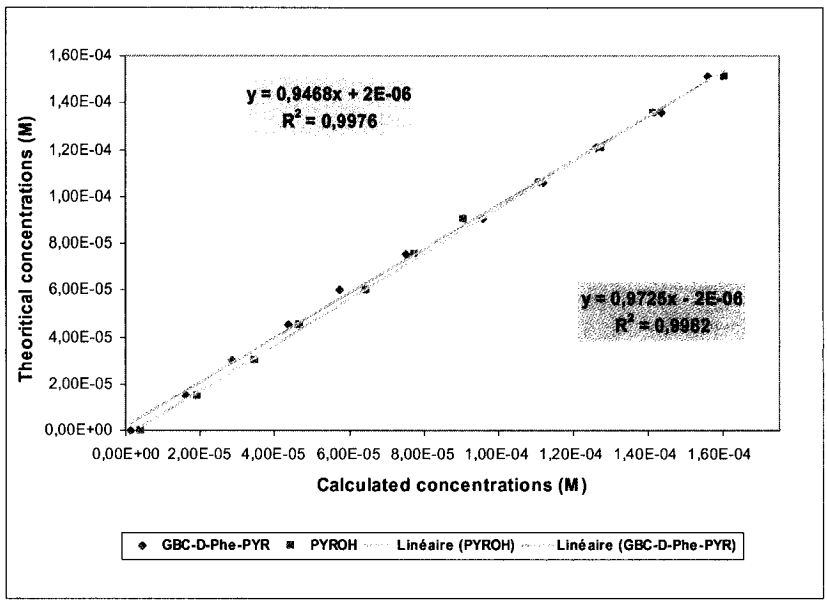

c) Non-selective: L-isomer varied while D-isomer constant at 7.55 x10^{-5} M (50 % hydrolysis, sln 12-22)

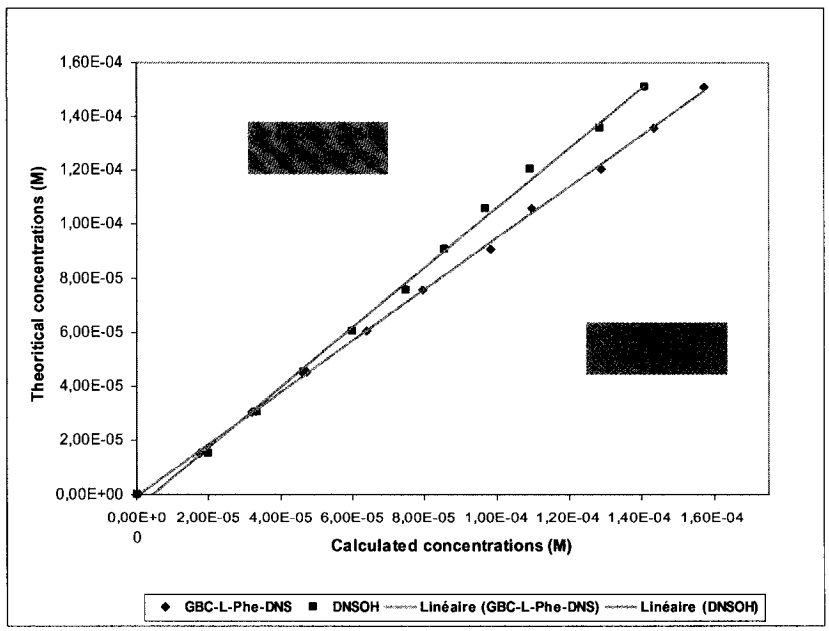

d) Non-selective: D-isomer varied while L-isomer constant at 7.55 x 10^{-5} M (50 % hydrolysis, sln 23-33)

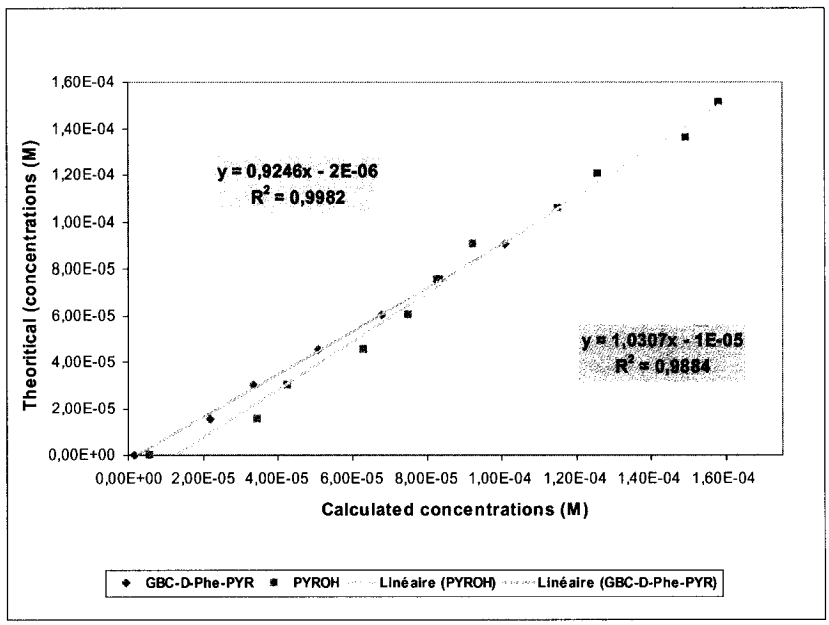

e) Random

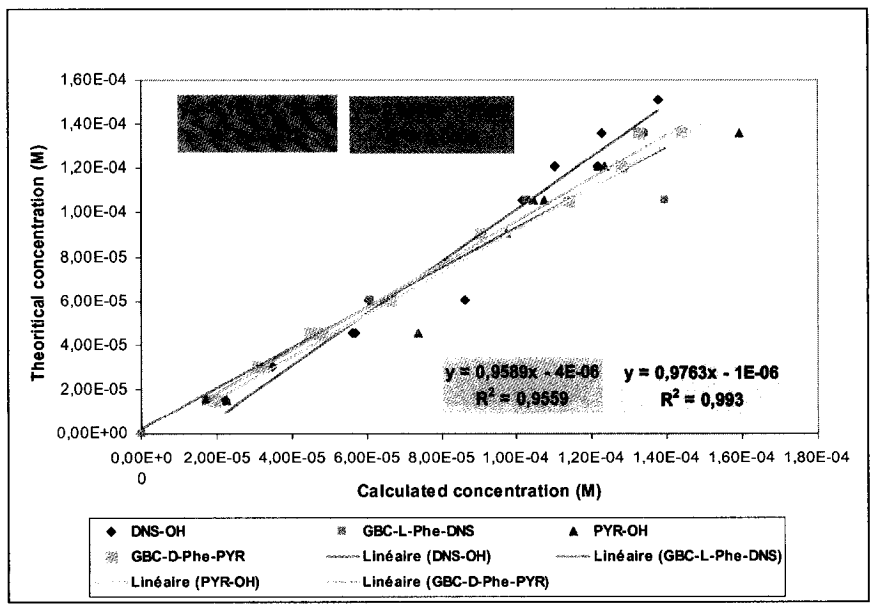

Fluorescence data

The same 55 solutions were submitted to the spectrofluorometer in a quartz cell (l = 1 cm) using the Advance Reads program. The excitation wavelength was at 370 nm and emission readings were done at 400 and 500 nm. The excitation/emission slits were adjusted at 5 nm.

sln	DNS-OH (500 nm)	PYR-OH (400 nm)
1	7,0877	-0,5693
2	14,1930	0,233
3	23,8864	0,6826
4	34,1575	1,5119
5	44,6389	2,4387
6	67,7465	4,0548
7	89,9749	5,3335
8	118,2514	7,0609
9	158,2987	10,1787
10	187,8733	11,6529
11	245,1886	14,7904
12	16,1388	52,6377
13	29,9947	62,6715
14	47,2128	74,7403
15	76,1688	102,5721
16	98,6810	115,1772
17	148,7852	157,6279
18	200,2797	191,4202
19	273,5866	238,4594
20	352,1794	307,6629
21	464,6108	375,2064
22	625,6498	497,8441
23	394,8537	997,3101
24	337,8207	769,0403
25	275,0441	534,6817
26	224,9686	356,244
27	196,5908	253,5634
28	157,4225	160,743
29	137,0534	112,5076
30	110,4941	66,7383
31	94,6670	37,5585
32	81,7683	18,9185
33	139,8482	8,5225
34	8,3217	-0,011
35	9,4899	5,1363

36	10,9524	12,4064
37	12,3655	20,9075
38	14,0270	35,1877
39	16,4099	52,3549
40	19,5802	78,6032
41	23,5395	118,6277
42	28,4510	172,0417
43	33,0483	241,4683
44	38,4380	322,0493
45	142,9282	345,003
46	298,3334	204,3225
47	47,9109	156,209
48	59,4628	14,27
49	189,3047	97,918
50	461,9653	991,0538
51	587,9391	588,9805
52	69,6988	170,8128
53	40,4723	16,4235
54	180,6224	35,2129
55	1000,0000	997,3465

Plots of the fluorescence intensities versus the calculated concentrations were established (***Figure 43 and 44***).

Solutions 1-11 and 34-44

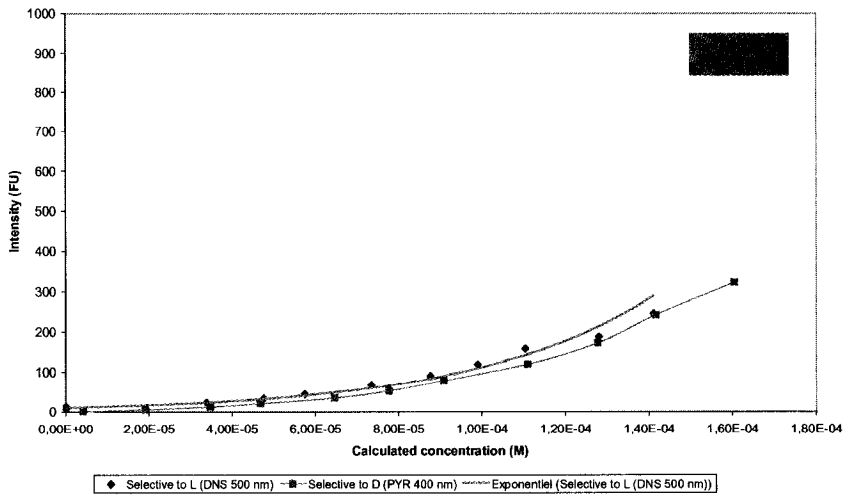

Solutions 12-22

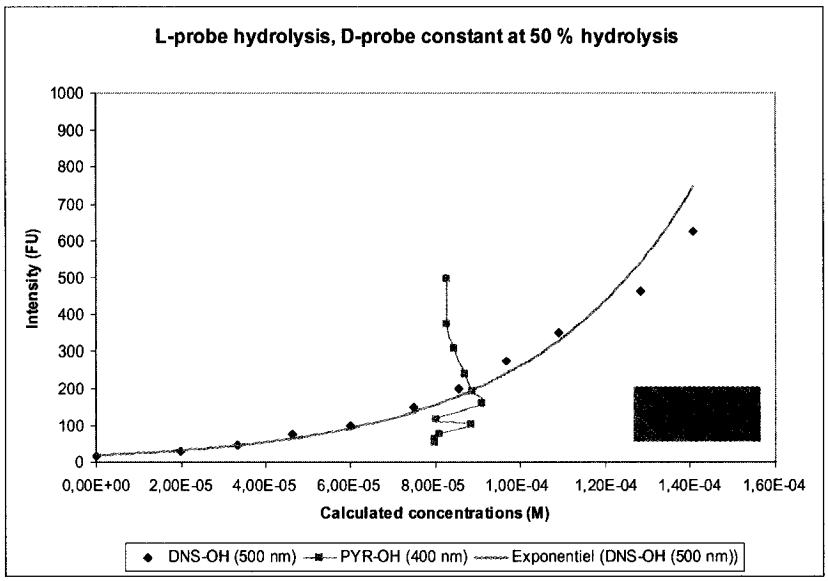

Solutions 23-33

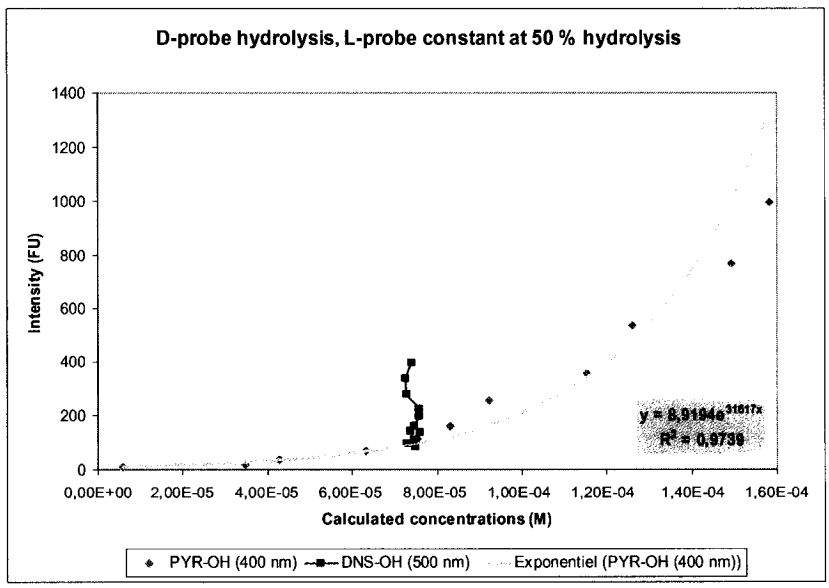

7.3.2.4 Calibration curves (attempt #2, Figure 45, 46 and 47)

55 solutions were prepared from stock solutions of each component with a 1 mL volumetric pipette and 5 mL volumetric flasks. All solutions were prepared in DCM.

GBC-L-Phe-DNS **121** = 7.640 x 10^{-4} M and * 8.327 x 10^{-4} M
GBC-D-Phe-PYR **124** = 7.812 x 10^{-4} M and * 9.084 x 10^{-4} M
DNS-OH **95** = 1.343 x 10^{-3} M
PYR-OH **102** = 1.312 x 10^{-3} M
GBC-D-Phe-OEt 125 = 1.065 x 10^{-3} M and * 1.226 x 10^{-3} M

Also, an internal standard, (L)-selector **90**, was added to each of them for HPLC measurements. (0.367 mL, 1.51 x 10^{-4} M; from a stock solution of 2.057 x 10^{-3} M)

The ratio of each component varied from 0 to 10 which correspond to a specific concentration:

10 ⇒ 1.51 x 10^{-4} M
9 ⇒ 1.359 x 10^{-4} M
8 ⇒ 1.208 x 10^{-4} M
7 ⇒ 1.057 x 10^{-4} M
6 ⇒ 9.06 x 10^{-5} M
5 ⇒ 7.55 x 10^{-5} M
4 ⇒ 6.04 x 10^{-5} M
3 ⇒ 4.53 x 10^{-5} M
2 ⇒ 3.02 x 10^{-5} M
1 ⇒ 1.51 x 10^{-5} M
0 ⇒ 0

sln	GBC-L-Phe-DNS	DNS-OH	GBC-D-Phe-PYR	PYR-OH	GBC-D-Phe-Oet
	Selective to L-probe				
1	10 (0,988 mL)	0 (-)	10 (1,05 mL)	0	0 (-)
2	9 (0,889 mL)	1 (0,056 mL)	10 (1,05 mL)	0	1 (0,071 mL)
3	8 (0,791 mL)	2 (0,112 mL)	10 (1,05 mL)	0	2 (0,142 ml0
4	7 (0,692 mL)	3 (0,169 mL)	10 (1,05 mL)	0	3 (0,213 mL)
5	6 (0,593 mL)	4 (0,225 mL)	10 (1,05 mL)	0	4 (0,284 mL)
6	5 (0,494 mL)	5 (0,281 mL)	10 (1,05 mL)	0	5 (0,354 mL)
7	4 (0,395 mL)	6 (0,337 mL)	10 (1,05 mL)	0	6 (0,425 mL)

8	3 (0,296 mL)	7 (0,394 mL)	10 (1,05 mL)	0	7 (0,494 mL)
9	2 (0,198 mL)	8 (0,450 mL)	10 (1,05 mL)	0	8 (0,567 mL)
10	1 (0,099 mL)	9 (0,506 mL)	10 (1,05 mL)	0	9 (0,638 mL)
11	0 (-)	10 (0,562 mL)	10 (1,05 mL)	0	10 (0,709 mL)
	Non-selective: D-probe constant at 50 % hydrolysis				
12	10 (0,988 mL)	0 (-)	5 (0,526 mL)	5 (0,288 mL)	5 (0,354 mL)
13	9 (0,889 mL)	1 (0,056 mL)	5 (0,526 mL)	5 (0,288 mL)	6 (0,425 mL)
14	8 (0,791 mL)	2 (0,112 mL)	5 (0,526 mL)	5 (0,288 mL)	7 (0,494 mL)
15	7 (0,692 mL)	3 (0,169 mL)	5 (0,526 mL)	5 (0,288 mL)	8 (0,567 mL)
16	6 (0,593 mL)	4 (0,225 mL)	5 (0,526 mL)	5 (0,288 mL)	9 (0,638 mL)
17	5 (0,494 mL)	5 (0,281 mL)	5 (0,526 mL)	5 (0,288 mL)	10 (0,709 mL)
18	4 (0,395 mL)	6 (0,337 mL)	5 (0,526 mL)	5 (0,288 mL)	11 (0,780 mL)
19	3 (0,296 mL)	7 (0,394 mL)	5 (0,526 mL)	5 (0,288 mL)	12 (0,851 mL)
20	2 (0,198 mL)	8 (0,450 mL)	5 (0,526 mL)	5 (0,288 mL)	13 (0,922 mL)
21	1 (0,099 mL)	9 (0,506 mL)	5 (0,526 mL)	5 (0,288 mL)	14 (0,992 mL)
22	0 (-)	10 (0,562 mL)	5 (0,420 mL)*	5 (0,288 mL)	15 (1,063 mL)
	Non-selective: L-probe constant at 50 % hydrolysis				
23	5 (0,494 mL)	5 (0,281 mL)	0 (-)	10 (0,575 mL)	15 (1,063 mL)
24	5 (0,494 mL)	5 (0,281 mL)	1 (0,084 mL)*	9 (0,518 mL)	14 (0,992 mL)
25	5 (0,494 mL)	5 (0,281 mL)	2 (0,166 mL)*	8 (0,460 mL)	13 (0,922 mL)
26	5 (0,494 mL)	5 (0,281 mL)	3 (0,249 mL)*	7 (0,403 mL)	12 (0,851 mL)
27	5 (0,494 mL)	5 (0,281 mL)	4 (0,332 mL)*	6 (0,345 mL)	11 (0,780 mL)
28	5 (0,494 mL)	5 (0,281 mL)	5 (0,415 mL)*	5 (0,288 mL)	10 (0,709 mL)
29	5 (0,494 mL)	5 (0,281 mL)	6 (0,499 mL)*	4 (0,230 mL)	9 (0,638 mL)
30	5 (0,453 mL)*	5 (0,281 mL)	7 (0,582 mL)*	3 (0,173 mL)	8 (0,567 mL)
31	5 (0,453 mL)*	5 (0,281 mL)	8 (0,665 mL)*	2 (0,115 mL)	7 (0,494 mL)
32	5 (0,453 mL)*	5 (0,281 mL)	9 (0,748 mL)*	1 (0,058 mL)	6 (0,425 mL)
33	5 (0,453 mL)*	5 (0,281 mL)	10 (0,831 mL)*	0 (-)	5 (0,354 mL)
	Selective to D-probe				
34	10 (0,988 mL)	0	10 (0,831 mL)*	0 (-)	0 (-)
35	10 (0,988 mL)	0	9 (0,748 mL)*	1 (0,058 mL)	1 (0,071 mL)
36	10 (0,988 mL)	0	8 (0,665 mL)*	2 (0,115 mL)	2 (0,142 ml0
37	10 (0,988 mL)	0	7 (0,582 mL)*	3 (0,173 mL)	3 (0,213 mL)
38	10 (0,988 mL)	0	6 (0,499 mL)*	4 (0,230 mL)	4 (0,284 mL)
39	10 (0,988 mL)	0	5 (0,415 mL)*	5 (0,288 mL)	5 (0,354 mL)
40	10 (0,988 mL)	0	4 (0,332 mL)*	6 (0,345 mL)	6 (0,425 mL)
41	10 (0,988 mL)	0	3 (0,249 mL)*	7 (0,403 mL)	7 (0,494 mL)
42	10 (0,988 mL)	0	2 (0,166 mL)*	8 (0,460 mL)	8 (0,567 mL)
43	10 (0,988 mL)	0	1 (0,084 mL)*	9 (0,518 mL)	9 (0,638 mL)
44	10 (0,988 mL)	0	0 (-)	10 (0,575 mL)	10 (0,709 mL)
	Random				
45	7 (0,635 mL)*	3 (0,169 mL)	2 (0,166 mL)*	8 (0,460 mL)	11 (0,677 mL)*
46	2 (0,181 mL)*	8 (0,450 mL)	6 (0,499 mL)*	4 (0,230 mL)	12 (0,739 mL)*
47	9 (0,816 mL)*	1 (0,056 mL)	3 (0,249 mL)*	7 (0,403 mL)	8 (0,493 mL)*
48	6 (0,544 mL)*	4 (0,225 mL)	9 (0,748 mL)*	1 (0,058 mL)	5 (0,308 mL)*
49	3 (0,272 mL)*	7 (0,394 mL)	7 (0,582 mL)*	3 (0,173 mL)	10 (0,615 mL)*

50	4 (0,363 mL)*	6 (0,337 mL)	1 (0,084 mL)*	9 (0,518 mL)	15 (0,924 mL)*
51	1 (0,091 mL)*	9 (0,506 mL)	4 (0,332 mL)*	6 (0,345 mL)	15 (0,924 mL)*
52	8 (0,725 mL)*	2 (0,112 mL)	3 (0,249 mL)*	7 (0,403 mL)	9 (0,554 mL)*
53	7 (0,635 mL)*	3 (0,169 mL)	8 (0,665 mL)*	2 (0,115 mL)	5 (0,308 mL)*
54	2 (0,181 mL)*	8 (0,450 mL)	9 (0,748 mL)*	1 (0,058 mL)	9 (0,554 mL)*
55	0 (-)	10 (0,562 mL)	2 (0,166 mL)*	8 (0,460 mL)	18 (1,108 mL)*

HPLC data

To measure the exact concentration of each component in the solutions, each of them was submitted on HPLC reverse phase (A: H2O, B: acetonitrile; 30 to 100 % B for 20 minutes and hold 100 % B for 15 minutes).

sln	Internal std	GBC-L-Phe-DNS	DNS-OH	GBC-D-Phe-PYR	PYR-OH	
1	16716825	16130845	0	22791126	0	
2	21573996	20632692	540583	28970238	0	
3	16954834	14828094	805401	22514616	0	
4	18867992	15524645	1409844	25603392	0	
5	19380966	15016182	2021204	26357450	0	
6	20304282	14395558	2488143	27732086	0	
7					0	
8	10026417	6090724	1729474	13676681	0	
9	18427682	10280622	3451442	24962134	0	
10	19868442	10208663		26963332	0	
11	8173488	3645714	2152342	10735466	0	
12	25147188	31107888	0	19060302	10372880	
13	23261726	27765688	1286371	18065098	9857409	
14	21711422	25093722	1665154	17973260	9380596	
15	20195402	21631496	1792028	15812492	8534663	
16	20288994	20670758	2791030	15707258	8221083	
17	20567954	19823240	2653045	16097701	8428042	
18	21447910	19412888	3337578	17282228	8629301	
19	25080916	21280554	4899526	18493400	10375933	
20	20463646	16855734	4479511	15299843	8509286	
21	20618228	15117507	5680037	16138548	8539132	
22	18753000	11959683	5561767	14165791	7835587	
23	24354032	28338954	3148659	881865	19720318	
24	20251046	23690528	2844130	3588194	14740331	
25	23807118	26419834	3363387	7630330	15179779	
26	21797084	22985200	3466912	9682639	11972854	
27	19477564	19799284	2447813	11481982	9472740	

28	20493054	20299046	3016399	15444790	8312318	
29	22383900	21532254	2855984	19662988	7493882	
30	17674580	15772140	2310455	17902142	4320020	
31	24508478	23080510	3113199	27845166	4123782	
32	28383814	21978288	4370596	35521572	2511524	
33	25452572	18869846	3677389	35894056	139542	
34	17502134	16546096	0	24110656	158219	
35	18158022	19311966	0	24184704	1565321	
36	19832376	21281858	0	22458498	3721831	
37	18713880	20932492	0	19088114	4843749	
38	18856134	22282508	0	15611199	6243429	
39	21527672	25847200	0	15308848	9039441	
40	18720482	23721596	0	10641982	9403477	
41	17648484	22932856	0	8557365	10415909	
42	19917206	27108540	0	6423930	13429911	
43	19305252	25860672	0	3310733	14278208	
44	19370348	27970918	0	507061	16147280	
45	18552830	22270512	1447949	5567554	12550603	
46	22966090	16317136	5380157	19205622	7461042	
47	28578926	35262752	613650	12289103	15928630	
48	24036398	19829944	3358735	30204584	2154315	
49	20943182	15372583	3815175	20881388	5092496	
50	22412816	22978728	3529371	3536048	16304265	
51	22000626	16654816	5319981	12711682	10510668	
52	20996412	12457546	1099247	9219189	11824099	
53	18253752	17350098	1447997	21009218	2844634	
54	21794976	12905129	4601474	27324446	2142039	
55	23481250	18206884	6810978	7170653	14797457	

Unfortunately, we were not able to separate adequately the GBC-L-Phe-DNS and the GBC-D-Phe-OEt, therefore the AUC shown in the GBC-L-Phe-DNS column represent both compounds. So, calculated concentrations were determined for the others only.

With the same calculations shown previously in 7.3.2.2b, exact concentrations of each component in the solutions could be obtained.

sln	DNS-OH		GBC-D-Phe-PYR		PYR-OH	
	theoretical	calculated	theoretical	calculated	theoretical	calculated
1	0,00E+00	0,00E+00	1,51E-04	1,79E-04	0,00E+00	0,00E+00
2	1,51E-05	9,96E-06	1,51E-04	1,76E-04	0,00E+00	0,00E+00
3	3,02E-05	1,89E-05	1,51E-04	1,74E-04	0,00E+00	0,00E+00

4	4,53E-05	2,97E-05	1,51E-04	1,78E-04	0,00E+00	0,00E+00
5	6,04E-05	4,15E-05	1,51E-04	1,78E-04	0,00E+00	0,00E+00
6	7,55E-05	4,87E-05	1,51E-04	1,79E-04	0,00E+00	0,00E+00
7	9,06E-05	9,06E-05	1,51E-04	#DIV/0!	0,00E+00	#DIV/0!
8	1,06E-04	6,86E-05	1,51E-04	1,79E-04	0,00E+00	0,00E+00
9	1,21E-04	7,45E-05	1,51E-04	1,78E-04	0,00E+00	0,00E+00
10	1,36E-04	1,36E-04	1,51E-04	1,78E-04	0,00E+00	0,00E+00
11	1,51E-04	1,05E-04	1,51E-04	1,72E-04	0,00E+00	0,00E+00
12	0,00E+00	0,00E+00	7,55E-05	9,94E-05	7,55E-05	7,49E-05
13	1,51E-05	2,20E-05	7,55E-05	1,02E-04	7,55E-05	7,69E-05
14	3,02E-05	3,05E-05	7,55E-05	1,09E-04	7,55E-05	7,84E-05
15	4,53E-05	3,53E-05	7,55E-05	1,03E-04	7,55E-05	7,67E-05
16	6,04E-05	5,47E-05	7,55E-05	1,02E-04	7,55E-05	7,35E-05
17	7,55E-05	5,13E-05	7,55E-05	1,03E-04	7,55E-05	7,44E-05
18	9,06E-05	6,19E-05	7,55E-05	1,06E-04	7,55E-05	7,30E-05
19	1,06E-04	7,77E-05	7,55E-05	9,67E-05	7,55E-05	7,51E-05
20	1,21E-04	8,71E-05	7,55E-05	9,81E-05	7,55E-05	7,55E-05
21	1,36E-04	1,10E-04	7,55E-05	1,03E-04	7,55E-05	7,52E-05
22	1,51E-04	1,18E-04	7,55E-05	9,91E-05	7,55E-05	7,58E-05
23	7,55E-05	5,14E-05	0,00E+00	4,75E-06	1,51E-04	1,47E-04
24	7,55E-05	5,59E-05	1,51E-05	2,32E-05	1,36E-04	1,32E-04
25	7,55E-05	5,62E-05	3,02E-05	4,21E-05	1,21E-04	1,16E-04
26	7,55E-05	6,33E-05	4,53E-05	5,83E-05	1,06E-04	9,97E-05
27	7,55E-05	5,00E-05	6,04E-05	7,73E-05	9,06E-05	8,83E-05
28	7,55E-05	5,85E-05	7,55E-05	9,89E-05	7,55E-05	7,36E-05
29	7,55E-05	5,07E-05	9,06E-05	1,15E-04	6,04E-05	6,08E-05
30	7,55E-05	5,20E-05	1,06E-04	1,33E-04	4,53E-05	4,44E-05
31	7,55E-05	5,05E-05	1,21E-04	1,49E-04	3,02E-05	3,05E-05
32	7,55E-05	6,12E-05	1,36E-04	1,64E-04	1,51E-05	1,61E-05
33	7,55E-05	5,75E-05	1,51E-04	1,85E-04	0,00E+00	9,95E-07
34	0,00E+00	0,00E+00	1,51E-04	1,81E-04	0,00E+00	1,64E-06
35	0,00E+00	0,00E+00	1,36E-04	1,75E-04	1,51E-05	1,56E-05
36	0,00E+00	0,00E+00	1,21E-04	1,49E-04	3,02E-05	3,41E-05
37	0,00E+00	0,00E+00	1,06E-04	1,34E-04	4,53E-05	4,70E-05
38	0,00E+00	0,00E+00	9,06E-05	1,09E-04	6,04E-05	6,01E-05
39	0,00E+00	0,00E+00	7,55E-05	9,33E-05	7,55E-05	7,62E-05
40	0,00E+00	0,00E+00	6,04E-05	7,46E-05	9,06E-05	9,12E-05
41	0,00E+00	0,00E+00	4,53E-05	6,36E-05	1,06E-04	1,07E-04
42	0,00E+00	0,00E+00	3,02E-05	4,23E-05	1,21E-04	1,22E-04
43	0,00E+00	0,00E+00	1,51E-05	2,25E-05	1,36E-04	1,34E-04
44	0,00E+00	0,00E+00	0,00E+00	3,43E-06	1,51E-04	1,51E-04
45	4,53E-05	3,10E-05	3,02E-05	3,94E-05	1,21E-04	1,23E-04
46	1,21E-04	9,32E-05	9,06E-05	1,10E-04	6,04E-05	5,90E-05
47	1,51E-05	8,54E-06	4,53E-05	5,64E-05	1,06E-04	1,01E-04
48	6,04E-05	5,56E-05	1,36E-04	1,65E-04	1,51E-05	1,63E-05
49	1,06E-04	7,24E-05	1,05E-04	1,31E-04	4,53E-05	4,41E-05
50	6,04E-05	6,26E-05	1,51E-05	2,07E-05	1,36E-04	1,32E-04
51	1,36E-04	9,62E-05	6,04E-05	7,58E-05	9,06E-05	8,67E-05

52	3,02E-05	2,08E-05	4,53E-05	5,76E-05	1,06E-04	1,02E-04
53	4,53E-05	3,15E-05	1,21E-04	1,51E-04	3,02E-05	2,83E-05
54	1,21E-04	8,40E-05	1,36E-04	1,64E-04	1,51E-05	1,78E-05
55	1,51E-04	1,15E-04	3,02E-05	4,01E-05	1,21E-04	1,14E-04

Plots of the theoretical concentration versus calculated concentration were established for each situation (***Figure 45***).

a) Selective to L-probe (sln 1-11)

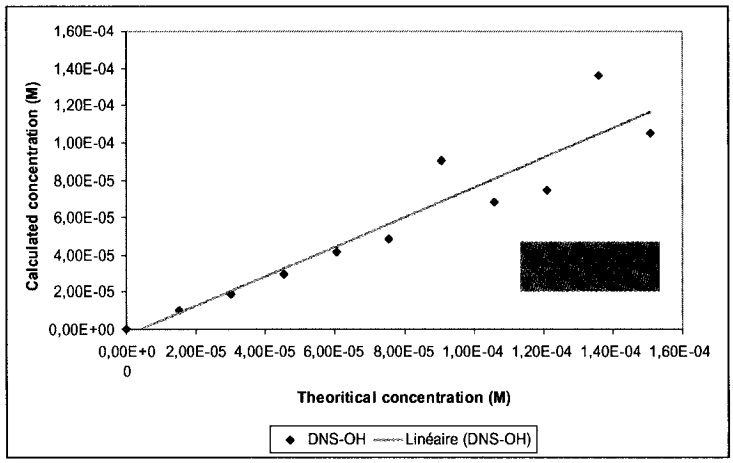

b) Selective to D-probe (sln 34-44)

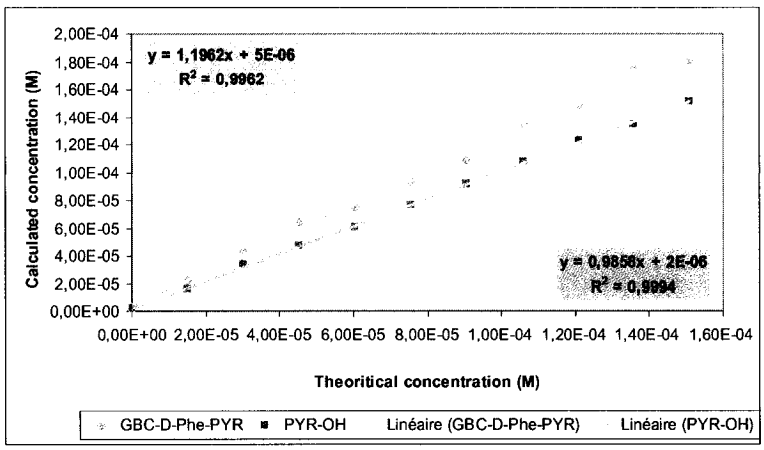

c) Non-selective: L-isomer varied while D-isomer constant at 7.55 x10^{-5} M (50 % hydrolysis, sln 12-22)

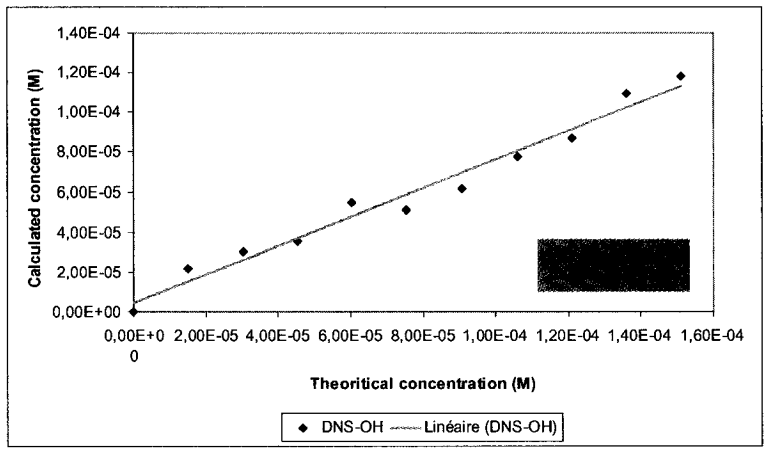

d) Non-selective: D-isomer varied while L-isomer constant at 7.55 x 10^{-5} M (50 % hydrolysis, sln 23-33)

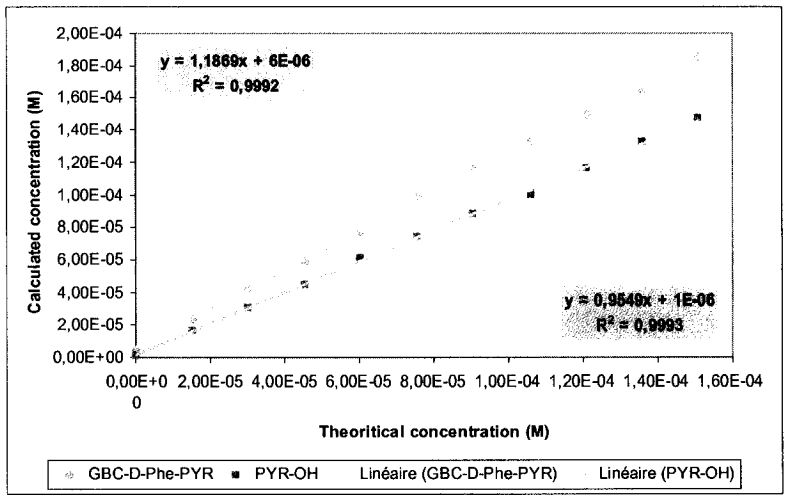

e) Random

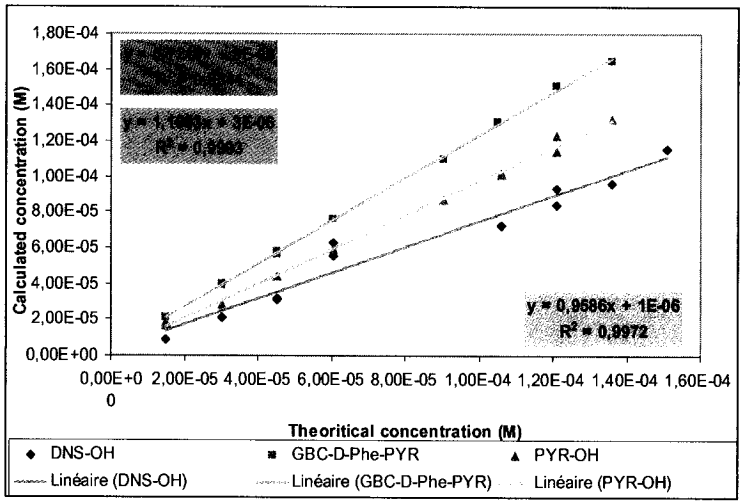

Fluorescence data

The same 55 solutions were submitted to the spectrofluorometer in a quartz cell (l = 1 cm) using the Advance Reads program. The excitation wavelength was varied for the solutions 1-11 and 34-44 and emission readings were done at 400 and 500 nm. For solutions 12-22, 23-33 and 45-55, the excitation wavelength was at 370 nm. The excitation/emission slits were adjusted at 10 nm.

	PYR (400 nm) slits = 10 nm					DNS (500 nm) slits = 10 nm				
sln	330 nm	340 nm	350 nm	360 nm	370 nm	330 nm	340 nm	350 nm	360 nm	370 nm
1	0	0	0	0	0	13,726	4,0819	0,8373	6,5873	28,3722
2	0	0	0	0	0	60,8757	29,5319	20,05	36,9095	98,7096
3	0	0	0	0	0	93,2294	48,8513	33,7166	58,0545	148,794
4	0	0	0	0	0	138,951	72,6098	51,7701	86,6268	218,316
5	0	0	0	0	0	177,735	94,7046	66,7925	112,478	278,649
6	0	0	0	0	0	217,222	116,797	84,3839	138,104	340,327
7	0	0	0	0	0	247,27	133,263	96,2848	158,044	388,936
8	0	0	0	0	0	293,453	157,273	113,556	187,406	455,99
9	0	0	0	0	0	335,389	183,861	135,009	217,07	521,841
10	0	0	0	0	0	398,3	218,227	160,311	259,079	618,064
11	0	0	0	0	0	431,084	235,756	173,018	280,684	671,09

12					159,161					31,8524
13					151,063					82,2972
14					184,099					136,464
15					160,984					172,982
16					170,02					227,395
17					158,009					258,305
18					178,453					329,24
19					211,007					424,65
20					205,091					467,69
21					198,05					518,805
22					255,664					664,171
23										361,452
24					337,83					288,763
25					302,115					290,419
26					277,018					311,036
27					217,984					291,353
28					189,292					291,513
29					145,894					289,707
30					91,0427					270,718
31					58,3764					269,955
32					21,3376					271,369
33					0					271,691
34	0	0	0	0	0	16,6299	5,9173	2,8118	8,7755	31,3349
35	17,2756	0	0	1,8897	38,0429	13,8135	4,3203	1,6698	7,3571	28,3711
36	55,5779	3,2361	0	25,2008	72,5357	12,9158	3,4936	1,0599	6,2038	26,187
37	106,752	35,3852	16,5179	60,2859	111,296	13,0517	4,0023	0,5909	6,574	27,2847
38	183,315	82,9162	54,8019	113,121	174,39	17,2145	6,0274	3,0004	9,0077	31,5441
39	214,537	95,9223	63,6863	128,103	201,453	15,761	5,3744	1,6649	7,9453	29,2233
40	329,849	185,454	139,749	213,024	280,64	19,461	7,8174	4,1526	10,8075	34,2494
41	417,777	237,429	181,047	275,657	355,85	24,1992	12,1588	7,9131	15,291	38,5079
42	426,364	231,315	170,063	273,013	371,434	24,116	11,7268	8,0289	15,4701	38,0978
43	527,399	308,522	239,684	349,677	442,002	27,4726	14,3938	10,2985	17,5487	41,3448
44	571,075	338,407	260,985	379,92	479,95	27,7411	14,4137	10,3353	17,9161	42,2973
45					223,78					168,402
46					123,594					422,734
47					193,588					81,4888
48					18,9377					234,109
49					79,5249					345,16
50					353,896					362,907
51					206,57					483,746
52					235,274					134,658

53					48,4746					179,58
54					24,996					436,716
55					306,115					572,822

Plots of the fluorescence intensities versus the calculated concentrations were established from each situation (***Figure 46*** and ***47***).

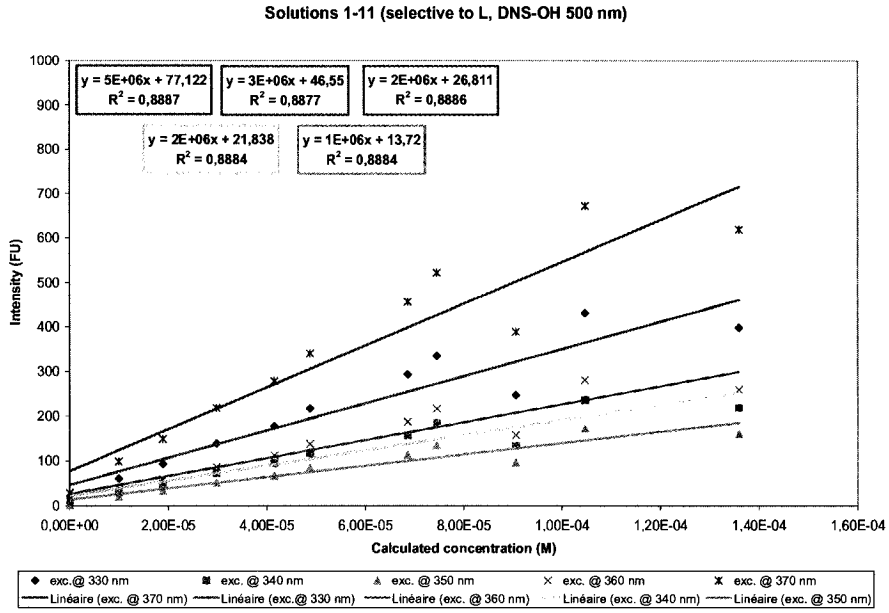

Solutions 12-22 (DNS-OH varying, PYR-OH constant at 7.55 x 10-5 M)

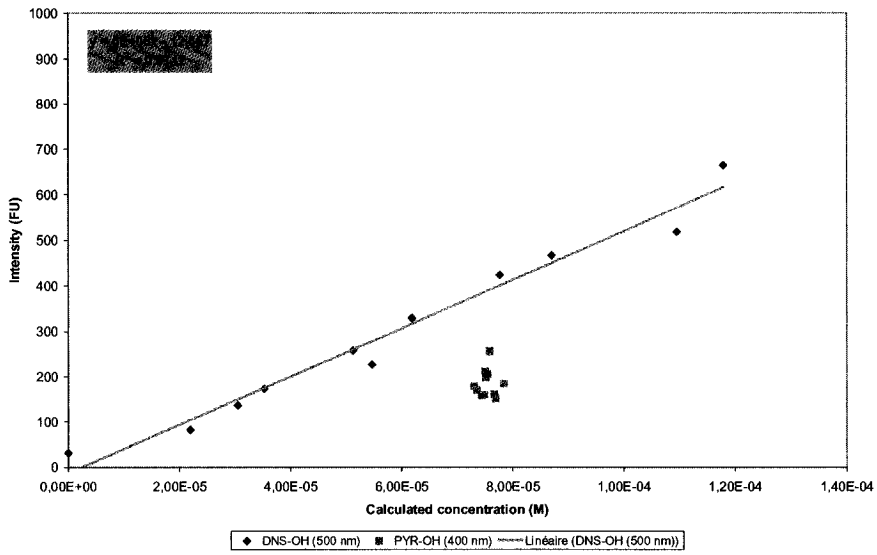

Solutions 23-33 (PYR-OH varying, DNS-OH constant at 7.55 x 10^{-5} M)

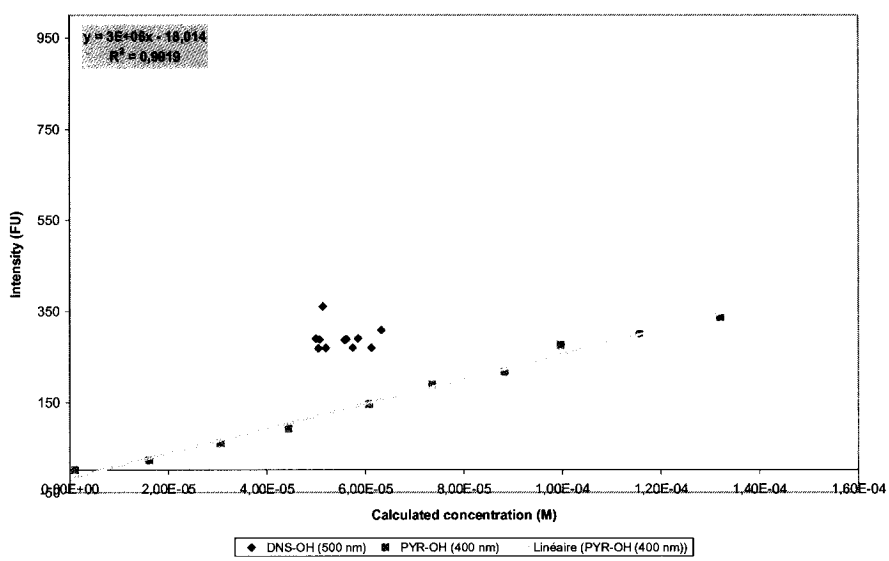

Solutions 34-44 (Selective to D, PYR-OH 400 nm)

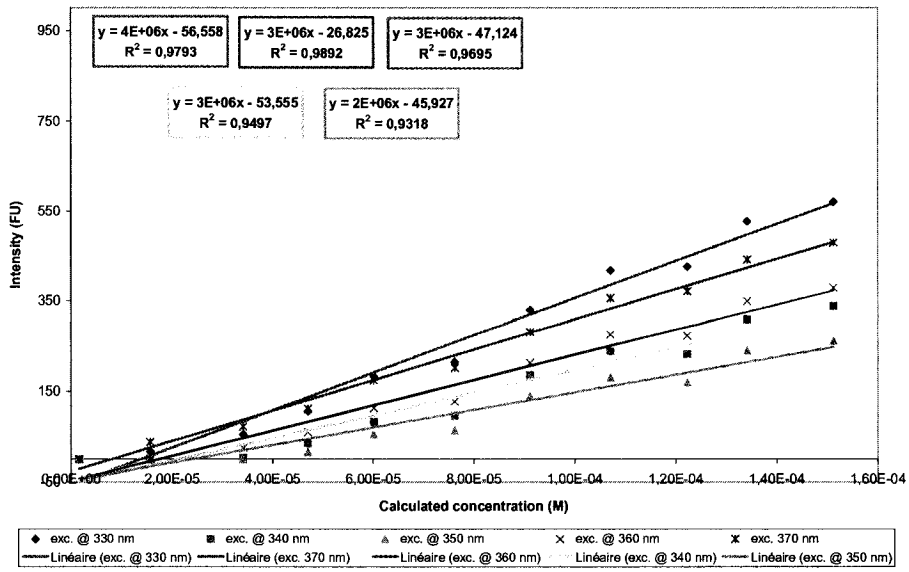

Solutions 45-55 (Random ratios)

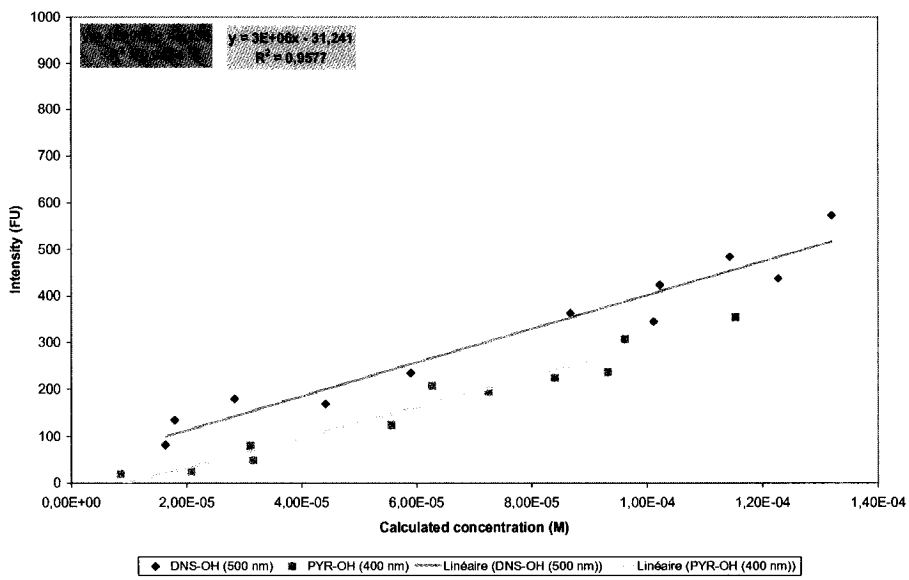

APPENDIX

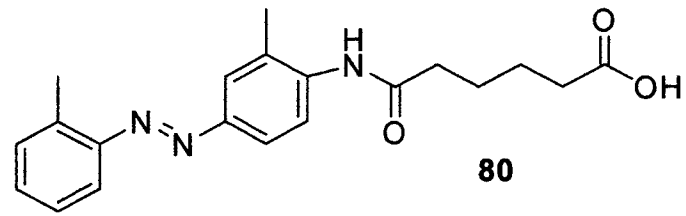

80

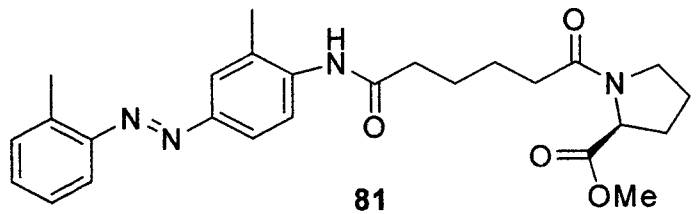
H
N
O
N
N
N
O
O
OMe

81

800
700
600
500
400
300
200
100
0
8.0
7.0
6.0
5.0
4.0
3.0
2.0
1.0
0.0
ppm (t1)

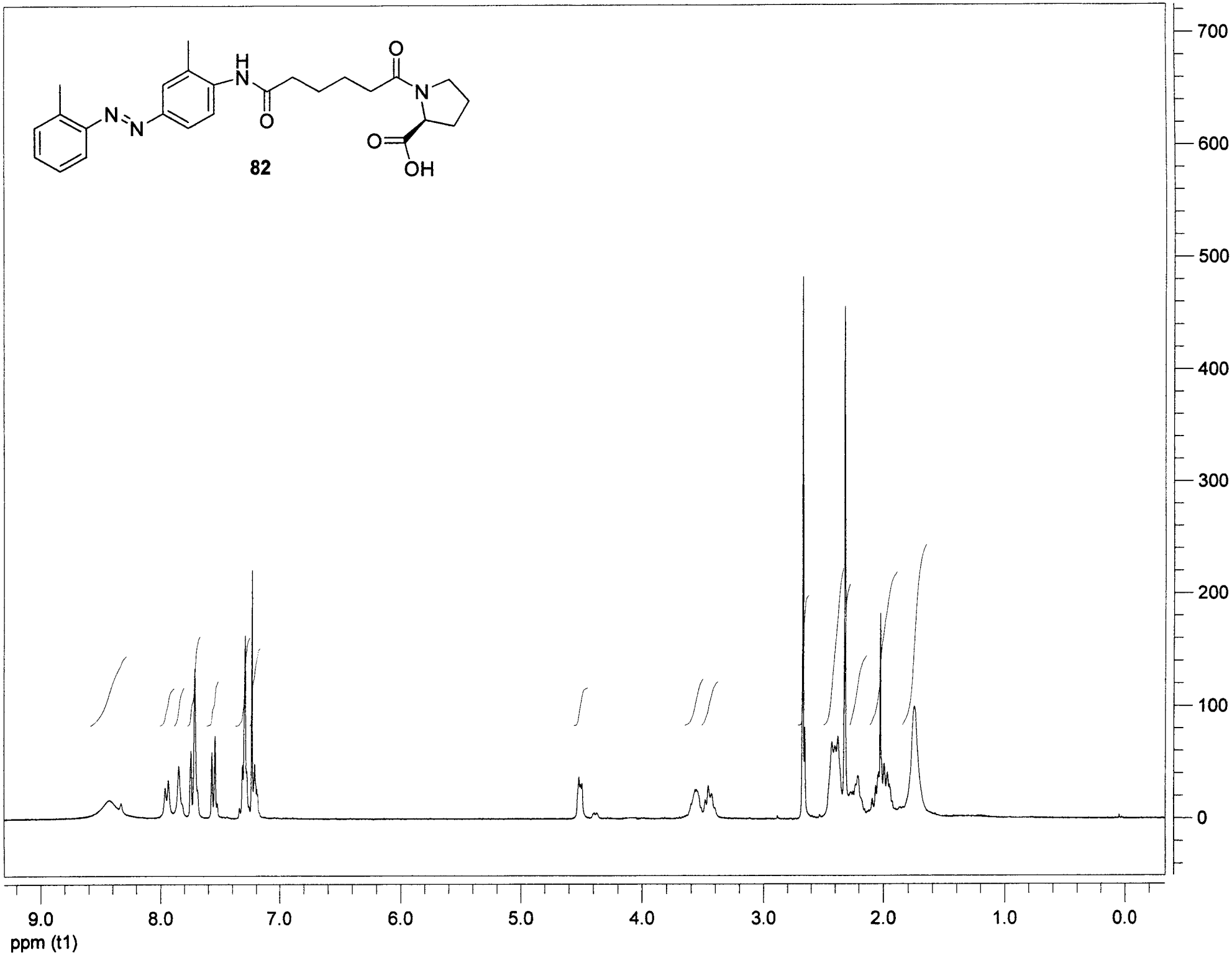
82
700
600
500
400
300
200
100
0
9.0
8.0
7.0
6.0
5.0
4.0
3.0
2.0
1.0
0.0
ppm (t1)

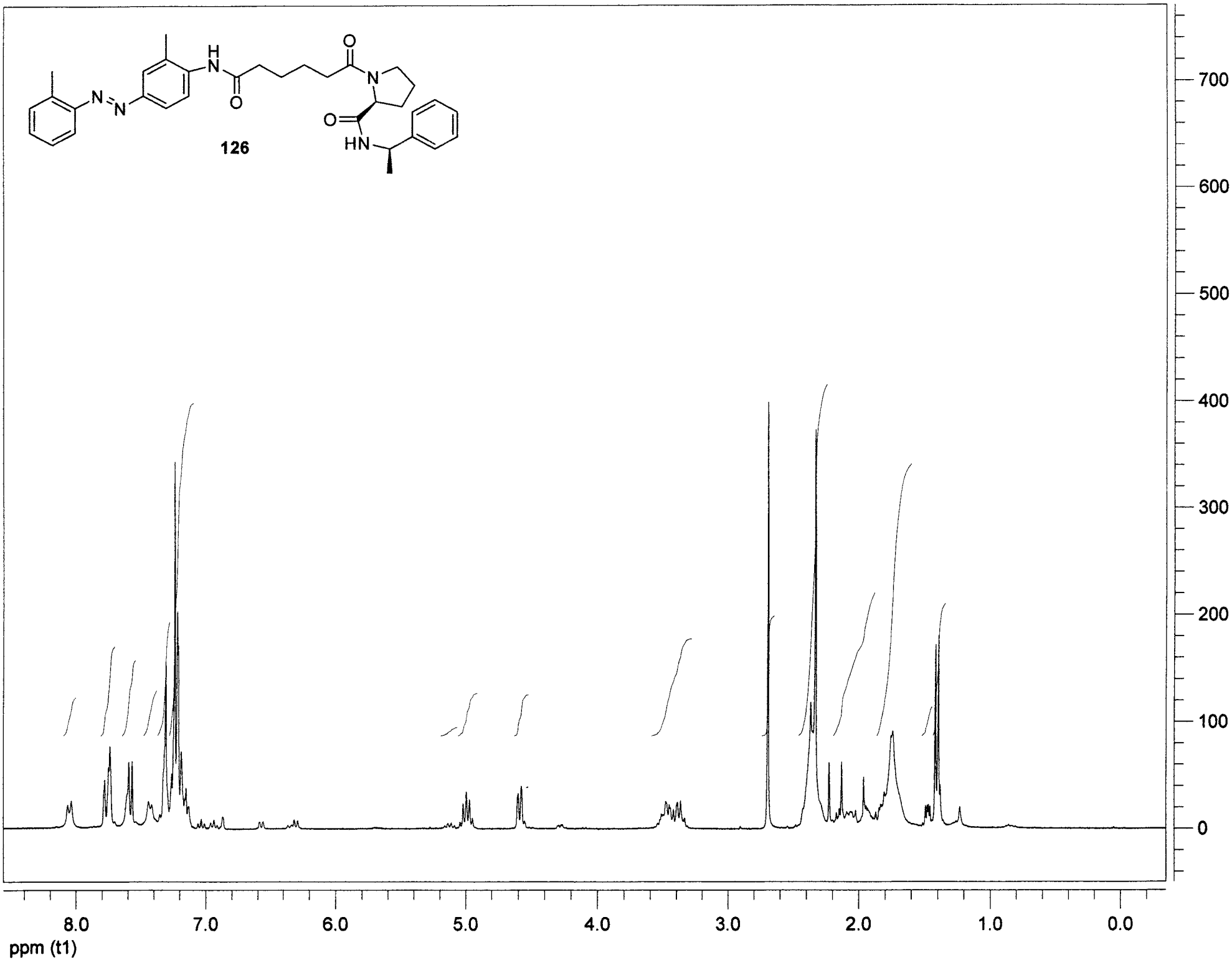
126
700
600
500
400
300
200
100
0
8.0
7.0
6.0
5.0
4.0
3.0
2.0
1.0
0.0
ppm (t1)

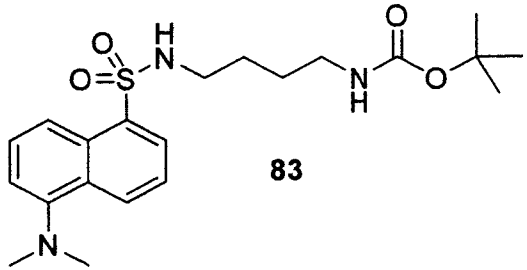

83

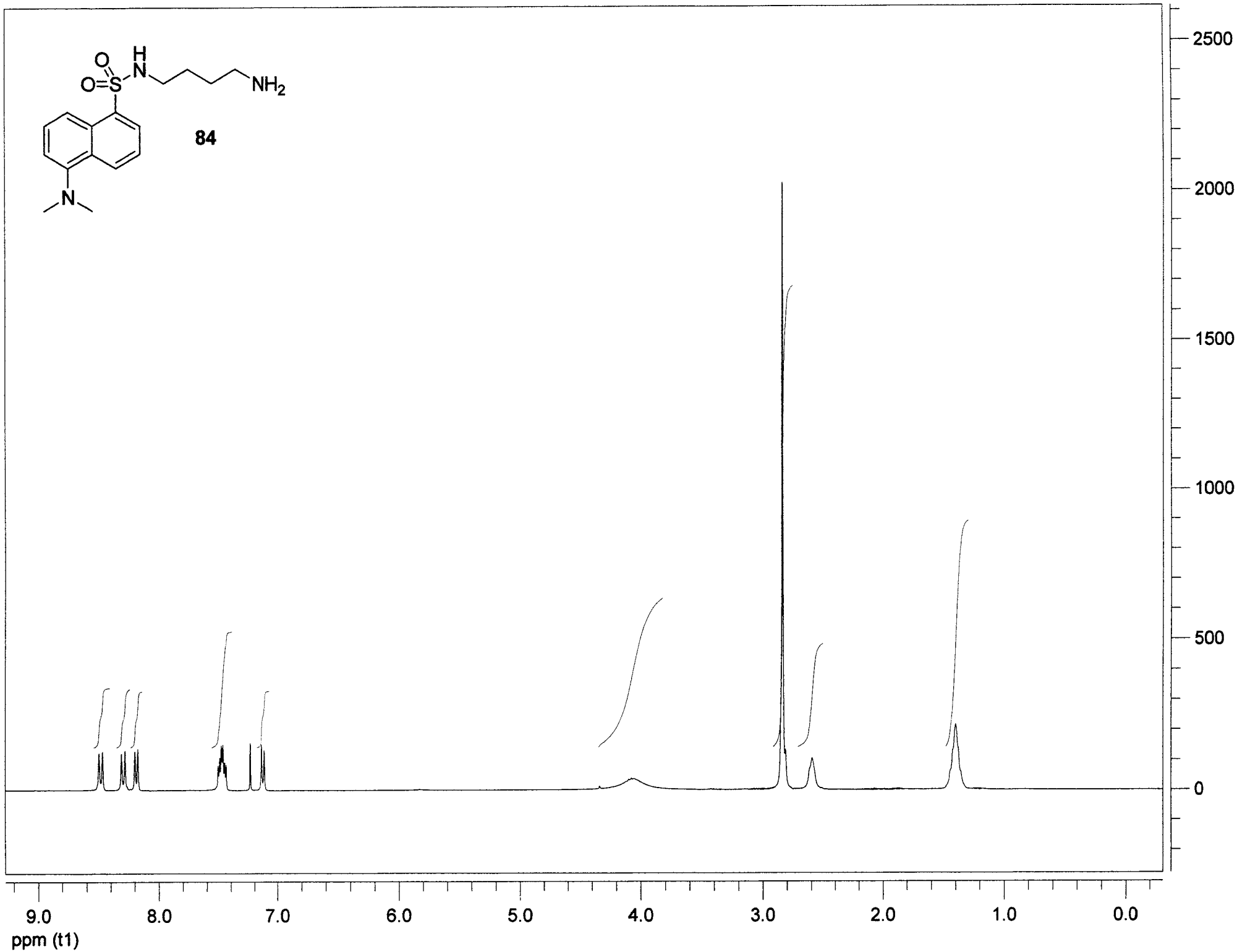
O
H
N
O=S
NH2
84
N
2500
2000
1500
1000
500
0
9.0
8.0
7.0
6.0
5.0
4.0
3.0
2.0
1.0
0.0
ppm (t1)

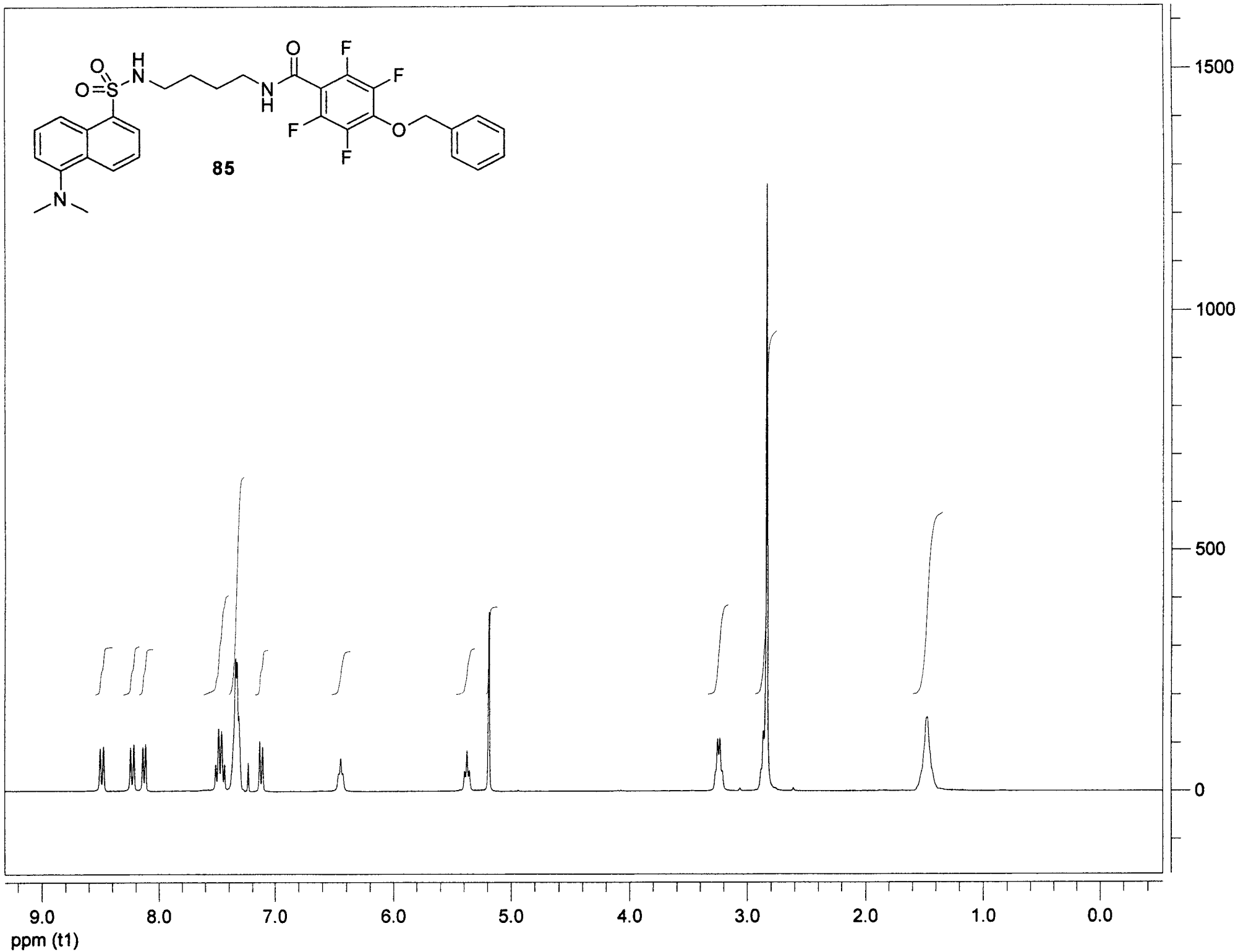
85
1500
1000
500
0
9.0
8.0
7.0
6.0
5.0
4.0
3.0
2.0
1.0
0.0
ppm (t1)

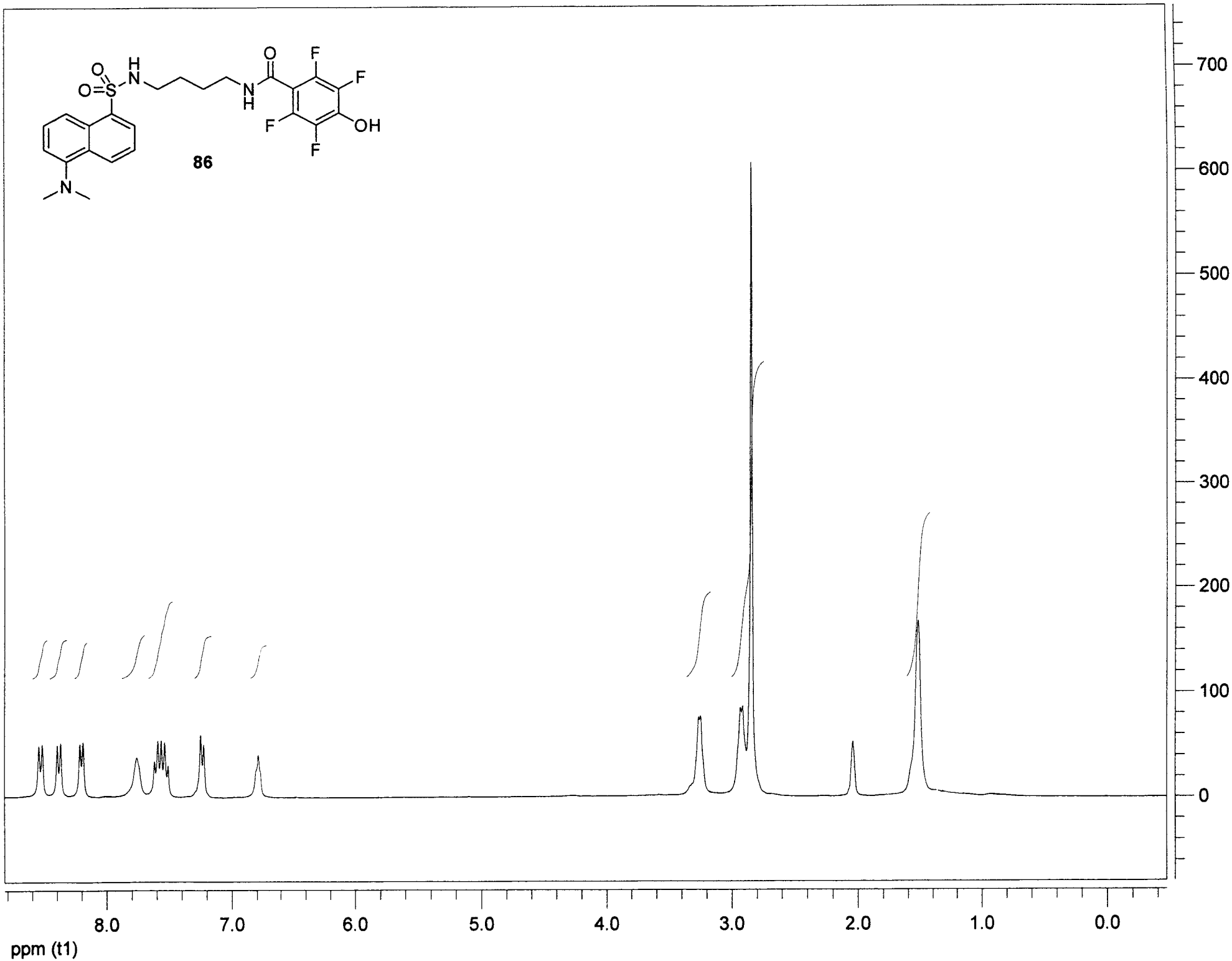
86
700
600
500
400
300
200
100
0
8.0
7.0
6.0
5.0
4.0
3.0
2.0
1.0
0.0
ppm (t1)

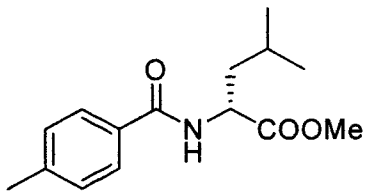

91

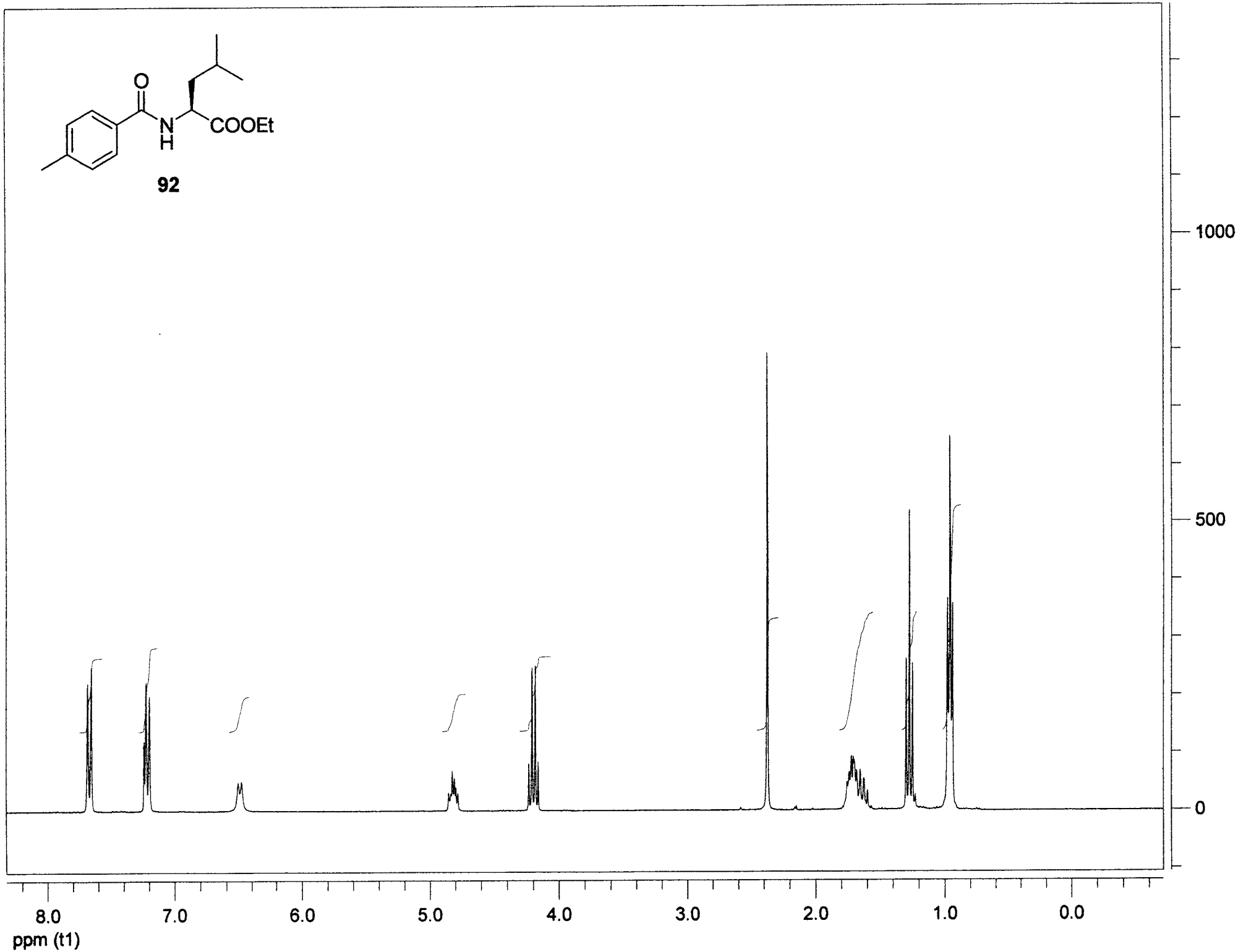
O
N
H
COOEt
92
1000
500
0
8.0
7.0
6.0
5.0
4.0
3.0
2.0
1.0
0.0
ppm (t1)

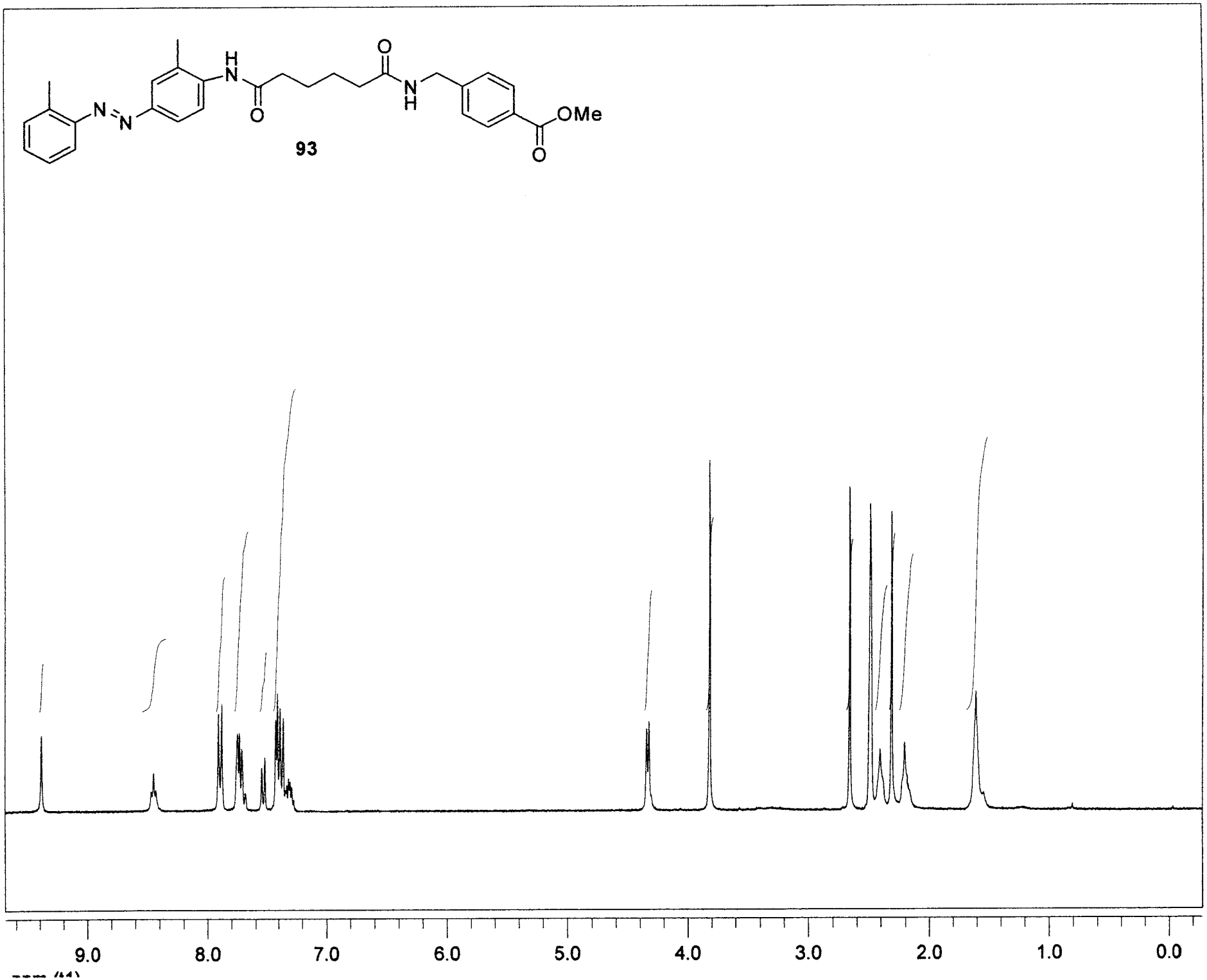
93
OMe
600
500
400
300
200
100
0
9.0
8.0
7.0
6.0
5.0
4.0
3.0
2.0
1.0
0.0

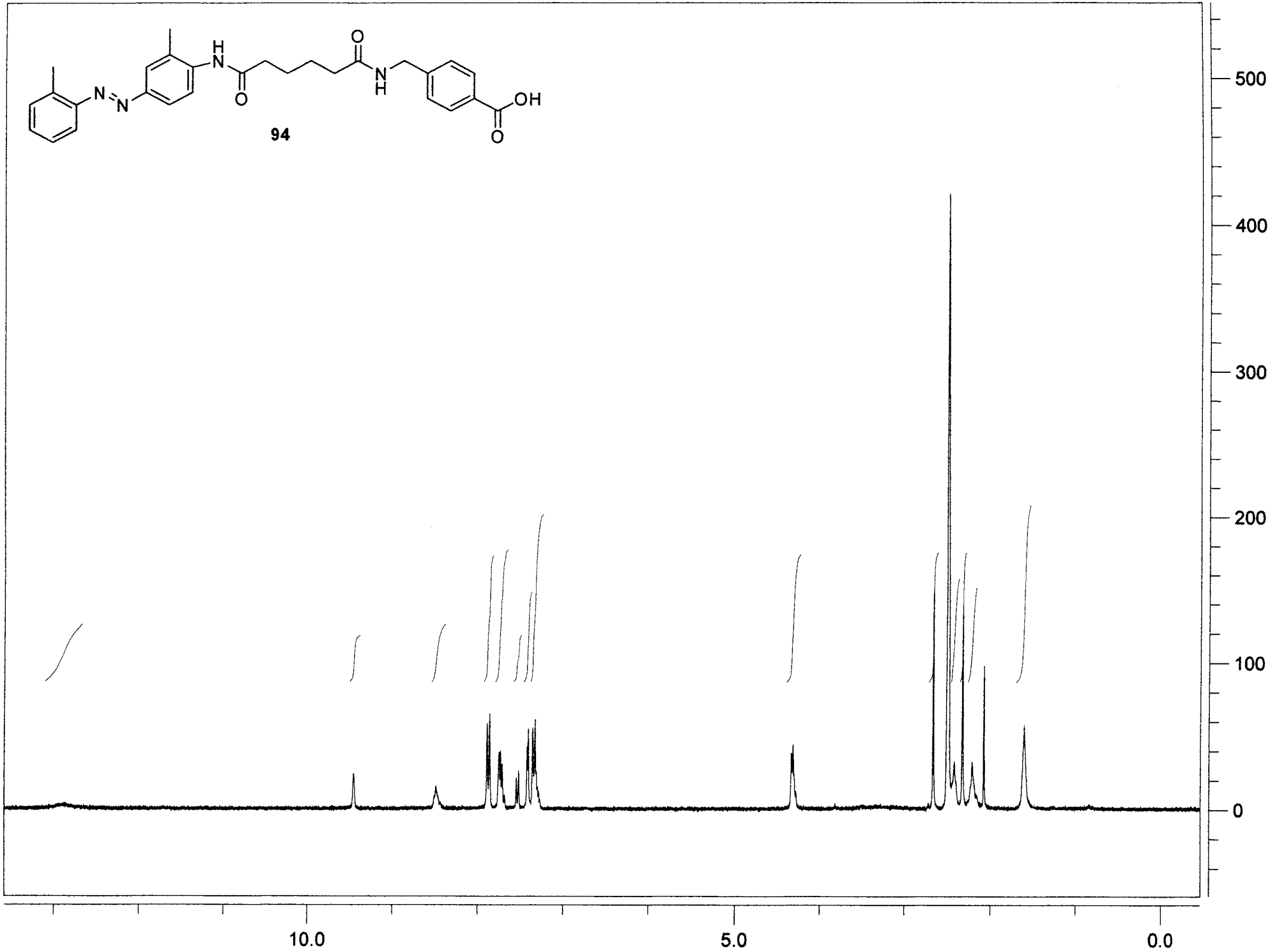
94
500
400
300
200
100
0
10.0
5.0
0.0
ppm (t1)

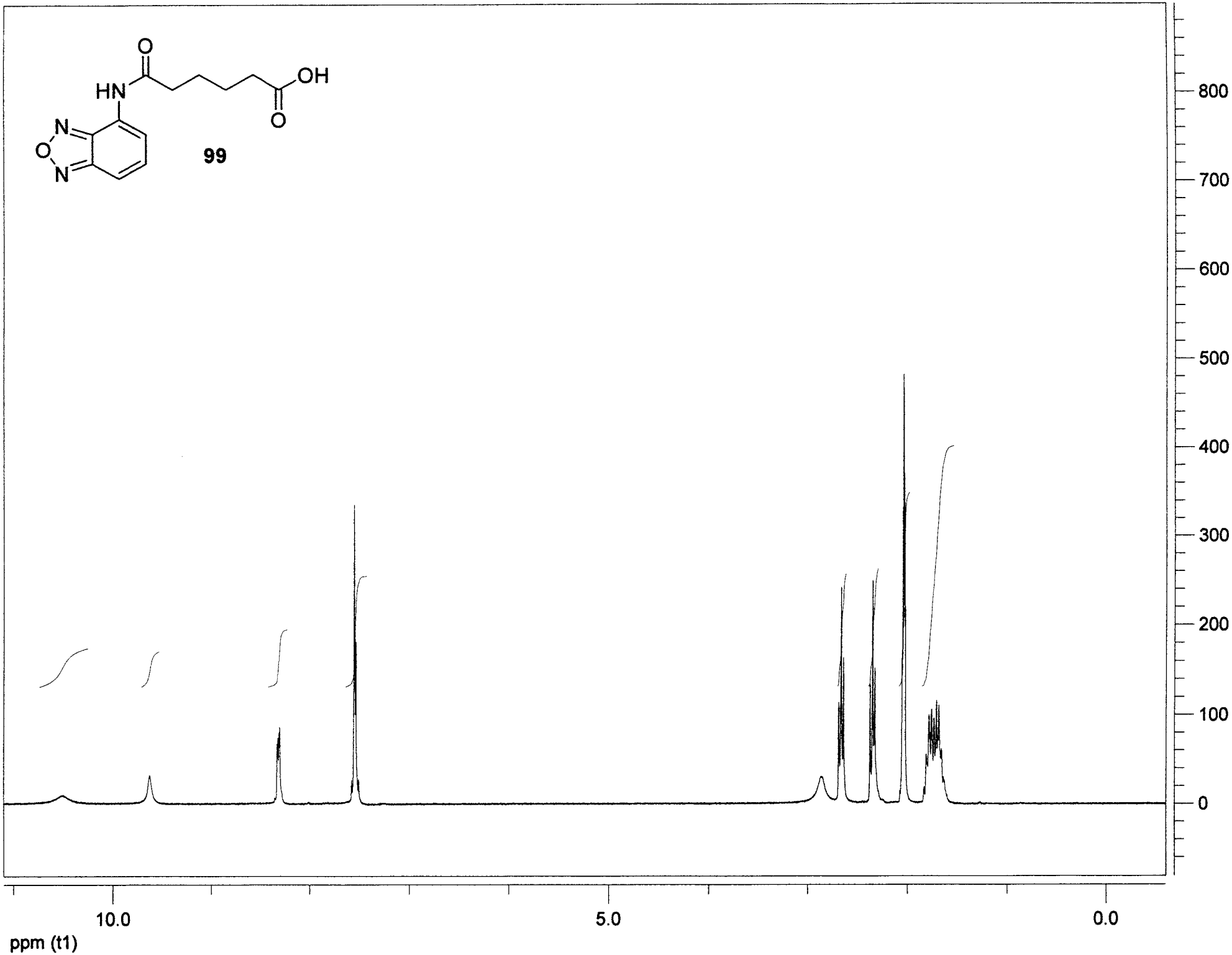
O
HN
OH
O
N
O
N
99
800
700
600
500
400
300
200
100
0
10.0
5.0
0.0
ppm (t1)

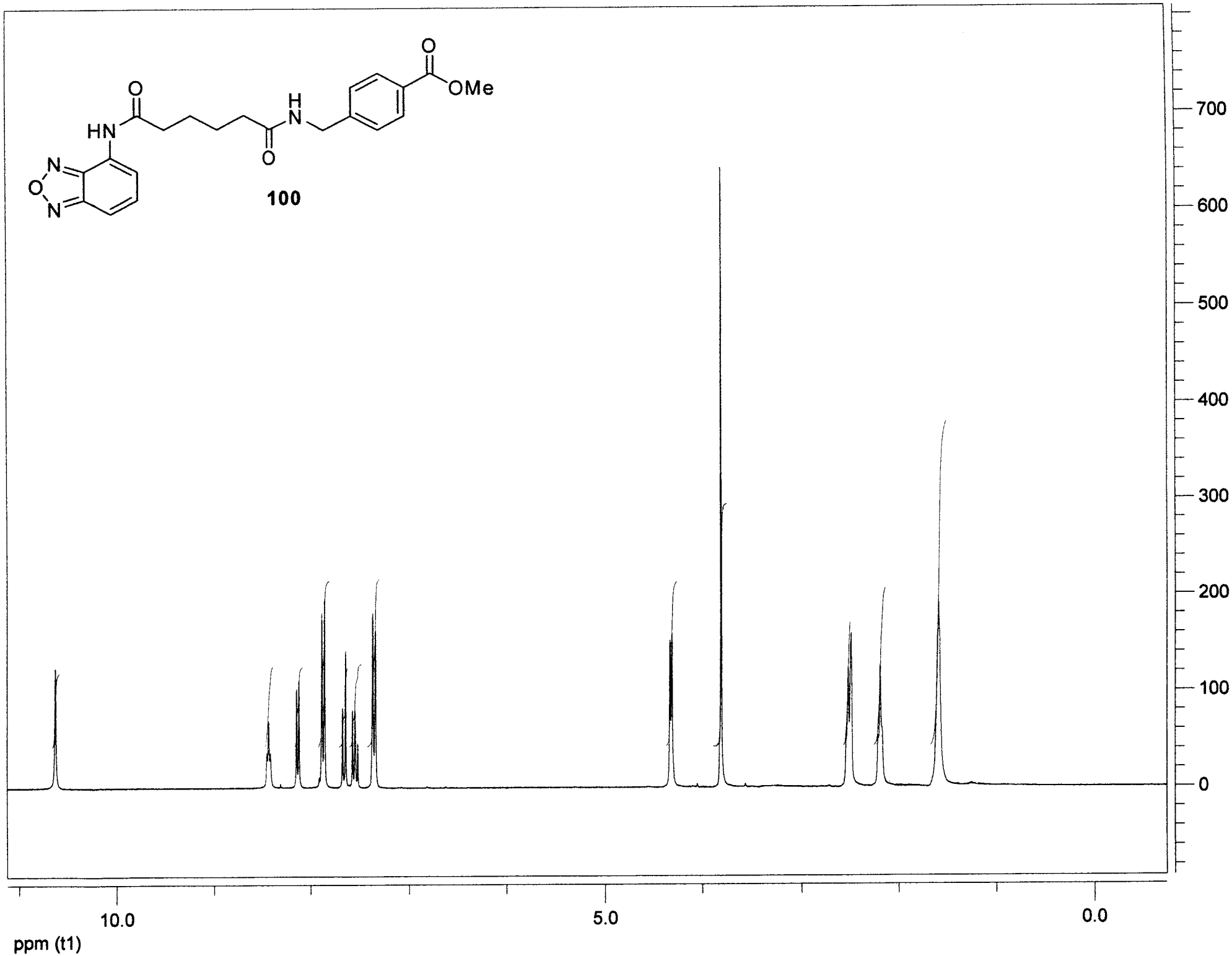
O
OMe
H
N
HN
O
O
N
O
N
100
700
600
500
400
300
200
100
0
10.0
5.0
0.0
ppm (t1)

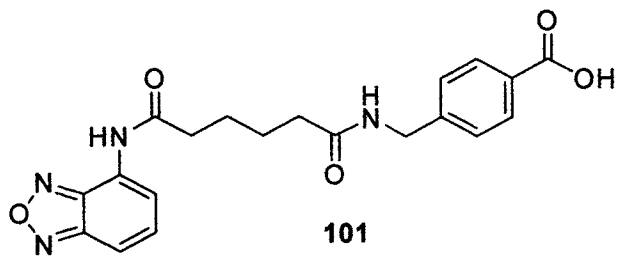

101

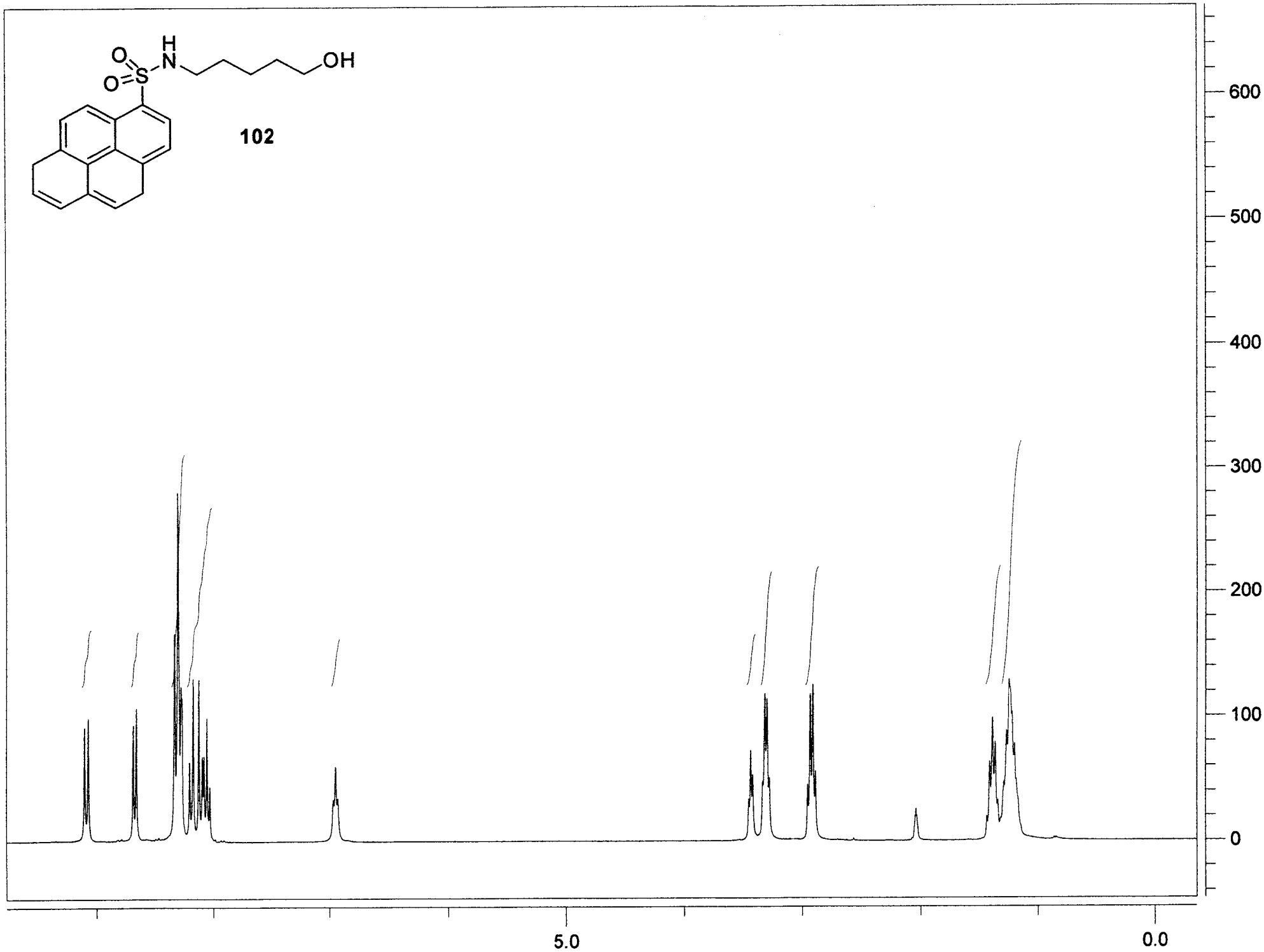
O
H
N
S
O
O
OH
102
600
500
400
300
200
100
0
5.0
0.0
ppm (t1)

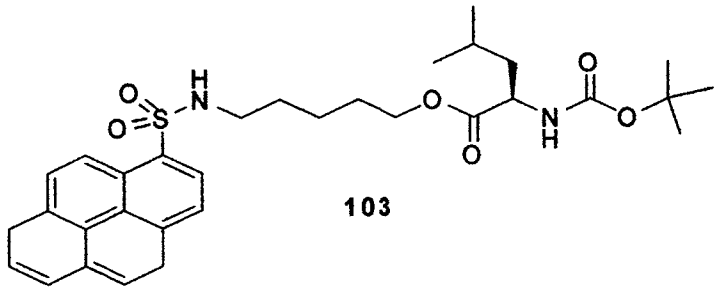

103

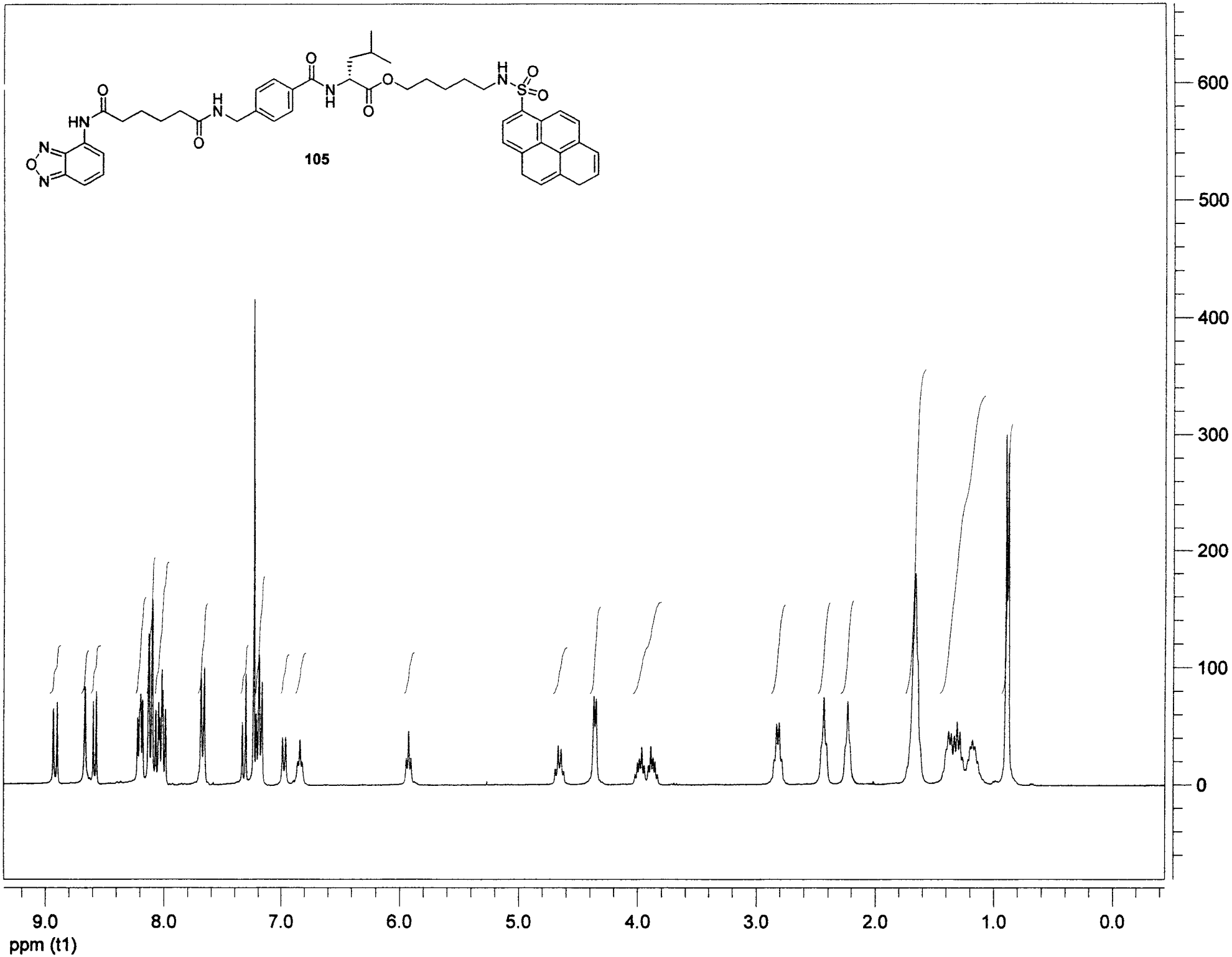
105
600
500
400
300
200
100
0
9.0
8.0
7.0
6.0
5.0
4.0
3.0
2.0
1.0
0.0
ppm (t1)

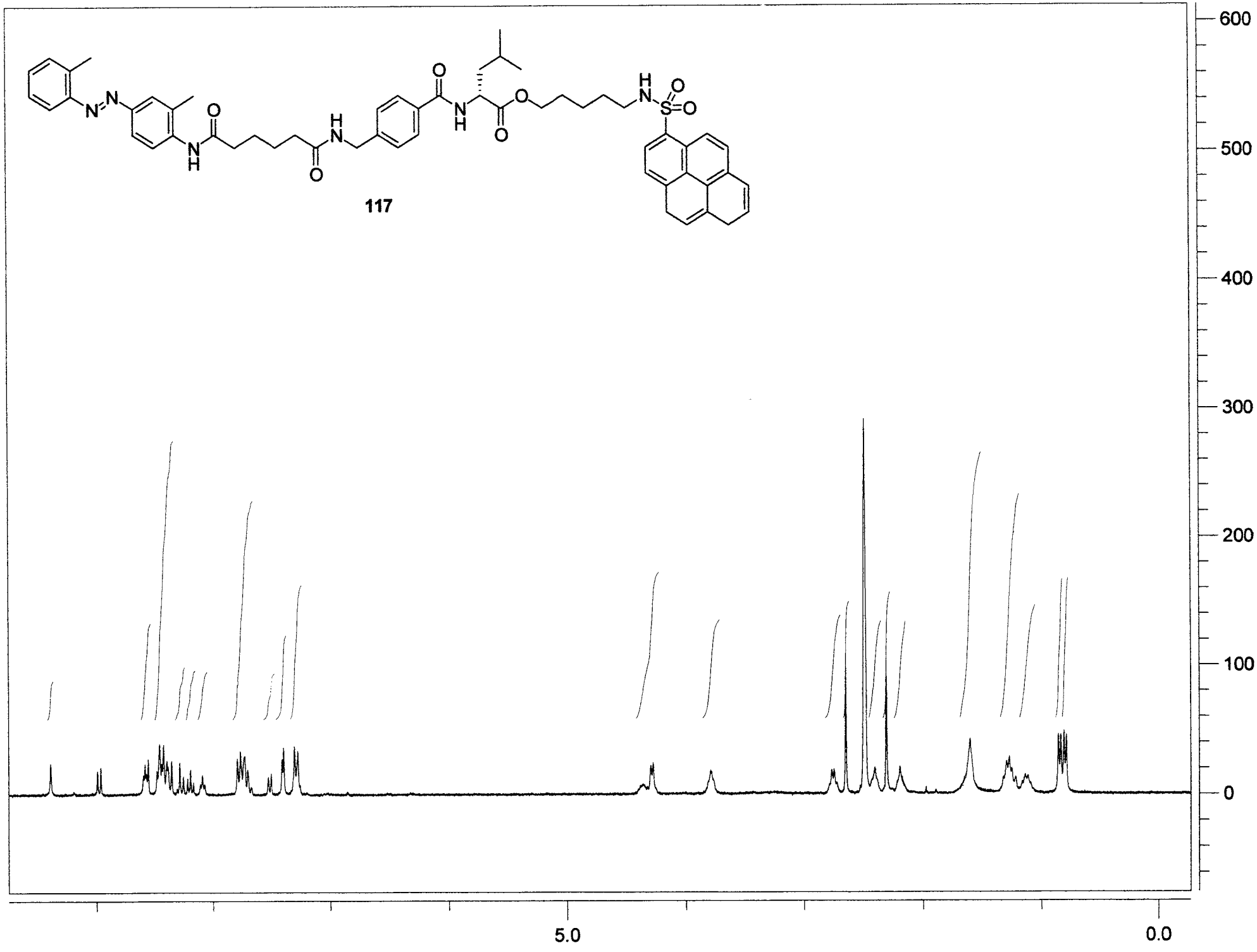
117
600
500
400
300
200
100
0
5.0
0.0
ppm (t1)

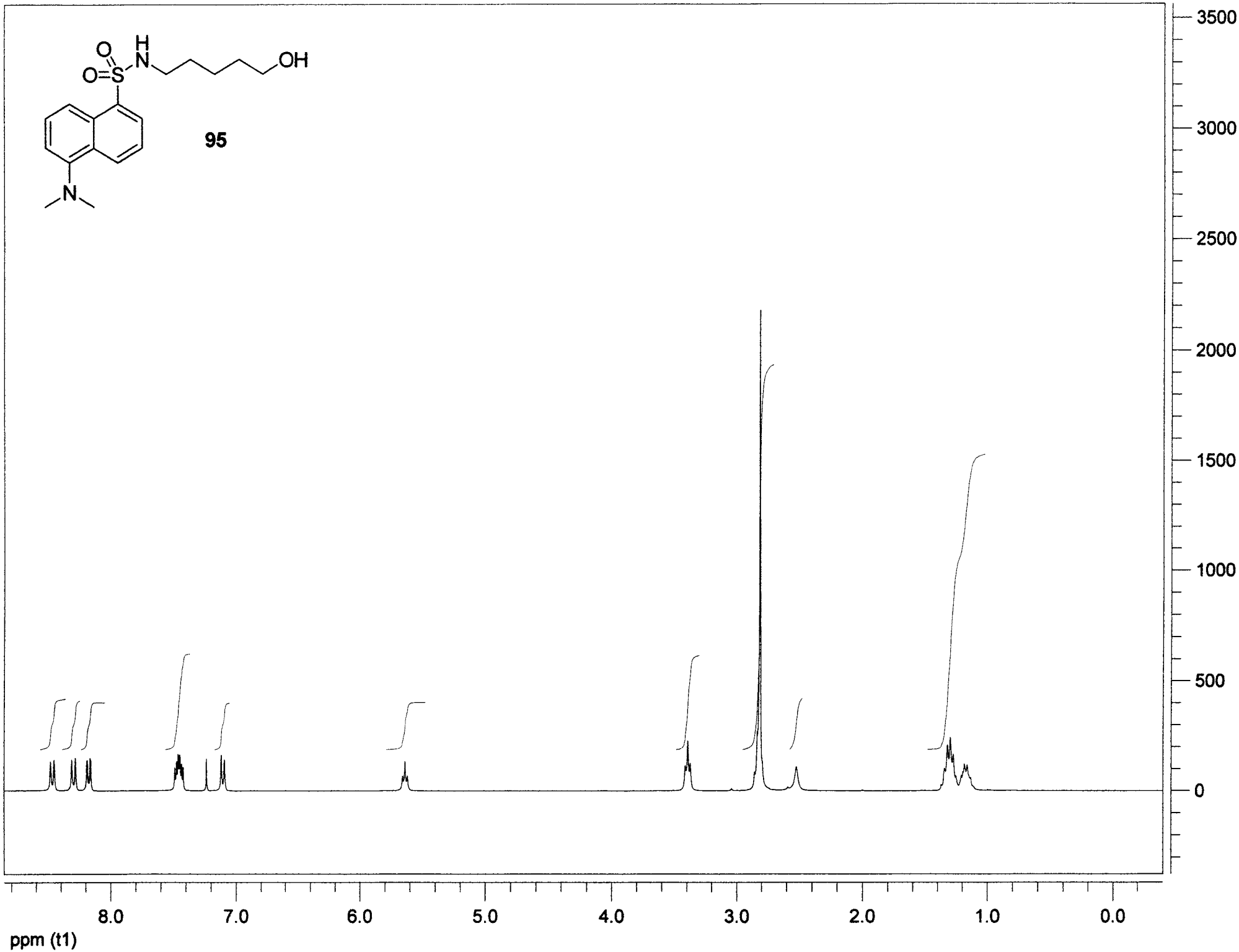
O
H
N
O=S
OH
95
N
3500
3000
2500
2000
1500
1000
500
0
8.0
7.0
6.0
5.0
4.0
3.0
2.0
1.0
0.0
ppm (t1)

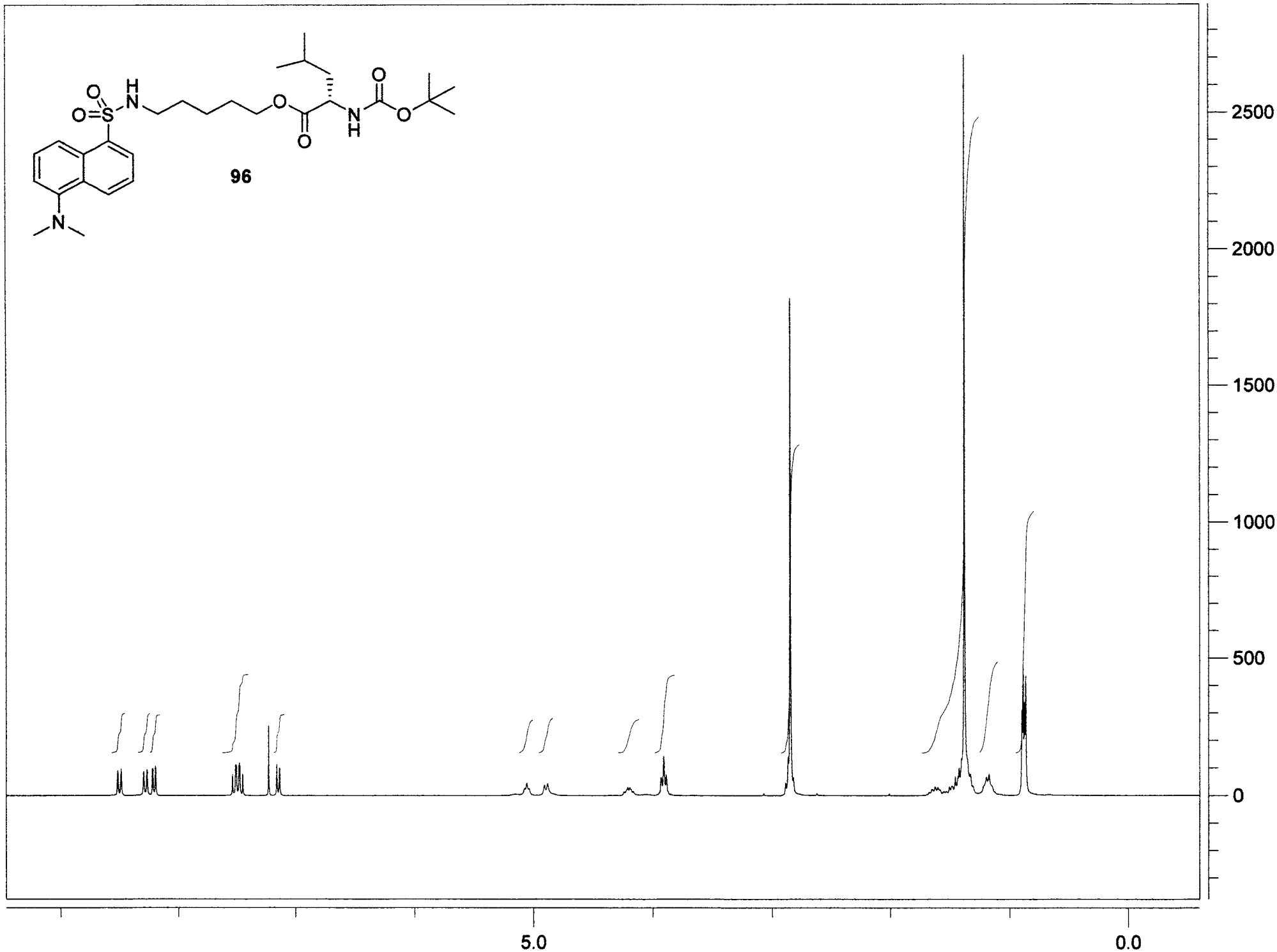
96
2500
2000
1500
1000
500
0
5.0
0.0
ppm (t1)

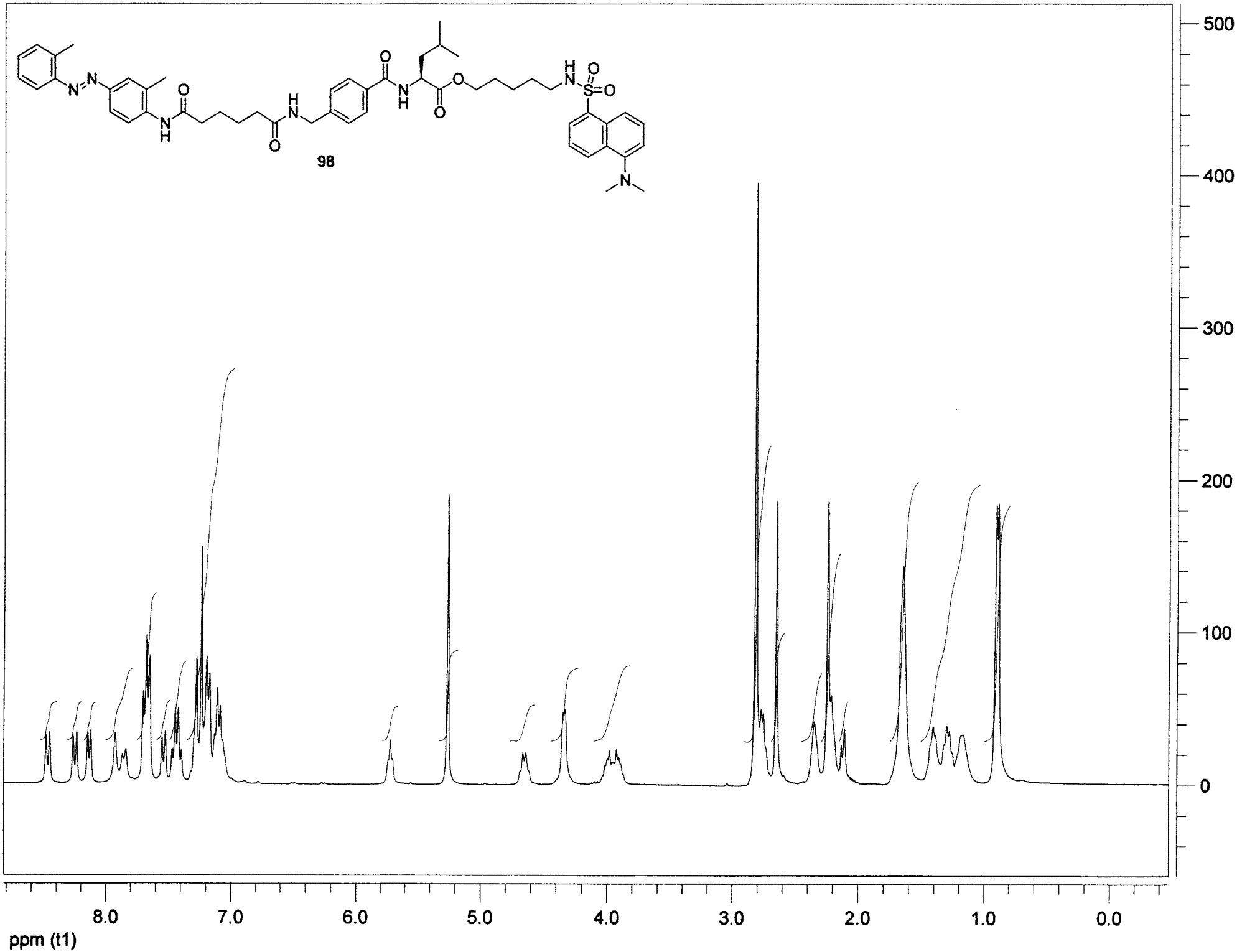
98
500
400
300
200
100
0
8.0
7.0
6.0
5.0
4.0
3.0
2.0
1.0
0.0
ppm (t1)

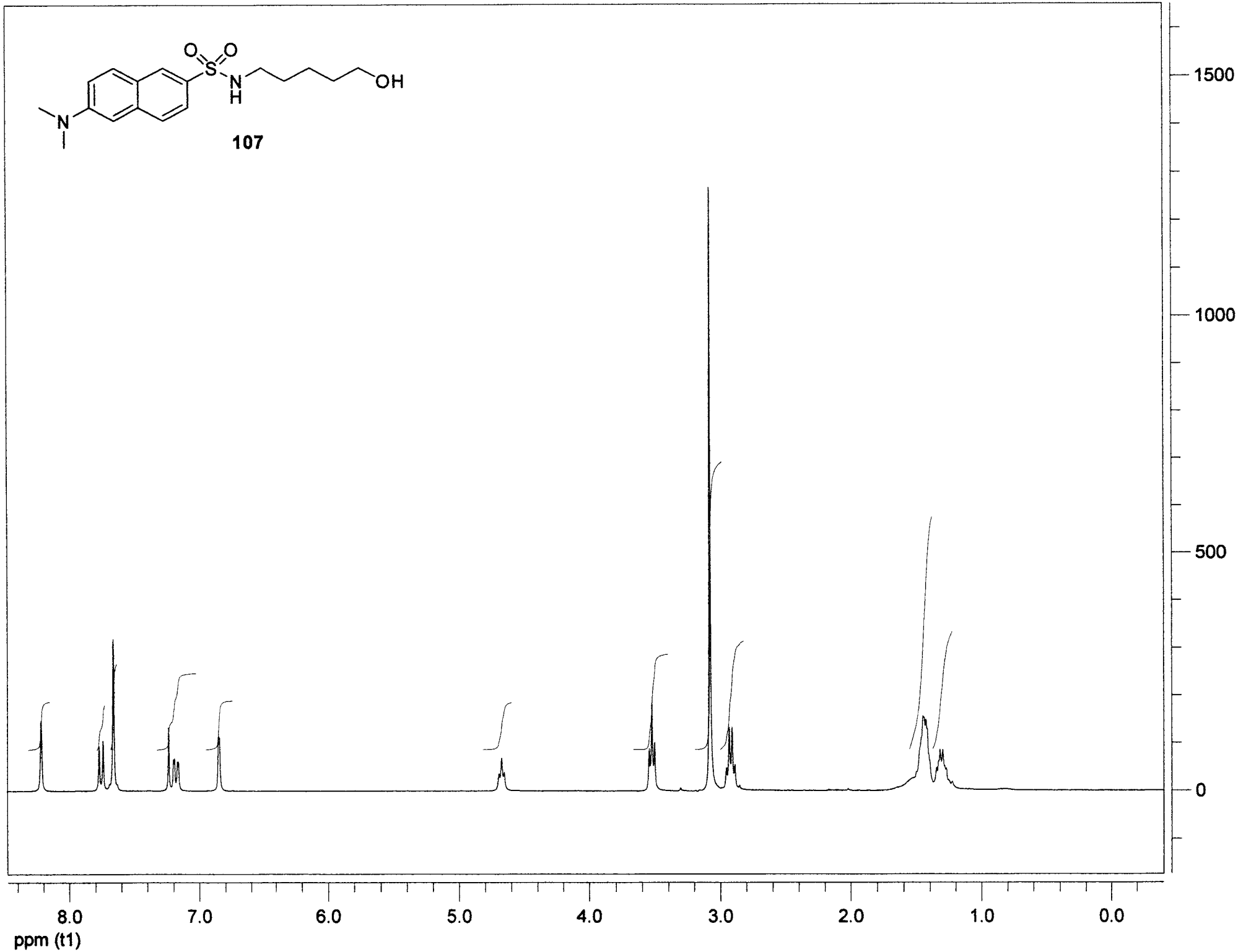
O
O
S
N
H
OH
N
107
1500
1000
500
0
8.0
7.0
6.0
5.0
4.0
3.0
2.0
1.0
0.0
ppm (t1)

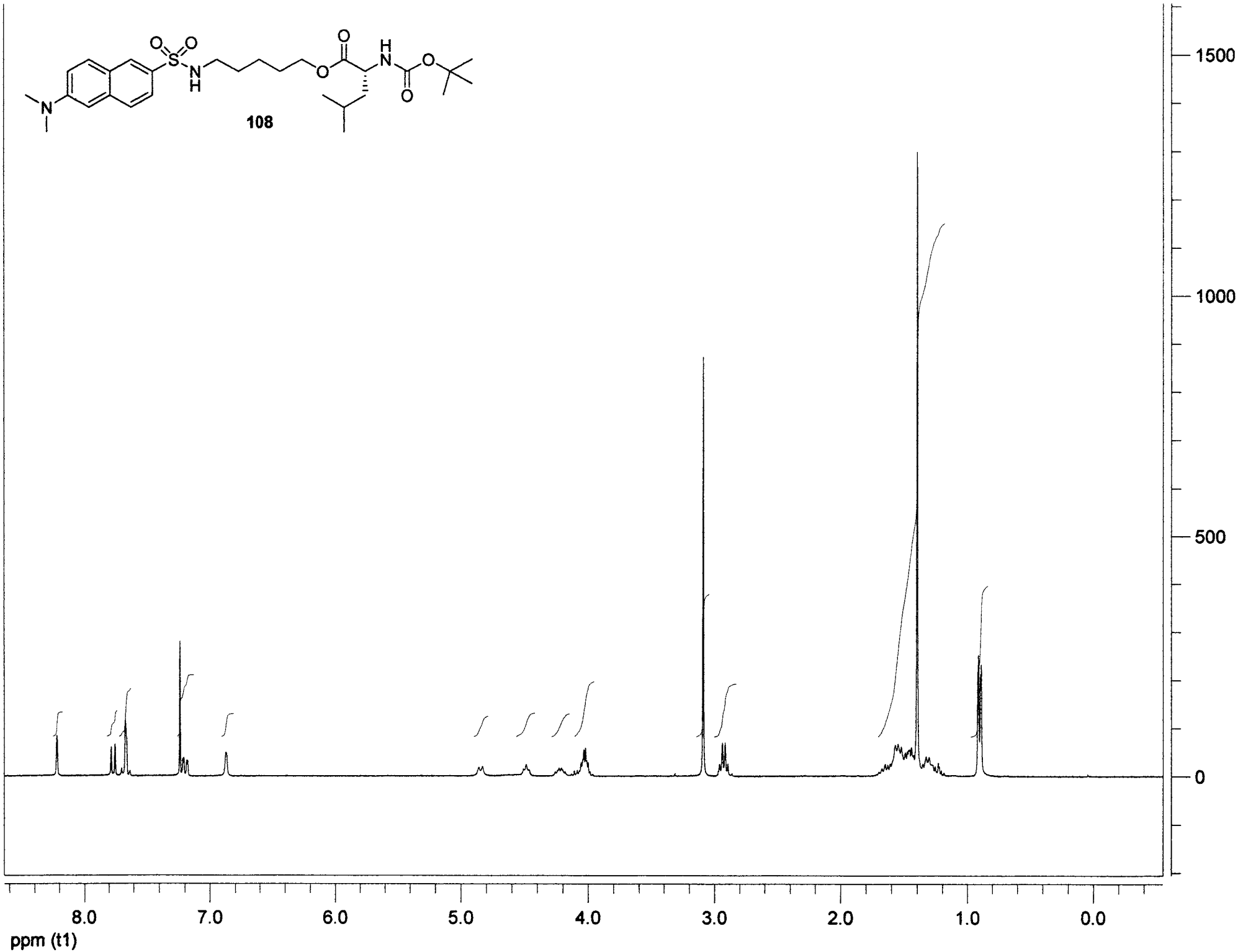
108
1500
1000
500
0
8.0
7.0
6.0
5.0
4.0
3.0
2.0
1.0
0.0
ppm (t1)

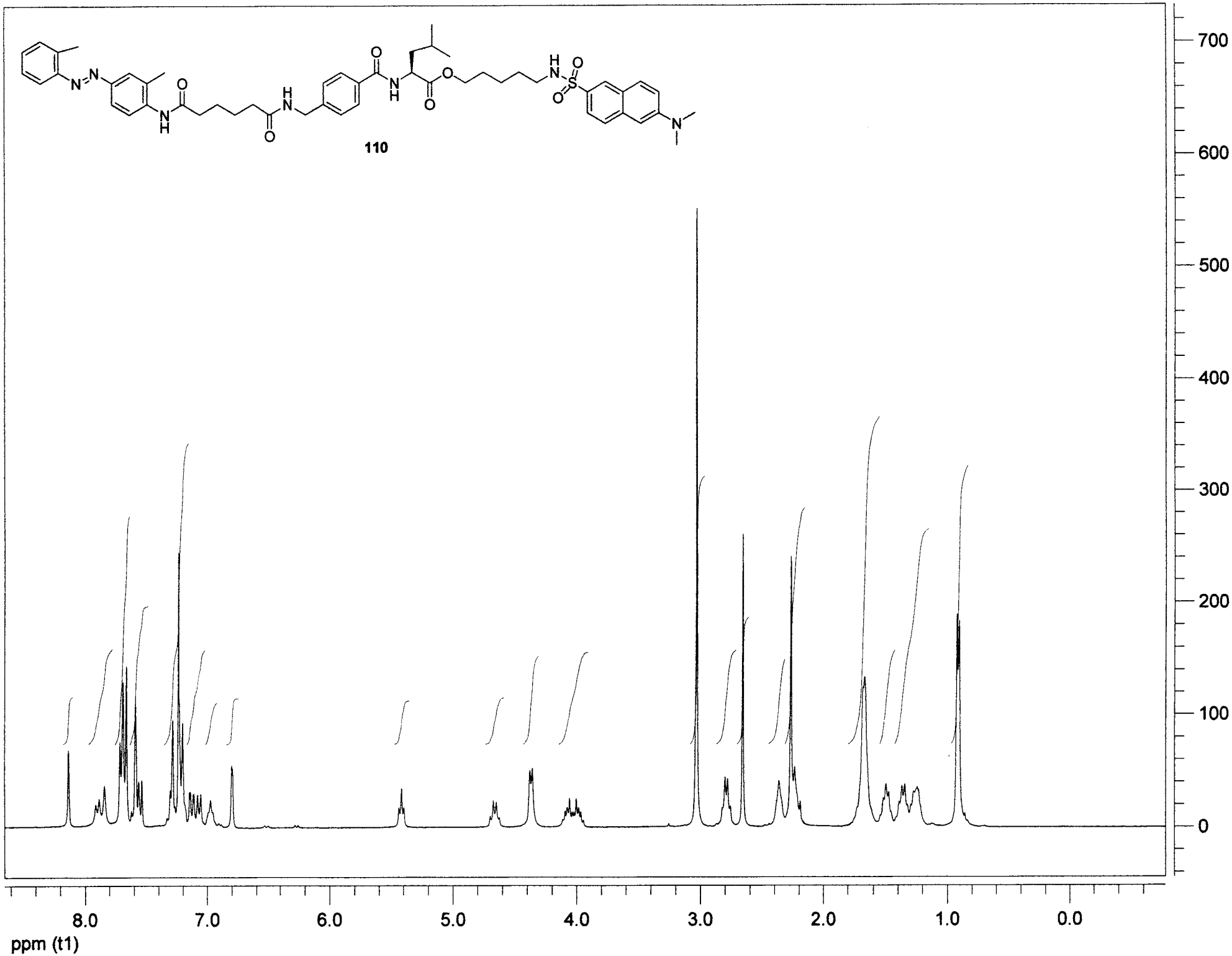
110
700
600
500
400
300
200
100
0
8.0
7.0
6.0
5.0
4.0
3.0
2.0
1.0
0.0
ppm (t1)

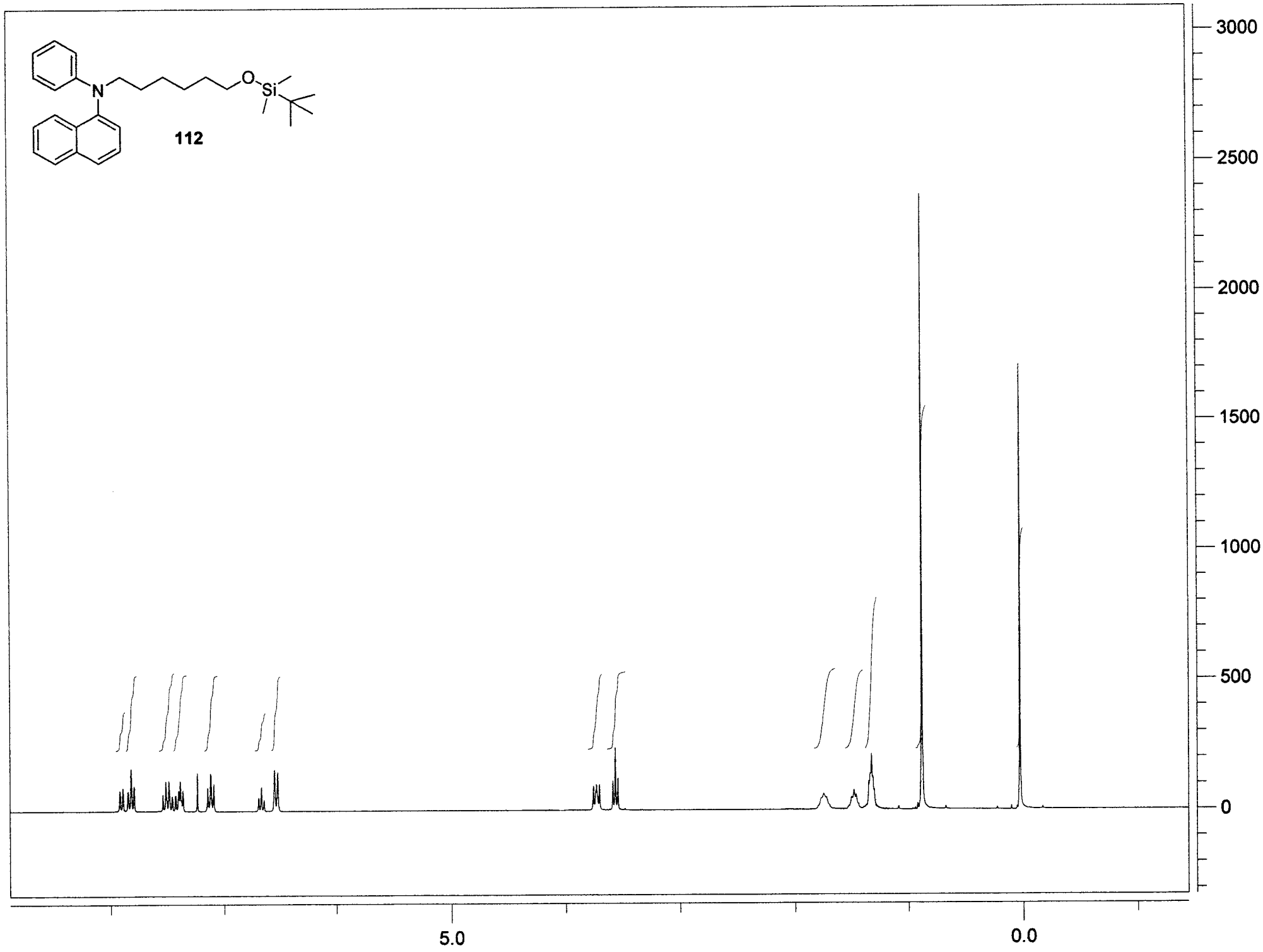
N
O
Si
112
3000
2500
2000
1500
1000
500
0
5.0
0.0
ppm (t1)

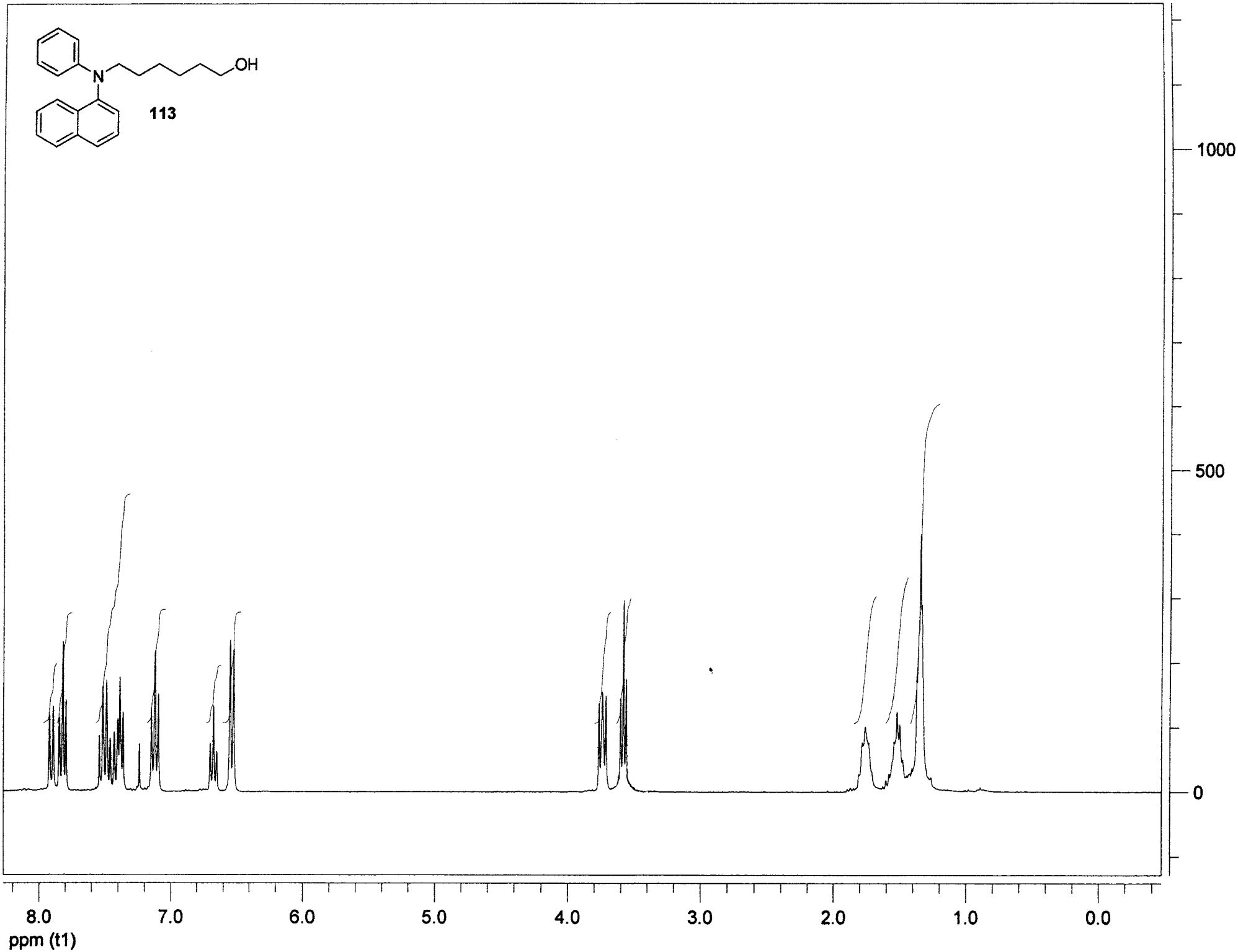
OH
N
113
1000
500
0
8.0
7.0
6.0
5.0
4.0
3.0
2.0
1.0
0.0
ppm (t1)

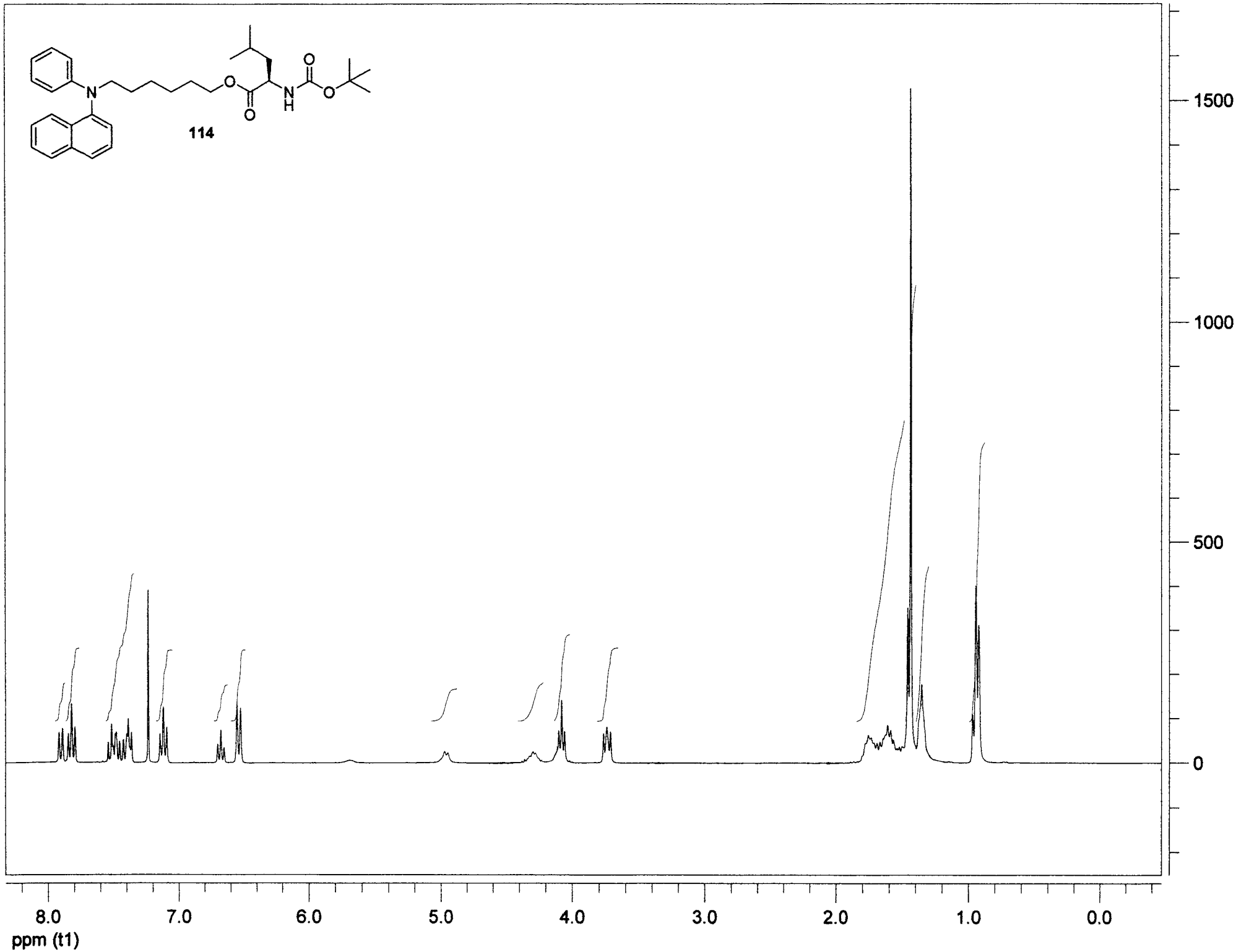
114
1500
1000
500
0
8.0
7.0
6.0
5.0
4.0
3.0
2.0
1.0
0.0
ppm (t1)

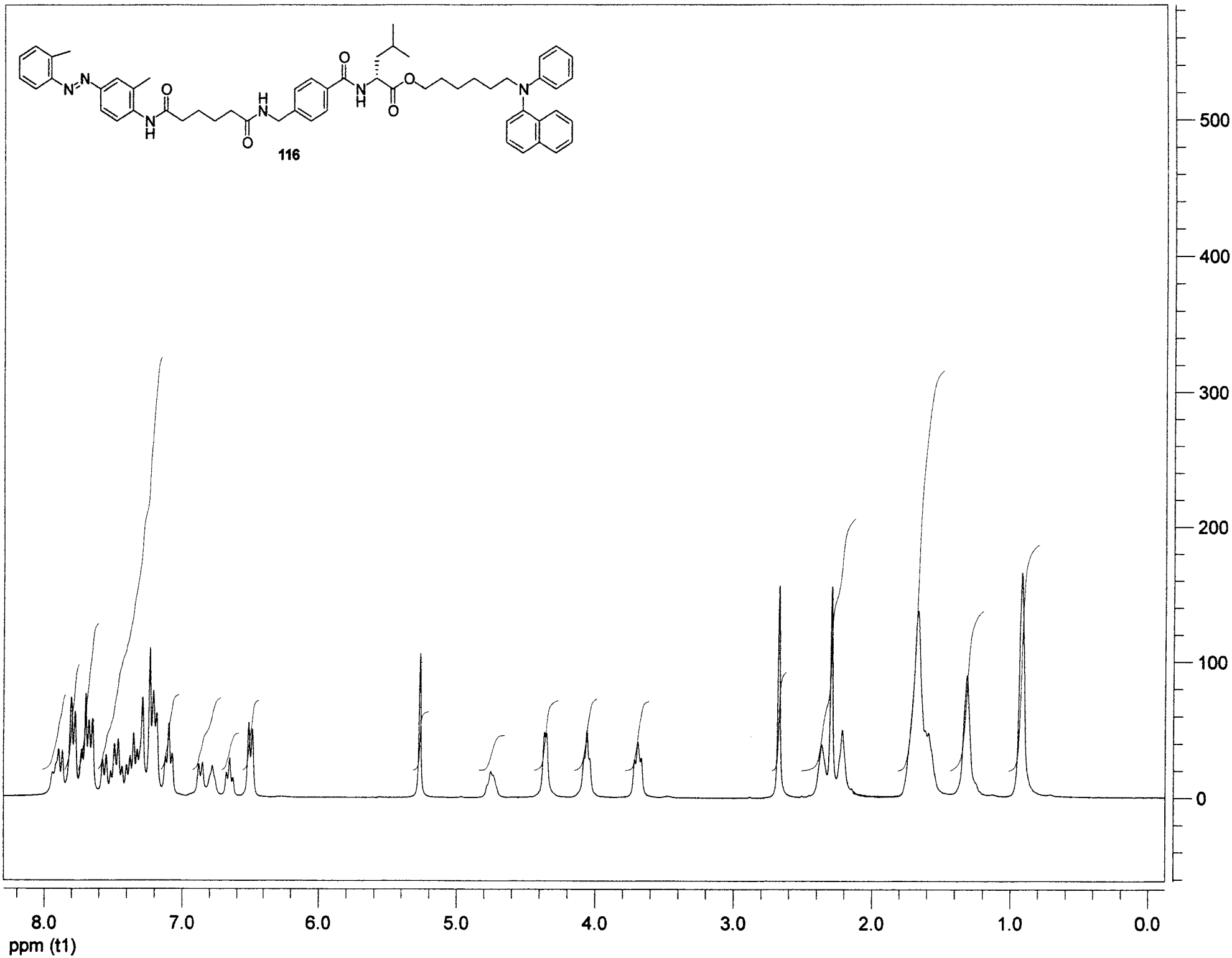
116
500
400
300
200
100
0
8.0
7.0
6.0
5.0
4.0
3.0
2.0
1.0
0.0
ppm (t1)

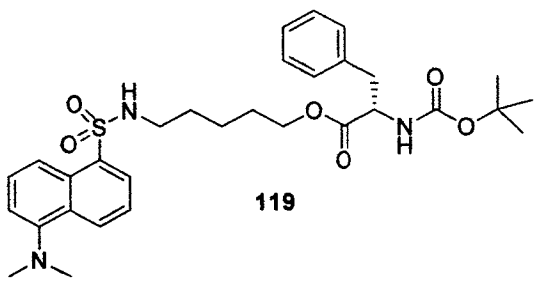

119

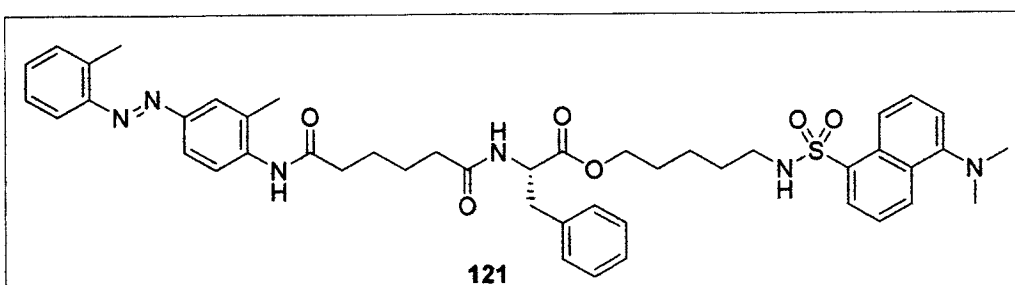

121

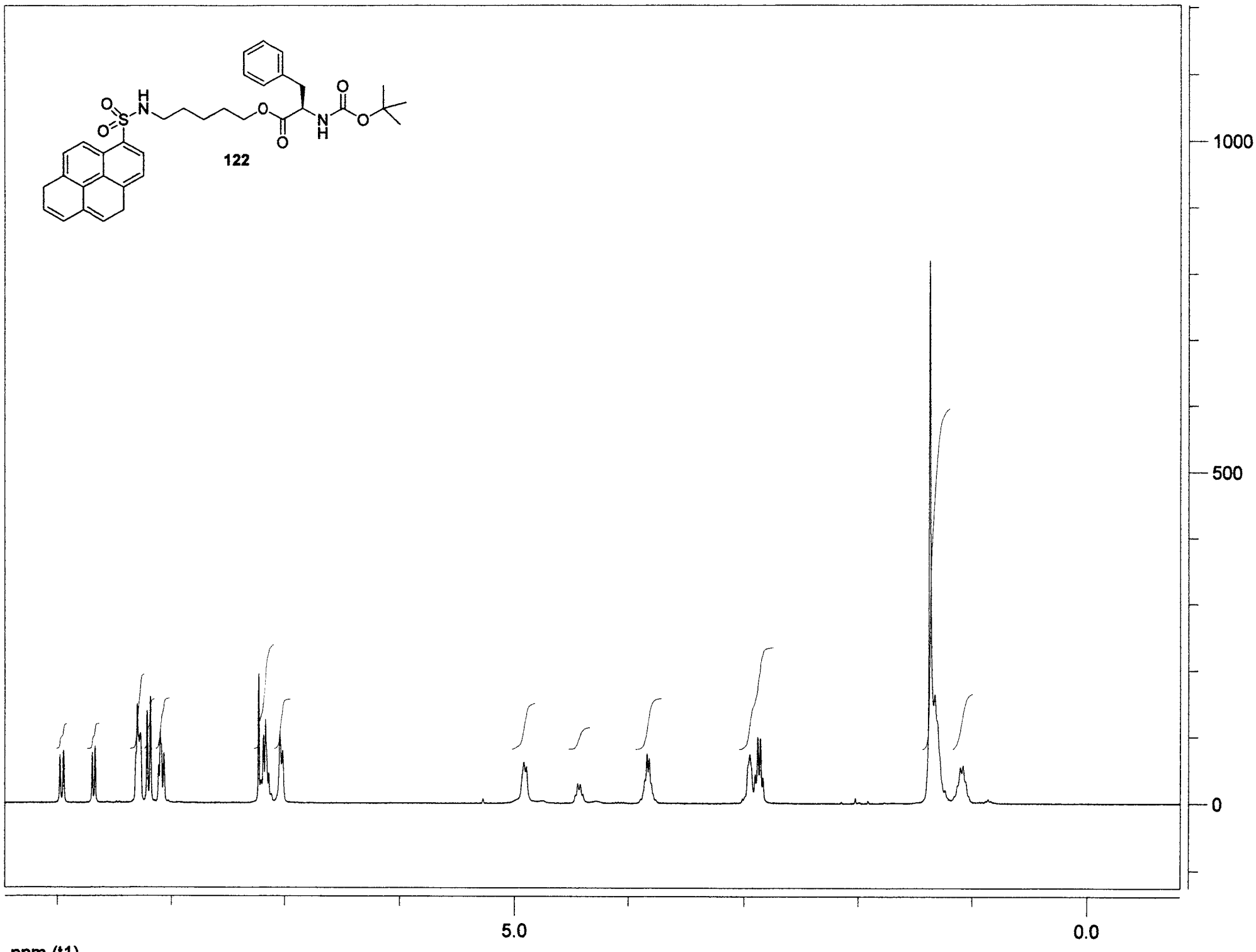
122
1000
500
0
5.0
0.0
ppm (t1)

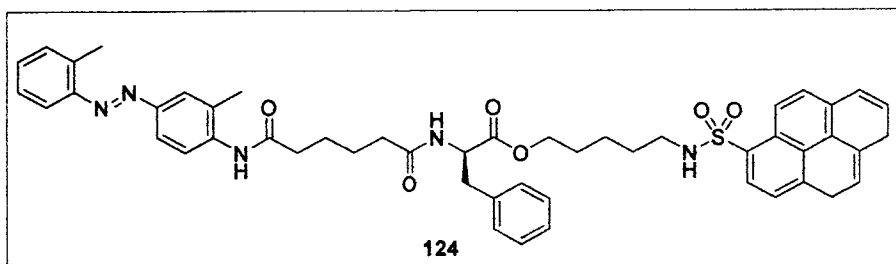

124